THE KINETICS OF CYCLOADDITION

BY FLUOROOLEFINS

A Thesis submitted for the degree of

DOCTOR OF PHILOSOPHY

of the University of London

by

Christos Tsiamis B.Sc. (Hon.), A.R.I.C.

ABSTRACT

The distinctive features of bonding in saturated and unsaturated fluorocarbons are discussed with special attention to their influence on the reactions of fluoroolefins. The theory of $\pi 2 + \pi 2$ cycloaddition reactions is reviewed. Using a combination of theoretical and thermochemical methods estimates are made of entropy and enthalpy changes in cycloaddition reaction of some fluoroolefins.

The gas phase thermal reactions of pure chlorotrifluoroethene and hexafluoropropene, and of their mixture at temperatures up to 725 K have been studied by the static method in a Pyrex reactor. The investigations were carried out both by making pressure observations and by chromatographic analyses. For each reaction, the (main) products were isolated and were identified by spectroscopic methods. These products were 1,2 cyclic dimers, formed as both the cis and trans isomers by homogeneous second-order reactions. At the upper end of the temperature range the reverse dissociation of the cyclic compounds was observed.

The order of reactivity of fluoroolefins in respect of cyclobutane formation is chlorotrifluoroethene dimerization > hexafluoropropene-chlorotrifluoroethene combination > hexafluoropropene dimerization. The specific rate constants are summarized partly as Arrhenius equations and also in terms of the transition state theory. For the dimerization of chlorotrifluoroethene the results cover an exceptionally wide temperature range and show that the Arrhenius equation is not obeyed. The enthalpy and entropy of the reactions are also given and are compared with values obtained from theoretical calculations.

The physicochemical properties of the products are discussed in relation to their structure. The alternative diradical and concerted mechanisms are considered and the corresponding activated complexes are discussed. The regioselectivity shown in these reactions suggests that the reactions proceed via a diradical intermediate.

To my Uncle Socrates

ACKNOWLEDGEMENTS

CONTENTS

Symbols

To avoid confusion the following symbols for compounds and physico-chemical quantities will be used throughout this thesis.

$A, _a$	=	Hexafluoropropene
$B, _b$	=	1,2-Di(trifluoromethyl)-hexafluorocyclobutane
C_m (M), $_c$	=	Chlorotrifluoroethene
$D, _d$	=	1,2-Dichloro-hexafluorocyclobutane
$E, _e$	=	1-Chloro-2-trifluoromethyl-hexafluorocyclobutane
R:	=	Diradical
Fc_i	=	chromatographic calibration factor
P_i, p_i	=	Partial pressure of component i (i=a,b,c,d,e)
P_t	=	Total pressure
P_o	=	initial pressure
$P^{\ominus}$	=	Standard pressure of 101,325 Pa (= 1 atm)
R	=	Gas constant 8.314 $JK^{-1}mol^{-1}$
$\dot{R}$	=	Gas constant 8.205×10^{-5} $m^3 atm$ $K^{-1}mol^{-1}$
$\dot{k}$	=	Boltzmann constant 1.3806×10^{-23} JK^{-1}
h	=	Planck constant 6.626×10^{-34} Js
T	=	Thermodynamic temperature
k_i	=	specific rate constant (i = 1,2,3..)
K	=	equilibrium constant
C	=	concentration (mol m^{-3})
H	=	molar enthalpy
S	=	molar entropy
Cp	=	molar heat capacity

FOREWORD

The present work is part of a programme of kinetic studies of the thermal reactions of perfluoro-alkanes and -alkenes and their chloro- derivatives. It is concerned with the thermal cycloaddition of chlorotrifluoroethene, hexafluoropropene and their mixture, and follows on similar studies of tetrafluoroethene by Trenwith [1] and Atkinson [2], of chlorotrifluoroethene by Stedman [3], of the cycloadduct of hexafluoropropene by Stockwell [4] and of perfluoro-cyclopropane by McKeagan. [5]

The thesis is arranged in four chapters. Chapter one, Introduction, in which thermal cycloaddition reactions of perfluoro- and chlorofluoro-carbons are reviewed together with selected topics of relevance to the present studies. Chapter two, Experimental, describes apparatus together with its method of use and application to sample preparation, and product analysis. Chapter three, Results, describes some physical and spectroscopic properties of the products, the reaction kinetics, the mathematical treatment of the experimental measurements and the application of the reaction rate theories to the results. The last chapter is a discussion of these results.

Chapter 1

INTRODUCTION

Bonding and Cycloaddition in Fluoroolefins

1.1. Bonding in Fluorocarbons

The unique properties of fluorocarbons are in evidence in the reactivities and reactions of fluoroalkenes. They behave in a markedly different manner from other alkenes and haloalkenes. In terms of reactivity, fluorinated ethenes undergo rather facile addition to themselves and to activated olefines and dienes to give cyclobutane derivatives[6,7,8], a type of addition virtually unknown to normal olefines which give the normal Diels-Alder products.

Fluorine replaces hydrogen in a wide range of chemical compounds without gross distortion of the geometry of the system because it is univalent, has a size moderately above that of hydrogen and, furthermore, forms a stable bond, which is among the strongest single bonds known. The electronic properties and size of fluorine relative to hydrogen and chlorine are set out in table 1.1.

Differences between hydrocarbon and fluorocarbon systems are likely to be influenced by the electronegativity differences, the existence of three unshared electron pairs on fluorine, the higher bond strength of C-F than C-H and the larger size of fluorine.

The presence of bulky atoms or groups (i.e. -CF_3) in a molecule may influence the reactivity and prevent reactions from taking place. The structure of the group contributes to interactions between non-bonded atoms or groups. Interactions between two non-bonded fluorine atoms have been considered to be the same as those between two isolated neon atoms. Although the exact nature of these interactions is very complicated, several effects, such as London dispersion and other van der Waals forces, may each contribute appreciably to the interaction energy. These interactions influence the physicochemical properties[13,14]. Viscosities

Table I.1. Electronic Properties

	H	F	Cl	
Electron configuration	$1s^1$	$..2s^2 2p^5$	$..3s^2 3p^5 3d$	
Internuclear distance r_e/nm (X_2)	0.0747	0.1435	0.1988	
Electronegativity (Pauling)	2.1	4.0	3.0	(9)
(Dewar)	3.9	6.0	4.2	(10)
Ionisation energy (kJ mol^{-1})	1318.0	1687.4	1256.5	
Electron affinity (kJ mol^{-1})	72.9	327.8*	348.9	(11)
Bond Energies of C–X in CH_3X	416.3	447.7	326.3	(12)
in CH_2X_2		485.6	325.9	
(kJ mol^{-1}) in CHX_3		479.5	327.6	
in CX_4		485.3	327.2	
Bond length of C–X in CH_3X	0.1090	0.1385	0.1782	(12)
(nm) in CH_2X_2		0.1358	0.1772	
in CHX_3		0.1332	0.1767	
in CX_4		0.1317	0.1766	
Average van der Waals radii X (nm)	0.12	0.135	0.180	(9)

of fluorocarbons are higher, by factors up to three, than those of the corresponding hydrocarbon, and deviations from the Principle of the Corresponding States behaviour between fluorocarbons, inert gases and hydrocarbons were related to the form of the interaction energy[15]. For fluorocarbons the potential energy curve is steeper in the attractive and repulsive region.

These molecular forces cause certain fluorine conformers to be preferred over others[16,17,18] and are responsible, at least in part, for the absence (or existence) of some rotational isomers[19]. Studies by Craig and others[18] on the stabilities of 1,2 dihalogenated ethenes, revealed that the cis form is more stable (cis effect). Non-bonding

orbital interaction between fluorine atoms superficially would lead to trans stabilization. In fact these interactions appear to be slightly bonding.

cis	CFH=CFH	C=C	0.1311*	C-F	0.1332	<FCH	110.5°[17]
trans	CFH=CFH		0.1320		0.1338	<FCH	115.2°
	$CF_2=CH_2$		0.1315		0.1321	<FCF	109.3°[22]
	$CF_2=CF_2$		0.1313		0.1313	<FCF	114°

*length in nm

trans 1,2-CHF=CHF

cis-1,2-CHF=CHF

$1,1-CF_2=CH_2$

$CF_2=CF_2$
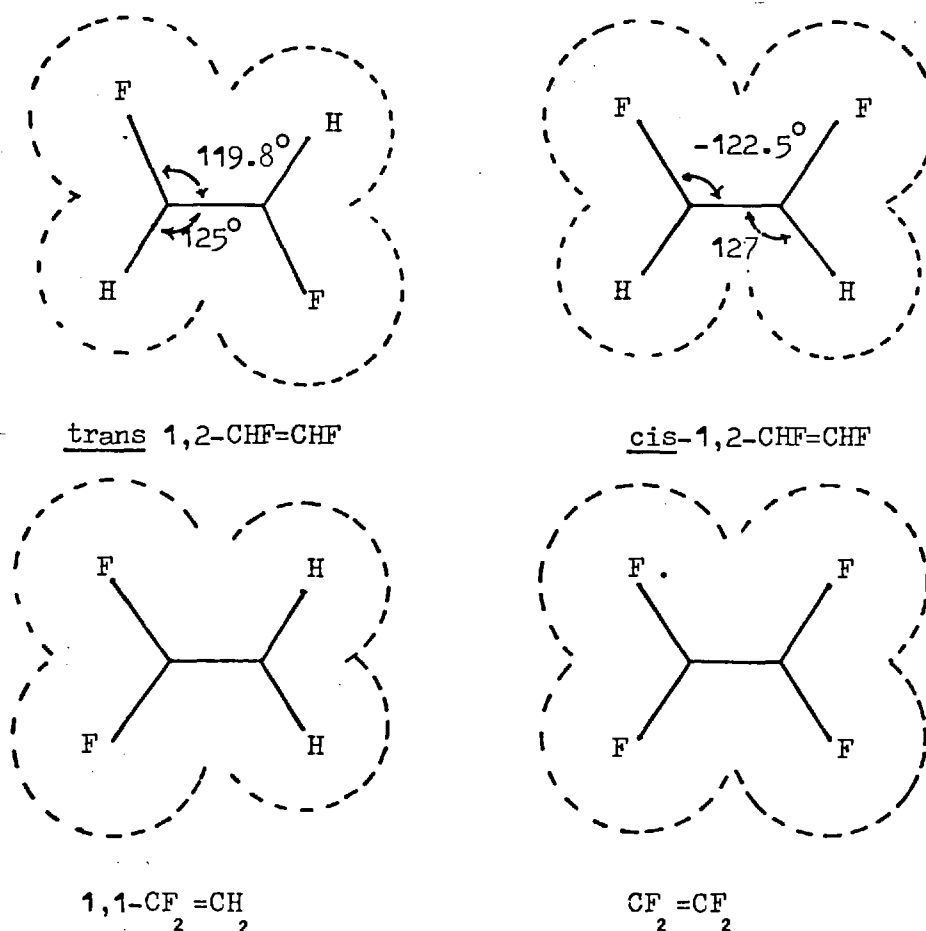
Fig. 1.1 Geometries and van der Waals radii of some fluoroalkenes

Hilderbrandt and others[20] used electron diffraction methods to study the effects on structure of fluorine-for-hydrogen substitution in organic molecules. The effect of fluorine on the structure depends also on the existence and position of other fluorine atoms as can be illustrated by difluorosubstituted ethenes[21]. The van der Waals radii of the atoms of these planar molecules were projected to the plane of symmetry to indicate the comparatively tight structure. The shorter C-C bond length and the larger size of fluorine mean that the fluorocarbon chain is much stiffer than the hydrocarbon chain.

The stiffer chain, the higher barrier of rotation about a C-C bond in fluorocarbons[23] and the low polarizability of fluorine indicate that the carbon atoms are more shielded from chemical attack than those shielded by hydrogen. A feature of fluorocarbons is their chemical stability which can be attributed not only to the intrinsic stability of the C-F bond but also to the difficulty of approach of chemical reagents to the carbon atom[24].

The strength, and the length of the carbon-fluorine bond is greatly influenced by the presence of other fluorine atoms. As fluorine replaces hydrogen, the C-F bond length shortens and simultaneously the bond strength increases. This change in bond length and strength with increasing fluorine substitution in methanes (Table I.1) is in striking contrast to the chlorinated and brominated methanes, in which no significant bond shortening and strengthening was observed.

The high electronegativity of fluorine implies that when fluorine is bonded to another atom (i.e. carbon) by a single electron-pair bond (σ bond) it will exert the greatest attraction for the electron pair, thus strongly polarizing the bond (Inductive and Field effect $-I_6$). As an increasing number of fluorines are bonded to carbon, the positive

charge density at carbon increases the positive character. Hence the amount of ionic character in C-F bonds in fluorinated methanes increases with increasing fluorine substitution. Increasing ionic attraction in the C-F bonds should shorten the C-F bond lengths and consequently strengthen the bonds.

Pauling[9] has discussed the bond shortening and strengthening in CF_4 in terms of contribution from resonance structures (so called "no bond-double bond" resonance).

$$
\begin{array}{c}
\quad\;\; F \\
\quad\;\; \| \\
F - C - F \\
\quad\;\; + \\
\quad\;\; F^-
\end{array}
\;\longleftrightarrow\;
\begin{array}{c}
\quad\;\; F \\
\quad\;\; | \\
F = C+ \\
\quad\;\; | \\
\quad\;\; F
\end{array}
\;\; F^- \;\longleftrightarrow\;
\begin{array}{c}
\quad\;\; F^- \\
\quad\;\; + \\
F - C - F \\
\quad\;\; \| \\
\quad\;\; F
\end{array}
\;\longleftrightarrow\; \text{etc.}
$$
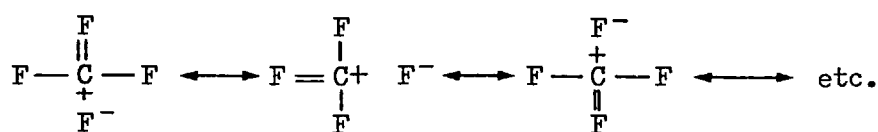
Streitwieser[25] argues against no-bond resonance 'fluorine hyper-conjugation' from observations on the rate of carbanion formation in tris (trifluoromethyl)methane and related compounds. In general we expect the normally strong inductive withdrawal of electrons by fluorine to be offset, to some extent, by the high electron density of the filled p-orbitals of fluorines. Klabunde and Burton[26], in order to explain the acidities of some polyfluorinated hydrocarbons suggested that, although many minor effects may be operative, the orders of acidity of those compounds could best be explained in terms of the inductive effect and the (electron donating +R) mesomeric effect.

When hydrogen on an sp^2 carbon is replaced by fluorine, the strong inductive effect of fluorine would be expected to act as a destabilizer to a greater extent than any other halogen, if olefin stabilities depended only on Pauling electronegativities. However, Hine and Flachskam[27] found that in monosubstituted olefins fluorine contributes more towards the stabilization of carbon-carbon double bonds than does chlorine or the -CN group. They attributed this to electron delocalization arising

from the overlap of the filled 2p orbitals of the substituent with the

2pπ system of the double bond. This contribution to stabilization seems

to be less than Hine and others[28] had suggested previously.

Multisubstitution of fluorine on the carbons of the C=C bond

results in significant weakening of the double bond. This effect can

be assessed from heats of addition. The heats of addition of halogen

and halogen acids to perfluoroolefins are observed to be more exothermic

(by about 17 to 21 kJ/F mol) than in the case of the corresponding

hydrocarbon systems[12]. The heat of polymerization of $CF_2=CF_2$ is

70 kJ mol^{-1} more exothermic than that of ethene[29].

Calculations based on Benson's[30] partial bond and group contri-

butions to enthalpy also substantiate the arguments that fluorine sub-

stitution on the carbons of a C=C bond results in a weakening of the

double bond. O'Neal and Benson[31] have shown that C-C π bond dissoci-

ation energy in tetrafluoroethene is only 175.5 kJ mol^{-1} (85.3 kJ mol^{-1}

weaker than in ethene).

$$HCF_2-CF_2H \rightleftharpoons \dot{C}F_2-\dot{C}F_2 + 2H\cdot$$

$$\Delta H_f^O = -912 \text{ kJ} \qquad \Delta H_f^O(R:) = ? + 2\Delta H_f^O$$

$$2\Delta H^O = 2D(C-H) = 2 \times 433 \text{ kJ mol}^{-1} \qquad 2\Delta H_f^O(\dot{H}) = 436 \text{ kJ mol}^{-1}$$

$$2\Delta H^O = (-866 + 436) \text{ kJ mol}^{-1} \qquad \Delta H_f^O(R:) = -482 \text{ kJ mol}^{-1}$$

$$CF_2=CF_2 \overset{(32)}{\longrightarrow} \dot{C}F_2-\dot{C}F_2$$

$$\Delta H_f^O = -657.7 \qquad \Delta H_f^O = -482 \qquad \text{then } \Delta H^O = +175.7 \text{ kJ mol}^{-1}$$
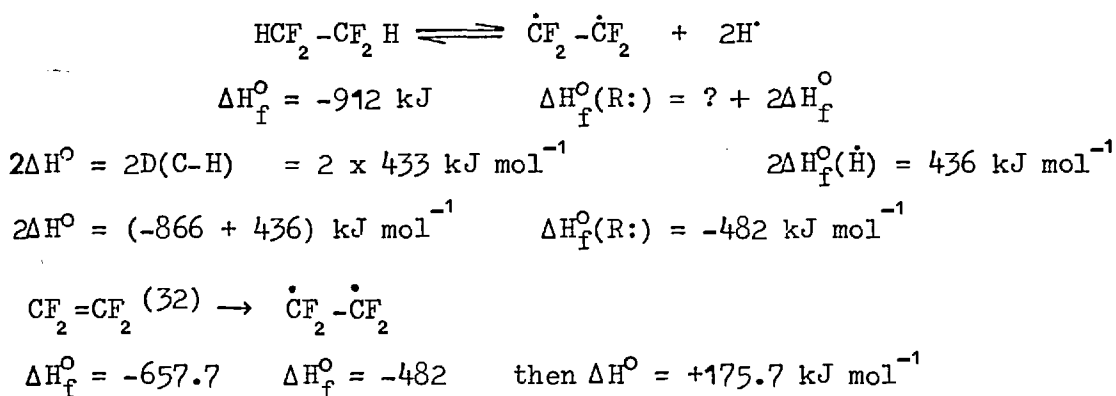
Thus only 175.7 kJ mol^{-1} is required to convert tetrafluoroethene

to the diradical, compared to 261 kJ mol^{-1} for ethene. The fluorine sub-

stitution has, therefore, destabilized the olefin by about 21 kJ/F mol.

Various electronic effects may contribute to the weakening of the

double bond by fluorine substitution. The inductive (through σ bonds)

and field effect (through space), resulting in electron withdrawal to fluorine has been discussed previously. Inductive and . . field effects also affect the polarization of π electrons ($-I_\pi$)

$$>C=C \xrightarrow{\overset{\delta-}{~~~~~} \overset{\delta+}{~~~~~}} F$$
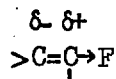
The influence of the existent unshared electron pairs of fluorine has been mentioned already. A repulsion[33] between electron pairs of fluorine and π electrons is termed Coulombic or Pauli repulsion ($+I_\pi$). There is a dichotomy in behaviour of fluorine because the ($-I$) inductive effects lead to electron withdrawal, whereas the Pauli repulsion would lead to return of electron density from fluorine. The tendency towards delocalization of the 'non bonding' electrons of the fluorine is much enhanced when fluorine is attached to an unsaturated group.

According to Bernett[22], the weakening of the double bond is due to the strain resulting from the change in hybridization. Bernett, on the basis of localized molecular orbital (MO) calculations relating hybridization with bond angles, argues that orbitals of carbon atoms used in forming the C-F bonds in gem-difluoro groups remain essentially sp^3 hybridized, even when the carbon atom is part of a double bond, carbonyl group, or three membered ring. The observed contraction in bond length, accounted by Walsh[34] in terms of changes in hybridization at the carbon centre, is supported by Bernett's calculations.

Bernett, on the basis of Bent's proposition[35], suggested that the carbon hybrid atomic orbitals used in forming the C-F bond in the series CF_4, CF_3H, CF_2H_2, CFH_3 show increasing p character (sp^3, $sp^{3.1}$, $sp^{3.18}$, $sp^{3.25}$).

Table |..2. Bond angles and carbon hybridization[22]

	C=C $\frac{1}{nm}$	<FCF	C-F,sp	<HCH	C-H,sp	C-F $\frac{1}{nm}$
CF_2H_2		108.3°±0.1	3.18	111.9°±0.8	2.83	0.1358
$CF_2=CH_2$	0.1315	109.3°±0.4	3.03	121.8°	1.89	0.1321
$CH_2=CH_2$	0.1335			117.2±0.6	2.19	
$CHF=CH_2$	0.1333	115.4°*	2.53			0.1334
$CF_2=CF_2$	0.1313	114°	3.00			0.1313
$CF_2=O$		108°±0.5	3.24			0.1312

Quantitative molecular orbital calculations on fluorocarbons were undertaken by Pople and others[36,37]. They used a semiempirical (approximate) self-consistent field (SCF) all-valence electron MO theory.

The salient point of their method is the complete neglect of differential overlap (CNDO/2) i.e. the overlap integrals between different atomic orbitals that need to be evaluated in normalizing molecular orbitals ψ_j that are linear combinations of valence atomic orbitals ϕ_i

$$\psi_j = \Sigma c_{ij} \phi_i \quad \text{or (matrix)} \quad \Psi = C\Phi \qquad 1.1$$

to which valence electrons are assigned in pairs. The method was used to calculate charge distribution and dipole moments which are in good agreement with experimental values.

Some more refined calculations by Pople and coworkers[38] using ab-initio methods reaffirmed noted trends and features caused by fluorine substitution.

These calculations make evident that fluorine, although it strongly
attracts σ electrons (fig. 1.2), is also a weak (H < CH$_3$ < F < OH <
< NH$_2$) π electron donor (called p-π interaction) and these electrons go
to β positions in large molecules, so that these positions are normally
negative. In the σ framework the charge density alternates, and with-
drawal is more effective at atoms at odd number of positions away from
fluorine. This effect, however, drops off very rapidly F-C-C-C .
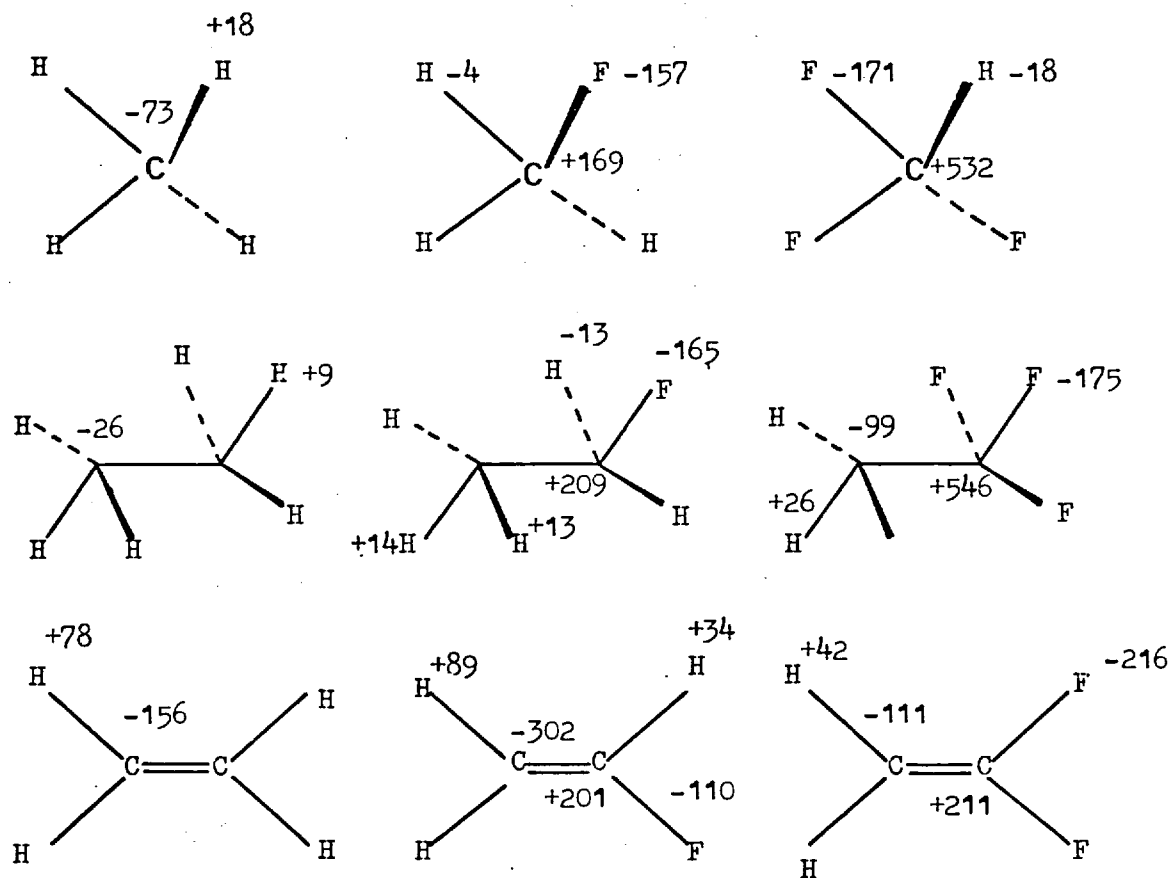
Fig. 1.2 Electron population in hydro- and fluorocarbons (10^{-3} electron).

The bond lengths and bond angles used were mean values and not
actual experimental values.

The alternation in induced charge density is associated with "back donation" of lone pair electrons of fluorine to molecular orbitals of π type relative to the C–F bond (that is, with a nodal plane through the C–F bond) and a σ type acceptance. Thus the β carbon acquires considerable negative charge leading to a relatively small dipole moment. These dipoles, attributed to π electron donation from a fluorine lone pair into the unsaturated group, result from a structure $\overset{\frown}{C}\overset{\cdot}{=}C\overset{\cdot}{-}F$, as can be seen from calculated π-electron population of some unsaturated molecules:

$$
\begin{array}{ccc}
\overset{0}{H}\ \underset{}{\overset{1.000}{-\!\!\!-}}\ \overset{1.000}{CH}\ =\ CH_2 &
\overset{0.993}{CH_3}\ \underset{}{-\!\!\!-}\ \overset{0.963}{CH}\ =\ \overset{1.044}{CH_2} &
\overset{1.939}{F}\ \underset{}{-\!\!\!-}\ \overset{1.006}{CH}\ =\ \overset{1.055}{CH_2}
\end{array}
$$

"Back donation" occurs even when no π system is directly involved as can be seen from numerical values of orbital and overlap population for difluoromethane (X=F) and fluoromethane (X=H) that are given below to illustrate the effect. The σ withdrawal of electrons from carbon
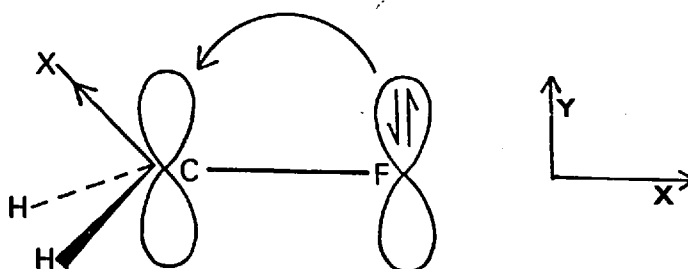
Population	Fluoromethane	Difluoromethane
$F(2p_y)$ orbital	1.966	1.943
$F(2p_z)$ orbital	1.966	1.964
$C(2p_y)$ – $F(2p_y)$ overlap	0.003	0.078
$C(2p_z)$ – $F(2p_z)$ overlap	0.003	0.014

Fig. 1.3. Electron donation from fluorine.

along the C-X bond (Fig. 1.3) decreases the occupancy of the carbon $2p_y$ orbital, which is then available to accept more electrons from the $2p_y$ lone pair of fluorine. This corresponds to some double-bond character in C-F bond and is reflected in a reduced gross population in the fluorine $2p_y$ orbital and an increased π_y overlap population between C and F. Pople's calculations make apparent the reasons for bond contraction in the carbon-fluorine bond as the number of fluorine atoms increases.

In the CNDO approximation, it was assumed that the two-centre repulsion integrals of the type (ii,kk) are independent of the relative orientations of the AO's φ_i and φ_K and under these conditions all integrals involving differential overlap can be neglected. In an improvement known as Intermediate neglect of differential overlap (INDO) introduced by Pople and others[39,40], one-centre products $\varphi_i(1)\varphi_j(1)$ involving different AO's φ_i and φ_j are retained only in one-centre integrals of the type (ij,ij). Other one-centre integrals involving orbital overlap vanish through symmetry. This procedure provides a more realistic description of atoms. Pople and others[39] tried to find a simple procedure that would reproduce the result that would be given by exact Hartree-Fock calculations, (were these possible) and the parameters in their treatment were chosen accordingly.

The parameters chosen by Pople in the INDO method failed to produce, among others, accurate enough heats of formation. This prompted Baird and Dewar[41] to use a different approach (Modified INDO) in order to obtain concordance between theoretical calculations and experimental data. They chose parameters (see Appendix I) that

would fit observed properties of suitable reference molecules,

rather than the results of a priori calculations. Second, the one-

centre integrals used in the molecular calculations were derived

from an analysis of the atomic spectra of the first-row elements.

Thirdly the various two-centre integrals were estimated by a scheme

analogous to that used in the Pariser-Parr treatment of π systems.

The MINDO method was further improved by Dewar and Haselbach[42]

and subsequently extended to fluorine systems by Dewar and Lo[43].

The heats of formation of fluorine compounds estimated by this

method are in good agreement with experimental data and with the

values determined by Pople and others[36]. The computed geometries

D_{2h}

$\Delta H_f^o = -662$
(-658.6)

$\Delta H_f^o = 50.4$
(52.4)

C_s

$\Delta H_f^o = -1129$
$(\quad ?)$

D_{4h}

$c-C_4H_8$

D_{2d}

$c-C_4F_8$

$\Delta H_f^o = -1570 \ (-1528)$

D_{4h}

$\Delta H_f^o = -1353$
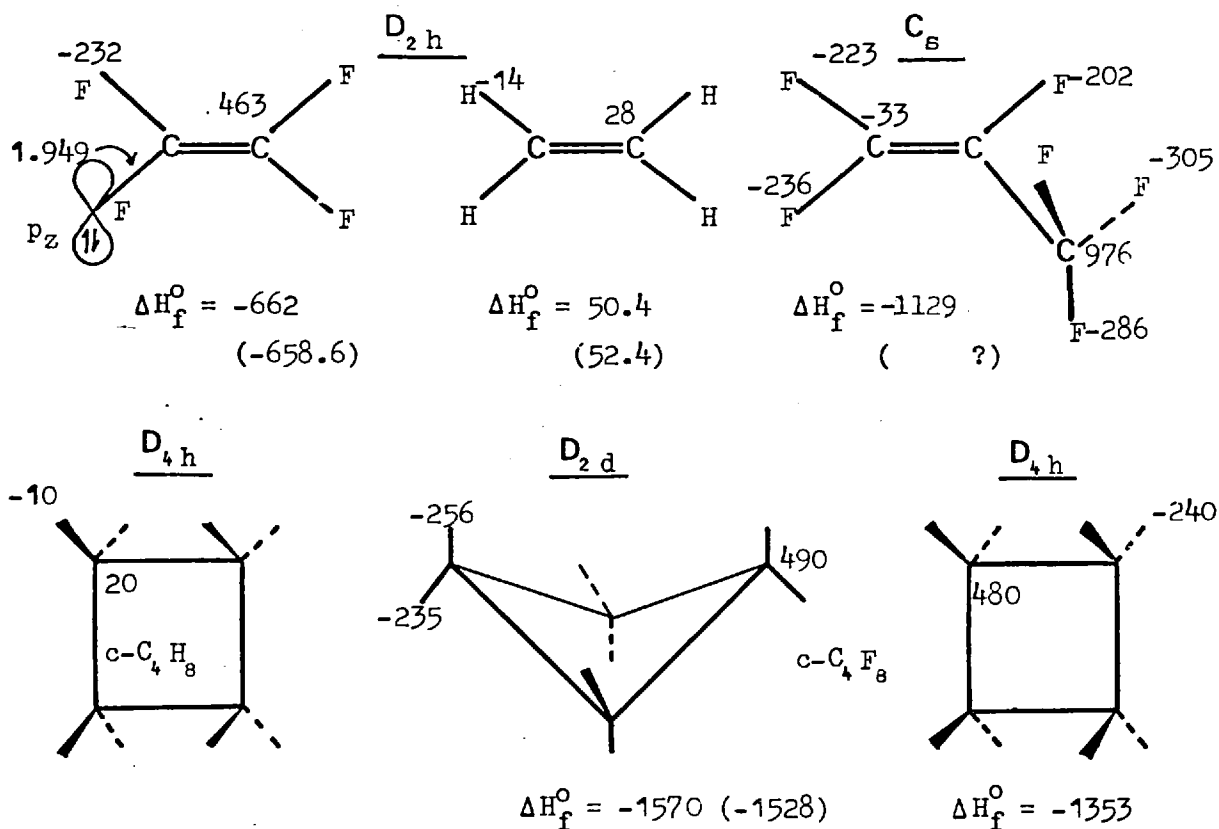
A. trans-1e,2e-DMC   (DMC = Ditrifluoromethylhexafluorocyclobutane)
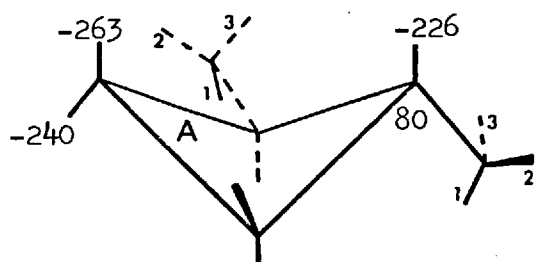
C_3 = 550 F_{11} = -287

C_5 = 955 F_{12} = -284

C_6 = 955 F_{13} = -284

ΔH^0_f = -2463

B. cis-1a,2e-DMC

C_2 = 77 F_{11} = -294

C_4 = 546 F_{12} = -278

$F_{4\alpha}$ = -249 F_{13} = -285

F_{4c} = -250 $_2F_a$ = -213
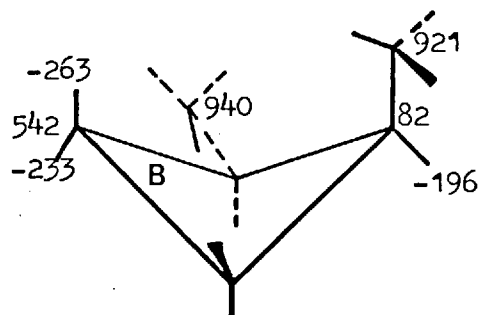
ΔH^0_f = -2382

C. trans-1a,2a-DMC

F_{11} = -296

F_{12} = -284

F_{13} = -281
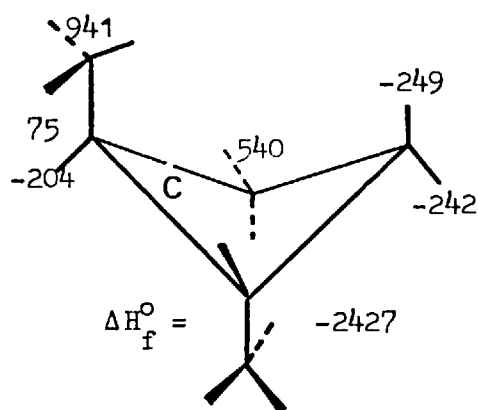
ΔH^0_f = -2427

D. trans-1a,3e-DMC

F_{11} = -299 F_{31} = 290

F_{12} = -284 F_{32} = 284

ΔH^0_f = -2446
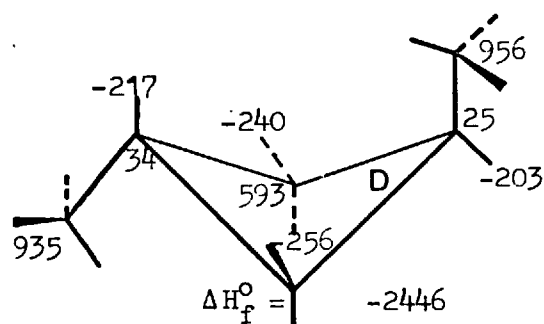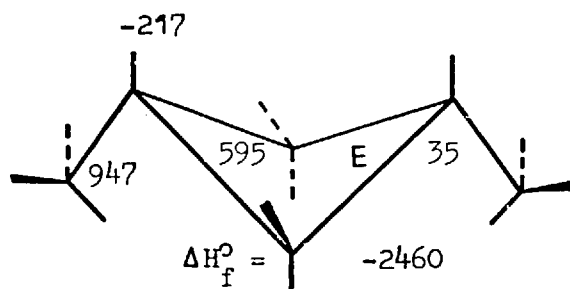
E. cis-1e,3e-DMC

F_{11} = -292 F_a = -269

F_{12} = -285 F_e = -230

ΔH^0_f = -2460

Fig. 1.4   Heats of formation (kJ mol^{-1}) and electron distribution (10^{-3} e)

that minimise the energy are in good agreement with the experimentally determined parameters, thus provided a detailed theoretical picture of the reasons for C-F bond contraction and FCF angle deformation.

As part of the work described in this thesis, the MINDO/2 method[44] (see Appendix I) was used to obtain information about a number of compounds. The geometries of the molecules were the experimentally determined ones (when available). Molecular coordinates were calculated employing the MOLTER computer programme[45] using as input data bond lengths and bond angles. The calculated heats of formation are, as expected, in excellent agreement with the experimentally determined ones (Figure 1.4.). It is also interesting to note that these calculations indicate for perfluorocyclobutane a D_{2d} structure rather than a D_{4h} form.

Epiotis[46] carried out INDO-type calculations for some fluorinated olefins to evaluate the importance of lone-pair interactions. In each fluorine or halogen, there might be two lone-pairs interacting with the lone-pairs of other halogen atoms and the olefinic bond as well. Interactions between p_z-p_z orbitals are referred to as p_π interactions, while p_x-p_x or p_y-p_y are denoted as p_σ interactions. The bond order of p_σ and p_π interactions is indicative of their extent. The lone-pair interactions for 1,1 and cis 1,2 - — difluoroethenes are attractive in nature. MINDO/2 and CNINDO calculations in our laboratory indicate that the magnitude of the bond orders for these interactions are rather small and the predictions of attractive or repulsive nature are different for the various computer programmes mentioned above.

Compound	p_π bond order	p_σ bond order	p_σ^* bond order
1,1 Difluoroethene	-0.0533	0.0873	0.0102+
cis-1,2-Difluoroethene	0.0475	-0.0242	0.0066+
Tetrafluoroethene			
Geminal fluorines			
Ref.(46)	-0.0403	0.0978+	
MINDO 2	-0.0511	0.1477‡	
CNINDO	-0.0424	0.0566‡	
Vicinal fluorines			
Ref.(46)	0.0403+	-0.0381‡	
MINDO/2	0.0511‡	0.0188+	
CNINDO	0.0424+	-0.0503‡	

p_σ^* bond order for p_x orbitals with large coefficients

+ bonding, ‡ antibonding

Liberles and others[47] in order to find a reasonable explanation for the greater stability of some cis disubstituted ethanes compared to trans, applied the total energy partition scheme suggested by Davidson and Allen[48] to quantum mechanical calculations for these molecules. The total energy E of the system is partitioned into kinetic energy of the electrons T, the attraction of the electrons for the nuclei V_{ne}, the interelectronic term V_{ee} and the internuclear repulsion term V_{nn}

The difference in energy between cis and trans isomers is given by $\Delta E = \Delta T + \Delta V_{ne} + \Delta V_{ee} + \Delta V_{nn}$

or $2\Delta E = \Delta V_{ne} + \Delta V_{ee} + \Delta V_{nn}$

therefore the relative stability of the isomers depends upon the magnitude of the above terms. The ΔV_{ne} term favours the cis

geometry, an attractive steric effect, while the last two components favour the _trans_ component. Fluorine, with its few electrons and small nuclear charge contributes more to the ΔV_{ne} term, which is larger than the sum $\Delta V_{ee} + \Delta V_{nn}$. This distribution leads to _gauche_ conformation and _cis_ isomers.

The electron delocalization and subsequently the large positive charge on the C = C carbon atoms and the weakening of the double bond is seen to be the driving force for the dimerization of fluorinated olefins to cyclobutane derivatives. In the dimerization the strength of C-F bond remains unchanged and the $C^+ - C^+$ repulsions decrease because of the much longer bond. The ring strain in perfluorocyclobutane is 117 kJ.mol^{-1}[49] compared with 110[50] kJ.mol^{-1} for cyclobutane.

1.2. Conformation of the cyclobutane ring.

There has been much interest in the molecular structure of cyclobutane-like four-membered rings and their derivatives, and a wide variety of methods have been applied in studying these compounds. Early investigations[51] suggested a puckered form (D_{2d}) for cyclobutane and a sufficiently low barrier of ring inversion such that an appreciable fraction of molecules would exist above the barrier in a planar form.

Recent infra red and Raman spectra studies by Stone and Mills[52] indicated the value 35° for the dihedral angle of cyclobutane and these results were confirmed by Miller and Copwell[53]. The NMR spectrum of cyclobutane in a liquid crystal (nematic) solvent[54] was consistent with D_{2d} symmetry of the molecule. The value of the

dihedral angle ranged between 23° and 27°. An interesting

feature is that the C-C-C planes do not bisect the HCH angle.

The CH_2 groups are tilted in a way which brings axial hydrogens

on the same side of the carbon ring together. The tilt of

'rocking' angle is 4°.

C-F = 0.1333 nm
C-C = 0.1566 nm
<FCF = $109.9 + 0.3^\circ$
<CCC = $89.3 + 0.3^\circ$
= $89.3 + 0.3^\circ$
α = 17.4°
β = -5.4° (Tilt)
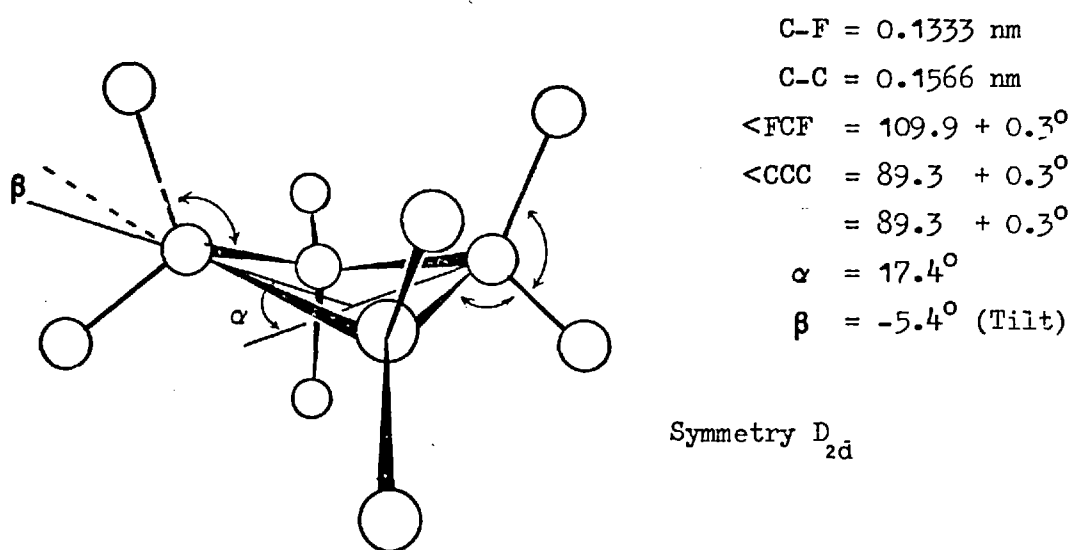
Symmetry D_{2d}

Fig. 1.5 Structure of octafluorocyclobutane[56].

Bauman and Bulking[55] re-examining the infra red (in gas

and liquid phase), Raman and NMR spectra of octafluorocyclobutane

concluded that the results were consistent with a bent ring of

symmetry D_{2d}, but not with a planar ring of D_{4h} symmetry or any

other form possessing a centre of symmetry. Refined electron

diffraction studies by Chang, Porter and Bauer[56] were compatible

with a D_{2d} structure. The dihedral angle was found to be 17.4°.

Their results are given in Fig. 1.5 and are in good agreement with previous data. The angle of tilt of axial atoms in cyclobutane which was indicated by the results of Meiboom and Snyder[54] and demanded by the calculations of Wright and Salem[57], Nelson and Frost[58] and Pasternak and Meyer[59] is also present in octafluorocyclobutane (β = -5.4). Miller and Capwell[60] have also determined and interpreted the Raman and infra red spectra of octafluoro- and octachlorocyclobutane in terms of a D_{2d} structure. They also found a D_{4h} structure for octahydrocyclobutane which was attributed to hydrogen bonding.

The unavoidable conclusion to be drawn from the results mentioned above is that cyclobutane and its octasubstituted derivatives are non planar molecules (see also ref 61). The D_{2d} structure was consistent with our calculations (Fig. 1.4). One consequence of the D_{2d} cyclobutane ring tilted structure is that a trans 1,2-disubstituted compound may exist in two conformational forms, namely diequatorial and diaxial, while the cis form would be in the axial-equatorial conformation. For a symmetrically 1,3 disubstituted cyclobutane the cis form can possess the diequatorial or diaxial conformation, while the trans may exist in axial-equatorial conformation as it has been confirmed experimentally[62]. It has also been suggested that 1,3 interaction causes flattening of the ring which is a less stable form.

1.3. Cycloaddition

The propensity of fluoroolefins for forming four-membered rings is one of their most intriguing characteristics. The dimerisation of tetrafluoroethene to octafluorocyclobutane[63], a

$_{\pi}2 + _{\pi}2$ reaction proceeds at a significant rate at 500 K, while the cyclodimerization of ethene, a similar reaction, has not been observed yet. Co-dimerisation will occur not only between different fluoroolefins but also between fluoroolefins and unsaturated hydrocarbons and, moreover, some of these co-dimerisations proceed more readily than the reaction involving only fluoroolefins. An impressive feature of the $_{\pi}2 + _{\pi}2$ cycloaddition of fluoroolefins is that it takes precedence over the Diels-Alder reaction. The presence of a gem $F_2C=$ group in the structure of fluoroolefin greatly facilitates cyclodimerisation. 1,2-difluoro-olefins -FC=CF- are much less reactive. Replacement of halogen with hydrogen, alkyl or perfluoroalkyl greatly reduces reactivity. Hexafluoropropene reacts quite sluggishly [at 500 K, 10^5 $k(CF_2=CFCF_3) \approx k(CF_2=CF_2)$]. A comprehensive review of cycloaddition reactions has been published by Huisgen and others[64]. Unfortunately this review does not include correlation with the reverse reaction of ring splitting.

Thermal cycloaddition can be conceived as proceeding by a surprising number of distinguishable mechanisms. Each mechanism implies a certain reaction path and a distinct transition state. The transition state requiring the minimum activation energy will dominate the course of the reaction. Ab-initio quantum mechanical calculation of the potential energy reaction surface connecting reactants and products would provide all the information about the reaction path, but computations of this magnitude are still unattainable. For concerted intermolecular cycloadditions, in which the passage from reactants to products occurs in a single step without any other species intervening, Woodward and Hoffman[65]
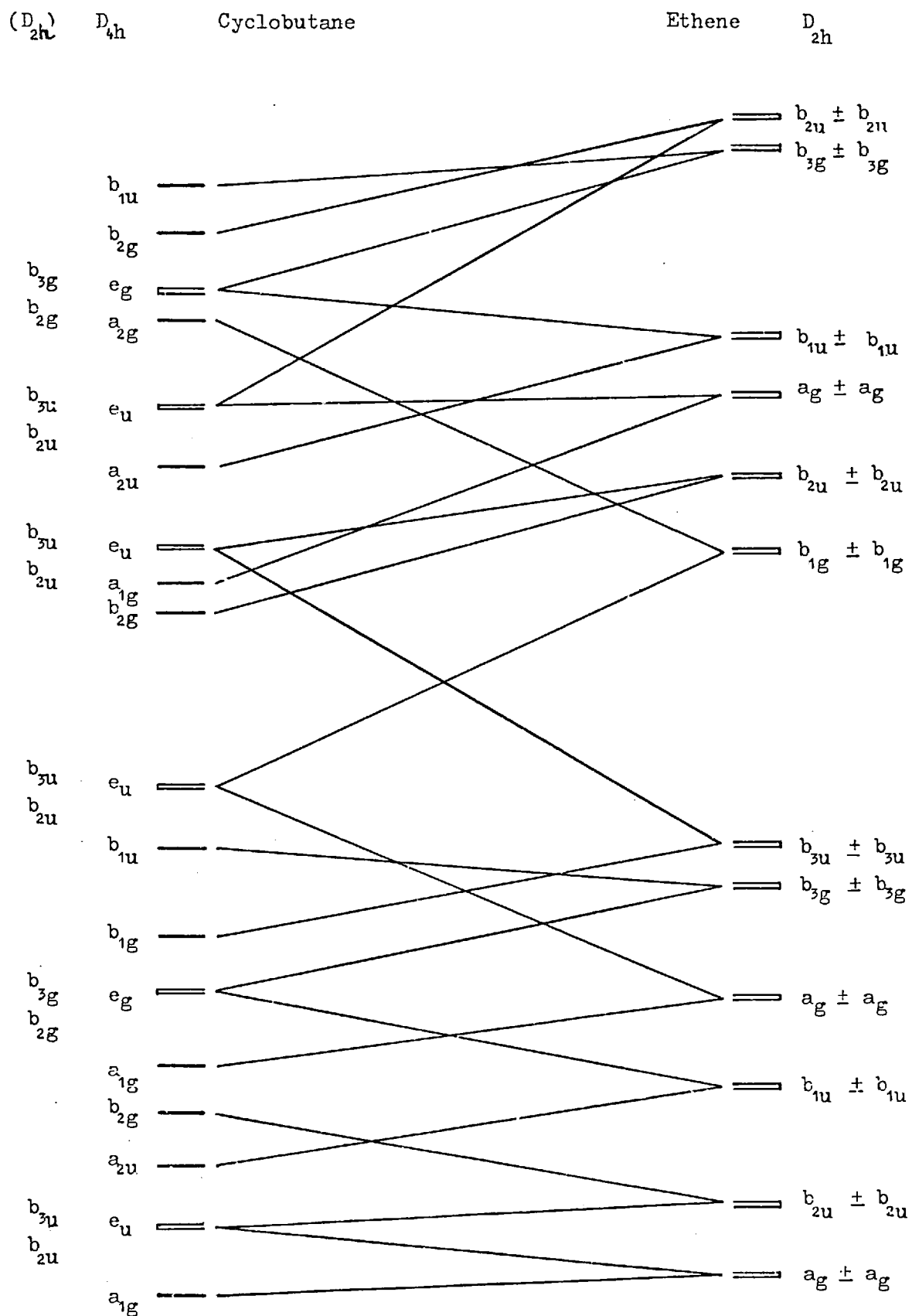
Fig. 1.6   Orbital correlation diagram for the cycloaddition (s + s)

of two ethene molecules.

have given rules which help in the choice of reaction path. In
practice until recently practically all calculations of reaction
route have been based on speculative selection of the transition
state, rather than exploration of the potential energy surface.

Calculation of molecular orbital (MO) energies of reactants
and products of known geometry can provide limited but very use-
ful information about the reaction path of cycloaddition reactions.
For this class of pericyclic reactions, Woodward and Hoffmann[65]
have established 'selection rules' on the basis of molecular
orbital symmetry. According to these 'rules' reactions occur
readily when there is congruence between orbital symmetry charac-
teristics of reactants and products, and only with difficulty when
that congruence does not obtain. The use of correlation diagrams,
suggested by Lonquet-Higgins and Abrahamson[66] is of high utility
in the treatment of cycloaddition reactions.

A complete correlation diagram for the thermal cycloaddition
of two ethene molecules (symmetry D_{2h}) to form planar cyclobutane
(symmetry D_{4h}) has been drawn (Fig. 1.6). In this suprafacial-
suprafacial addition, denoted $_\pi 2_s + _\pi 2_s$, two ethene molecules
approach each other with their planes parallel, moving along the
maximum orbital interaction-least motion path. The character
tables used are those of Wilson, Decius and Cross[67]. The z
axis was taken perpendicular to planar cyclobutane, with the y
axis bisecting the gem $H_2C=$ angle of the ethene and the x axis
perpendicular to the nodal plane of the double bond. The energies
of the MO were calculated by the MINDO/2 method.

The reaction transfers two electron pairs from π bonding

orbitals (b_{3u}) to σ orbitals. Two of the electrons occupying

b_{3u} orbitals would finish up in (b_{3u}) antibonding orbitals of

higher energy and the cyclobutane would be formed in a high-energy

excited state. Therefore a significant amount of energy would have

to have been acquired during the concerted change in order to reach

the excited state. The non-crossing rule indicates that the path

actually followed would be that of the full line, which leads to

formation of ground state cyclobutane, but which indicates the

presence of an energy barrier to the concerted cycloaddition.

The barrier height crudely about half the energy gap between the

highest occupied (HOMO) and the lowest vacant (LVMO) orbitals, is

estimated by recent calculations[66,68] to be about 500 kJ.mol^{-1}.

The reaction is 'forbidden' in the Woodward-Hoffman sense, which

means that this mechanism will not be observed as a fast reaction

at room temperature, while at higher temperature, because of the

high activation energy, other reactions, such as decompositions,

might prevail. There may of course be other mechanisms for cyclo-

addition which have lower barriers.

The approach in which the two $p\pi$ carbon orbitals of the react-

ants interact with each other in an antarafacial-antarafacial mode

($_{\pi}2_a + _{\pi}2_a$) is also symmetry 'forbidden'.
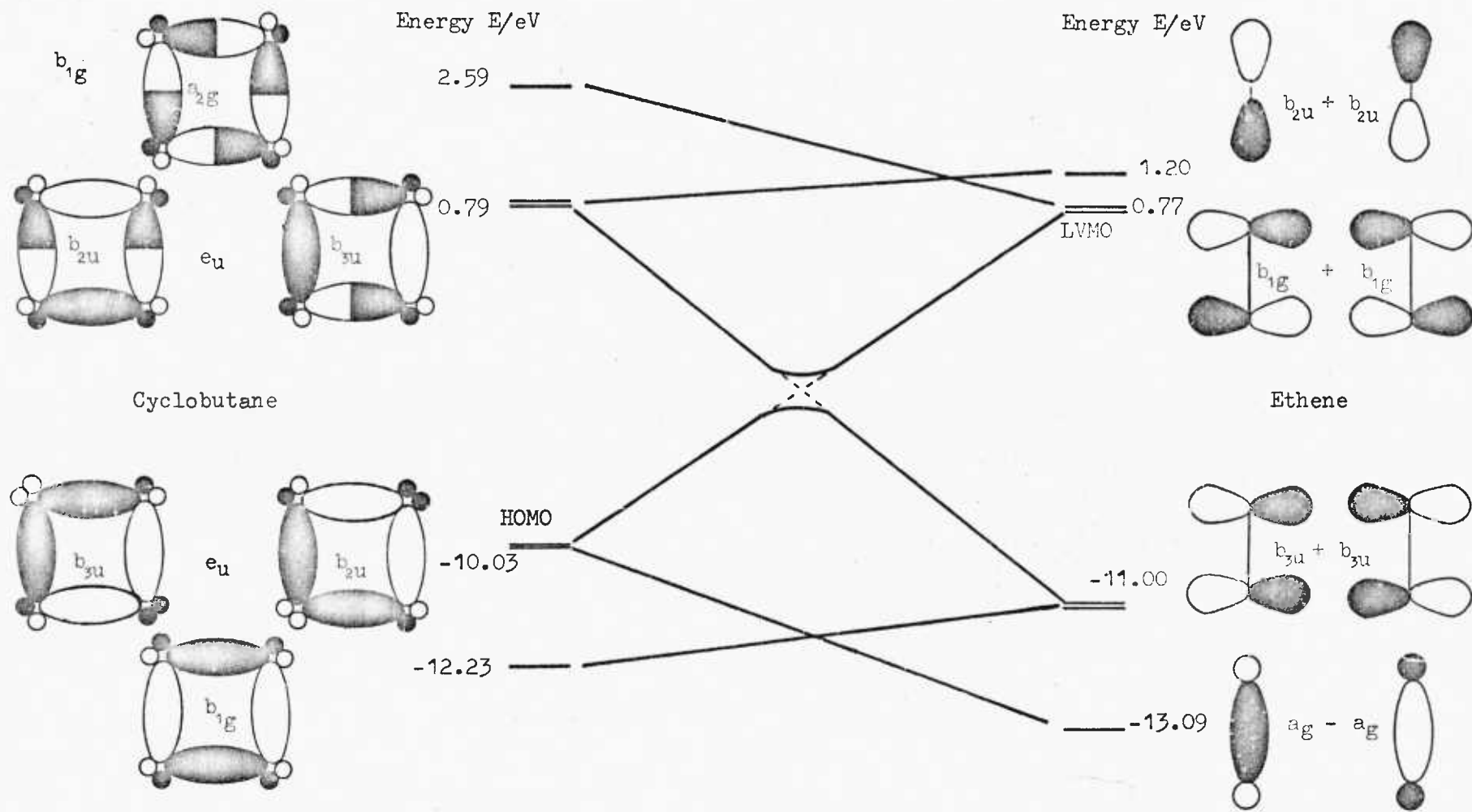
Fig. 1.7. Energies and Orbital correlation for ethene cyclodimerization.

$\pi^2_a + \pi^2_a$

$\pi^2_s + \pi^2_a$
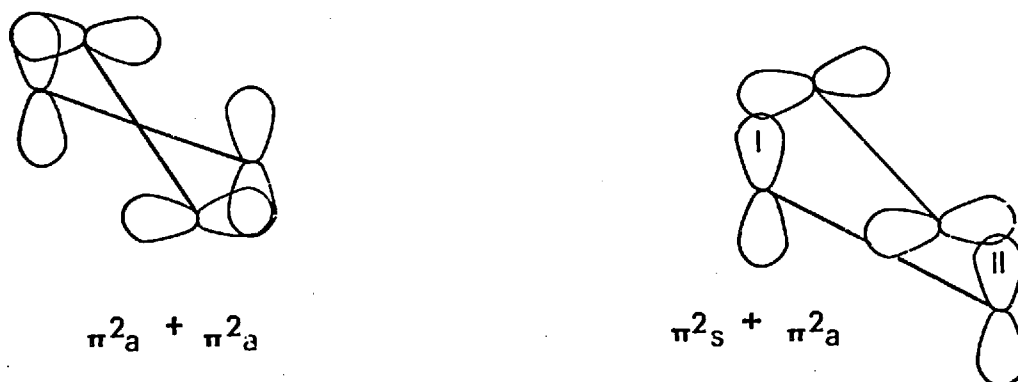
Figure 1.8 Modes of approach for cycloaddition of two ethene molecules

The approach in which one of the reactant molecules exercises a suprafacial interaction to one of the $p\pi$ orbitals and an antarafacial interaction to the other (Fig. 1.8 I, II) is termed a supra-antara process. It can be seen that in order to achieve maximum overlap of the relevant orbitals the reactants must approach one another orthogonally. A correlation diagram may be constructed for a $\pi^2_s + \pi^2_a$ reaction using a two-fold axis of symmetry which bisects both the ethylenic bonds.

$$\pi_i \pm \pi_i' = \pi_1 , \pi_1^*$$
$$\sigma_i \pm \sigma_i = \sigma_1 , \sigma_1^*$$
$$\sigma_j \pm \sigma_j = \sigma_2 , \sigma_2^*$$
$$\pi_j \pm \pi_j = \pi_2 , \pi_2^*$$
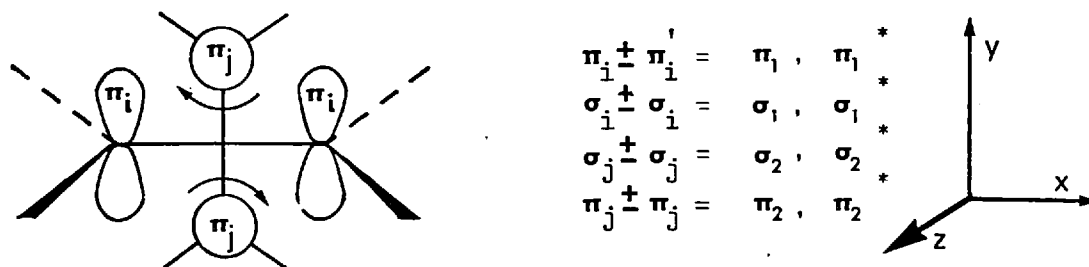
Figure 1.9 Orientation of two ethene molecules and orbitals

for correlation diagram of a $\pi^2_s + \pi^2_a$ process.

The orbitals of interest are the occupied $\sigma_1, \sigma_2, \pi_1, \pi_2$ and the unoccupied $\sigma_1^*, \pi_1^*, \sigma_2^*, \pi_2^*$. The symmetry is C_{2v} and these orbitals may be assigned to representations of the C_{2v} point group.

A_1	σ_1 ,	σ_2 ,	π_2
A_2	π_1^*		
B_1	σ_1^*		
B_2	π_1 ,	π_2^* ,	σ_2^*

The three lowest molecular orbitals are derived from combinations (three) of the orbitals of the A_1 representation

$\sigma_1 + \sigma_2 + \pi_2$ $\sigma_1 + \sigma_2 - \pi_2$ $\sigma_1 - \sigma_2 + \pi_2$ $\pi_1 + \pi_2^* + \sigma_2^*$
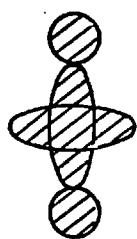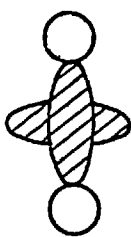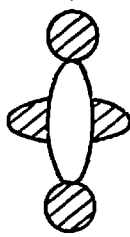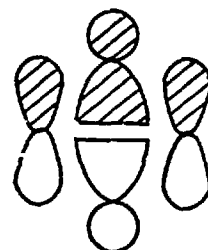
<u>a</u>   <u>b</u>   <u>c</u>   <u>d</u>

The total energy of <u>a</u> , <u>b</u> , <u>c</u> , will be slightly higher than the sum of the orbital energies in the separated molecules. The combination is slightly antibonding as all possible levels are occupied. The fourth lowest occupied molecular orbital <u>d</u> is derived from the orbitals of the B_2 representation and will be close to pure π_1.

If the lobe (carbon atom) j turns towards i to make a ring,

the four lowest orbitals of the cyclobutane ring are produced.

The concerted reaction is 'permitted' in so far as the correlation
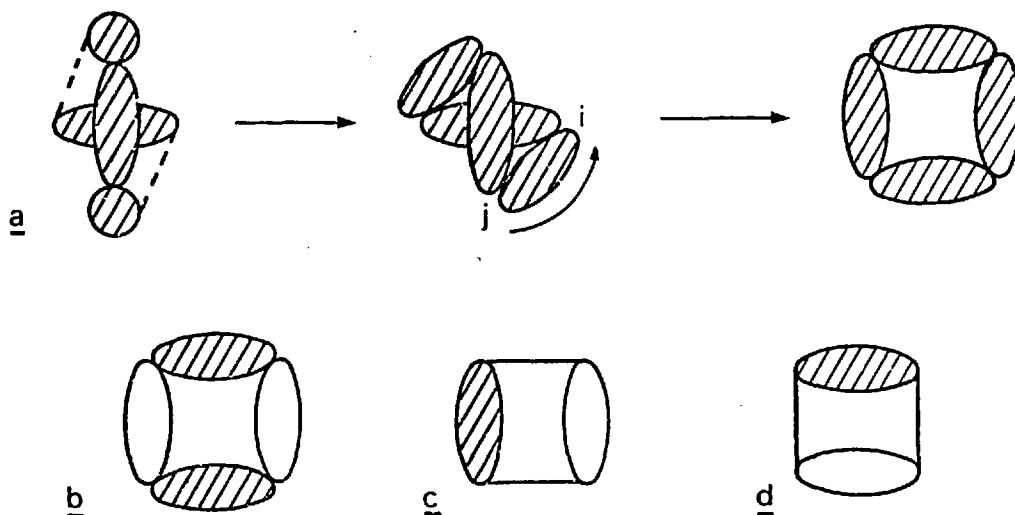
of orbitals is concerned, but there is energy required to produce

the distorted structures involved in the transition state. The

initial interaction between two orthogonal ethene molecules is⁻

similar to the repulsive interactions between two saturated mole-

cules. This repulsion is compensated for only when the molecules

turn to form a puckered ring.

In their treatment of cycloaddition of an m to an n electron

system, Woodward and Hoffmann presented selection rules in which

the geometry of addition is taken into account (Table 1.3), but

they give no guide concerning the strain energy which may be in-

volved.

Table I.3. Selection rules for Cycloaddition reactions.[65]

m + n	Allowed in Ground State Forbidden in Excited State	Allowed in Excited State Forbidden in Ground State
4q	$m_s + n_a$ $m_a + n_s$	$m_s + n_s$ $m_a + n_a$
4q + 2	$m_s + n_s$ $m_a + n_a$	$m_s + n_a$ $m_a + n_s$

The same conclusion can be reached by following the Dewar[69] -Zimmerman[70] representation. A 4q electron cycloaddition is allowed in the ground state if the Mobius topology of interaction can be achieved, namely, an array with an odd number of sign inversions as in the s + a process. It should be emphasised that the principle of conservation of orbital symmetry is valid, whether or not a formal correlatin diagram can be constructed. The presence of substituents in an ethene molecule can be dealt with by replacing them with their isoelectronic carbon groupings or, if their electronic demands are trivial, by hydrogen atoms. In the concerted cycloaddition of ethene to propene there is no symmetry in the transition state. The methyl group has reduced all levels to the same symmetry. One might be tempted to conclude that methyl substitution has made the thermal cycloaddition ($_\pi 2_s + {}_\pi 2_s$) symmetry allowed. The perturbation caused by the presence of methyl is a very small one and a bonding level of reactants has again moved to high energy in the transition state. The reaction still remains symmetry-forbidden.

Using correlation diagrams, the energetic behaviour of each orbital as it transformed from reactant to product was carefully considered and the importance of the first excited state was indicated. Fukui[72,73] and co-workers evolved the 'Frontier Orbital' theory which correlated reactivity with properties of the highest occupied (HOMO) and lowest vacant (LVMO) orbitals of the reactants since the most significant interactions are considered to be between the HOMO of one molecule and the LVMO of the other. The overall energy change resulting from the mutual perturbing influence of one molecule upon the other can be calculated to a reasonable degree of accuracy using perturbation methods[10]. Mathematical correlations of the frontier orbital concepts[73] with perturbation theory (PMO) were demonstrated and the relation-ship of both PMO theory and the frontier orbital method to the orbital-symmetry reactivity concepts has also been extensively discussed[10,70,73]. Herndon[74] presented the theory of cyclo-addition reactions in terms of PMO while Hudson[75] used the same approach for the whole spectrum of chemical reactivity.

The essential feature of the PMO is that, in the incipient state of the reaction, the wave functions of the perturbed system is given by appropriate combinations of the wave functions of the two unperturbed molecules. The magnitude of stabilization will depend on the nature and the extent of interactions of the MO's of the two cycloaddends. The result of the interactions will be to lower the energy of the occupied levels and to raise the energy of unoccupied levels. The stabilization energy (SE) for two polyenes A and B, when the doubly occupied MO M of A interacts

with the vacant MO , N of B and the doubly occupied MO K of

polyene B interacts with an unfilled MO L of polyene A, is given

by

$$SE = N[C_{mi} \ C_{nj} + C_{mr} \ C_{ns})^2 \ \gamma^2 \quad \frac{1}{E_m - E_n} \ ] \ +$$

$$N[(C_{li} \ C_{kj} + C_{lr} \ C_{ks})^2 \ \gamma^2 \quad \frac{1}{E_k - E_l} \ ] \quad {}^{(76)} \qquad 1.2$$

where N is the number of electrons occupying the energy levels E_z

C_{zx} is the coefficient of the xth p atomic orbital of polyene P,

γ is the resonance integral between the two interacting p atomic

orbitals at the union sites and E_2 is the energy associated with

the MO Z.
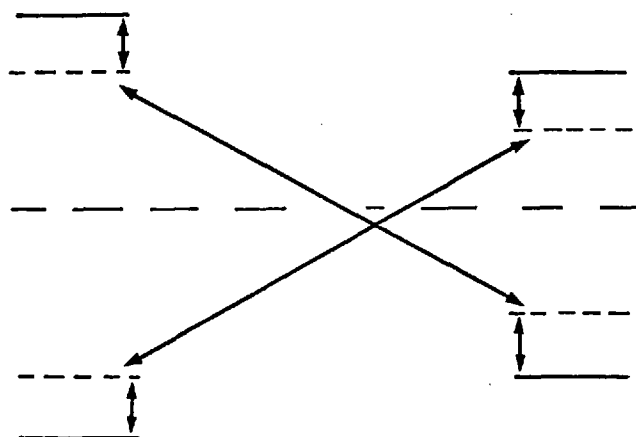
Figure 1.10. Schematic diagram of the effect of MO interaction

upon the energy levels of the cycloaddends. Broken lines depict

the energy levels of the two molecules prior to interaction. Full

lines depict the energy levels of the two molecules after the

interaction. Arrows indicate interacting energy levels.

On the basis of equation 1.2 which incorporates all the features

of the Woodward-Hoffmann rules, Epiotis[76] argued that the type of

approach (a + a, s + s, s + a) and, therefore, the selective

formation of one of the possible stereoisomers can be predicted
as well as the preferential orientation (regioselectivity) of
the reactants to form one particular isomer.

It has been suggested that face compatibility alone of the
MO is a necessary but not sufficient condition for concerted
process and the energy separation of the interacting MO of the
cycloaddends should be taken into account. The latter may be
studied by using interaction diagrams. An interaction diagram
depicts the relevant MO energy levels of the reactants, the dis-
tribution of electrons in these MO and the dominant interactions
of the MO of the two cycloaddends, which can be ascertained by
noting the degree of proximity of the energy levels corresponding
to the interacting. Such an interaction diagram can be construct-
ed using computed figures or experimental data (Fig. 1.11)
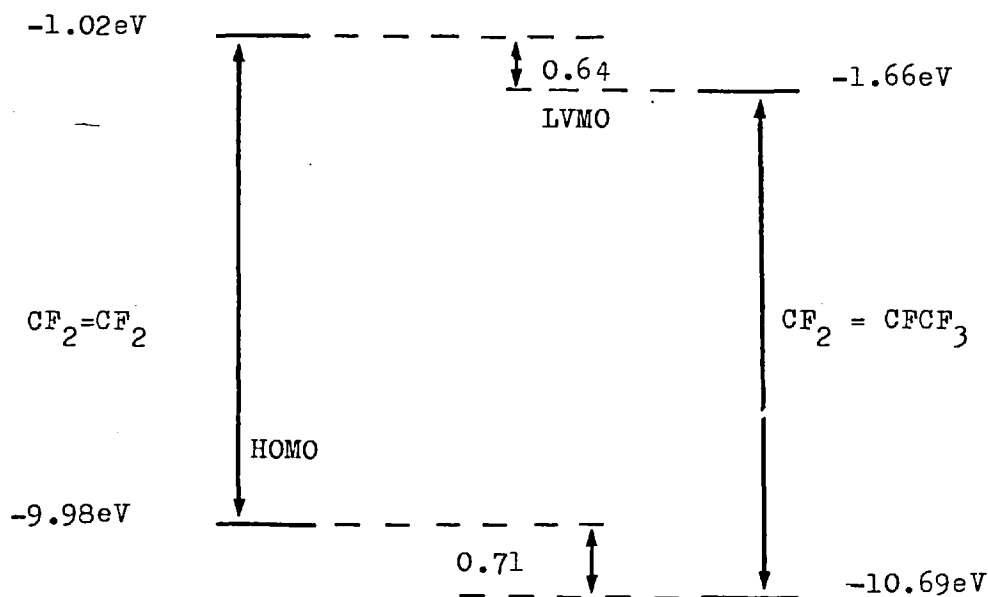
Figure 1.11 Interaction diagram for the case of $C_2F_4 + C_3F_6$
cycloaddition. Orbital energies calculated by the MINDO/2 method
(for spectroscopic data see ref. 77).

Most of cycloaddition reactions can be.described in terms of donor-acceptor relationships. The difference $(E_{Ha} + E_{LVa})$ - $(E_{Hd} + E_{LVd}) = \lambda > 0$ indicates that reactant d acts as donor while cycloaddend a acts as an acceptor in a given cycloaddition. Their interaction in the transition state can be defined as a resonance hybrid involving no bond (NB) and charge transfer (CT) contributing structures. For cyclodimerizations or, in

$$d....a(NB) \longleftrightarrow d^+ \quad a^- \quad (CT)$$

general, $\lambda \simeq 0$, the contribution of the CT structure will be negligible, while for $\lambda > 0$ the contribution of the NB structure will be negligible. The examination of phase compatibility
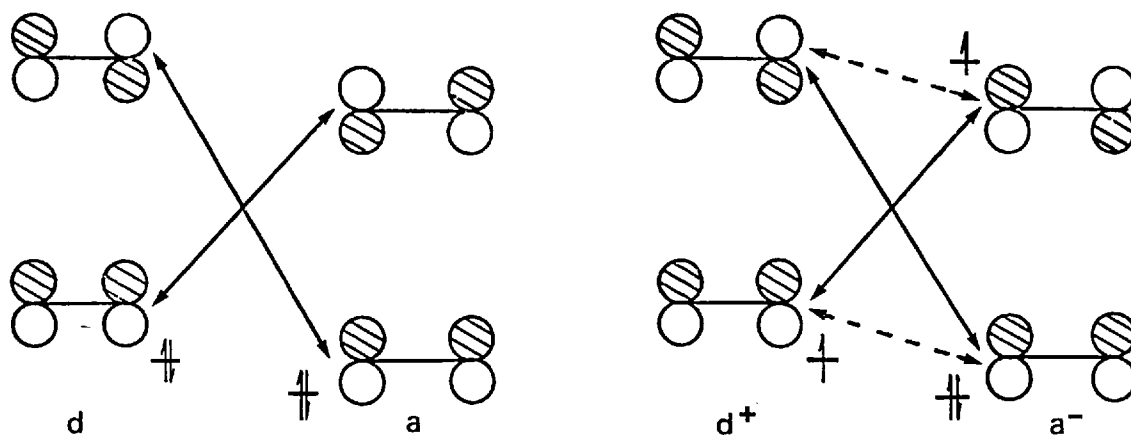
Figure 1.12. Schematic diagram of the resonance formations of the transition state of a cycloaddition reaction. Solid arrows indicate dominant interactions stabilizing the s + a transition state, while broken arrows indicate dominant interactions stabilizing the s + s transition state.

(signs and magnitude of the quantities C_{ZX}) of the appropriate orbitals corresponding to the interacting energy levels indicates

that the π^2_s + π^2_a path is preferred when the d...a (NB) contribution to the transition state prevails. The preferred mode of union of two cycloaddends is determined jointly by steric and electronic effects. The rotation of a bond demanded by the s + a process will preferentially occur within the acceptor moiety. Steric effects caused by the presence of bulky substituents will dominate the overlap effects γ_i and will influence the stereochemistry as well as the rate of the reaction. From consideration of steric effects alone the rate of dimerization of some fluorinated olefines is expected to decline as bulky substituents replace fluorine.

$$CF_2 = CF_2 > CF_2 = CFCl > CF_2 = CCl_2 > CF = CFCF_3 \gg CF_2 = C(CF_3)_2$$
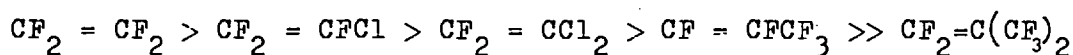
Epiotis also discussed[78] the regioselectivity of concerted cycloadditions. Rearrangement of equation A for two distinct regiochemical modes of union, namely, the head-to-head (HH) and head-to-tail (HT) cycloadditions, gives:

$$SE(HH) = [4\gamma^2/(E_1 - E_2)] (C_{11}C_{21} + C_{12}C_{22})^2 \qquad 1.3$$

$$SE(HT) = [4\gamma^2/(E_1 - E_2] (C_{11}C_{22} + C_{12}C_{21})^2 \qquad 1.4$$

where E_1 and E_2 are the energies of the frontier MO's of the reactant undergoing cycloaddition and $\underline{i}$ in Cij denotes the appropriate MO and j the appropriate carbon atom. Since $C_{12} \simeq C_{21}$ = a and $C_{11} \simeq C_{22}$ = b and substituting $K = 4\gamma^2/(E_1 - E_2)$ equations 1.3 and 1.4 become

$$SE(HH) \quad = \quad K(2ab)^2 \qquad 1.5$$

$$SE(HT) \quad = \quad K(a^2 + b^2)^2 \qquad 1.6$$

therefore the regioselectivity of a reaction will be determined from the inequality $a^2 + b^2 > 2ab$ which holds for all positive

values of a and b except a = b$\geq$0. Epiotis postulated that a re-
action will proceed regiochemically in a manner which involves
union of the two atoms of highest frontier orbital electron density
and union of the two atoms of the lowest frontier orbital electron
density. For olefines substituted by electron withdrawing groups
the mode of addition is expected to be head-to-tail. Furthermore,
the geometry of a $_\pi 2_s$ + $_\pi 2_a$ transition state is sterically unfavour-
able and the orbital interactions which stabilize such a transition
state are very weak since, as it is the case, the frontier orbitals
of the cycloaddends have substantially different energies. Also,
it has been found that $_\pi 2$ + $_\pi 2$ cycloaddi-tions yield mainly head-
to-head products. The alternative to a concerted reaction is a
stepwise mechanism with one of the new bonds forming first, and
leading to a definite, though short-lived, bifunctional intermed-
iate (diradical or dipolar ion), whose free end then combine to
close the ring. Such a mechanism would explain regioselectivity of
these reactions since 'head' in this context is the most stable
radical formed, as well as the relative absence of stereoselectiv-
ity[6,7,8].

It has been suggested that a particular requirement for the
stepwise process is the presence of the $F_2C=$ group or 1,1 electro-
negative substituents. Bartlett and Wheland[79] argued that a
geminal pair of fluorine atoms or highly electronegative substitu-
ents is neither a necessary nor a sufficient condition for reactiv-
ity in the diradical mechanism of cycloaddition. They suggested,
on the grounds of the sensitivity of this reaction to structure,
the dependence of the reaction on three important factors:

(1) exothermicity of double bond opening.

(2) accommodation of the odd electrons on the potential diradical.

(3) ease of approach of reactants in formation of the initial new bond.

Benson suggested semiempirical methods for estimating thermo-dynamic properties[30] of organic compounds. These methods are based upon additivity schemes in which the basic units are the atoms or bonds, or groups which comprise the molecule. Group additivity methods proved to be the most successful schemes developed. For simple molecules it is possible by these methods to estimate the heats of formation ($\Delta H^{\ominus}_f$), heat capacities ($Cp^{\ominus}$) and entropies ($S^{\ominus}$)[30,80] to a high degree of accuracy. Error limits of the order of $\pm$ 4 kJ.mol^{-1} in $\Delta H^{\ominus}_f$ and $\pm$ 4J.K^{-1}.mol^{-1} in $\Delta S^{\ominus}$ can be easily achieved. Known correction factors for ring strain steric factors and resonance effects can be introduced with a similar degree of accuracy. So, heats of reaction can be calculated to a reasonable degree of accuracy ($\pm$ 8kJ.mol^{-1}).

Within the transition-state theory framework, a chemical re-action involves the passage of reactants along a reaction surface into products _via_ a transition complex. The thermodynamic prop-erties of reactants and products can be calculated as well as those of _model_ intermediates and possible transition complexes including strain, resonance, and relative stability parameters for unstable species[81].

The main disadvantage of this method is the _a priori_ selection of a model for the activated complex. Though thermochemical evaluations may match experimental data, any aspects of quantum-mechanical restrictions which might pertain to the reaction cannot be revealed, and such coincidence cannot be interpreted without

further proof as evidence for the accuracy of the model in repres-

enting the details of the actual chemical entity under consider-

ation. Selection of a number of possible intermediates would make

the choice less arbitrary, without increasing unduly the amount

of calculation.

O'Neal and Benson[30,49] applied the thermochemical method in

their analysis of cyclobutane ring-cleavage reactions with consid-

erable success. They assumed that the ring opening proceeds via

a putative, non-interacting, 1,4-diradical. Summarizing the

Salem-Rowland[82] definition, diradicals are molecules with two

(weakly interacting) odd electrons in degenerate or nearly de-

generate molecular orbitals. For thermochemical evaluations the

electronic properties of these short-chain-length diradicals are

not considered in detail. They may be important in discussing

stereoselectivity and estimation of bond rotation barriers[83]

influenced by through space overlap and through bond interactions.

Stephenson and Gibson[83] found that this omission did not affect

the validity of Benson's method and suggested the same rotational

barrier for singlet and triplet species. For corrections in the

entropy of the system, only the spin degeneracy of the singlet

$(g_i = 1)$ is taken into account[30b,31].

According to O'Neal and Benson, the diradical is an inter-

mediate and not the transition state. The heats of formation of

these non-interacting diradicals are 25-42 kJ.mol^{-1} less than that

of the corresponding activated complex. The failure to intercept

any such diradical by radical scavengers could be accounted by

its short life-time (10^{-10} s). These free radicals would correspond

to shallow potential energy minima near the transition state
region along the reaction surface. Extended HMO calculations by
Hoffmann and others[84] on the tetramethylene diradical yielded a
smooth surface with only one maximum between cyclobutane and
ethylene decomposition products. No secondary minimum was found
in the many dimensional potential energy surface but only a very
flat region, where the system - named twixtyl - spends a relatively
long time exploring its way out. Calculations for the trimethyl-
ene diradical by Goddard's generalized valence bond method[85] did
not indicate a secondary minimum.. A priori SCF calculations with
Slater type orbitals[88] favour a minimum on the triplet state
surface. Pople[86] has shown that the lowest energy route
for ring closure through an orbital crossing region is _via_ the
triplet state. Stephenson and others[87] suggested two possible
reasons for observed discrepancies between thermochemical and MO
calculations. The first reason, calculation of the heat of forma-
tion of the diradical by employing the same C-H bond dissociation
energy in removing the second hydrogen as when removing the hydro-
gen, can be debated. Benson and O'Neal[31] assign the value 410 kJ
as dissociation energy for one C-H bond and an average value
433 kJ per C-H bond for the diradical. The second reason is the
approximations employed in MO calculations. Doering and Sachdeu[88]
from kinetic data of thermal isomerization studies, suggested that
1,3 diradicals constituted the transition state while 1,4 diradi-
cals might exist as an intermediate. With the present understand-
ing of these short-chain-length diradicals, thermochemical calcu-
lations remain very useful and facilitate evaluation of Arrhenius
parameters and rates of reaction.

1.4   Energetics of cycloaddition reactions.

Using Benson's procedure[31], the enthalpy and the entropy

of activation of certain reactions of special interest in this work

have been calculated. The figures relate to ring formation in the

biradical mechanism. The thermodynamic path from reactants to the

transition state employed for pre-exponential factor calculations

that follow, involves estimates of changes in entropy, enthalpy

and heat capacities in the manner described.

(a)   association of reactants to the corresponding

diradical (nonresonance form) at room temperature

(298 K):

(b)   incorporation of resonance to the diradical (if

resonance exists):

(c)   correction of the thermodynamics of the reaction to

the diradical from 298K to the reaction temperature

by using the estimated average reaction heat capacity

over this temperature range ($\Delta C_{p_{T-298}}^{\ominus}$):

(d)   formation of the transition state from the diradical:

(e)   incorporation of the reaction path degeneracy of

the reaction.

Detailed calculation for a few compounds are given below. The

notation is that of Benson[30,31]. For sake of brevity $X_{298}^{\ominus}$ is

written as $X^{\ominus}$

A   Ethene——>cyclobutane

(a). 1.   Ethene

$$2[C_d - (H)_2]$$

$$\Delta H_f^{\ominus} = 2 \times 26.2 \qquad = \qquad 52.4 \text{ kJ.mol}^{-1} (1kJ = 0.239kcal)$$

$$S^{\ominus} = 2 \times 115.52 - R\ln 4 = 231.04 - 11.52 = 219.50 \text{ J K}^{-1}\text{mol}^{-1}$$

$$\bar{C}p_{700-300} = (2 \times 0.5)(21.34 + 38.91)^{-} = 60.25 \text{ J K}^{-1}\text{mol}^{-1}$$

2. Diradical (R:) $= \overset{\bullet}{C}H_2 CH_2 CH_2 \overset{\bullet}{C}H_2$

$$H(CH_2)_4 H \longrightarrow {}^{\bullet}(CH_2)_4^{\bullet} + 2H^{\bullet}$$
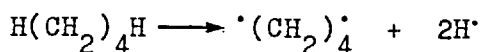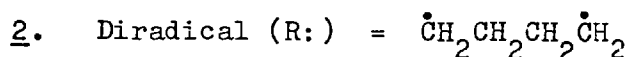
$$\Delta H_f^{\ominus} (R:) = 2D(C-H) + \Delta H_f^{o} \text{ (n-butane)} - 2\Delta H_f^{o} (H^{\bullet})$$

$$303.1 = 866.1 - 127.03 - 435.97 = 303.1 \text{ kJk}^{-1}\text{mol}^{-1}$$

$$R: = 2 [\overset{\bullet}{C} - (C)(H)_2] + [C - (C)_2(H)_2]$$
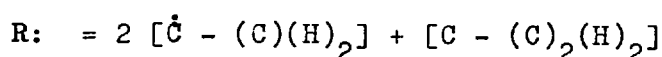
$$\sigma = \sigma_{int} \times \sigma_{ext} = 4 \qquad R\ln 4 = 11.52$$

$$S^{\ominus} = 2[130.54 + 39.41] - R\ln 4 = 328.4 \text{ JK}^{-1}\text{mol}^{-1}$$

$$\bar{C}p_{700-300} = (2 \times 0.5)(25.06 + 41.00 + 23.01 + 42.68) =$$
$$= 131.75 \text{ kJ.mol}^{-1}$$

3 Reaction $\qquad 2CH_2 = CH_2 \longrightarrow$ (R:)

$$\Delta H_a^{\ominus} = \Delta H_f^{\ominus} (R:) - 2\Delta H_f^{\ominus} (CH_2 = CH_2)$$

$$303.1 - 2 \times 52.4 = 198.3 \text{ kJ mol}^{-1}$$

$$\Delta S^{\ominus} = 328.4 - 2 \times 219.50 = 110.6 \text{ J K}^{-1}\text{mol}^{-1}$$

$$\Delta \bar{C}p = 131.75 - 2 \times 60.25 = 11.25 \text{ J K}^{-1}\text{mol}^{-1}$$

(b,c) $\Delta H_{700}^{\ominus} = \Delta H^{\ominus} + \Delta \bar{C}p(T_2 - T_1) = 198.3 + 11.25 \times 402 = 202.86$

$\Delta S_{700}^{\ominus} = \Delta S^{\ominus} + \Delta \bar{C}p \int dT/T = 110.6 + 11.25 \times 0.847 = -101.07$
$$\text{J K}^{-1} \text{ mol}^{-1}$$

$\Delta H \quad CH_2{=}CH_2 \quad \xrightarrow{198.34}$ ... $\xrightarrow{4.52}$ ...
$\Delta S \quad CH_2{=}CH_2 \quad \xrightarrow{-110.6}$ 298 K $\qquad \xrightarrow{9.53}$ 700K
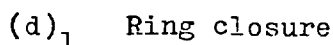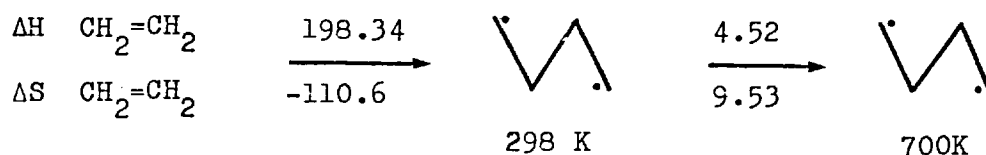
(d)$_1$ Ring closure

$$\Delta H^{+}\text{ring closure} = (Et^{\bullet} \longrightarrow E_t^{\bullet})_{27.6} \quad 27.6 \text{ kJ mol}^{-1}$$

$$\Delta S^{+} = -S^{\ominus}(Et^{\bullet} \longrightarrow Et^{\bullet})_{27.6} = -10 \text{ J K}^{-1}\text{mol}^{-1}$$

$$\overline{\Delta C}_p^+ = 0.5(8.79 + 9.62) = 9.20 \quad J \cdot K^{-1} mol^{-1}$$

$$\Delta H_{rc}^+ = \Delta H_{r.c.300}^+ + \overline{\Delta C}_p^+ (700-30) = 27.6 + 9.2 \times 0.4 = 31.28 \, kJmol^{-1}$$

$$\Delta S_{700}^+ = \Delta S^+ + \Delta C_p \ln(700/300) = = 10 + 9.2 \ln 2.33 = 17.79$$
$$J \, K^{-1} mol^{-1}$$

ΔH

ΔS

298 K   700K
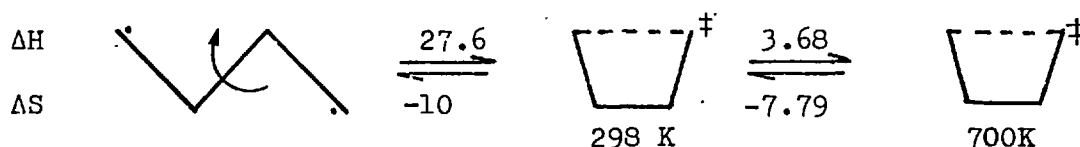
(d)$_3$ Cyclic activated complex

$$2CH_2 = CH_2 \longrightarrow (\quad []^\ddagger \quad)$$

$$\Delta H^\ddagger = 202.86 + 31.28 = 234.14 \quad kJ \cdot mol^{-1} \quad (-55.96 \, kcal)$$

$$\Delta S_{int}^\ddagger = -101.07 - 17.79 = -118.86 \quad J \cdot K^{-1} \cdot mol^{-1}$$

(e)

Symmetry (D_{2d}) correction - $R\ln\sigma = -11.52 \quad (\sigma=4)\Delta S^\ddagger = -130.38 JK^{-1}$

$$\therefore \Delta S^\ddagger = -130.4 \, J \cdot K^{-1}$$

(d)$_2$ Diradical formation process - 'Open' activated complex

The concerted process for formation of the 1,4 butanyl diradical from ethene is depicted as

$$2CH_2 = CH_2 \underset{-1}{\overset{1}{\rightleftharpoons}} (\quad)^\ddagger \underset{-2}{\overset{2}{\rightleftharpoons}} \text{/\\/}$$
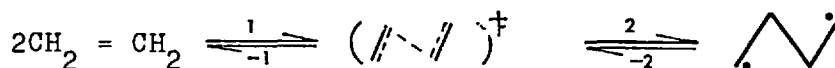
Thus, proceeding from the diradical to the activated complex as suggested previously (path -2),

$$\Delta \overline{X}^\ominus = \overline{X}^\ominus[-2(CH_2 \longrightarrow n\text{-}Pr)_{25} -2(C\text{-}C)_{420} - (C - C)_{900}$$

$$+(P_{3e})_t + (P_{4e})_t + 2(C\text{-}C\cdot C)_{290} + (S_f - S_h)_{17}$$

$$\Delta \overline{S}^{\ominus}_{700} = \Delta S^{\ominus} + \Delta \overline{C}_p \int dT/T = [-2(9.20) - 2(3.8) - 0.8 + 4.0 + 0.8 +$$

$$+ 2 \times 12.0 + 0.8] + [-(2 \times 0.5)(7.5 + 8.8) - (2 \times 0.5)(12.0)$$

$$-0.5(4 + 4.4) + 0.5(6.3 + 7.9) + 0.5(2.9 \times 7.1)+0+0]x0.847 = -18.1kJ$$

$$\Delta S = -101.07 - 18.1 = -119.2 \ JK^{-1}$$

5 Cyclobutane

$$4[C-(C)_2(H)_2] + \text{ring correction}$$

$$\Delta H^{\ominus}_f = 4(-20.71) + 109.62 = 26.78 \ kJ \ mol^{-1}$$

$$S^{\ominus} = 4(39.41) + 124.68 - 8.3141 \ln 8 = 265.03 \ JK^{-1} \ mol^{-1}$$

$$\Delta \overline{C}_p = 2(23.01 + 42.68) + 0.5(-19.21 - 9.45) = 117.0 \ J \ K^{-1} mol^{-1}$$

6 Reaction $\qquad 2CH_2 = CH \longrightarrow c-C_4H_8$

$$\Delta H^{\ominus}_R = 26.78 - 2 \times 52.4 = -78 \ kJ \ mol^{-1}$$

$$\Delta S = 265.03 - 2 \times 219.5 = -164 \ J \ K^{-1} \ mol^{-1}$$

$$\Delta \overline{C}_p = 117 - 2 \times 60.25 = -3.5 \ J \ K^{-1} \ mol^{-1}$$

at 700K $\Delta H^{\ominus}_{R700} = \Delta H^{\ominus}_{R300} + \Delta C_p \int dT = -78 - 3.5x400x10^{-3}$
$$= -79.4 \ kJ \ mol^{-1}$$

Using the quantities obtained in this manner, a reaction co-ordinate diagram is constructed (Fig. 1.13). The values of the thermochemical quantities are in good agreement with the experiment-al data of Beadle and others[90] obtained from the pyrolysis of cyclobutane. The difference in the heat of formation of the di-radical between these calculations and the value of Beadley is eliminated if the calculation is based on heats of formation of
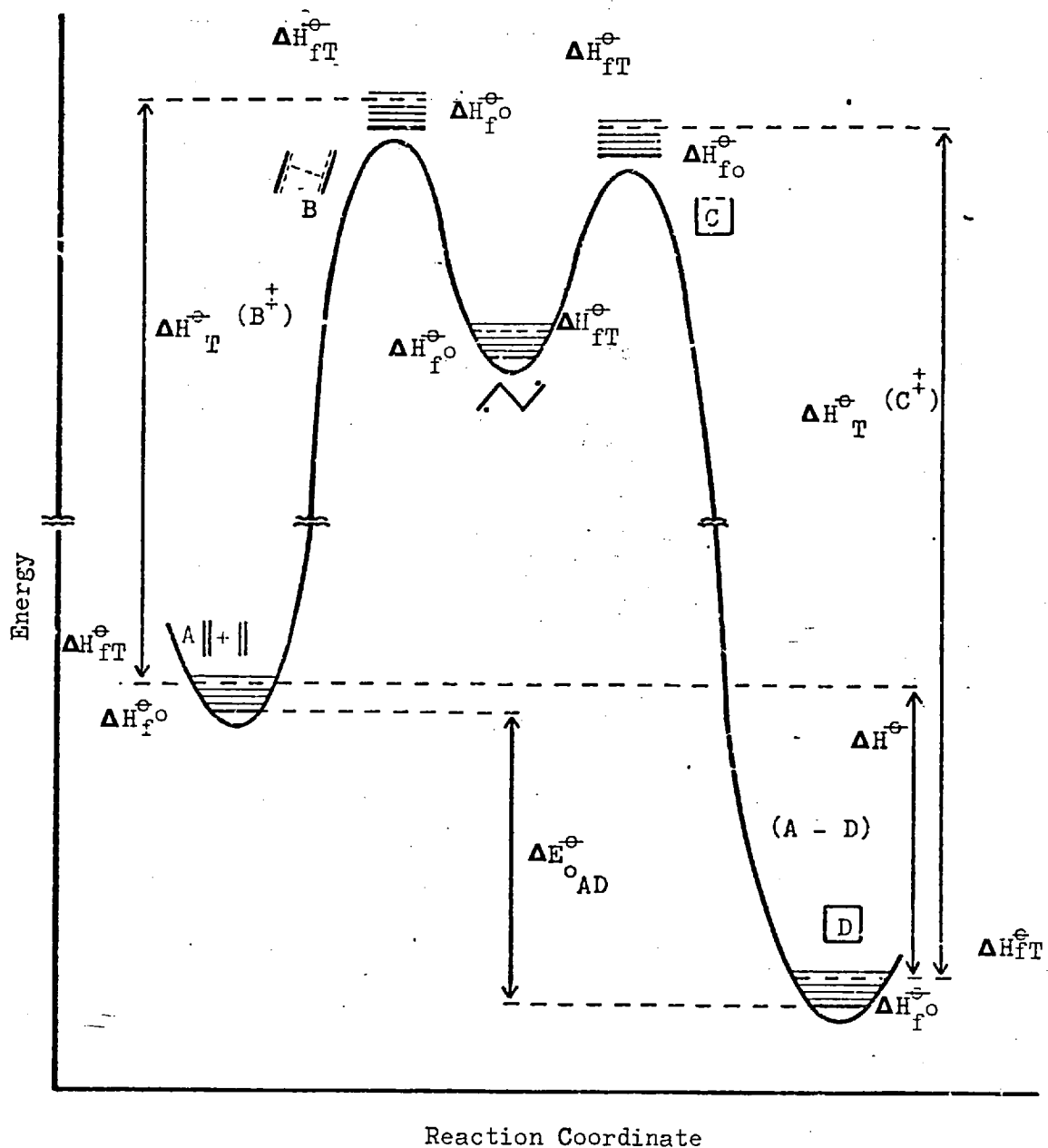
Figure 1.13   Reaction coordinate diagram for ($_\pi 2$ + $_\pi 2$) cyclo-
addition and cycloisomerization reactions. The structure (☐)
represents the transition state for <u>cis</u> - <u>trans</u> (geometric)
isomerizations. The structure (⟋⟍⟋) represents the transition
state for structural decomposition (formation of substituted
ethenes) of cyclobutane derivatives.

radicals[49,81]

B.   Tetrafluoroethene $\longrightarrow$ Octafluorocyclobutane

(a).1 Tetrafluoroethene[32]

$$\Delta H_f^{\ominus} = -658.56 \text{ kJ mol}^{-1}, \quad S^{o} = 300, \quad \overline{C}_{p_{700-300}} = 95.81 \text{ J K}^{-1} \text{ mol}^{-1}$$

2   Diradical $(\overset{\bullet\bullet}{R_f}) = \dot{C}F_2 \, CF_2 \, CF_2 \, \dot{C}F_2$

$$H(CF_2)_4 \, H \longrightarrow {}^{\bullet}(CF_2)_4^{\bullet} + 2H^{\bullet}$$
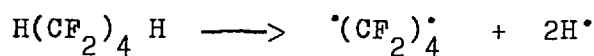
ΔH_f^{o} (R:) $= 2DH(C-H) + \Delta H_f^{o}(n\text{-}CF_2HCF_2CF_2CF_2H) - \Delta H^{o}(H) = -1297.9$

$\qquad = 866.1 \qquad\qquad -1728 \qquad -435.97$

$S^{\ominus}$ (R:) $= S^{\ominus}, (n\text{-}C_4F_8H_2) - 3R\ln \dfrac{R:}{n\text{-}C_4F_8H_2} - 2S^{\ominus}(C-H)_{3100}$

$\qquad -4(F\overset{\displaystyle \overset{C}{\diagup\diagdown}}{\quad}H)_{1450} - 0.5R\ln \dfrac{Ir(R:)}{Ir(RH_2)} + R\ln g_i + S_{rotor}(n\text{-but-rad})$

$\qquad = 476.14-0.25-0.25-0.5+0+0+0 = 475.14 \text{ J K}^{-1} \text{ mol}^{-1}$

$$\overline{C}_{p_{700-300}} = 224.26 - 0 - 0.63 - 4 \times 2.26 + 0 = 214.6 \text{ J K}^{-1} \text{ mol}^{-1}$$

3   Reaction $2CF_2 = CF_2 \longrightarrow (\overset{\bullet\circ}{R_f})$

$$\Delta H_{\alpha}^{\ominus} = 19.22, \quad \Delta S^{\ominus} = -124.86, \quad \Delta\overline{C}_p = 22.98$$

(b,c) $\Delta H_{700}^{\ominus} = 28.4$ kJ $\Delta S_{700}^{\ominus} = -105.4 \text{ J K}^{-1}$

(d) Ring closure

$$\Delta H^{+} = \Delta H(CF_2CF_2 \longrightarrow \infty)_{60} \cong (t\text{-Bu} \longrightarrow \infty)_{60} = \Delta\overline{C}_p \int dT$$

$$= 60 + 9 \times 0.4 = 63.6 \text{ kJ}$$

$$\Delta S^{+}_{700} = -\Delta S^{\ominus}_{300} - \Delta C_p \quad dT/T = 26.5 + 9.2 \times 0.847 = -34.3 \ J \ K^{-1}$$

The assignment of 60 kJ barrier to internal rotation is justified[81] by the tightness of the C-C bond and the mass of fluorine atoms.

(d_3) Cyclic activated complex

$$\Delta H^{\ddagger} = 28.4 + 63.6 = 92 \ kJ.mol^{-1} \ (93 \ kJ \ mol^{-1}) \ [63]$$

$$\Delta S^{\ddagger} = -105.4 - 34.3 - Rln = -157 \ (156.9 \ JK^{-1} \ mol^{-1})$$

5   Octafluorocyclobutane

$$\Delta H^{\ominus}_f = 1528 \ kJ \ mol^{-1} \quad S^{\ominus} = 400 \ JK^{-1} \ mol^{-1} \quad \Delta C_{p_{23}} = 207.4 \ JK^{-1}mol^{-1}$$

6.   Reaction $2CF_2 = CF_2 \longrightarrow c\text{-}C_4F_8$

$$\Delta H^{\ominus}_R = 210.9 \ kJ. \quad , \quad \Delta S^{\ominus}_R = -200 JK^{-1}, \quad \Delta Cp = 15.8 \ JK^{-1}$$

7   Reaction $c\text{-}C_4F_8 \longrightarrow (c\text{-}C_4F_8)^{\ddagger}$

$$\Delta H^{\ddagger}_R = 92 + 210.9 = 302.9 \ kJ.mol^{-1} \ (303.8 \ kJ \ mol^{-1})$$

$$\Delta S^{\ddagger}_R = -157 + 200 = 43 \ J.K^{-1} \ mol^{-1} \ (44.3 \ JK^{-1} \ mol^{-1})$$

Agreement between the calculated and the experimental values[63] is good. Nevertheless, thermochemical calculations for fluorinated compounds lack the precision that is common in hydrocarbons, mainly due to rarity of relevent data. Although cycloaddition reactions of fluorinated alkenes dominate the work of Bartlett[8] and his team, kinetic measurements have rarely been made. Atkinson and co-workers[2-4,63,91] have supplied reliable kinetic data for a number of compounds and this work aims to extend the range of observations and to include new reactions and compounds.

1.5.   Object of the present work.

The main aim of the present work was to obtain kinetic

parameters and thermochemical quantities for the thermal cyclo-

dimerization of chlorotrifluoroethene, hexafluoropropene and the

intermolecular cyclic product of the two compounds.

The literature survey has shown that the general mechanism

of fluoroolefin cycloaddition has not been unambiguously settled

and details still remain to be elucidated. It was expected that

this work would provide information concerning the reactivity of

the compounds under investigation and that the geometry of the

products would provide indications about the probable mechanism

of the reaction.

Chapter 2

EXPERIMENTAL

Introduction

The purpose and aim of the experimental work was to investigate the dimerization of chlorotrifluoroethene and perfluoropropene and the inter-combination of the two compounds, and to determine the activation energies and pre-exponential factors for these reactions. To achieve this aim, a vacuum system and an analytical system were needed. Throughout the work it was planned to use gas chromatography as a means of extending measurements to conditions in which it would otherwise be impossible to make accurate measurements.

The vacuum system was designed so that starting materials and products could be handled and stored free from atmospheric contamination. Several storage globes and traps were incorporated into the system. Facilities were provided for vapour pressure and molecular weight determination, and for taking samples for examination of infra-red, nuclear magnetic resonance and mass spectra. For preparative work, a gas chromatograph was linked to the system.

Samples for analysis were drawn from the middle of a specially designed reaction vessel. Analyses were carried out in a second gas chromatograph equipped with a flame ionization detector.

2.1. APPARATUS

2.1.1. The Vacuum System

A vacuum system of conventional design (Fig. 2.1), constructed of Pyrex glass, consisted of a preparation and sampling section, gas storage section, and gas mixing and reaction section. The system was pumped out by an Edwards "Speedivac" rotary oil pump, backed by a two stage mercury diffusion pump. A trap between the vacuum line and the pumps was kept cooled in liquid nitrogen to improve the vacuum and to prevent contamination of the system. A side arm of the vacuum line pumped out by a second mercury diffusion pump was used exclusively to evacuate quickly and efficiently a gas sampling valve.

The system was normally maintained at a vacuum better than 0.01 Pa. The degree of vacuum was measured on two Edwards Pirani gauges, model G5C-2. Incorporated into the system were a number of manometer tubes which indicated roughly the vacuum at any part of the system.

2.1.1.a Preparation and Sampling Section

The Preparation and Sampling Section consisted of three traps (shown A in Fig. 2.1.) each of which had a volume of about 50 cm^3. At the end of the section there were two standard joints B 10/19. Ordinary glass taps greased with Apiezon L were used in this section.

Gases were admitted into the system and samples were taken out of it through the standard joints. The traps were used for trap to trap distillation, as well as for the collection of fractions of gases puri-fied by gas chromatography. For this purpose a Pye 'Panchromatograph' was employed and it was easily connected to the system by the B 10/19 joints.
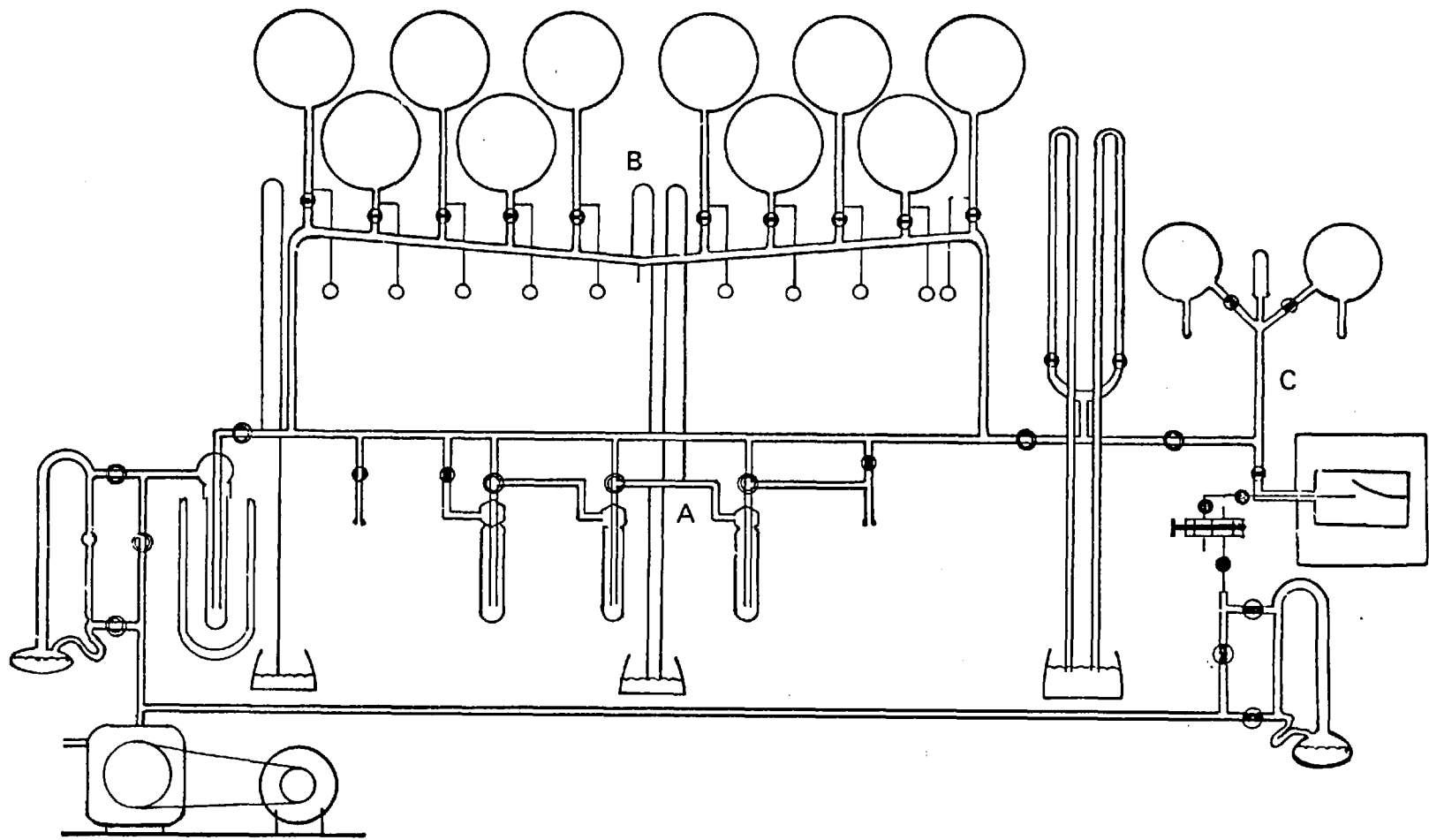
Figure 2.1   The Vacuum System

Samples were injected directly from the vacuum system into the columns, using a modification of the sampling device[92] (Fig. 2.2) described by McKeagan[5]. The sample loop was about 50 cm^3 total volume. The 3mm o.d. copper tubing supplying the carrier gas was connected to 6mm glass tubing of the sampling device and to the packed glass column by means of Cajon Ultra Torr reducing unions. The connections were made leak proof using Viton A washers.

In the usual operation of the Panchromatograph carrier gas would flow from the 3mm o.d. copper pipe _via_ the Cajon brass connector directly into the packed glass column in the chromatograph. The sampling arrangement allows a quantity of gases to be taken (A and B of Figure 2.2) from the vacuum system and then injected into the chromatographic column (C of Figure 2.2). As the column inlet pressure was about 200 kPa, spring loaded stopcocks were used; rather frequent regreasing was required in order to avoid leaks.

A thermal conductivity detector was connected to the outlet of the chromatographic column. The detector was a Gow-Mac hot wire device Type 9285-D with a four filament bridge, each arm being a code W2 tungsten filament. This was used in conjunction with a Gow-Mac regulated D.C. power supply, Model 9999-CS. A Honeywell Electronik 194 recorder was used to measure detector output.

The Panchromatograph is provided with a thermostated oven with place for two columns. Each column is surrounded by an aluminium cylinder. A length of metal tubing wound spirally around both aluminium cylinders allows cooling water or other fluid to be circulated for cooling the columns to below ambient temperature. A separate oven holds the thermal conductivity detector, and can be thermostated at a different temperature. The operating range in both ovens, when heated, is 325-525 K.

To
Handling Section

N_2 →

A

To
Gas Chromatograph

B

C
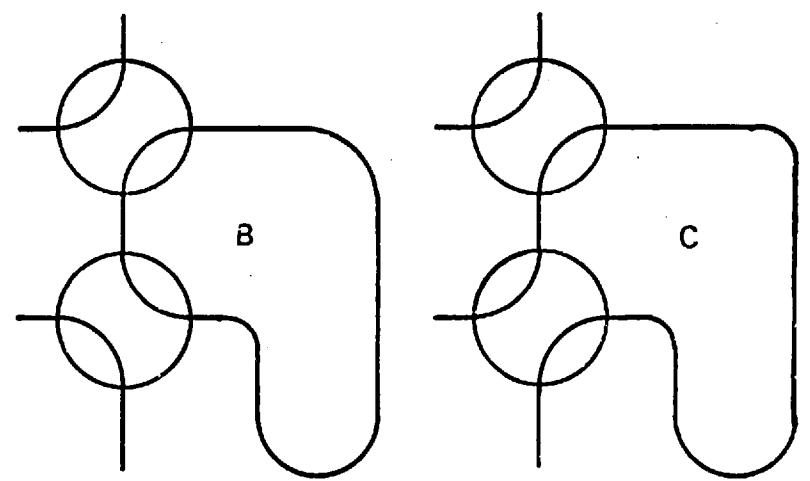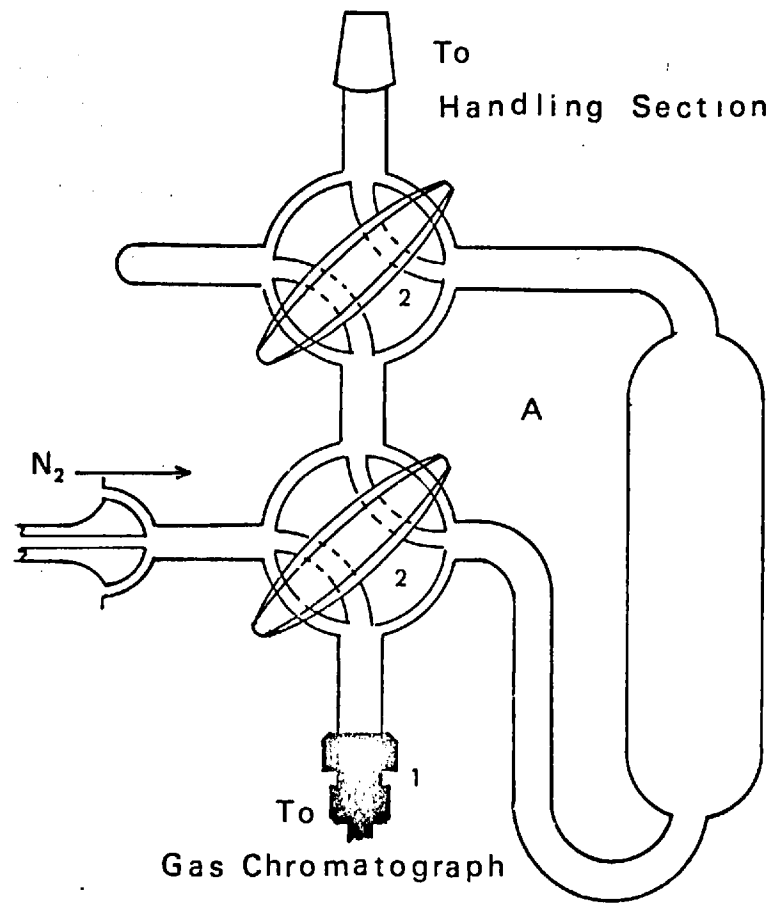
1 Cajon Ultra Torr Reducing Union

2 Spring Loaded Stopcocks

A Sampling Position

B Sample Ready Position

C Sample Injection Position

Figure   2.2   Sampling   Device

Nitrogen was used exclusively as the carrier gas. The flow to the columns and to the column simulator used in conjuction with the thermal conductivity detector was controlled with Edwards vacuum needle valves. Four rotameters in the chromatograph monitored inlet flow ; bubble flow meters were used to measure the flow directly and to calibrate the rotameters. The outlet of the thermal conductivity detector was connected via 3mm o.d. metal piping, a brass reducing union and a B 10/19 standard joint to the vacuum system (A in Fig. 2.1). The stream of gases emerging from the detector was diverted into the traps which were kept in liquid nitrogen. A single fraction could be separated and collected using the three way stopcocks of this section.

2.1.1.b Storage and Handling Section

Ten globes of about two litres total capacity each (shown B in Fig. 2.1) provided space for storing the gases. Each storage globe was attached to a bulb in which the gases could be condensed by using liquid nitrogen, thereby permitting complete transfer of the gas to be stored to the storage globe. Each globe could be sealed off by a 'Rotaflo' TF6/13 tap.

2.1.1.c Mixing and Reaction Section

The principal parts of this section (C in Fig. 2.1)were two globes of about 560 cm^3 each, two wide bore mercury manometers, a reaction vessel and two pressure transducers.

Each globe had a condensing nipple 10mm o.d., 70mm long, and contained a small magnet sealed in glass, to facilitate thorough mixing of the gases. Sovirel 'Torion' valves were used extensively in this part of the system. The pressure measurements were effected by means of a pressure
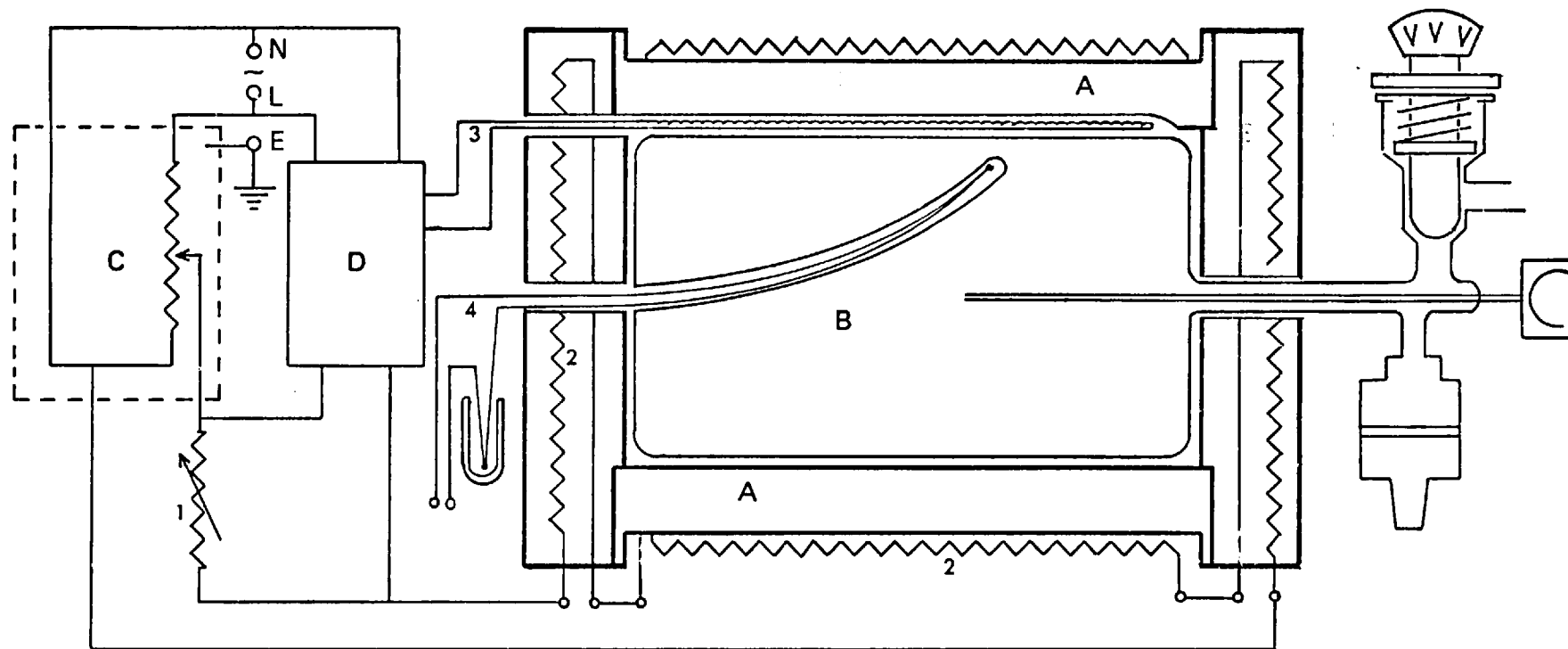
A	Aluminiun Furnace	1	Rheostat
B	Reaction Vessel	2	Heater Coils
C	Variable Transformer	3	Pt Resistance Thermometer
D	RT3 Controller	4	Thermocouple

Figure   2.3   Reaction Vessel, Furnace and Heating Circuit

transducer (Bell and Howell, type No. 4-366, range 0-100 k Pa) attached

to the tubing connecting the two globes.

The main limbs of the manometers were of 14mm i.d. tube, 100 cm long [93].

The mercury reservoir was common. The difference in levels was measured

by a cathetometer.

The reaction vessel was cylindrically shaped and had a thermocouple

well in the centre. The reactor's external dimensions were length

11.9 cm and diameter 7.5 cm. Its capacity was 458.7 cm^3. The length of

the thermocouple well was 70 mm. The reaction vessel was connected to

the vacuum line via a 7 mm o.d., 11 cm long tube. A 'Rotaflo' TF6/13

greaseless valve was used on the reactor inlet.

An extension, consisting of 6 mm i.d. kovar-glass graded seal, was

provided in the connecting tube and a suitable socket was brazed to the

kovar side to accommodate a pressure transducer (Bell and Howell, type

4-326 L101 range 0-70 k Pa).

For experiments in which samples were to be taken by the gas chrom-

atography sample valve, another reaction vessel was introduced (Fig. 2.3).

Its external dimensions were, length 12.2 cm and diameter 7.4 cm. The

4 mm i.d. 7.5 cm long thermocouple well, starting from the centre of the

base of the cylindrical reactor, and having a slight curvature, ended

10 mm from the walls of the reactor[94]. The reaction vessel was connected

to the vacuum line by a 7 mm o.d. 12 cm long tube having a 3 mm o.d.

concentric tube along the axis of the cylinder. The narrow tube was

extended 5 cm inside the reaction vessel. A 'Hone' No. 4310/2 high vacuum

stainless steel valve was attached to the other end of the narrow tubing.

A Sovirel 'Torion' valve was used in the main inlet and a side tube was

provided for the pressure transducer. The total capacity of the reaction

vessel was 474.6 cm^3, and the surface-to-volume ratio was approximately

0.57 cm^{-1}. The volume was measured by filling one of the adjacent calibrated globes with pure nitrogen, at known pressure and temperature. Then the globe was opened to the reaction vessel and the pressure change was measured. The 'dead' volume was estimated to be no more than 4 cm^3, that is approximately 1 per cent of the total volume.

2.1.2. Pressure Transducer Calibration and Measurements

The pressure transducer incorporates a diaphragm which converts fluid pressures to a controlled strain in an excited Wheatstone bridge of strain gauge windings, in which all four arms are active. Pressure variations are indicated by the variation in the resistance of the Wheatstone bridge. The inbalance can be measured by potentiometric methods.

The electrical excitation of the bridge was achieved by means of 10 V D.C. provided by an 'Accuron' X 470 twin power supply unit, taking 240 V A.C. mains supply.

The control circuitry for the transducer is described in Fig.2.4 It has facilities for connection to a potentiometer or recorder, as well as for 'backing off' a portion of the output signal using a constant voltage Mallory cell (1.35 Volt). Thus the full range of the recorder, covering a suitable small fraction of the transducer range, could be used to indicate pressure changes during runs.

The transducers were calibrated using oxygen-free nitrogen. The pressured indicated on the 14 mm i.d. wide bore manometers were read with a cathotometer to 0.03 mm. These figures, corrected to 273.1 K temperature and standard gravity[93] were plotted against the transducer output. The best line for the whole range is given by the equation

$$\text{Pa} = 1498.27 \pm 0.01 \times \text{mV, for transducer A}$$

$$\text{Pa} = 2622.84 \pm 0.03 \times \text{mV, for transducer B}$$
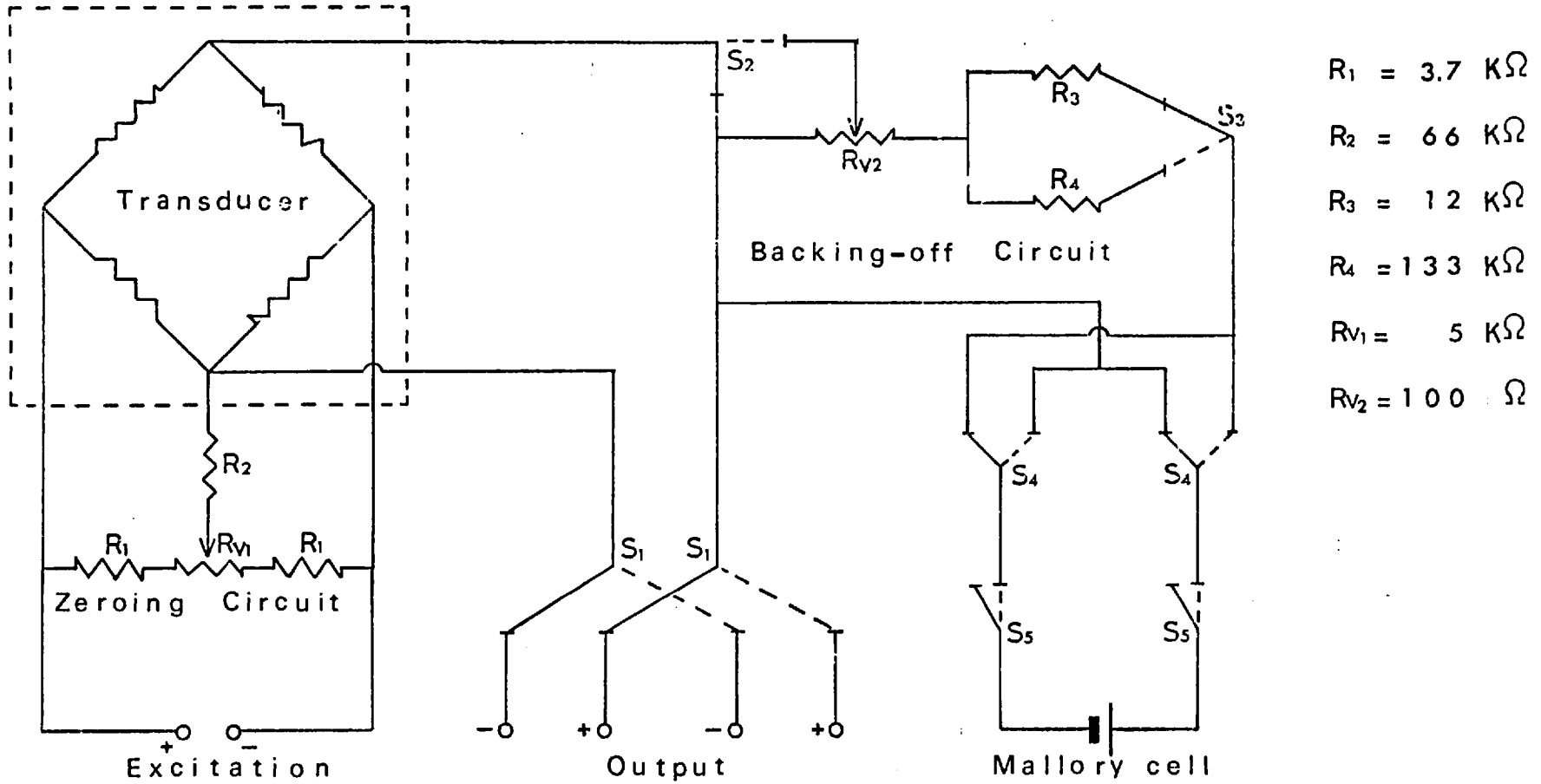
Figure 2.4 Transducer Control Circuit

$R_1 = 3.7$ KΩ

$R_2 = 66$ KΩ

$R_3 = 12$ KΩ

$R_4 = 133$ KΩ

$R_{V_1} = 5$ KΩ

$R_{V_2} = 100$ Ω

which are in excellent agreement with the manufacturers calibration records.

The transducer output was read on a Universal Precision Potentiometer (Pye Cat. No. 7565) combined with a galvanometer modulator (Pye Cat. No. 11353 'S'), amplifier-indicator (Pye Cat. No. 11343 'S') and Standard (Cadmium) Weston cell (H. Tinsley, type 1149).

The 'backing off' output of the Mallory cell was controlled with a 100 ohm helical potentiometer having 10 main divisions, each with 100 sub-divisions. The sensitivity of this arrangement was 1.1 mV per main division and was checked frequently.

The output of the 'Accuron' transformer-rectifier was measured periodically using either a D.C. Microvoltmeter ('Philips' type PM 2435/03) or the Precision Potentiometer and a voltage division arrangement as follows.

Potentiometer

MΩ   kΩ

Accuron
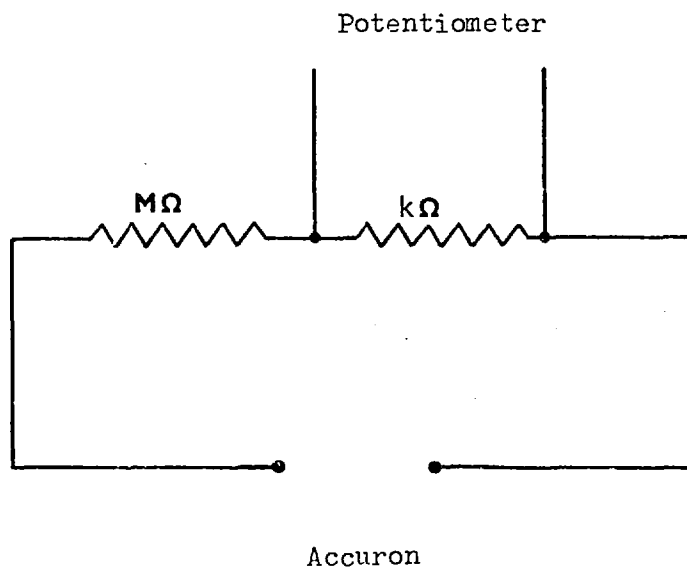
2.1.3. Temperature Measurement and Control.

The furnace (Fig.2.3   ) consisted of a 12.8 cm long aluminium
cylinder having 8.5 cm internal diameter. A groove was cut on the inside
of the cylinder to accommodate a 10 Ω platinum resistance thermometer
for use with the temperature controller. A 4 cm thick aluminium block
formed the front end of the furnace. It was cut in half so that the
reaction vessel could be easily and safely placed. A hole was provided
in the middle for the reactor inlet. The block at the back end had the
same thickness. It had a hole aligned to the groove to pass the Pt
resistance thermometer and another in the centre as a thermocouple inlet.
The three parts were held together by four 27 cm long stainless steel
bolts.

The outside of the main part was covered with asbestos paper and
about 44 ohm of 2.75 ohm per metre nichrome wire was wound on. A thick
layer of alumina cement was applied on top of it. In the end blocks
four horizontal holes were cut and about 20 ohm of heating wire was
placed in each end. The heating wire from each section was connected
to separate terminals on the box containing the furnace. The furnace
was placed in a metal frame in the middle of the furnace box.

The furnace box constructed of sindanyo board was 30.5 cm wide,
30.5 cm high, and 38 cm long. A piece of sindanyo just behind the front
end block of the furnace divided the box into two parts. A block of
'Marinite' 2.5 cm thick was placed in each side of the furnace. Five
blocks were placed behind the back end of the furnace. A hole was
cut in them to pass the thermocouple. The remaining cavities were filled
with mica. In the front end a divided block of Marinite was inserted.
The rest of the space was packed with asbestos wool. These arrangements
gave good insulation.
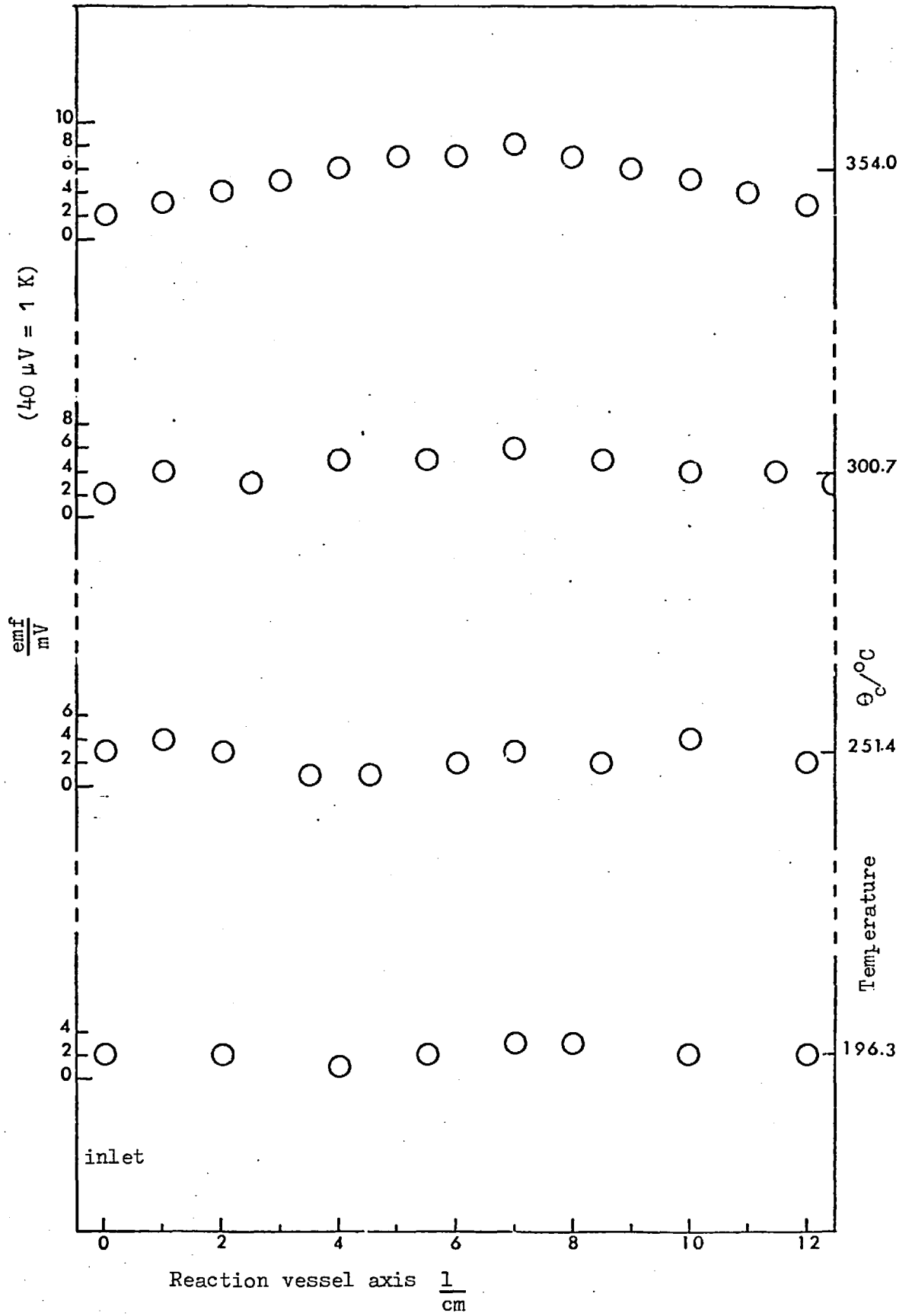
Figure   2.5   Temperature   Profile

The heating current was supplied by means of a Philips type E401/8A variable transformer. The controller was an A.E.I. type RT3 platinum resistance thermometer device. A 40 ohm, 3A rheostat was connected in series (shown 1 in Fig. 2.3).

Control is effected by the RT3 controller periodically bypassing the suitably adjusted rheostat and increasing the load power. The on-off cycle of the controller corresponded to a 7.75:10.00 current variation.

A Chromel-Alumel thermocouple was used to measure the temperature of the reaction vessel. It was calibrated against the melting points of 'Analar' grade tin, lead, and zinc keeping the cold junction in melting ice. The thermal e.m.f. were measured with the precision potentiometer and a calibration graph was drawn. The agreement with the thermal e.m.f. given in the literature[95] was excellent.

The control arrangement was found to give good temperature stability even over the longest experiments (72 hours). The combined uncertainty from the calibrations of the thermocouple and the measurement of the temperature should not be greater than 0.15 K and there were no thermal gradients present in the reaction vessel to this accuracy.

The temperature profile (Fig. 2.5) was obtained using a thermo-couple that could easily probe the interior of the reaction vessel. An asbestos wool plug filling the empty space between the inlet and the thermocouple prevented heat losses due to free air circulation.

A 'KENT' Mark 3 recorder was used during kinetic experiments for continuous recording of the temperature. The input range of this instru-ment is 10 mV and it was necessary to 'back off' a portion of the thermocouple output. The circuitry of the 'backing off' device is shown
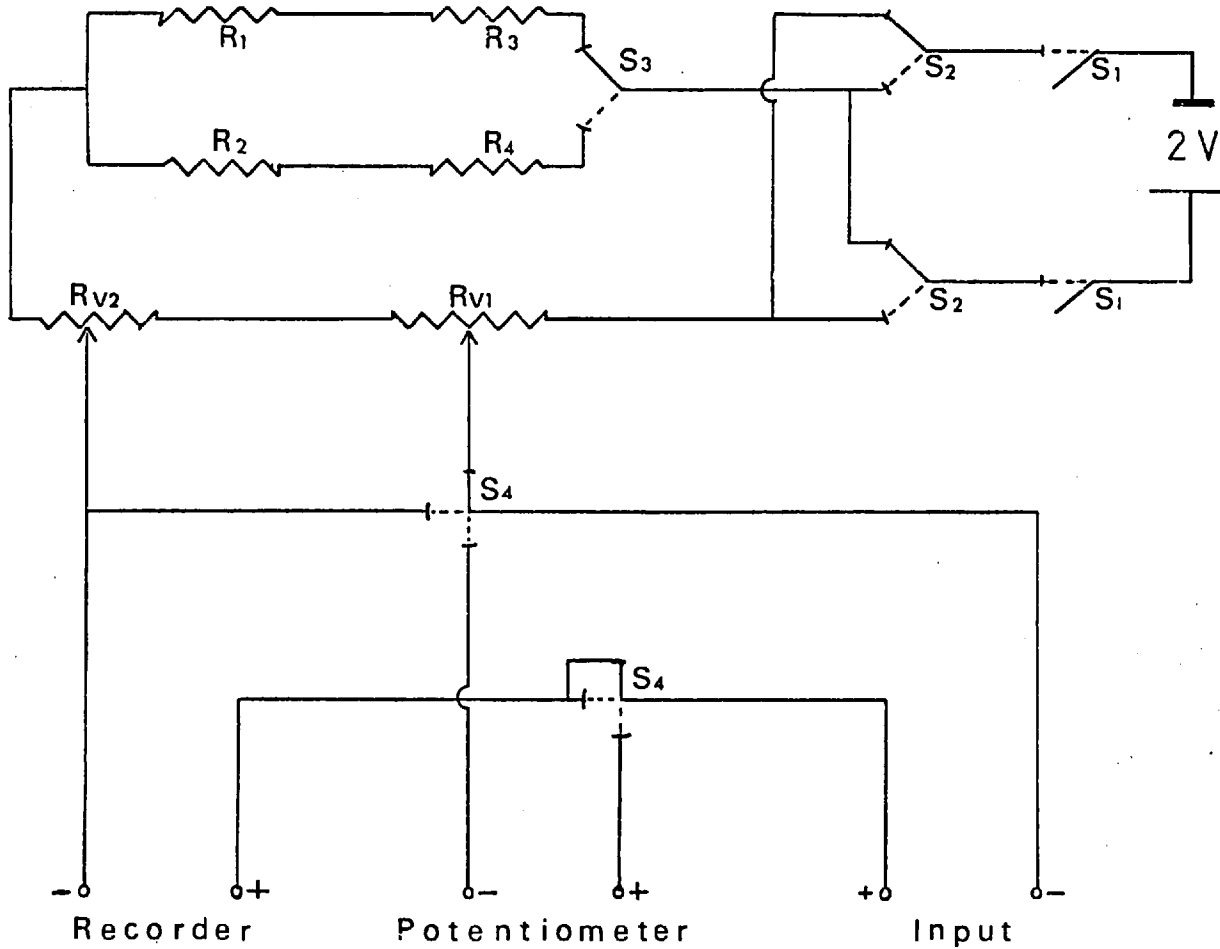
Figure 2.6   Thermocouple   Backing-off Circuit

R_1 = 4.7 KΩ

R_2 = 1.5 KΩ

R_3 = 15 KΩ

R_4 = 8.2 KΩ

R_{V1} = 100 Ω

R_{V2} = 10 Ω

in Figure 2.6

The sensitivity of the recorder is 0.1 mV or 2.5 K per division for the Chromel-Alumel thermocouple, therefore a high impedance thermocouple amplifier was used to increase the sensitivity to 0.1 K per division. The amplifier circuit is shown in Figure 2.7.

A cause of uncertainty in the measured initial temperature of reaction was cooling by gases entering the reaction vessel. McKegan[5] using the same furnace observed a drop of 0.3 K at 587.1 K and indicated that the extent of the temperature variation depends both on the pressure of the reactants and on their temperature and that of the reaction vessel. The temperature being observed is actually that of the thermocouple within its well. Because of the poor conduction through the glass the indicated temperature undoubtedly lags behind the gas phase temperature. In this work, a temperature change of 4.5 K was observed at 633 K, 12 seconds after the moment of admission of the reactant (24,754 Pa). It was found that the time taken for the admission of the reactant (from 1 to 10 seconds) affected the size of the temperature change and the time at which its lowest point was reached. Also the position of the thermocouple well had a critical effect. In the first reactor, the well was close to and in line with the inlet. In the modified reaction vessel with the well off axis the transient temperature drop was significant (0.5 K) only at temperatures higher than 675 K.

In a detailed study of temperature changes at the time of admission of gases into a reaction vessel, using built-in silica coated thermocouples, Fine et al[96] found that the duration of the cooling period was no more than 5 seconds.
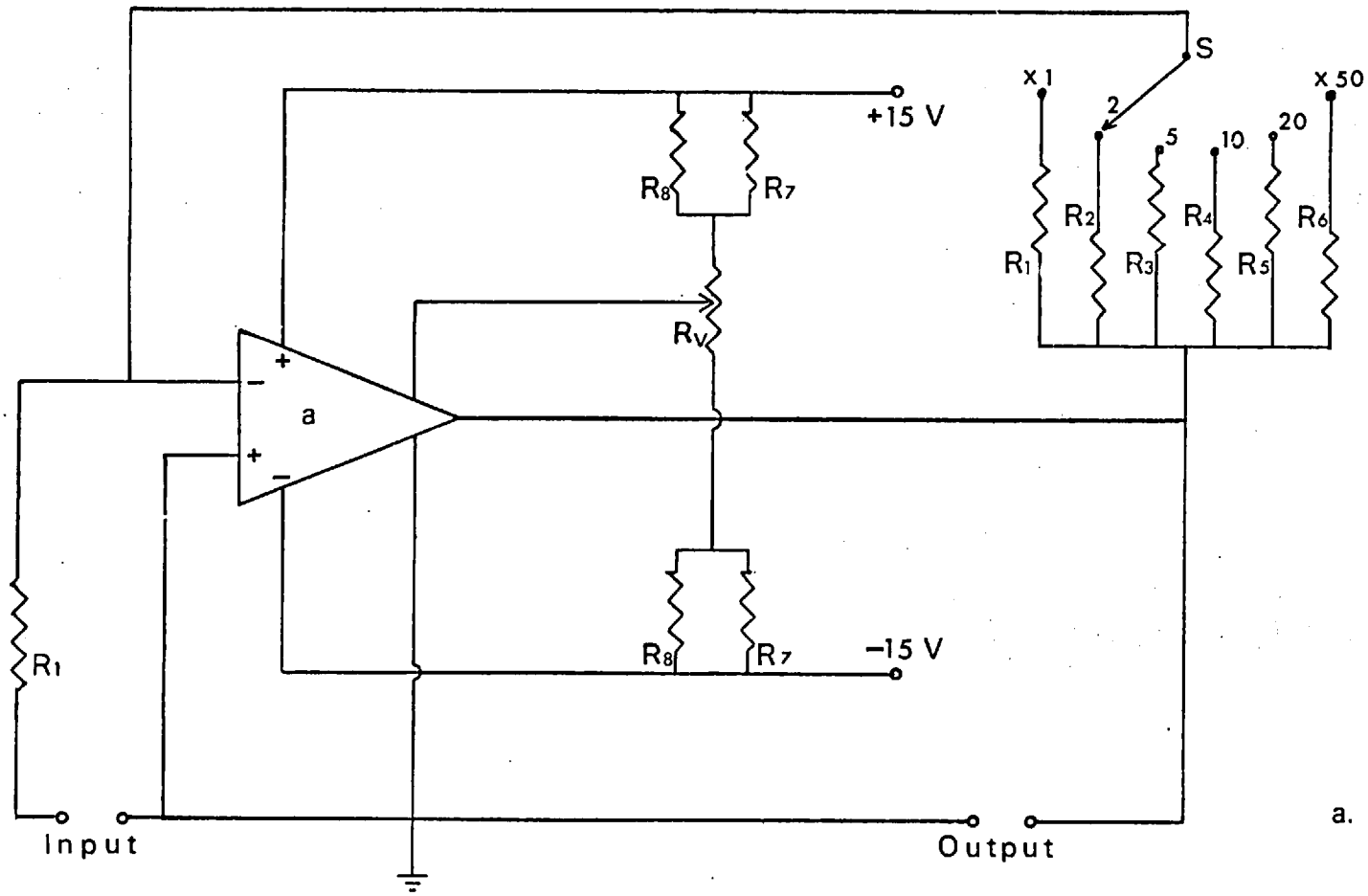
$R_1 =$	470	Ω
$R_2 =$	940	Ω
$R_3 =$	2.35	$K\Omega$
$R_4 =$	4.70	$K\Omega$
$R_5 =$	9.40	$K\Omega$
$R_6 =$	23.5	$K\Omega$
$R_7 =$	75.0	$K\Omega$
$R_8 =$	27.0	$K\Omega$
$R_V =$	10.0	$K\Omega$

a.   Philbrick   Nexus
1701

Figure   2.7   Thermocouple   Amplifier

2.2. ANALYTICAL METHODS

2.2.1. Gas Chromatography

The gas chromatography equipment served two main functions; as a mode for purifying materials and as an analytical tool. A Pye 'Panchromatograph', having a Gow-Mac katharometer as a detector, was used for preparative work. The purity of the compounds as well as the composition of mixtures of gases were determined using a Pye series 104 chromatograph equipped with a dual flame ionisation detector (F.I.D.).

Analysis by gas chromatography was the only source of kinetic observations whenever the product yield was as low as 0.1 to 0.01 per cent of the reaction mixture. This method also extended the range of kinetic measurements to fairly low percentage yields at low initial pressures, another circumstance that was beyond the limit of resolution of the pressure transducer. The method also allowed individual observations on concurrent reactions.

The response of the flame ionisation detector to compounds such as perfluoropropane and chlorotrifluoroethene and even some of their dichloro-derivatives are 10 to 10^3 times greater than their electron capture responses[97]. Since sensitivity was the major consideration the greater response of the flame ionisation detector and its extremely wide linear dynamic range over which major components of a mixture could be analysed at the same time as minor, or trace, components favoured its selection as the detection system.

To achieve a satisfactory performance from the F.I.D. it was important to ensure that air and hydrogen supplies were free from dust, moisture, and organic impurities. For this purpose Pye gas purifying bottles containing molecular sieve 13X were placed in all gas lines to the equipment. The packing was re-activated every six months. The gas supplies

were taken from cylinders fitted with dual gauge head regulators. Adjustable flow indicators mounted on the analyser unit controlled the flow rate of the gases.

The effects of increased standing current in a detector with increased temperature are largely overcome by the use of two similar column/detector systems. The currents from the two flame ionisation detectors are summed and the summation current (10^{-14} A to 2×10^{-7} A) is applied to the input of the Ionization Amplifier (Pye cat No. 12304). Appropriate adjustment could be made to the amplifier attenuation by an 18 steps switch, thus allowing a suitable on-scale deflection in the recorder for each component in a mixture. The recorder used was an eight chart speed 1 mv Honeywell Electronic.

2.2.1.a Selection of Chromatography Columns

The extreme sensitivity required in this work imposes stringent limitations on the choice of liquid phase and the temperature at which it can be used. For temperature control, the columns were housed in a high performance forced air circulation temperature programmed oven. The high sensitivity allows very small $(\frac{\sim 1 \mathrm{pg}}{\mathrm{cm}^3})$ samples to be separated and so the column can be prepared with a low amount of liquid phase on the support ($\sim 4\%$). This allows comparatively low temperatures to be used which reduces the amount of stationary phase bleed considerably. The column requirements can be easily met by using solid adsorbents as stationary phase.

A very wide range of liquid phases has been suggested for the analysis of highly fluorinated compounds. The compounds suggested include chloro-fluoro-compounds, esters of phthalic acid, fluoro-compounds, polymers, silicones, and thiourea. It has been found[98] that hydrocarbons such

as squalane and hexadecane give excellent separations, provided that the loading of the column is kept low. Exceptionally good separations of low molecular weight fluorocarbons were achieved[99] using Poropak, a porous hydrocarbon polymer, as stationary phase. Poropak Q was used[100] successfully to separate mixtures of C_1 and C_2 halocarbons.

Several stationary phases were tested, packed in stainless steel, glass, copper and nylon columns. The air flow rate was 8 cm^3/s and that of hydrogen and nitrogen 3.5 cm^3/s, unless otherwise stated. The oven of the chromatograph was held at room temperature (298-302 K). A gas mixture consisting of hexafluoropropene, its cyclic dimer, and chlorotrifluoroethylene was injected. The following columns did not achieve significant separation or any separation at all.

Column: 3 m 6 mm o.d. stainless steel

Packing: 5% w/w Carbowax 20 M on Chromosorb P

Flow-rate: 0.3 cm^3/s

Separation: Rather poor

Column: 3 m 6 mm o.d. stainless steel

Packing: 15% w/w Fluorosilicone oil D.E. 30% on Siliconised Diatomite C

Flow-rate: 0.2 cm^3/s N_2

Separation: Very poor

Column: 8 m 3 mm o.d. nylon

Packing: 20% w/w Di-butyl-tetrachlorophthalate on Chromosorb W

Flow-rate: 0.5 cm^3/s N_2

Separation: None

Column: 4 m 3 mm o.d. nylon

Packing: 20% Bis-methoxy-ethyl-adipate on Chromosorb P

Flow-rate: 0.5 cm^3/s N_2

Separation: Poor

Column: 1.5 m 6 mm o.d. glass

Packing: 10% methyl silicone gum E-30 on Siliconised Diatomite C

Flow-rate: 0.5 cm^3/s N_2

Separation: Unsatisfactory

Column: 3 m 6 mm o.d. stainless steel

Packing: 10% w/w Fluorolube oil No 3 on Celite

Flow-rate: 0.5 cm^3/s N_2

Separation: Rather poor

Satisfactory separation of chlorotrifluoroethene from its cyclic dimer was achieved (Fig. 3.3) using a column having squalane as stationary liquid. The supporting material was Chromosorb W.

Column: 8 m long, 3 mm o.d. nylon[101]

Packing: 20% w/w squalane on 60-80 mesh Chromosorb W

Packing density: 0.75 g/m

Flow-rates: 0.14 cm^3/s nitrogen, 0.33 cm^3/s hydrogen, 8 cm^3/s air

Retention times: C_2F_3Cl 228 s , $c-C_4F_6Cl_2$ 1764 s
                                 3.8 min   29.4 min

Column efficiency: C_2F_3Cl ~ 2200, $c-C_4F_6Cl_2$ ~ 500

H.E.T.P.: C_2F_3Cl 0.4cm , $c-C_4C_6Cl_2$ 1.6cm

Resolution: 12

(This column will be referred to as column A).

Solid adsorbents as stationary phase gave still better results. Trials using a 1.10 m long, 6 mm o.d. glass column packed with Poropak R at various temperatures indicated complete separation, though the retention times were too long (4 hours for the dimer) and some tailing was present. The operation at elevated temperatures (150-180 K) and higher carrier gas flow rates (1 cm^3/s) shortened the retention time for the dimer but was

unsuitable for the monomer.

It was estimated that a rather short column 28-40 cm should give good separation. Highly satisfactory performance was achieved with such a column.

Column: 32 cm long, 6 mm o.d. L-shaped glass column

Packing: Poropak Q

Packing density: 5.5 g/m

Flow-rates: 0.35 cm^3/s nitrogen, 0.4 cm^3/s hydrogen, 8 cm^3/s air

Temperature: 357 K

Sample size: 0.01 cm^3

Retention times: C_3F_6 1.75min, $c-C_4F_6(CF_3)_2$ 35 min

Column efficiency: C_3F_6 ~ 133, $c-C_4F_6(CF_3)_2$ ~70

H.E.T.P.: C_3F_6 0.24cm, $c-C_4F_6(CF_3)_2$ 0.46cm

Resolution: 3.65

The size of the sample was critically important. Large sizes, mainly of the cyclic dimers, affected the shape of the peak indicating that the mechanism of the sorption followed the Langmuir isotherm. In all the analytical samples the size was kept well below saturation of the adsorbing surface.

2.2.1.b Sampling

Samples could be injected into the gas chromatograph either using a gas microsyringe or by connecting a gas sampling valve in the carrier gas stream.

A S.G.E. 500 microlitre gas syringe with repeating adaptor was used in conjunction with a sampling tube (Fig. 2.8). The sampling tube was
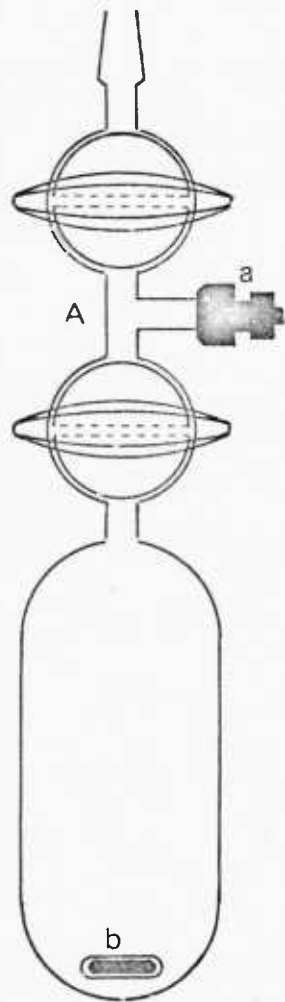
A. Sampling Bottle

a. Ultra Torr Reducing Union

B. Sampling Tube

b. Magnetic Stirrer

c. Graded Seal

d. Septum Holder
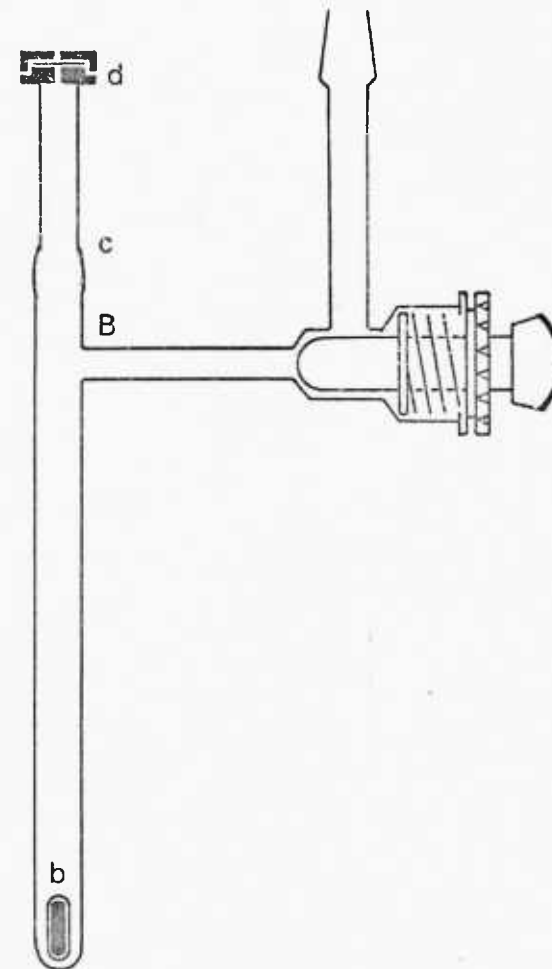
Figure 2.8   Sampling Bottle and Tube

constructed from a 6 mm kovar-glass graded seal. The metal part was fitted with a septum holder and a magnet-in-glass was inserted into the glass tube for mixing purposes. A "Torion" valve forming a side arm of the tube secured the admission and trapping of gases. The sampling tube could be attached to the vacuum system by means of a standard joint at the end of the torion valve.

Gas mixtures were admitted into the gas sampling valve by means of a sampling bottle (Fig. 2.8). Mixtures that had been condensed into the bottle were left to evaporate and were brought to room temperature by immersing the bottle into a water bath. Thorough mixing was ensured using a magnetic stirrer. By opening the bottle tap the gas mixture was allowed to fill the evacuated sample loop of the sample injector.

The sample injector was an eight-part piston valve (Fig. 2.9) supplied by Mechanism Ltd. (Negretti and Zambra). It was found that the Viton A rings were outgassing and spurious peaks appeared at vital places in the chromatograms. To remedy this, the rings were replaced and Nitrile rings outgassed at 355 K for 24 hours under vacuum were fitted.

The sampling valve was connected to the reaction vessel and to the vacuum line by means of two 'Hone' high vacuum miniature valves and a stainless steel flexible tubing. Cajon "Ultra-torr" unions were used for glass-to-metal connections.

Samples were taken after carefully evacuating the sample injector and the connections to the reaction vessel. Then, the injector was cut-off from the vacuum line, the valve in the capillary tube was opened and the reaction mixture was allowed to fill the evacuated sample loop. The sampling sequence was timed, and under very similar conditions various modifications were tried in order to establish the best technique. As

1   Gas   Sampling   Valve

2   Pressure   Transducer

3   Stainless   Steel   Valves

4   Torion   Valve
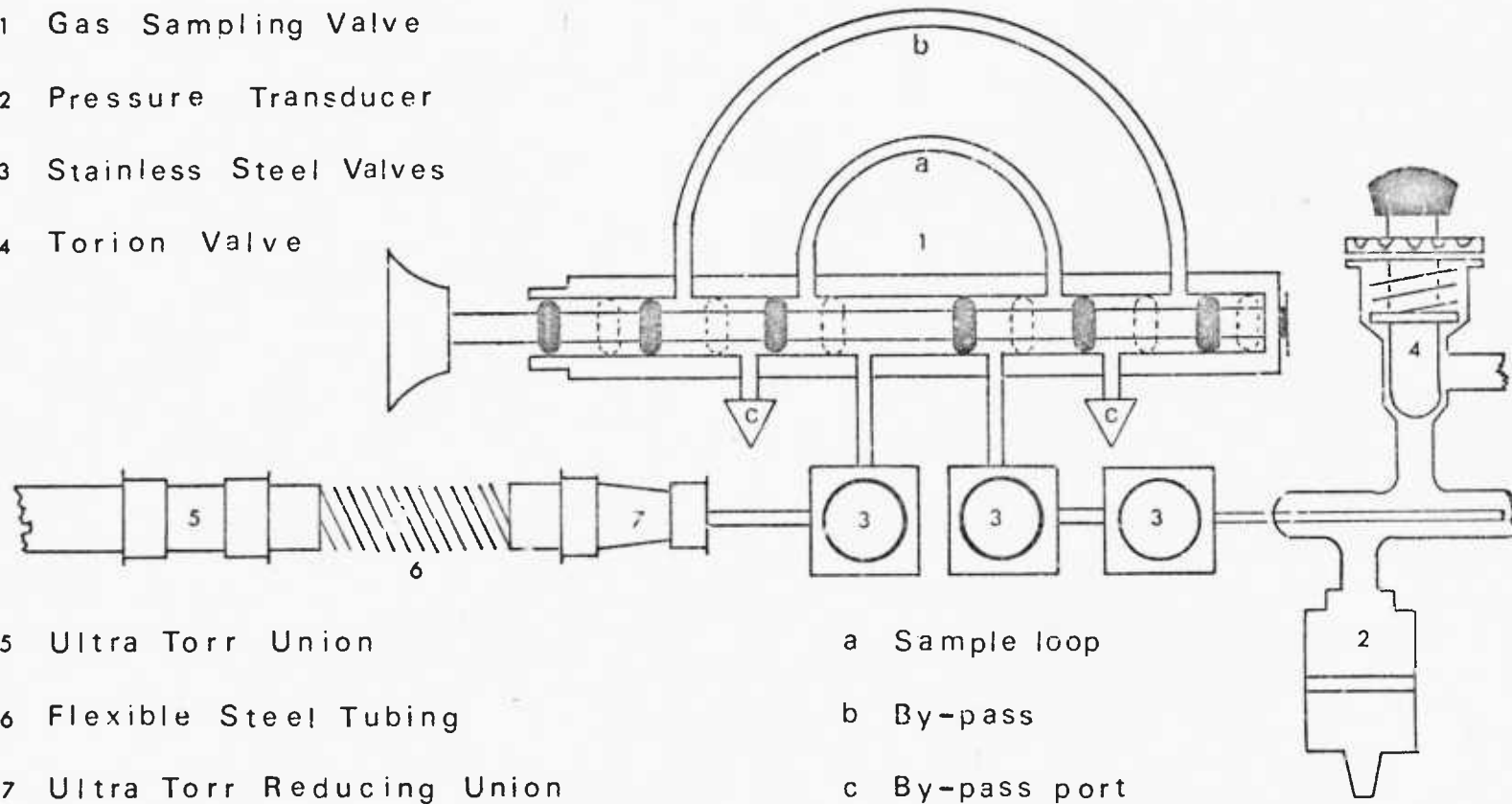
5   Ultra   Torr   Union

6   Flexible   Steel   Tubing

7   Ultra   Torr   Reducing   Union

a   Sample loop

b   By-pass

c   By-pass port

Figure   2.9   Gas   Sampling   Valve   and   Accessories

part of the procedure for flushing the capillary tube the first and second

sample were discarded and a third sample was taken so drawing gases from

the middle of the reaction vessel. The most consistent results were

obtained when the whole operation was completed within 60 to 80 seconds

and the time elapsed between the second and the third sample did not

exceed 40 seconds.

A number of interchangable loops ranging in capacity from 0.03 to

0.25 cm^3 were constructed to provide for suitable sample size.

2.2.1.c   Chromatographic Calibrations

The apparatus was calibrated by injecting into it samples of known

concentrations of pure compounds in prepared mixtures. Calibration

factors were calculated from the respective peak areas and these were

used to calculate the concentrations of these compounds present in the

unknown pyrolysis sample.

The precision of Gas Chromatographic analysis depends on the precision

with which the critical variables (temperature, flow rate) are controlled,

and on the precision of the techniques of sample handling, injection and

the measurement of peaks.

1 Sample preparation

Several test mixtures were prepared, each containing the relevant

pure compounds in concentrations covering the ranges necessary for the

subsequent analysis of the unknown sample.

For this purpose, the precalibrated globes of the mixing section

(Fig. 2.1) and two specially constructed bottles were used. The cap-

acity of the bottles was 57.658 cm^3 and 9.603 cm^3 respectively. Samples

were prepared by measuring the pressure (2.5 - 30 kPa) of each pure

constituent in a calibrated flask, with the pressure transducer.
Occasionally, these readings were checked against the catheto-
meter readings. Then the calibrated globe and bottle were opened
and tne pressures of the constituents were allowed to equilibrate.
The gases were transferred into one flask by condensation. The
mixture was brought to room temperature and homogeneity was en-
sured by magnetic stirring.

2 Injection

The gas sampling valve was used invariably for the injection
of the sample. Samples were admitted to the gas injector _via_
the reaction vessel. There were certain advantages in using the
reaction vessel since the sampling conditions were similar to
those of the actual kinetic experiments. This method required
significant amounts of mixtures to achieve the desired pressure,
and it was not entirely reliable at higher temperatures when the
mixture reacts.

The limitations of this method were largely overcome by
employing the sampling bottle, provided that due care was taken
in transferring the mixture to the sampling bottle. The results
obtained using the sampling bottle were less consistent than
those of the previous method. Nevertheless differences by either
method did not exceed the error ($\pm$ 3%) associated with the use of
this type of injection[102].

To inject the sample the by-pass ports of the gas sampling
valve (c in Fig. 2.9) were connected to the carrier gas stream
at the column entrance. The carrier gas was diverted into the

sample loop for 25 seconds to sweep up the gases.

3. Measurement of Peak areas

The peak area is, over a wide range, directly proportional to the mass of substance chromatographed. In order to establish whether or not a linear relationship existed between the various components of a mixture, calibration mixtures were prepared covering the composition range likely to be encountered in kinetic measurements. Since the accuracy of the calibration depends largely on the accuracy with which the peak area is measured, the following methods were used

a Peak height – times– width at half height (h x w/h)

b Triangulation

c Planimetric

Selection of a particular method for application in kinetic measurements was based on the consistency and accuracy achieved in measuring calibration mixtures. All measurements were duplicated and those using the planimeter were made in triplicate. Measurements for calibration purposes were compared with the results of a second set of measurements made after a week's time and were repeated until concordance was achieved.

4 Calibration factors

The change in the integrated detector signal which is produced for a unit change in concentration of a compound being chromatographed, is known as the response factor. The relative

response factor is defined simply as the ratio of the detector

response factor to any amount of selected standard component.

It is calculated for each component from the peak areas, obtained

on chromatographing the calibration mixtures, and the weights of

components in the mixture. The compound having the highest

concentration in a set of mixtures was taken as the standard.

Relative response factors are calculated from

$$R_f = \frac{A_i \times W_s}{A_s \times W_i}$$

where R_f is the relative response factor, A_s and A_i are the peak

areas of standard and component, and W_s and W_i are their masses

in the calibration mixture. Peak area in the calibration is

expressed as the equivalent value at 10^{-14} A by multiplying the

area by the ratio of the actual current range to 10^{-14}A.

Another expression for the relative response factor R_f is

derived as follows:

Let V_s be the volume of the calibrated flask containing the

standard at pressure P_s, and V_i the volume of the calibrated

bottle containing the component at pressure P_i. At low pressure

(it is assumed that) the gases behave ideally.

Since $W_s = \dfrac{P_s V_s}{RT_s} \times MW_s$

and $W_i = \dfrac{P_i V_i}{R T_i} \times MW_i$

then at $T_s = T_i$, $\dfrac{W_s}{W_i} = \dfrac{P_s V_s}{P_i V_i} \times \dfrac{MW_s}{MW_i}$

so $\qquad R_f \qquad = \qquad \dfrac{A_i}{A_s} \times \dfrac{P_s V_s}{P_i V_i} \times \dfrac{MW_s}{MW_i}$

therefore $\qquad \dfrac{A_i}{A_s} \qquad = \qquad Fc_i \times \dfrac{P_i V_i}{P_s V_s}$.

where $\qquad F_{ci} \qquad = \qquad R_f \times \dfrac{MW_i}{MW_s}$

is the calibration factor and MW_s and MW_i are the molecular weights of standard and component. Calibration factors Fc_i were obtained from the slopes of graphs in which ratios of peak areas $\dfrac{A_i}{A_s}$ were plotted against $P_i V_i / P_s V_s$. These plots were straight lines passing through the origin.

For a given calibration mixture at least three samples of different size were chromatographed. One important fact which was observed for a large number of injections of the same sample at different attenuations was that, within the uncertainty of the calibration figures, the area conversion procedure was found to give consistent results regardless of attenuation.

The concentration of each component is calculated from

$$C_i \qquad = \qquad \dfrac{A_i / R_f(i)}{(A/R_f)} \times 100$$

where C_i is the concentration of any component i and A_i and $R_f(i)$ represent its peak area and relative response factor respectively.

<u>4a</u> The system of chlorotrifluoroethene and its cyclic dimer

The column used for calibration and analysis of this system

was the squalane column (column A) operating under the conditions

given in 2.2.1a. Mixtures containing up to 10% cyclodimer were

prepared and samples were chromatographed as described previously.

The ratio of peak area A_i for the compound to A_s for the standard

was plotted against the ratio of $P_i V_i / P_s V_s$ (Fig. 2.10) giving a

straight line. The response factor of 1,2-dichloro-hexafluoro-

cyclobutane relative to chlorotrifluoroethene was $R_{fi} \simeq 0.775$

and the calibration factor for this system was $Fc_i = 1.55 \pm 0.05$.

<u>4b</u> The system of hexafluoropropene and its cyclic dimer

The Poropak Q column operating at 348K was used for this

system. Since the dimer peak was not totally symmetric   best

results for area measurement were achieved using a planimeter.

There was a comparatively wide scattering of the points corres-

ponding to low cyclodimer concentration arising from the diffi-

culty of preparation and the relatively large errors in preparing

these mixtures. Nevertheless, based on the behaviour of small

samples, it was assumed that the linearity holds for all the

mixtures of low cyclodimer concentration (cyclodimer $<1 \times 10^{-3}$

monomer). The graph of A_i / A_s against $P_i V_i / P_s V_s$ gave a straight

line passing through the origin. The response factor of the

cyclodimer relative to hexafluoropropene was $R_{fi} \simeq 0.996$ and

the calibration factor for this system was $Fc_i = 1.99 \pm 0.06$.

<u>4c</u> The system of hexafluoropropene and 1-chloro-2-trifluoro-
methyl hexafluorocyclobutane

The column calibrated for this system was the Poropak   Q

column (column B) operating at 358K. At this temperature though the relative retention times were long, especially that for the cyclodimer of chlorotrifluoroethene, the separation of the peaks was quite good and the peaks themselves well shaped. No interference from other peaks was observed and the calibration was carried out using purified hexafluopropene and 1-chloro-2-trifluoromethyl hexafluorocyclobutane. Peak areas were calculated by measuring peak heights and the width at half height. The response factor of 1-chloro-2-trifluoromethyl hexafluorocyclobutane R_{fi} = 0.858 relative to hexafluoropropene and the calibration factor Fc_i = 1.33 $\pm$ 0.05 were calculated by plotting peak area ratios A_i/A_s against P_iV_i/P_sV_s . The calibration curve, a straight line, passed through the origin.

4d The system of hexafluoropropene and chlorotrifluoroethene

The same column B (Poropak Q) operating at 358K was used for hexafluoropropene-chlorotrifluoroethene mixtures. Peak areas were calculated by measuring the peak height and the width at half height. There was some overlapping of the peaks and calibration for mixtures containing less than 3% chlorotrifluoroethene was difficult. To offset the effect of peak overlap, the width from the middle of the peak to the undistorted side multiplied by two was taken as the true value. Mixtures containing up to 20% chlorotrifluoroethene were prepared (hexafluoropropene as standard) and the values for the relative response factor and the calibration factor were R_{fi} = 1.07 and Fc_i = 0.83 $\pm$ 0.02 respectively.
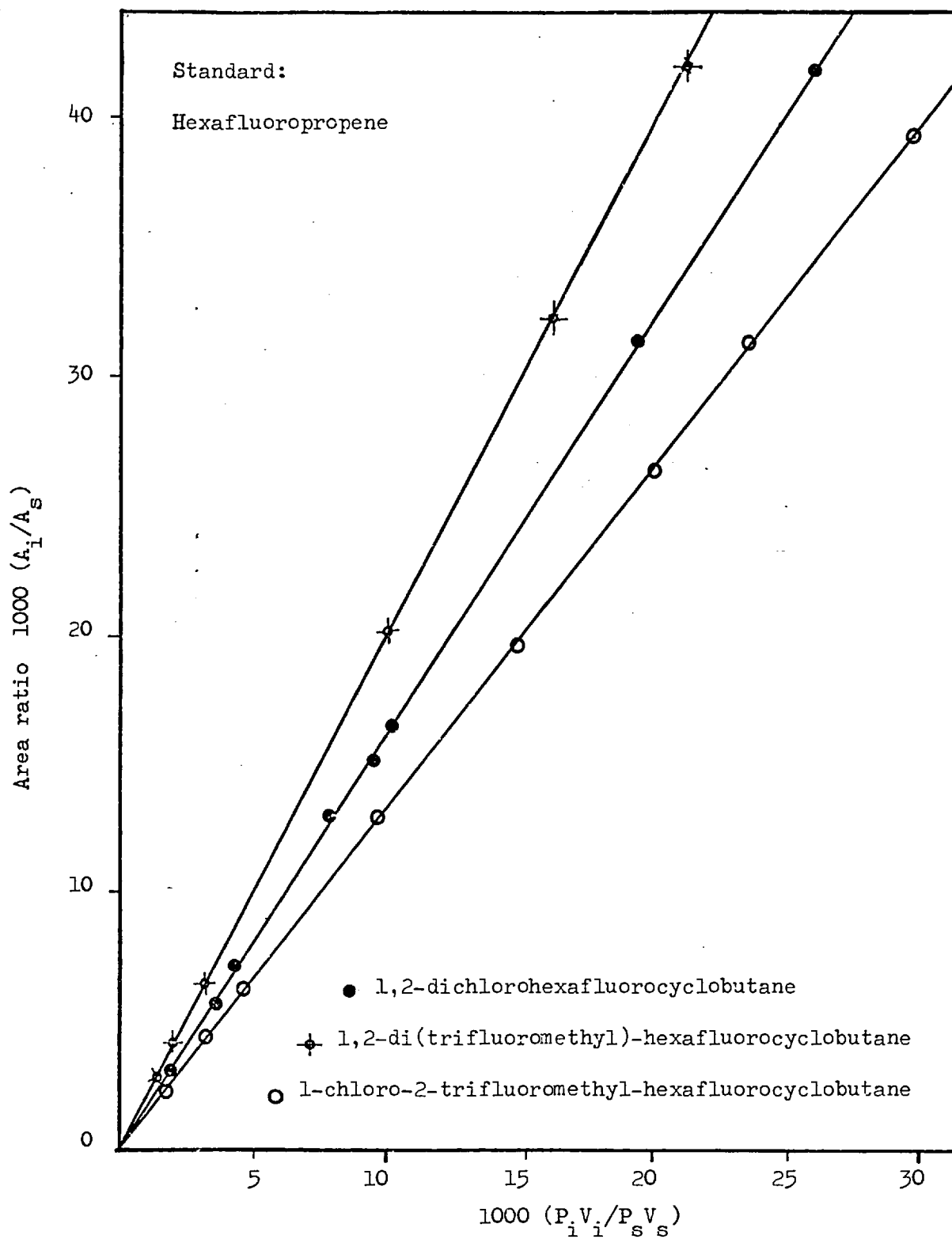
Figure 2.10   Calibration graph for chromatographic analysis

3.2.2. Spectroscopy.

3.2.2a Infrared Spectroscopy

Infrared analysis was used for identification of compounds and to determine if impurities were present when chromatographic analysis was not considered sufficient. For rough work a Perkin-Elmer 457 Infra-red grating spectrophotometer was used, which covered the range 600-3000 cm^{-1}. For greater sensitivity and higher resolution in the range 4000-600 cm^{-1} a Grubb-Parsons spectromaster was used. The scanning speed was set at 1μ per minute. All spectra of the compounds were measured in the gas phase using a gas cell. The path length of the light beam through the cell was 10cm. The gas cell was fitted with a B 10 socket so that it could be attached to the vacuum line. The cell was pumped out and then filled to a known pressure equal or less than 1,333 Pa. Pressures usually had to be in the range of 250 - 650 Pa because absorbancies caused by the C-F vibrations were very large. The measurements obeyed the Beer-Lambert law over the pressure range of samples used.

3.2.2b Mass Spectroscopy

The low resolution mass spectra of the compounds were measured on a modified A.E.I. machine model MS9 with a resolving power of 1000. A Perkin-Elmer 270 instrument was used whenever the combination of gas chromatography and mass spectroscopy was thought to be advantageous.

2.2.c   Nuclear magnetic resonance spectroscopy.

The ^{19}F NMR spectra were recorded on a modified Varian Associates H.A. 100 spectrometer at 94.1 MHz by Mr Stephen Roberts and Dr. Michael Kinns using the continuous wave technique. The temperature of the sample at which measurements were made was 308 K. All samples were diluted by 'Analar' grade (Hopkin and Williams) carbon tetrachloride. The concentration of solute ranged from 15% to 30% $^{V}/v$. The tube (Perkin-Elmer) containing the sample had 5 mm o.d. and was rotated at about 25 revolutions per second. Spectra were internally referenced to hexafluorobenzene and were calibrated in Hz by the usual side-band technique. Chemical shifts δ are given in ppm and a positive value means that resonance occurs at a lower field than the reference. Peak areas were measured using a planimeter.

2.3. CHEMICALS

2.3.1. Hexafluoropropene

The compound was purchased from 'Peninsular Chemical Reagents'. Gas chromatography and the infrared spectrum indicated the presence of impurities such as tetrafluoroethene, perfluorocyclopropane and dimers of hexafluoropropene. Attempts to remove the impurities using a 3 m long 6 mm o.d. copper column packed with 20% squalane on Chromosorb W did not give entirely satisfactory results.

A 2 m long 6 mm o.d. trombone shaped glass column packed with Poropak R produced very pure hexafluoropropene. Samples of approximately 0.25 grams of impure material were trapped into the sample loop (Figure 2.9) and injected into the column. The column as well as the katharometer were maintained at 27°C. Nitrogen at a flow rate of 25 cm^3/min was used as carrier gas.

The infra red spectrum of the purified compound was in excellent agreement with that reported in the literature[103, 104]. Its purity, as determined by gas chromatography, was found to be better than 99.99%.

2.3.2. Chlorotrifluoroethene

The material supplied by The Matheson Co. Inc. was found to contain a limited amount of impurities. These impurities, mainly tetrafluoroethene and hexafluoropropene, were removed by preparative gas chromatography. The column employed was a 3 m long 6 mm o d. trombone shaped copper column having 20% squalane on Chromosorb W as stationary phase and it was held at room temperature ($25-27^{o}$C). The carrier gas flow rate was 0.3 cm^3/s. Trace amounts of impurities that remained in the purified gas were not present if the Poropak R column was used instead of the squalane one.

The infra red spectrum of the purified compound agreed with that reported in the literature. Its purity as determined by gas chromatography was found to be 99.98%.

2.3.3. Di-(trifluoromethyl)-hexafluorocyclobutane

A mixture of isomers of 1,2 Di-(trifluoromethyl)-hexafluorocyclobutane were obtained from the pyrolysis products of hexafluoropropene at temperature of 650 K and pressure about 100 kPa (1 standard atmosphere) for 7-9 hours. The non-condensable gases were removed from the reaction mixture by keeping it cooled in liquid nitrogen and continuous pumping for 10 minutes. The unreacted hexafluoropropene was separated by trap to trap distillation using melting toluene (178.1 K) and collecting it in a trap cooled in liquid nitrogen.

Any remaining impurities were removed by preparative gas chromatography. The flow-rate of the carrier gas was increased to 1 cm^3/s and the Poropak R glass column was held at 350 K. Recycling was found necessary for complete purification. The collected fraction of the second cycle had less than 0.02% total impurities as it was found by analysis by gas chromatography.

A series of N M R spectra taken at a later stage indicated that the cyclic dimer consisted of approximately 48.5% cis isomer and 50.6% trans isomer and ~ 0.9% cis - trans -1,3 isomers

2.3.4. 1,2-Dichloro-hexafluorocyclobutane

The compound was prepared by pyrolysing chlorotrifluoroethene at 625 K and pressure about 100 kPa for two hours. The unreacted chlorotrifluoroethene was separated by trap to trap distillation using a slush bath

consisting of toluene cooled by carbon dioxide (194.6 K) and was recovered in a liquid nitrogen trap. Further purification was achieved by preparative gas chromatography. The column employed was the 6 mm o.d. 3 m long copper column (20% w/w squalane on Chromosorb W) and the flow rate of the carrier gas was 0.35 cm^3/s. Analysis of the collected material by gas chromatography indicated that impurities did not exceed 0.02%.

2.3.5. 1-Chloro-2-trifluoromethyl-hexafluorocyclobutane

The compound was prepared by pyrolysing mixtures consisting of 90% v/v hexafluoropropene and 10% v/v chlorotrifluoroethene at pressures about 100 kPa (1 standard atmosphere) and at temperature 675-700 K for 3-4 hours. The products of the reaction were separated from the reactants by trap to trap distillation using melting toluene (178.1 K). The reactants, which were recycled, were collected in a trap cooled in liquid nitrogen. The cyclic dimer of hexafluoropropene and that of chlorotrifluoroethene as well as other substances were removed by gas chromatography.

At room temperature, the vapour pressure of the cyclic compounds mentioned above is rather low. To increase the amount of the mixture injected, the sampling device (Fig. 2.2) was heated to about 355 K using a hair-dryer. The Poropak R glass column was held at 350 K and the flow rate of the carrier gas was 0.75 cm^3/s.

The efficiency of the column under these conditions had decreased drastically, mainly due to non-instant injection of the sample and to tailing. The collected fraction contained as much as 8% Di-(trifluoromethyl)-cyclobutane. To minimize these shortcomings and still maintain a comparatively rapid process, an L shaped, 25 cm long glass column packed with Poropak Q was connected to the outlet of the sampling device. Although

the central part of the peak was collected, it was found necessary to recycle the purified fraction twice to achieve 99.5% content in Chloro-trifluoromethyl-hexafluorocyclobutane.

2.6   Pyrolysis procedure

A standard procedure had been adopted in performing kinetic experiments. For each selected temperature, although thermal equilibrium was reached within 2-5 hours, the furnace was left undisturbed for 24 hours before commencing experiments. During the experiments the temperature was either recorded continuously or at suitable time intervals. A certain amount of reactants was transferred from the storage globes into the calibrated flask adjacent to the reaction vessel and their pressure was monitored by the pressure transducer. A vacuum below 0.01 Pa was maintained inside the seasoned reactor for at least two hours before admitting the purified material. Gases entered the evacuated reaction vessel by opening the inlet tap (Fig.   2.9) to the calibrated flask for about two seconds. At the end of this period a chronometer was started to time the reaction.

The distribution of gases between the reaction vessel and the calibrated flask was in accordance with the gas laws. The initial pressure of the starting material inside the reaction vessel could be estimated (to a good approximation) from the pressure of the gases in the calibrated flask before the start of the experiment. This speeded up the accurate measurement of the pressure of the reacting material and facilitated the selection of suitable pressures in the calibrated flask to achieve the desirable pressure inside the reactor.

Chapter 3

RESULTS

3.1. THE KINETICS OF THE THERMAL CYCLODIMERIZATION OF CHLOROTRIFLUOROETHENE

The thermal reactions of chlorotrifluoroethene have been investigated at a wide range of conditions. Thus, Harmon[105] performed the pyrolysis under pressure in a steel bomb as did Henne and Ruh [106]. Buxton, Stacey et al [107] investigated the dimerization by flow methods. Flow methods were also used by Miller[108]. These investigators found that at temperatures below 825K the main product is cis, trans 1,2-dichlorohexafluorocyclobutane. Park, Lacher and Holler[109], reported about 50% of each isomer in the product of dimerization at 400K to 500K. Solomon and Dee[110] studying the relative yield of cis and trans isomers at 450K to 600K and pressures from below ambient to 7kPa found that the cycloaddition provides a cis-trans dimer ratio of 56:44.

The kinetics of the cyclodimerization of chlorotrifluoroethene

$$2CF_2=CFCl \underset{k_{-1}}{\overset{k_1}{\rightleftharpoons}} C-C_4F_6Cl_2 \qquad 3.1.1.$$
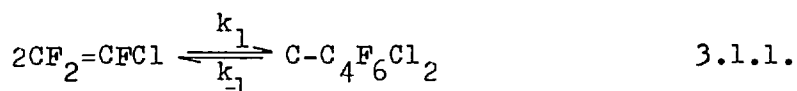
have been studied by Lacher, Tompkin and Park[111], by the static method in a Pyrex vessel. They used pressure changes to follow the reaction at 577 to 782K and at pressures between 13.3kPa and 80.0 kPa. The reaction was found to be homogeneous and second order, and the rate constant was independent of the initial pressure and the extent of the reaction (up to 70 to 80%). The reverse reaction was apparently not detected nor was any cis-trans isomerization reported. The results are summarized in the equations

$$- \frac{1}{2} \frac{d[CF_2=CFCl]}{dt} = k_1 \ [CF_2=CFCl]^2 \qquad\qquad 3.1\text{-}2$$

$$k_1 = 1.765 \times 10^4 \ exp(-110,120 \ /RT) \ m^3 mol^{-1} s^{-1}$$

In a more detailed study of the same reaction, Atkinson and Stedman[3] also investigated the reverse reaction, as well as the cis, trans isomerization of the product. For the cyclic dimerization they covered the same temperature and pressure ranges (570K to 820K,13.5 kPa to 80.0 kPa), also in a static system. Their results are summarized in the equations

$$2M \longrightarrow D \qquad k_1 \qquad\qquad k_1 = 2.14 \times 10^4 \ exp(-111,300/RT) m^3 mol^{-1} s^{-1}$$

$$D \longrightarrow 2M \quad k_{-1} \qquad\qquad k_{-1} = 2.5 \times 10^{15} \ exp(-273,220/RT) \ s^{-1}$$

where k_1 is defined by equation 3.1-2, M (or C_m) and D represent the chlorotrifluoroethene and 1,2-dichlorohexafluorocyclobutane respectively and R is expressed in $J \ K^{-1} \ mol^{-1}$.

The purpose of the work described here was to extend downwards the range of temperature covered in measurements of the cyclo-dimerizations. Initially the reaction was observed by recording pressure changes and by analysis of the mixture at the end of the run. The sampling tube fitted with a serum cap (see 2.2.1b) was connected to the vacuum line and was thoroughly evacuated. At the end of the experiment the reaction vessel was opened and the pressure was allowed to equilibriate between the hot and cold parts of the system including the sample tube. A sample

was then taken into the gas syringe (section 2.2.1b) for injection to the chromatograph.

The obvious disadvantage of this method was inability to follow the reaction by analysing samples at suitable intervals. Furthermore part of the gases entering the sampling tube came from the 'dead space'. The sample was not accurately representative of reaction mixture. These shortcomings prompted the construction of the improved reaction vessel described in 2.1c (Figure 2.3) from which samples could be taken directly to a gas sampling valve (Figure 2.9). All the analytical results presented later (sections 3.1.2, 3.1.4) were obtained by the improved method which is described in section 2.2.1b.

3.1.1. Characterisation of 1,2-dichlorohexafluorocyclobutane.

Quantities of 1,2-dichlorohexafluorocyclobutane were prepared and purified as described in 2.3.4. Samples of the same isomeric composition were used to determine the infrared, NMR and mass spectra.

3.3.1a Infrared spectrum of 1,2-dichlorohexafluorocyclobutane.

The infrared spectra of pure cis and trans isomers have been reported[112,113] as well as that for the isomeric mixture[114]. The spectrum of the mixture served to characterize the compound. The agreement between wavenumber absorption values reported in the literature and the present work was very good. However the spectrum recorded in a Perkin-Elmer model 325 spectrophotometer

was better resolved. Differences between literature values and the present work are given below

| Reference (112) | | Reference(113) | | Reference(114) Raman | Present work |
cis	trans	cis	trans	cis-trans	cis-trans
1246	1245	1239	1236	1243	1243-1238
1188	1188	1183	1181	1190	1185-1180
1122	1122	-	-	1111	1123-1118
893	-	890	-	910	893
-	-	-			886
					875
					870

The relative absorption intensities of the isomers are not given in the literature and determination of the composition from the infra red spectrum alone was not possible.

3.1.1b Mass spectrum of 1,2-dichlorohexafluorocyclobutane

The mass spectrum of 1,2-dichlorohexafluorocyclobutane appearing in Figure 3.1 was recorded as described in section 2.2.2b. The molecular ion (M^+) peak is not observed. The salient feature of the spectrum is the symmetrical rupture of the cyclobutane ring to give chlorotrifluoroethene molecular ions (m/e = 116,118). The peak height ratio m:m+2 is, as expected, 3:1. Fragmentation across the other two opposite carbon-carbon bonds, giving tetra-fluoroethene and 1,2-dichloro-1,2-difluoroethene molecular ions
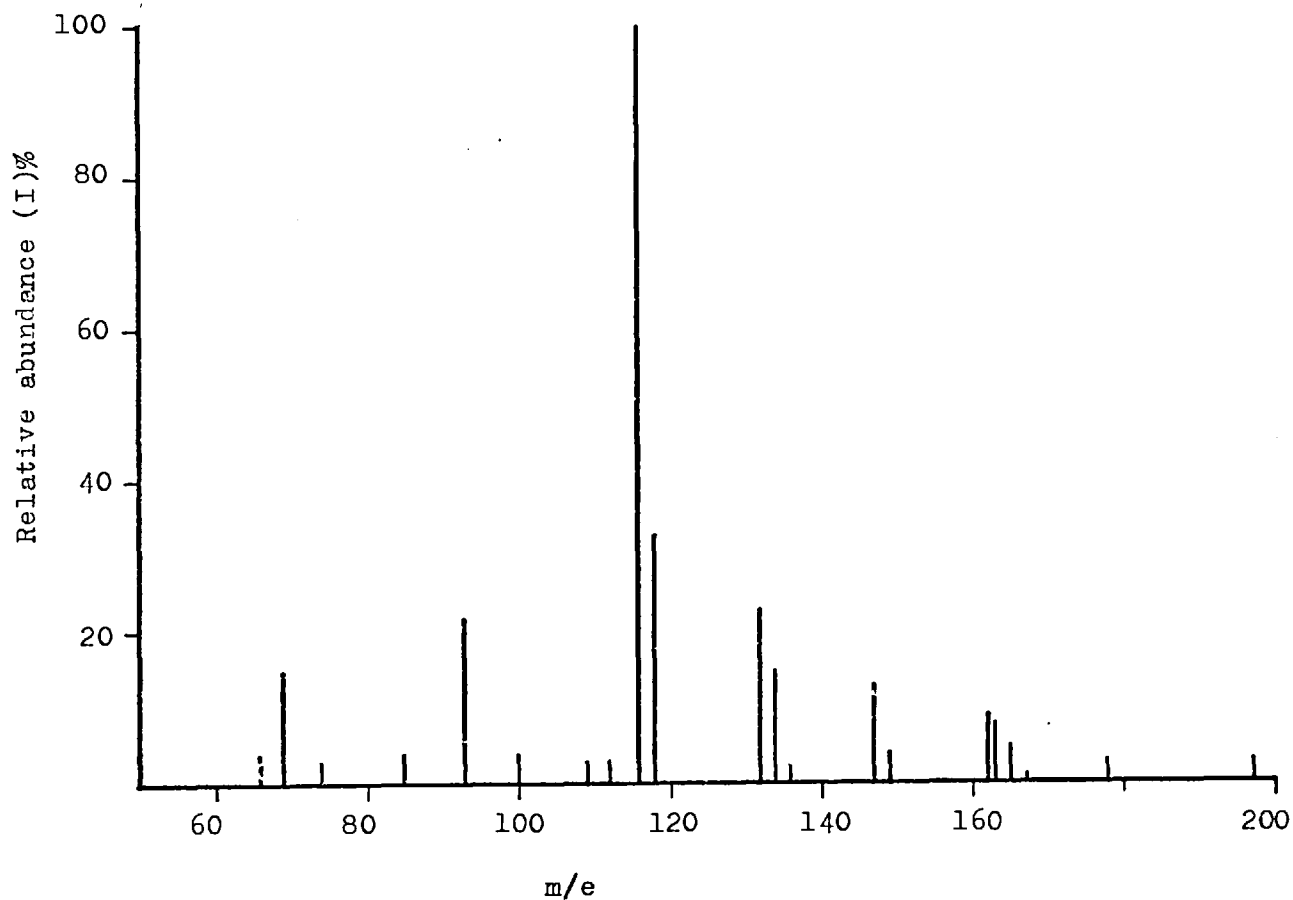
Ion	m/e	I%			Ion	m/e	I%	
$C_4F_6Cl_2$	232,+2,+4	0,	0, 0		C_3F_2Cl	109,+2	3, 1	
C_4F_5Cl	178,+2	3,	1		C_2F_4	100	4	
$C_3F_3Cl_2$	163,+2,+4	8,	5,~1		C_3F_3	93	22	
C_4F_6	162	9			CF_2Cl	85,+2	4, 1	
C_3F_4Cl	147,+2	13,	4		C_3F_2	74	3	
$C_2F_2Cl_2$	132,+2,+4	23,	15, 25		CF_3	69	15	
C_2F_3Cl	116,+2	100,	32		$CFCl$	66,+2	4, 1	
C_3F_4	112	3			CF_2	50	2	

16 eV

Figure 3.1. Mass spectrum of 1,2-dichlorohexafluorocyclobutane

is also significant. Only two groups of three peaks were attributed to segments with two chlorine atoms at m:m+4. In each group the peak height ratios m:m+2:m+4 were as expected for two chlorines[115] 5.6:3.7:0.6. The first of these fragments corresponding to m/e 132,134,136 (CFCl $\overset{+}{\div}$ CFCl) was more abundant than the other group (CF$_2$ = CCl - $\overset{+}{C}$FCl) both in the 70eV ionization potential (I.P.) spectrum and in the 16eV I.P. spectrum. The greater abundance of CFCl $\overset{+}{\div}$ CFCl was associated with the simultaneous formation of a stable double bond in CF$_2$=CF$_2$. The group CF$_3$ although is not present in the molecule gives a relatively intense peak at m/e 69. This peak, common in the spectra of polyfluorocyclobutanes, might be associated with 1 $\longrightarrow$ 3 fluorine atom transfer. A similar explanation applies for the presence of the CF$_2$Cl ion which is as intense as CF$_2$ $\overset{+}{\div}$ CF$_2$. The relative abundancies of the fragments are very close to those reported[124] for the _trans_ isomer. Figure 3.2 depicts diagrammatically the proposed fragmentation mechanism for 1,2-dichlorohexafluorocyclobutane.

3.1.1c The nuclear magnetic resonance spectrum.

The ^{19}F NMR spectra of pure _cis_ and _trans_ isomers of 1,2-dichlorohexafluorocyclobutane have been reported by Atkinson and Stedman[3]. The spectrum of a mixture consisting of approximately equal parts of _cis_ and _trans_ isomers diluted in CFCl$_3$ was reported by Solomon and Dee[110].

The present ^{19}F NMR spectrum of 1,2-dichlorohexafluoro-
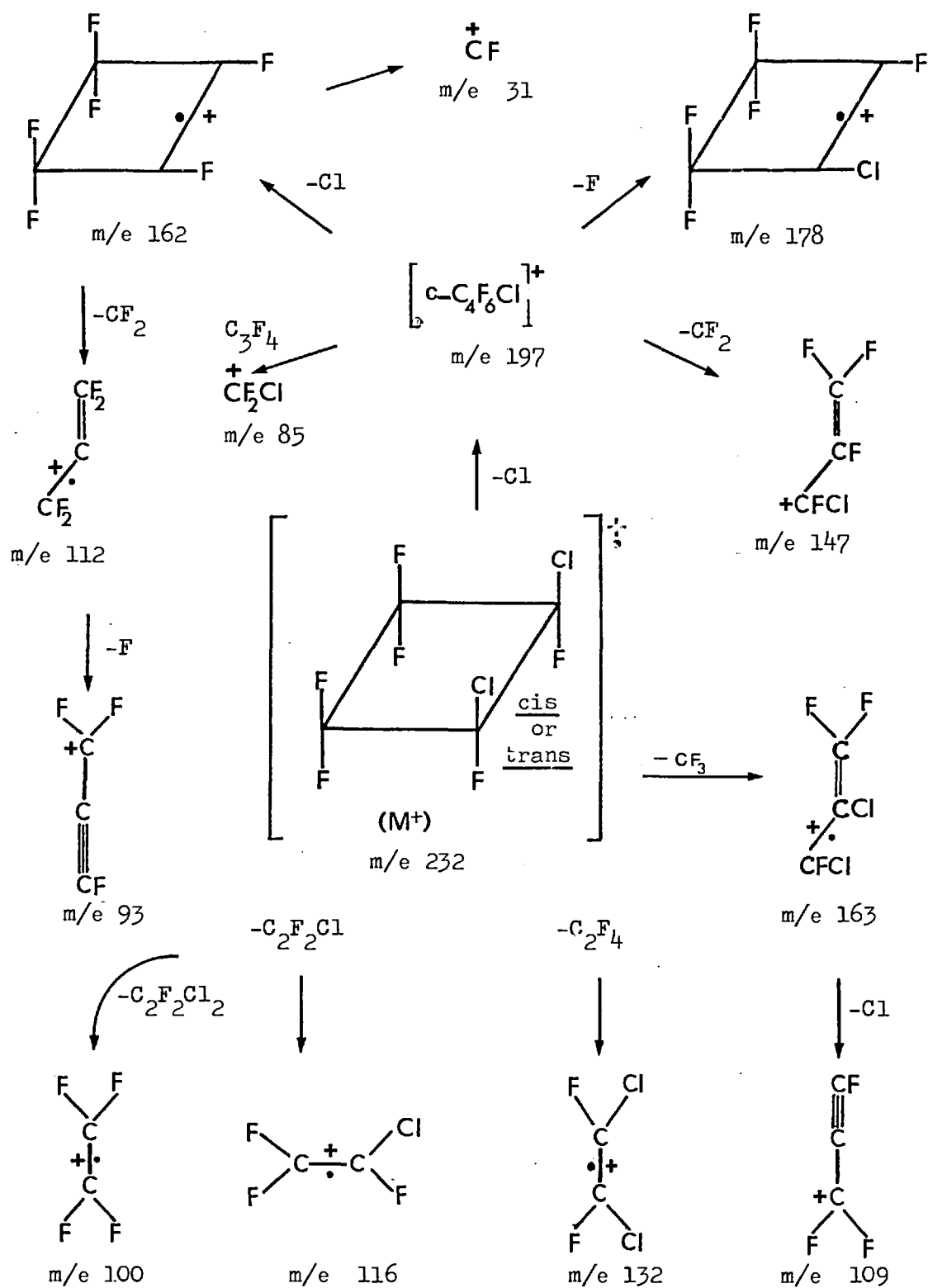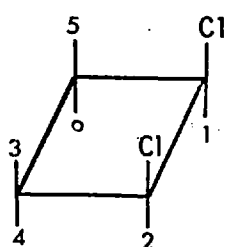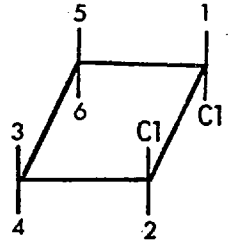
Figure 3.2   Proposed fragmentation mechanism for 1,2-dichloro-

hexafluorocyclobutane

cyclobutane, recorded as described in 2.3.4, comprised nine well

separated peaks at $\underline{a}$ = 4270, b = 4052, c = 3912, d = 3698,

e = 3479, f = 3255, g = 3110, h = 2893, i = 2362 Hz. Peak $\underline{f}$ in

fact is a combination of two separate peaks f_1 = 3255 Hz and

f_2 = 3263 Hz, the main peak f_1 being a triplet (J $\simeq$ 3Hz) with

overlapping bands.

The non planar geometry of the ring in cyclobutane molecule

is well established but vibrations of the ring make the average

structure seen in NMR spectrum planar[116]. Therefore, both

cis and trans 1,2-dichlorohexafluorocyclobutane form an $A_2B_2C_2$

system, the $-CF_2-$ groups forming two AB pairs. Each pair of these

doublets forms a quartet. The peaks were assigned to doublets

employing the characteristic spin-spin coupling constant

(J $\simeq$ 220 Hz) of asymmetric $-CF_2-$ groups in cyclobutanes.

The doublets $\underline{ab}$ and $\underline{gh}$ centred[117] on 3581 Hz were assigned

to the cis quartet by assessing the effect of chlorine substitu-

tion. The usual effect of substituting chlorine into a fluoro-

carbon is for fluorine resonance to be shifted to lower applied

fields. One parameter determining the magnitude of the shift is

the proximity of the resonating nucleus to the substituent and to

the C-Cl bond. Feeney and others[116] have shown that the magni-

tude of the chemical shift of a ^{19}F nucleus in halogenated

cyclobutanes can be calculated from the calculated electric fields

at the fluorine nucleus. Their results indicate that the F_3, F_5

nuclei in the cis isomer, being the most influenced by the

chlorine atoms, would resonate at a lower field, as it has been

found experimentally[3,110]. The chemical shift for the $\underline{a,b}$

Fluorine nucleus		Chemical shifts (δ =0.0 for $CFCl_3$)				$J(-CF_2-)$
		ref. 116	ref. 3	ref. 110	Present	work
	3,5	-119.8	-119.0	-119.1	-118.8	218 Hz
	6,4	-130.2	131.2	-131.1	-130.9	217 Hz
	3,4	10.4	12.2	12.0	12.1	
	1,2		-138.0	-137.6	-137.8	
	3,6	-120.3	-123.0	-123.1	-122.8	214 Hz
	5,4	-129.6	-127.1	-127.2	-126.8	216 Hz
	3,4		4.1	4.1	4.0	
	1,2		-128.4	-128.9	-128.3	

The chemical shift of $CFCl_3$ relative to hexafluorobenzene was taken as δ = 162.9 and relative to C_4F_8 as 135.2 ppm

(F_3,F_5) doublet relative to hexafluorobenzene is 44.10 ppm whilst that for the g,h doublet, associated with the F_4,F_6 nuclei, is only 32.00 ppm. The chemical shift between two fluorine nuclei in the -CF_2- groups is, therefore. 12.1 ppm.

The trans quartet is formed by the remaining doublets c,d δ = 40.13 and ef$_2$ δ = 36.12. In this case the chemical shift between the two fluorine nuclei in the -CF_2- group is only 4.0 ppm.

There is sufficient evidence that the arguments presented previously are valid, Therefore, peak i, δ = 25.10, should be associated with the -CFCl- of the cis isomer. In the trans isomer the -CFCl- fluorine nuclei are nearer to the two chlorine atoms and to the C-Cl bonds than in the case of the cis isomer.

Thus, peak f_1 at $\delta = 34.59$ was assigned to the _trans_ isomer.

This analysis agrees with the results reported in the literature[3,110].

To assess the influence of chlorine atoms on the chemical shift of ^{19}F of the -CF_2- groups δ may be taken as the sum of the chemical shift resulting from the effect of the neighbouring -CFCl- group and the same group two carbon atoms away $\delta = \delta_1 + \delta_2$. The chemical shift amounts to 12.1 ppm for the _cis_ isomer but is restricted to 4.0 ppm for the _trans_ isomer. It might be concluded that for -CF_2- groups adjacent to a single -CFCl-group would have a value 8.05 ppm. When the -CFCl- group is two carbon atoms away from the -CF_2- fluorine atoms the value is only 4.05 ppm. In the case of chloroheptafluorocyclobutane (undiluted) Stedman[112] found $\delta_1 = 7.98$ and $\delta_2 = 3.95$.

The peak areas of the isomers of 1,2-dichlorohexafluorocyclo-butane in the mixture examined were roughly equal.

3.1.2. Preliminary kinetic analysis.

The early experiments were designed to establish the condi-tions for accurate measurements by gas chromatography and to compare and correlate pressure changes with results obtained by chromatographic analysis.

To diminish the possibility of reaction with the walls of the reactor, it was first 'aged' by performing a series of pyrolyses of chlorotrifluoroethene covering a total period of

several days. In fact no evidence of interference by wall reactions was ever obtained.

In the first experiment Al-1 at 586.1K (Table III.1.1) the initial pressure was 5.978 kPa and pressure changes were followed for ten hours when there was 17.5% reaction as indicated by the pressure change. In the next experiment Al-2 (initial pressure 5.723 kPa) pressure measurements were made every 30 minutes for the first six hours. Measurements were continued intermittently for a total of 73 hours and the final pressure change indicated 65% reaction.

In the experiment Al-3 the initial pressure was increased to 8.960 kPa. Since the pressure changes were greater, measure-- ments were made every 10 minutes for the first four hours and every 15 minutes for another two hours. More pressure measurements were made from time to time until the reaction had proceeded for 24 hours.

—In all these experiments the temperature (586.1 K) was recorded continuously.

In experiments at about 500 K it was easier to follow the early stages of the reaction both by pressure changes and chroma- tographic analysis. Rapid changes in composition did not occur and this minimized the error in defining the reaction time at which samples were taken. This error results from the presence of a cold space in the concentric tube through which samples are taken (Fig. 2.3). The sequence always involved discarding two samples to vacuum before taking the sample which was analysed (see 2.2.1b).

Thus the cold section contained reaction mixture as at the time of taking the second discarded sample. The error amounts to no more that 30 seconds in the overall reaction time, which corresponds to about 0.8% for a period of one hour.

In experiment A2-1 at 523.5K, pressure 39.790 kPa, measurements were made continuously for the first five minutes and then every 10 to 15 minutes for a period of 2.55 hours (2h - 33min) when a sample was taken for chromatographic analysis using a squalane column (see section 2.2.4$\underline{a}$). The dimer to monomer $P_d : P_m$ was in good agreement with the concentration ratio calculated from chromatographic analysis, as shown in the table below.

Experiment A2-1

Time (t/min)	Pressure (P_t/Pa)	C_m area[+]	D area[+]	Area ratio $\frac{D}{C_m}$	Conc. ratio $\frac{D}{C_m}$	Press. ratio $\frac{P_d}{P_c}$
153	39,790	14.9×10^5	$70.0 \times 6 \times 10^2$	23.4×10^{-3}	18.17×10^{-3}	18.2×10^{-3}
211		$29.1 \times 5 \times 10^4$	$36.1 \times 3 \times 500$	37.2×10^{-3}	24.0×10^{-3}	23.8×10^{-3}

In order to test the reproducibility of the methods the experiment was duplicated, experiment A2-2. Again, as the table below shows, the concentration ratio agreed with the pressure ratio. Also the rate constants derived from A2-2 were in agreement with those from experiment A2-1 (see Table III 1.2). Good agreement was also observed in the next experiment A2-3 in which the pressure was only 25.434 kPa (see next page).

Experiment A2-2

Pressure	Time	C_m^+ area	D^+ area	Area $\frac{D}{C_m}$ ratio	Conc. $\frac{D}{C_m}$ ratio	Press. $\frac{P_d}{P_c}$ ratio
40,552	47.5	$32.2 \times 5 \times 10^4$	$46.4 \times 3 \times 100$	8.64×10^{-3}	5.58×10^{-3}	5.58×10^{-3}
39,711	135	$30.7 \times 5 \times 10^4$	$62.9 \times 3 \times 200$	24.6×10^{-3}	15.8×10^{-3}	15.9×10^{-3}
38,506	245	$30.1 \times 5 \times 10^4$	$44.1 \times 3 \times 500$	43.9×10^{-3}	28.4×10^{-3}	28.1×10^{-3}

Experiment A2-3

Pressure	Time	C_m^+ area	D^+ area	Area $\frac{D}{C_m}$ ratio	Conc. $\frac{D}{C_m}$ ratio	Press. $\frac{P_d}{P_c}$ ratio
25,434	63.5	$19.0 \times 5 \times 10^4$	$43.6 \times 3 \times 50$	7.67×10^{-3}	4.95×10^{-3}	4.94×10^{-3}
24,939	151	$18.8 \times 5 \times 10^4$	$54.3 \times 3 \times 100$	17.3×10^{-3}	11.1×10^{-3}	11.2×10^{-3}
24,366	308	$18.2 \times 5 \times 10^4$	$51.8 \times 3 \times 200$	33.8×10^{-3}	21.8×10^{-3}	21.6×10^{-3}

$+$Area in 10^{-12} A ($= cm^2$ x chart speed x attenuation.)

The chromatographic analysis of the reaction mixture in the above experiments did not indicate the presence of any other compounds at detectable levels, even when the Poropak column was used. All the additional peaks that appeared in chromatograms of material from pyrolysis in more rigorous conditions were missing.

Stedman[112] reported that at 689.1 K for 28% reaction ($P_m : P_o = 110:150$, t = 10 min) the amount of the only by-product, 1,4-dichlorohexafluorobut-2-ene, was about 2% of the unreacted chlorotrifluoroethene. The following experiments at higher temperature (622.6 K) were planned to give information about the factors affecting the formation of side products.
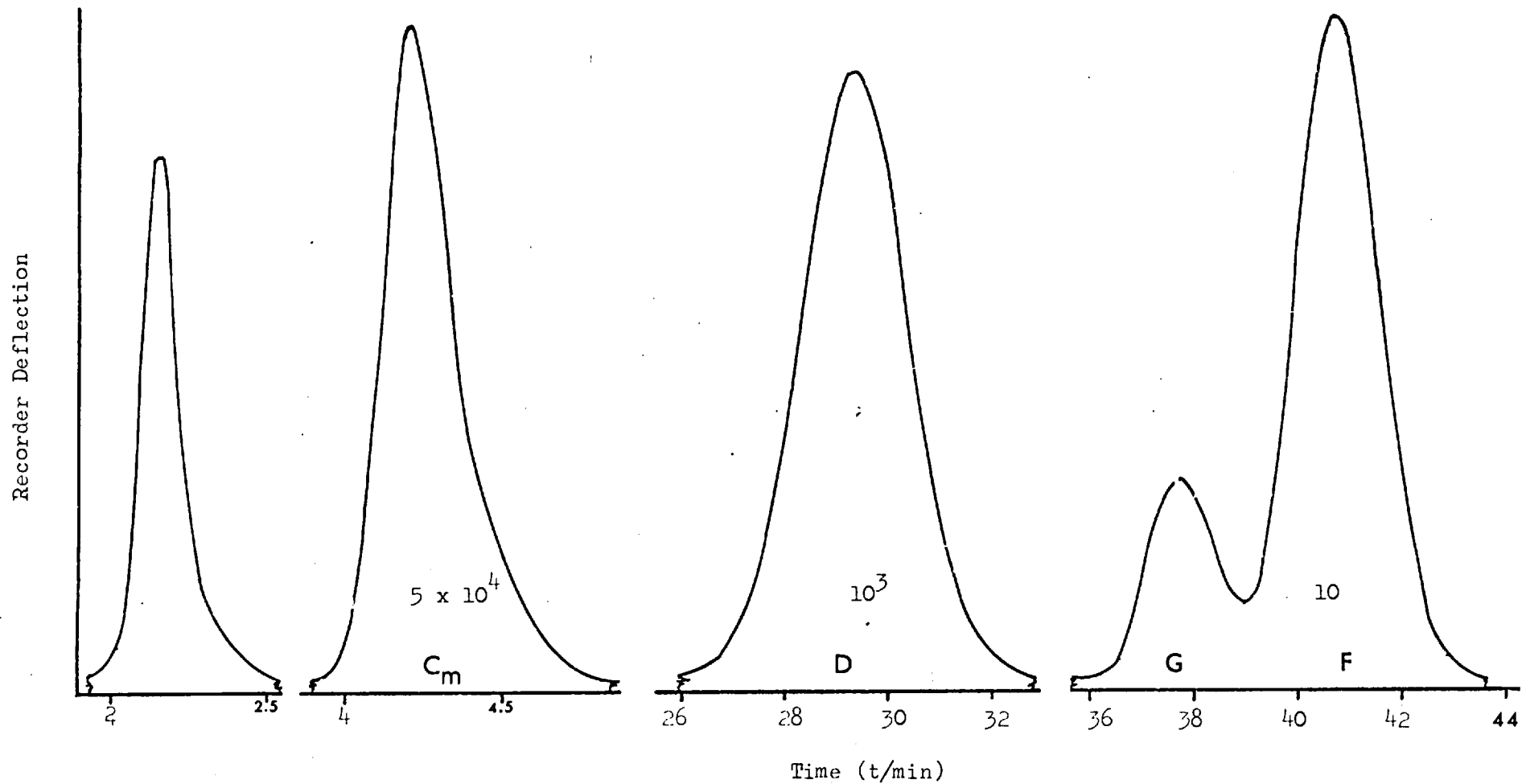
Figure 3.3 Chromatogram of chlorotrifluoroethene pyrolysis mixture
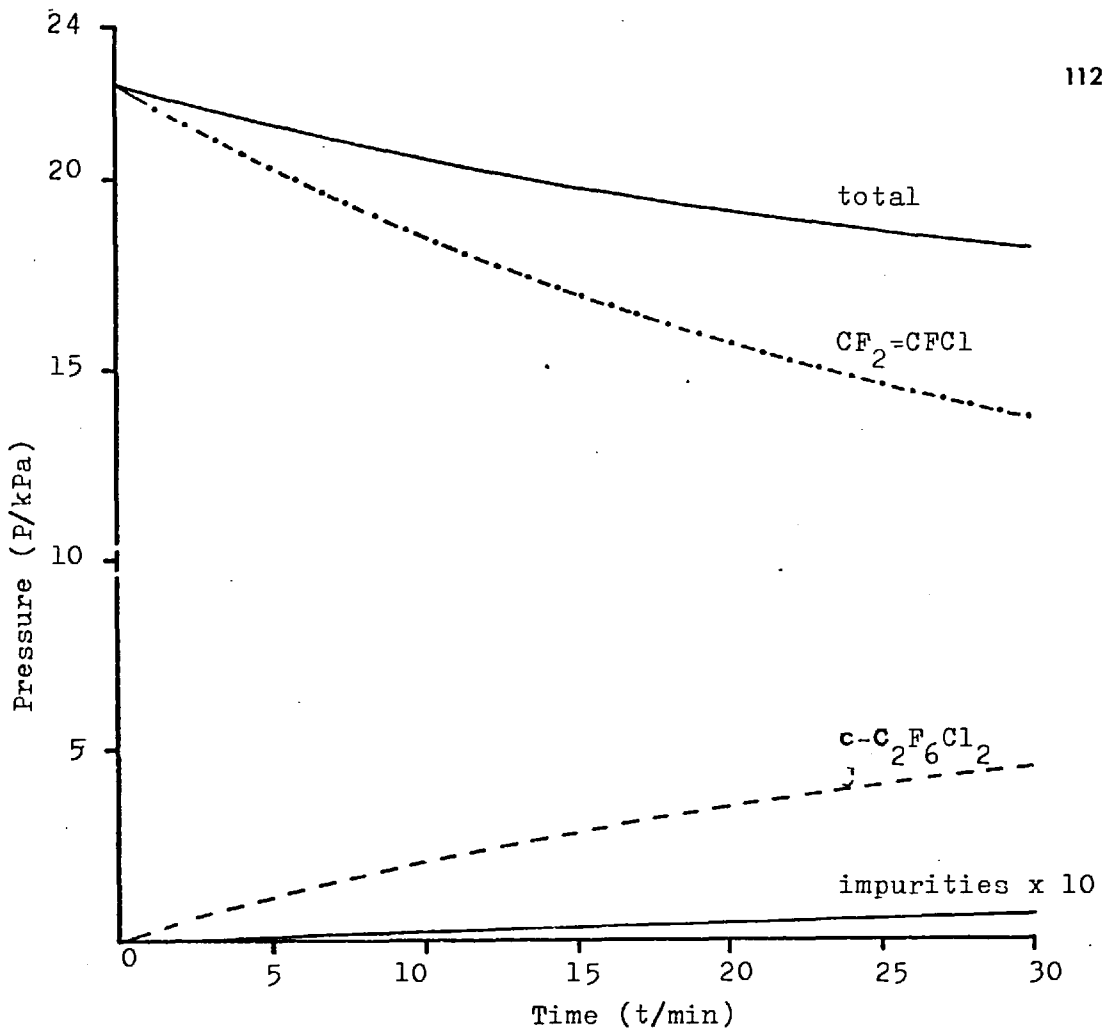
Figure 3.4. Pyrolysis of chlorotrifluoroethene (672.2 K)

In experiment A10-1 pressure was recorded continuously for the first 80 minutes at which point a sample was taken for analysis. The two peaks (G,F in Figure 3.3) in addition to those already characterized clearly indicated the presence of new compounds. A second sample taken after 150 min. total reaction time established that the compound corresponding to peak F increased as the reaction proceeded. A replicate experiment (A10-2) confirmed these observations. The initial pressure (experiment A10-3) seems not to have any effect on the formation of these compounds since the peak sizes were, by and large, independent of it. The peak area ratios (F area/D area) were less than $1:10^3$. Figure 3.4 shows the composition of a reaction mixture as a function of time. It can be seen that the amounts of side products are insignificant.

The dependence of reaction rate on the pressure of the reactants P_i, all the other variables being kept constant, can be expressed thus,

$$\text{reaction rate} \qquad r = \frac{-dP_i}{dt} = k \prod_{i=1}^{s} P_i^{n_i} \qquad \text{3.1-3}$$

or taking logarithms

$$\log r = \log k + \sum_{i=1}^{s} n_i \log P_i \qquad \text{3.1-4}$$

where n_i is the order of reaction.

A graph in which the logarithm of the rate r is plotted against the logarithm of the chlorotrifluoroethene pressure P_m should be a straight line if the rate law(3.1-2) is obeyed. The slope of this line indicates the order of the reaction n_i. Such graphs were drawn for all the above experiments and the straight lines obtained all had a slope close to 2.00 indicating a second order reaction.

The data obtained from the above experiments make evident the following features of the reaction.

a. Invariant stoichiometry

b. The rate is unaffected by the presence of small
    amounts of product (reverse reaction negligible).

c. A reaction order of two, independent of
    temperature and pressure.

The constant reaction order and the reproducibility of the results indicate that the surfaces of the reaction vessel,

conditioned by the production of carbon film, are inert.

The correlation and consistency of results obtained by making pressure observations and performing chromatographic analyses suggest that the methods complement each other and can be used in combination to study the reaction.

3.1.3 Treatment of experimental measurements

The chemical equation for the system is

$$2 \text{ CF:CFCl} \underset{k_{-1}}{\overset{k_1}{\rightleftharpoons}} \text{C} - \text{C}_4\text{F}_6\text{Cl}_2 \qquad 3.1\text{-}1$$

or

$$2\text{M} \underset{k_{-1}}{\overset{k_1}{\rightleftharpoons}} \text{D}$$
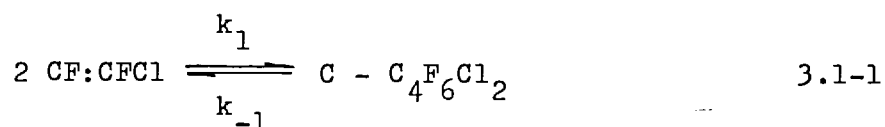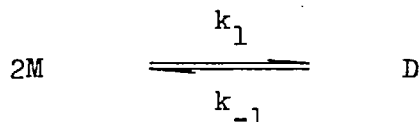
for the forward second order reaction, k_1 is definied by

$$-\frac{1}{2} \frac{dC_m}{dt} = k_1 C_m^2 \qquad 3.1\text{-}2$$

and it is expressed in $m^3.\text{mol}^{-1}\text{s}^{-1}$. The integrated form is

$$k_1 = \frac{1}{2t} \ C_m^{-1} - C_o^{-1} \qquad 3.1\text{-}5$$

where C_m is the concentration of monomer at time t and C_o is the initial concentration.

The pressure of the reaction mixture P_t at any time is equal to the sum of the partial pressures of its constituents. (The subscripts refer to monomer ($_m$) and dimer ($_d$)).

$$P_t = \sum_{i=1}^{s} P_i = P_h + P_d \qquad\qquad 3.1\text{-}6$$

Let P_o be the initial pressure. By the stoichiometry of the reaction (App. III)

$$_oP_h = P_h + 2P_d \qquad\qquad 3.1\text{-}7$$

therefore
$$P_h = 2P_t - P_o \qquad\qquad 3.1\text{-}8$$

Since
$$P_h = C_h \, R \, T_h \qquad\qquad 3.1\text{-}9$$

equation 3.1-5 becomes
$$k_1 = \frac{RT_h}{2t} \left(\frac{1}{2P_t - P_o} - \frac{1}{P_o} \right) \qquad 3.1\text{-}10$$

where the gas constant $R = 8.3143$ J K^{-1} mol^{-1}

Taking into account the 'dead' space, equation 3.1-10 is modified (appendix III, 3I_23) to

$$k_1 = \frac{1+b}{1+2b} \; \frac{RT_h}{t} \left(\frac{b}{P_t(1+2b) - P_o(1+b)} - \frac{1}{P_o} \right) \quad 3.1\text{-}11$$

where
$$b = \frac{V_h \, T_c}{V_c \, T_h} = \beta \, \frac{T_c}{T_h} \qquad\qquad 3.1\text{-}12$$

It can be easily seen that for high values of b (i.e. $\beta > 500$) equation 3.1-11 is reduced to 3.1-10.

At the upper end of the temperature range (T > 625K) the value of P_o could not be measured accurately because of the rapid changes

in pressure. Tentative values for P_o were assigned and graphs were constructed in which $1/(2P_t - P_o)$ values were plotted against time. P_o was estimated by extrapolating this graph. A satisfactory graph gave a straight line having an intercept close to $1/P_o$

At temperatures and pressures where the changes in composition are not so fast, the value of P_o could be measured with an error not exceeding the experimental error ($\pm$ 0.002μV). Pressure measurements were made at equal time intervals and graphs were constructed in which $\dfrac{b}{P_t(1+2b) - P_o(1+b)} = -f(a)$ was plotted against time, having an intercept close to $f(a_o) = -\dfrac{1}{P_o}$, and a slope equal to $k' = \dfrac{1+2b}{1+b}\, k_1/RT$.

The calculation of the specific rate constant using a graphical method is advantageous[118] since it is of importance to evaluate the contribution of each experimental observation to the average value of k_1 so obtained.

Let $\delta_j = f(\alpha_j) - f(\alpha_o) - k'_{av}\, t_j$ 3.1-13

be the deviation of the jth point and k'_{av} the slope of the line drawn through the experimental points according to the condition that $\displaystyle\sum_{j=1}^{n} \delta_j = 0$ 3.1-14

and equation 3.1-11 becomes

$$\sum_{j=1}^{n} f(\alpha_j) = \sum_{j=1}^{n} f(\alpha_o) - k'_{av} \sum_{j=1}^{n} t_j \qquad 3.1-15$$

or

$$k'_{av} = \frac{nf(\alpha_o) - \sum\limits_{j=1}^{n} f(\alpha_j)}{\sum\limits_{j=1}^{n} t_j} \qquad 3.1-16$$

Thus with exception to the initial value every other value of α derived from experimental observation is equally weighted. Most of the observations were made at equally spaced time intervals. Writing τ for $t_j = t_1$, 2τ for $t_j = t_2$ and so on, then

$$\sum_{j=1}^{n} t_j = \sum_{j=1}^{n} jt = \frac{n(n+1)\tau}{2} = \frac{n}{2} t_{(n+1)} \qquad 3.1-17$$

Therefore

$$_a k_v = \frac{(1+b)}{(1+2b)} \frac{RT}{t_{(n+1)}/2} \left[\sum_{j=1}^{n} \frac{b/n}{P_t(1+2a)-P_o(1+a)} - \frac{1}{P_o} \right] \qquad 3.1-18$$

Clearly, the average value of k obtained graphically using a set of observations made at equally spaced time intervals is determined by the ratio of the difference between the value of 1/Po and the unweighted average of the $b/[P_t(1+2b) - Po(1+b)] = 1/P_h$ elapsed to exactly midway in the experiment.

Equation 3.1-11(3I-15a) can be rearranged to

$$k_1 = \frac{(1+b)}{(1+2b)} \frac{RT_h}{tP_o} \frac{P_o - P_h}{P_h} \qquad 3.1-19$$

from 3l-9 follows that

$$n_b \cdot \frac{1+2b}{1+b} = {_o}n_h - n_h \qquad \text{3.1-20a}$$

$$P_d \frac{1+2b}{1+b} = P_o - P_h \qquad \text{3.1-20b}$$

Therefore

$$k_1 = \frac{RT_h}{tP_o} \cdot \frac{Pd}{P_h}$$

$$= \frac{RT_h}{t\,P_o} \; \frac{C_b}{C_h} = \frac{RT_h}{tP_h} \; \frac{A_r}{f_{ci}} \qquad \text{3.1-21}$$

where A_r is the chromatographic peak area ratio and f_{ci} is the calibration factor (see section 2.2.1).

The 'dead' space has also an effect on composition of the reaction mixture whenever samples are taken out of the reaction vessel.

Let $\rho = P_d / P_a$ as determined by analysis. At time t, before taking the last sample, the composition was

$P_t = P_a(1+\rho) + dP_a(1+\rho-b)$. The term $-dP_a b$ arises from the contribution of the 'dead' space, P_a is the pressure of the compound undergoing dimerization and $b = \dfrac{T_h}{T_c} \dfrac{V_c}{V_h}$. Let $1-b=a$.

Obviously $dP_a(1+\rho-b) = dP_t = dP_a(a+\rho)$

Since ρ, b and dP_t are known then dP_m can be calculated

The composition of the mixture before taking the sample,

disregarding all other effects, was

$$P_{t_1} = P_a + dP_a \cdot a + \rho(P_a + dP_a)$$

$$= P_{a_1}\left(1 + \rho \, \frac{P_a + dP_a}{P_{a_1}}\right)$$

By the same reasoning

$$P_{t_2} = P_{a_1}\left(1 + \rho\frac{(P_a + dP_a)}{P_{a_1}}\right) + \delta P_{a_1}\left(1 + \rho\frac{(P_a + dP_a)}{P_{a_1}} - b\right)$$

$$P_{t_2} = P_{a_1} + \delta P_{a_1} \cdot a + (P_{a_1} + \delta P_{a_1})\left(\rho \cdot \frac{(P_a + dP_a)}{P_{a_1}}\right)$$

Again $\quad \delta P_{a_1}\left(1-b + \rho \, \frac{(P_a + dP_a)}{P_{a_1}}\right) = \delta P_{t_2}$

and P_{a_1} can be calculated since all the other quantities are known.

$$P_{t_2} = (P_{a_1} + \delta P_{a_1} \cdot a)\left(1 + \rho \frac{(P_a + \delta P_{a_1})}{(P_a + \delta P_{a_1} \cdot a)} \cdot \frac{P_a + dP_a}{P_{a_1}}\right)$$

$$= P_{a_2}\left(1 + \rho \frac{(P_{a_1} + \delta P_{a_1} \cdot a)}{P_{a_2}} \cdot \frac{(P_a + dP_a)}{P_{a_1}}\right)$$

Before sampling the composition was

$$P_{t_3} = P_{a_2}\left(1 + \rho \, \frac{P_{a_1} + \delta P_{a_1} a}{P_{a_2}} \cdot \frac{(P_a + dP_a)}{P_{a_1}}\right) +$$

$$+ \delta P_{a_2}\left(-1 - b + \rho\left(\frac{P_{a_1} + \delta P_{a_1} \cdot a}{P_{a_2}} \cdot \frac{P_a \, dP_a}{P_{a_1}}\right)\right)$$

For typical values of a = 0.985 and p = 0.001 to 0.1 the
P_b/P_a ratio does not vary more than 1% which is within the
experimental error.

3.1.4 Quantitative Measurement of the Reaction Rate of
chlorotrifluoroethene cyclodimerization.

It was shown in sections 3.1.1 and 3.1.2 that the main
product of the thermal reaction of chlorotrifluoroethene below
675 K is cis and trans 1,2-dichlorohexafluorocyclobutane. It
was also demonstrated that the course of the reaction can be
followed by either observing pressure changes or analysing samples
of the reaction mixture or both. The reaction was studied by
these methods.

3.1.4a Pressure measurements

Pressure changes were used almost exclusively to study the
reaction at the upper end of the temperature range. The monomer-
cyclodimer equilibrium is well on the dimer side so that the
reverse reaction is negligible. Treatment of the data as for a
simple second order reaction does not introduce significant
error, at least in the early stages of the reaction. The experi-
mental measurements were treated as described in section 3.1.3.
For each experiment a graph of $[P_t(1+2b) - P_o(1+b)]^{-1}$ against
time was plotted. Occasionally, at the higher temperatures, it
was necessary to adjust the value of P_o to meet the conditions for

Table III 1.1.

Specific rate constants for the cyclodimerization of Chlorotrifluoroethene

Experiment	Temperature $\frac{T}{K}$	$\frac{kK}{T}$	Pressure $\frac{P}{Pa}$	Correction factor $\underline{1 + b}/\underline{1 + 2b}$	$\dfrac{k_1}{m^3\ mol^{-1}s^{-1}}$	$-log_{10}\ \dfrac{k_1}{m^3\ mol^{-1}\ s^{-1}}$
A6 - 1	672.2	1.488	22,512	0.5055	4.55×10^{-5}	4.342
A9 - 1	647.6	1.544	13,095	0.5054	2.27×10^{-5}	4.645
A9 - 2	647.6	1.544	6,670	0.5054	2.25×10^{-5}	4.647
A5 - 1	633.0	1.580	25,695	0.5052	1.44×10^{-5}	4.843
A5 - 2	633.0	1.580	24,661	0.5052	1.42×10^{-5}	4.846
A10 - 1	622.6	1.606	13,865	0.5051	1.05×10^{-5}	4.980
A10 - 2	622.6	1.606	14,094	0.5051	1.06×10^{-5}	4.974
A10 - 3	622.6	1.606	21,042	0.5051	1.04×10^{-5}	4.984
A1 - 1	586.1	1.706	5,723	0.5048	2.94×10^{-6}	5.532
A1 - 2	586.1	1.706	5,978	0.5048	3.00×10^{-6}	5.523
A1 - 3	586.1	1.706	8,960	0.5048	2.93×10^{-6}	5.532
A3 - 1	550.1	1.818	17,178	0.5045	6.80×10^{-7}	6.167
A3 - 2	550.0	1.818	14,503	0.5045	6.79×10^{-7}	6.168

Table III 1.1. contd.

Experiment	Temperature $\frac{T}{K}$	$\frac{kK}{T}$	Pressure $\frac{P}{Pa}$	Correction factor $\underline{1+b}/\underline{1+2b}$	$\frac{k_1}{m^3 \, mol^{-1}s^{-1}}$	$-log_{10} \frac{k_1}{m^3 \, mol^{-1} \, s^{-1}}$
A4 - 1	525.3	1.904	24,693	0.5043	2.35×10^{-7}	6.629
A4 - 2	525.3	1.904	24,924	0.5043	2.36×10^{-7}	6.627
A2 - 2	523.5	1.910	40,552	0.5043	2.10×10^{-7}	6.678
A2 - 1	523.5	1.910	39,790	0.5043	2.09×10^{-7}	6.679
A7 - 1	473.4	2.121	20,962	0.5039	1.71×10^{-8}	7.807
A8 - 1	448.1	2.232	19,839	0.5039	4.50×10^{-9}	3.347

a straight line. The rate constant was calculated from equation 3.1-18 and, whenever a chromatogram was taken, from 3.1-21.

Replicate experiments were carried out whenever the accuracy of the observations was limited by the small extent of the reaction. The effect of pressure on the value of the specific rate constant was found to be insignificant. The initial pressure ranged from   kPa to 40.5 kPa. The results are given in Table III .1.1

3.1.4b Chromatographic measurements

Chromatographic measurements were made to confirm the composition of pyrolysed material indicated by pressure measurements and to extend downwards the temperature range covered. At low temperatures the pressure changes were too small to be measured accurately. Samples were taken as described in sections 2.2.1b and 3.1.2. Chromatographic peak areas were expressed in $cm^2 \, 10^{-12}A$. Specific rate constants were calculated from equation 3.1-21 and a weighing factor was introduced to allow for pressure changes due to taking samples.

At the later stage of the quantitative experiments the squalane column had shown signs of deterioration. It was replaced by a slightly shorter column (7.80m). The calibration factor was, within experimental error, the same. The results of the chromatographic analyses are given in Table III 1.2.

Table III 1.2.

Analyses and specific reaction constants for the cyclodimerization of chlorotrifluoroethene

Experiment	Temperature T/K	Pressure P/Pa	Time t/min	$CF_2:CFCl$ area $+A_{r1}$	$C.C_4F_6Cl_2$ $\ddagger A_{r2}$	$\dfrac{C.C_4F_4Cl_2 \times 10^3}{C_2F_3Cl}$	$\dfrac{k_1}{m^3\ mol^{-1}s^{-1}}$	$-log_{10}\dfrac{k_1}{m\ mol^{-1}s^{-1}}$
A2 – 1.1	523.5	39.790	153	14.9 x 10	70.0 x 20	18.2	2.16×10^{-7}	6.665
– 1.2		38.024	211	29.1 x 5	36.1 x 50	24.0	2.04×10^{-7}	6.690
A2 – 2.1	523.5	40.552	47.5	32.2 x 5	46.4 x 10	5.6	2.10×10^{-7}	6.677
2.2		39.711	135	30.7 x 5	62.9 x 20	15.8	2.13×10^{-7}	6.658
2.3		38.506	245	30.1 x 5	44.1 x 50	28.4	2.08×10^{-7}	6.681
A2 – 3.1	523.5	25.434	63.5	19.0 x 5	48.6 x 5	4.95	2.220×10^{-7}	6.654
3.2		24.939	151	18.8 x 5	54.3 x 10	11.1	2.05×10^{-7}	6.688
3.3		24.366	308	18.2 x 5	51.3 x 20	21.8	2.100×10^{-7}	6.678
A16 – 1.1	498.2	40.041	91	29.2 x 5	50.5 x 5	3.35	6.34×10^{-8}	7.198
1.2		39.379	187	29.2 x 5	50.6 x 10	6.71	6.24×10^{-8}	7.205
1.3		38.717	307	28.4 x 5	81.5 x 10	11.1	6.46×10^{-8}	7.189
A16 – 2.1	498.2	25.198	160	17.8 x 5	83.9 x 2	3.66	6.26×10^{-8}	7.203
2.2		24.764	262	17.5 x 5	84.1 x 5	5.99	6.35×10^{-8}	7.197
2.3		24.317	422	17.3 x 5	87.5 x 5	9.78	6.40×10^{-8}	7.194

$+$ A_{r1} = area in $cm^2.10^{-8}A$ $\ddagger$ A_{r2} = area in $cm^2.3.10^{-11}A$

Table III 1.2. cont.

Experiment	Temperature T/K	Pressure $P3Pa$	Time t/min	$CF_2{:}CFCl$ area $^+A_{r1}$	$C.C_4F_6Cl_2$ $^\ddagger A_{r2}$	$\dfrac{C.C_4F_4Cl_2 \times 10^3}{C_2F_3Cl}$	$\dfrac{k_1}{m^3\ mol^{-1}s^{-1}}$	$-log_{10}\dfrac{k_1}{m\ mol^{-1}s}$
A17 - 1.1	473.0	42,434	150	34.1 x 5	72.7 x 2	1.65	1.70×10^{-8}	7.770
1.2		41,895	270	33.6 x 5	49.4 x 5	2.85	1.65×10^{-8}	7.783
1.3		41,390	391	33.1 x 5	72.2 x 5	4.22	1.71×10^{-8}	7.769
A17 - 2.1	473.0	30,144	274	23.2 x 5	63.4 x 2	2.12	1.68×10^{-8}	7.774
2.2		29,631	383	22.8 x 5	34.9 x 5	2.96	1.71×10^{-8}	7.768
A17 - 3.1	473.0	24,787	171	19.2 x 5	27.6 x 2	1.12	1.70×10^{-8}	7.769
3.2		24,495	317	18.9 x 5	48.6 x 2	1.99	1.68×10^{-8}	7.775
3.3		24.226	466	18.7 x 5	28.7 x 5	2.97	1.70×10^{-8}	7.770
*A10 - 1.1	471.4	14,180	1310	12.3 x 5	11.0 x 5	3.80	1.34×10^{-8}	7.873
1.2		14.100	2332	19.4 x 5	24.5 x 10	10.56	1.67×10^{-8}	7.777
1.3		13.909	3065	24.5 x 5	14.5 x 20	10.00	1.50×10^{-8}	7.824
*A15 - 1.1	447.9	25.687	1121	29.8	17.8 x 1	1.68	3.71×10^{-9}	8.422
1.2		25.554	1423	30.4	23.6 x 1	2.18	3.93×10^{-9}	8.406
1.3		25.367	2348	33.7	22.5 x 2	3.82	3.73×10^{-9}	8.428

* sample loop chart speed different from the rest of the data

Table III 1.2. cont.

Experiment	Temperature T/K	Pressure $P3Pa$	Time t/min	$CF_2{:}CFCl$ area $^+A_{r1}$	$C.C_4F_6Cl_2$ $^‡A_{r2}$	$\dfrac{C.C_4F_4Cl_2 \times 10^3}{C_2F_3Cl}$	$\dfrac{k_1}{m^3\ mol^{-1}s^{-1}}$	$-log_{10}\dfrac{k_1}{m\ mol^{-1}s^{-1}}$
*A11 - 1.1	445.6	17.138	1275	19.6 x 10	12.3 x 5	1.32	3.77×10^{-9}	8.424
1.2		17.085	1890	19.6 x 10	18.1 x 5	1.96	3.76×10^{-9}	8.425
1.3		17.012	2728	19.3 x 10	25.6 x 5	2.79	3.74×10^{-9}	8.427
A18 - 1.1	437.7	52.514	390	21.2 x 10	40.9 x 2	0.747	2.21×10^{-9}	8.656
1.2		51.981	1410	20.9 x 10	29.1 x 10	2.69	2.22×10^{-9}	8.654
1.3		51.305	1959	21.7 x 10	39.9 x 10	3.73	2.22×10^{-9}	8.654
A18 - 2.1	437.7	52.949	721	21.6 x 10	30.0 x 5	1.35	2.14×10^{-9}	8.670
2.2		52.347	1217	21.1 x 10	48.9 x 5	2.25	2.13×10^{-9}	8.672
2.3		52.232	3508	21.1 x 10	71.6 x 10	6.57	2.16×10^{-9}	8.665
*A12 - 1.1	426.1	16.613	1280	18.87 x 10	7.42 x 2	0.334	9.58×10^{-10}	8.987
1.2		16.532	1800	15.6 x 10	9.93 x 2	0.540	9.60×10^{-10}	8.979
1.3		16.488	8181	15.6 x 10	13.6 x 2	0.730	9.58×10^{-10}	9.022
*A13 - 1.1	423.1	53.233	1259	15.5 x 5	8.4 x 2	0.915	8.02×10^{-10}	9.096
1.2		52.997	1634	16.8 x 5	11.9 x 2	1.202	8.13×10^{-10}	9.090
1.3		52.728	2667	17.2 x 5	19.3 x 2	2.70	8.00×10^{-10}	9.097

Table III 1.2. cont

Experiment	Temperature T/K	Pressure P3Pa	Time t/min	$CF_2:CFCl$ area $^+A_{r1}$	$C.C_4F_6Cl_2$ $^‡A_{r2}$	$\dfrac{C.C_4F_4Cl_2 \times 10^3}{C_2F_3Cl}$	$\dfrac{k_1}{m^3\ mol^{-1}s^{-1}}$	$-log_{10}\dfrac{k_1}{m\ mol^{-1}s^{-1}}$
*A13 - 2.1	423.1	53.203	1563	19.5 x 5	13.0 x 2	1.13	8.00×10^{-10}	9.097
2.2		52.970	1733	18.2 x 5	13.6 x 2	1.26	8.07×10^{-10}	9.093
2.3		52.757	2871	16.1 x 5	19.6 x 2	2.05	8.05×10^{-10}	9.094
A19 - 1.1	413.3	57.504	1410	23.9 x 10	35.5 x 2	0.575	4.06×10^{-10}	9.392
1.2		56.986	2430	23.9 x 10	62.6 x 2	1.01	4.16×10^{-10}	9.381
1.3		56.485	2800	23.8 x 10	27.8 x 5	1.13	4.03×10^{-10}	9.395
A19 - 2.1	413.3	52.956	991	22.0 x 10	20.7 x 2	0.370	4.04×10^{-10}	9.394
2.2		52.480	1411	21.7 x 10	30.3 x 2	0.539	4.10×10^{-10}	9.387
2.3		52.001	2431	21.4 x 10	52.2 x 2	0.942	4.22×10^{-10}	9.375
2.4		51.528	2870	21.2 x 10	60.4 x 2	1.10	4.10×10^{-10}	9.387
*A14 - 1.1	403.9	50.813	129 0	15.9 x 5	7.3	0.252	2.15×10^{-10}	9.668
1.2		50.574	2516	15.6 x 5	12.8	0.464	2.05×10^{-10}	9.688
1.3		50.352	3840	16.3 x 5	20.6	0.714	2.00×10^{-10}	9.699
*A14 - 2.1	403.9	54.182	1404	15.6 x 5	7.8	0.280	2.06×10^{-10}	9.686
2.2		53.998	2626	15.9 x 5	14.2	0.500	2.04×10^{-10}	9.690
2.3		53.821	4083	16.1 x 5	20.2	0.727	1.99×10^{-10}	9.701

* sample loop chart speed different from the rest of the data
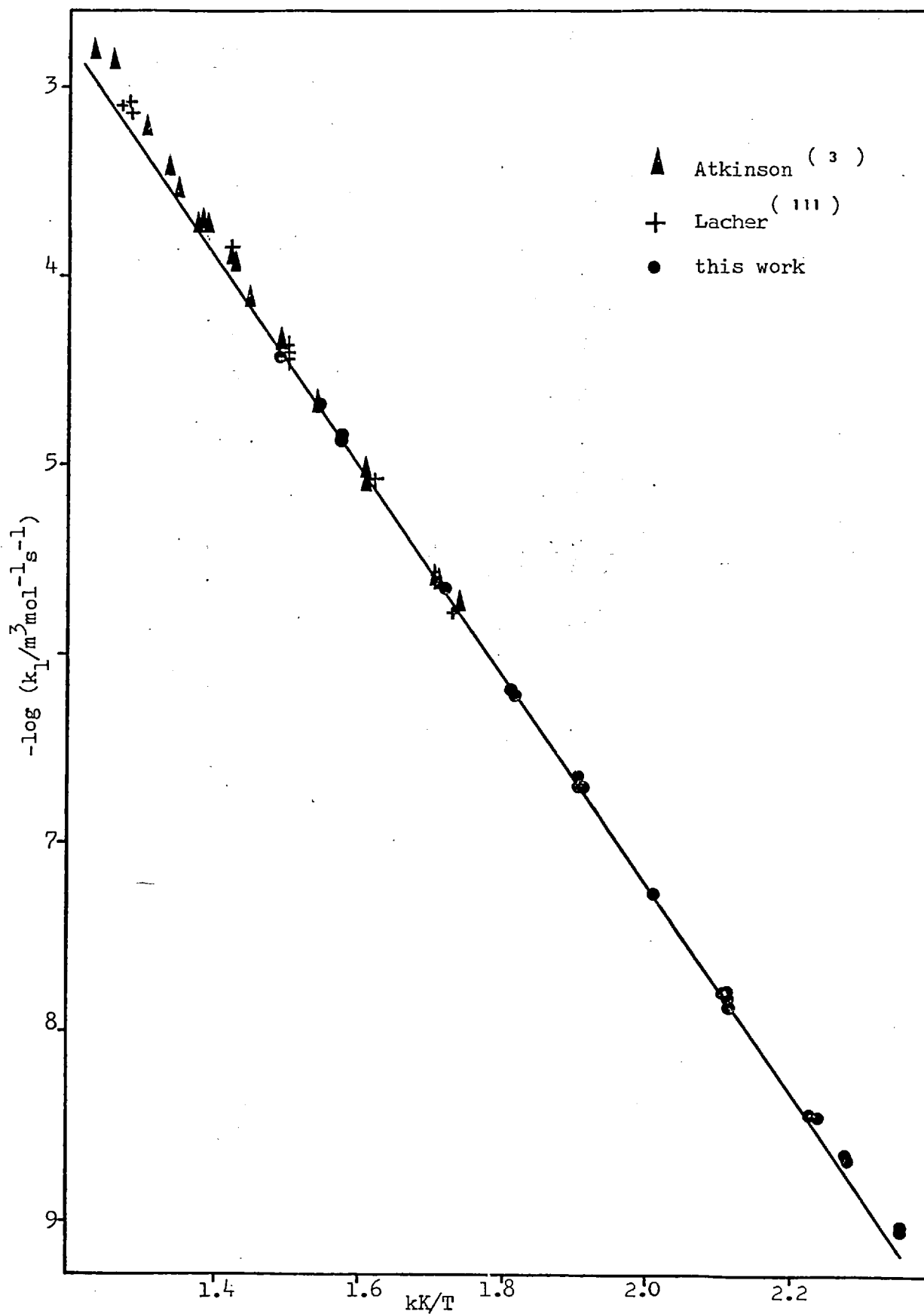
Figure 3.5   Graph of the logarithms of specific rate constants (k_1)

v. the reciprocal of temperature for the cyclodimeri-

zation of chlorotrifluoroethene

3.1.4c   Correlation of the rate constants

Experiments were made over the temperature range 400K to 672K and the pressure range 5.5 kPa to 53 kPa. The specific rate constants are given in Table III.1 An Arrhenius graph of log k_1 against the inverse of temperature $\frac{K}{T}$ is given in Figure 3.5. This includes the constants measured by Lacher and others [111] and by Atkinson and Stedman [3]. Regression analysis for a linear relationship by the method of least squares produced the equation log k_1 = 3.93 - 5536/T. However the points corresponding to both ends of the temperature range are above the straight line fitted by this method.

A modified equation of the form

$$\log k_1 = A + B \log T + C/T \qquad \qquad 3.1\_22$$

was fitted to the whole set of the results. The parameters A = -9.92, B = 4.321 and C = 4444.2 were determined by using a least squares solution of simultaneous equations in the form [119]

$$an + b\Sigma x + c\Sigma z = \Sigma y = - \Sigma \log k_1$$
$$a\Sigma x + b\Sigma x^2 + c\Sigma xz = \Sigma yx$$
$$a\Sigma z + b\Sigma xz + c\Sigma z^2 = \Sigma yx$$

where $x = \log T$ and $z = T^{-1}$

Experiments in which the value of log k differ by more than $\pm$ 0.035 from the calculated ones using equation 3.1_22 were not included in the calculation. All values used appear in the computer printout.

```
******  C H L O R O T R I F L U O R O E T H Y L E N E  ******
******  C H L O R O T R I F L U O R O E T H Y L E N E  ******

** ** ** ** ** ** ** ** ** ** ** ** ** ** ** ** ** ** ** ** ** ** ** **
```

SX	SXX	SY	SYY	SZ	SZZ
149.65411	529.37637	-355.37360	2059.85031	3.11242	0.00019246

SXZ = 5.3116673   **** SYZ = -0.6249967   **** SYZ = -981.8894687

A1A -5544.3295'   B2B -254.57185   C3C -5535.89206   D -252.63997

THE VALUE IS A = -0.3375
THE VALUE IS B = 4.3713
THE VALUE IS C = -5444.17   95.0815

NC 68	VARIANCE 0.000218	ST DEVIATION 0.014757	SAMPLE VAR 0.003229	ST ERROR 0.015134	DEVIATION 0.033431	0.25269	0.06039

NC	TEMP	LOG T	1/T (Z)	LOG K EXPERIMENTAL	K EXPERIMENTAL	*LOG K* CALCULATED	*K* CALCULATED	**LOG K** DIFFERENCE
1	823.1	2.91545	1.1312149	-2.7389	1.829E-03	-2.7320	1.854E-03	-0.0060
2	742.2	2.93332	1.1312794	-3.1214	7.561E-04	-3.11	7.703E-04	-0.0114
3	741.8	2.9931	1.1312791	-3.1217	7.556E-04	-3.1138	7.695E-04	-0.0079
4	741.8	2.8931	1.1312701	-3.1179	7.361E-04	-3.1138	7.695E-04	0.0059
5	785.7	2.93249	1.1312849	-3.1223	7.546E-04	-3.1245	7.508E-04	0.0022
6	740.7	2.83249	2.1312849	-3.1365	7.303E-04	-3.1245	7.508E-04	-0.0121
7	781.6	2.93243	1.1312811	-3.1366	7.331E-04	-3.1254	7.491E-04	-0.0112
8	770.5	2.88677	1.1312979	-3.2071	6.203E-04	-3.2245	5.963E-04	0.0175
9	769.6	2.83627	1.1312994	-3.2033	6.310E-04	-3.2334	5.842E-04	0.0334
10	752.0	2.87622	1.1313299	-3.4050	3.936E-04	-3.412	3.872E-04	0.0077
11	739.5	2.86896	1.1313523	-3.5533	2.618E-04	-3.5434	2.862E-04	-0.0066
12	739.4	2.86888	1.1313524	-3.5263	2.973E-04	-3.5444	2.855E-04	0.0184
13	723.5	2.85944	1.1313802	-3.7133	1.936E-04	-3.7173	1.917E-04	0.0043
14	723.5	2.85944	1.1313522	-3.7420	1.811E-04	-3.7173	1.917E-04	-0.0247
15	713.5	2.85337	2.1314.15	-3.8333	1.468E-04	-3.6295	1.481E-04	-0.0037
16	712.9	2.85307	1.1314027	-3.8413	1.445E-04	-3.8363	1.458E-04	-0.0039
17	712.2	2.85269	1.1314041	-3.8436	1.431E-04	-3.8443	1.431E-04	0.0037
18	705.3	2.85122	1.1314113	-3.8791	1.321E-04	-3.8397	1.291E-04	0.0108
19	690.2	2.83897	1.1314489	-4.1363	7.413E-05	-4.1101	7.9.5E-05	-0.0279
20	675.9	2.82994	1.1314795	-4.2741	5.321E-05	-4.2776	5.277E-05	0.0036
21	672.2	2.82751	1.1314877	-4.3429	4.550E-05	-4.3241	4.741E-05	-0.0179
22	669.1	2.82543	1.1314945	-4.3599	4.467E-05	-4.3534	4.331E-05	0.0134
23	668.0	2.82478	1.1314970	-4.4526	3.957E-05	-4.3774	4.193E-05	-0.0252
24	666.7	2.82393	1.1314999	-4.4434	3.95.E-05	-4.3941	4.36E-05	-0.0093
25	666.7	2.82393	1.1314999	-4.4269	3.742E-05	-4.3941	4.036E-05	-0.0328
26	666.5	2.82393	1.1315004	-4.4035	3.943E-05	-4.3966	4.012E-05	-0.0070
27	647.6	2.81134	1.1315442	-4.6450	2.265E-05	-4.6452	2.263E-05	0.0002
28	633.0	2.31146	1.1315799	-4.8462	1.425E-05	-4.8463	1.425E-05	0.0032
29	633.0	2.8146	1.1315798	-4.8431	1.435E-05	-4.8463	1.425E-05	0.0032
30	623.3	2.73473	1.1316944	-5.0710	9.977E-06	-4.9945	1.036E-05	-0.0165
31	623.1	2.79456	1.1316949	-4.9971	1.0735E-05	-4.9974	1.029E-05	0.0004
32	622.6	2.73421	1.1316062	-4.9741	1.0615E-05	-4.9347	1.0612E-05	0.0206
33	622.6	2.73421	1.1316.62	-4.991	1.0473E-05	-4.9947	1.0612E-05	0.0014
34	622.6	2.71159	1.1316.62	-4.9337	1.0734E-05	-4.9347	1.0612E-05	0.0110
35	620.7	2.79333	1.1316134	-5.0057	9.870E-06	-5.0222	9.501E-06	0.0165
36	619.8	2.73225	1.1316134	-5.0413	9.082E-06	-5.0354	9.218E-06	-0.0064
37	586.1	2.75797	1.1317562	-5.5317	2.945E-06	-5.5526	2.8 2E-06	0.0212
38	586.1	2.75797	1.1317562	-5.5324	2.935E-06	-5.5526	2.8 2E-06	0.0202
39	586.1	2.76797	1.1317562	-5.5223	3.000E-06	-5.5526	2.8 2E-06	0.0297
40	583.6	2.76613	1.1317135	-5.5524	2.559E-06	-5.5931	2.552E-06	0.0011
41	583.2	2.76532	1.1317147	-5.5776	2.649E-06	-5.5396	2.514E-06	0.0226
42	550.1	2.74045	1.1318179	-6.1683	6.737E-07	-6.1678	6.796E-07	-0.0005
43	550.1	2.74045	1.1318179	-6.1775	6.645E-07	-6.1678	6.796E-07	-0.0097
44	525.5	2.72057	1.1319029	-6.6287	2.351E-07	-6.6318	2.335E-07	0.0031
45	525.5	2.72057	1.1319029	-6.6275	2.358E-07	-6.6318	2.335E-07	0.0043
46	523.5	2.71992	1.1319102	-6.6776	2.101E-07	-6.6713	2.132E-07	-0.0063
47	523.5	2.71992	1.1319102	-6.6791	2.094E-07	-6.6713	2.132E-07	-0.0077
48	523.5	2.71992	1.1319102	-6.6780	2.099E-07	-6.6713	2.132E-07	-0.0067
49	523.5	2.71992	1.1319102	-6.5743	2.113E-07	-6.6713	2.132E-07	-0.0027
50	523.5	2.71992	1.1319102	-6.6791	2.094E-07	-6.6713	2.132E-07	-0.0077
51	498.2	2.6974	1.1319772	-7.1965	6.361E-08	-7.1953	6.376E-08	-0.0012
52	498.2	2.6974	1.1319772	-7.1981	6.333E-08	-7.1953	6.378E-08	-0.0027
53	473.0	2.67435	1.1321142	-7.7750	1.679E-08	-7.7652	1.706E-08	-0.0070
54	473.0	2.67435	1.1321142	-7.7711	1.694E-08	-7.7652	1.706E-08	-0.0030
55	473.0	2.67435	1.1321142	-7.7715	1.692E-08	-7.768	1.706E-08	-0.0035
56	471.4	2.67370	1.1321213	-7.9239	1.53.E-08	-7.8963	1.562E-08	-0.0176
57	447.9	2.65113	1.1322336	-8.4220	3.784E-09	-8.3969	4.010E-09	-0.0251
58	445.6	2.64895	1.1322442	-8.4251	3.753E-09	-8.4577	3.456E-09	0.0327
59	437.7	2.64118	1.1322847	-8.6545	2.215E-09	-8.6713	2.132E-09	0.0168
60	437.7	2.64118	1.1322847	-8.6481	2.141E-09	-8.6713	2.132E-09	0.0233
61	426.1	2.63051	1.1323469	-8.9551	1.035E-09	-8.9381	1.0648E-09	0.0131
62	426.1	2.63051	1.1323459	-9.0201	9.5537E-10	-8.9381	1.0648E-09	-0.0219
63	574.3	2.75902	1.1317397	-5.7230	1.892E-06	-5.7362	1.927E-06	0.0152
64	760.6	2.93627	1.1312904	-3.2193	6.039E-04	-1.2334	5.842E-04	0.0144
65	769.4	2.33625	1.1312997	-3.2171	6.067E-04	-3.2354	5.815E-04	0.0184
66	676.2	2.8315	1.1314789	-4.2393	5.146E-05	-4.2739	5.323E-05	-0.0151
67	661.9	2.82070	1.1315128	-4.4703	3.388E-05	-4.4560	3.500E-05	-0.0140
68	642.1	2.8076	1.1315574	-4.7393	1.824E-05	-4.7200	1.905E-05	-0.0190

Computer printout: Temperature, specific rate constants and kinetic parameters

3.2. THE THERMAL CYCLODIMERIZATION OF HEXAFLUOROPROPENE

A number of investigators have studied the pyrolysis of hexa-fluoropropene over a wide range of temperature. Atkinson and Atkinson[2] described the kinetics of the reaction hexafluoropropene ⟶ per-fluoroisobutene in the temperature range 870 - 950 K. R. A. Matula[120] investigated the rate of the same reaction in the range 820 K - 950 K. H. C. Brown[121] described a product from the dimerisation of hexa-fluoropropene in an autoclave at 675 K. He assumed by analogy with the head-to-head dimerisation of other alkenes

$$2 \, CF_2 = CFCF_3 \rightleftharpoons c - C_4F_6(CF_3)_2 \qquad 3.2 - 1$$
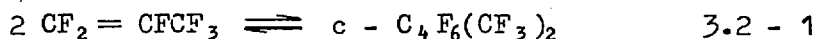
that the compound was a 1,2 - cyclic dimer. Hauptschein et al[122] confirmed that hexafluoropropene undergoes cyclic dimerisation under pressure in the temperature range 525 K to 720 K by characterizing the products as a mixture of isomers of di(trifluoromethyl) hexafluoro-cyclobutane. They also found that at temperatures above 725 K per-fluoroisobutene is the principal product. Atkinson and Stockwell[4] confirmed the characterization of the products of the cyclic dimeri-sation and identified the isomers. They also studied the dissociation of cis and trans 1,2 - isomers to hexafluoropropene, as well as the rates of isomerisation. These earlier investigations had established that the cyclic dimerisation of hexafluoropropene is a much slower reaction than the dimerisation of tetrafluoroethene or other fluorinated ethenes. At normal pressures (~ 100 kPa) yields are very low. Raising the temperature introduces the competing reaction to perfluoroisobutene and instability in the cyclic dimer.

3.2.1   Characterization of Di-(trifluoremethyl)-hexafluorocyclobutanes

.Successive chromatographic analyses during the pyrolysis of hexa-
fluoropropene at 650 K indicated that there was one major product. This
product, isolated and purified as described.in section 2. 3. 3, was cha-
racterized as a mixture of di-(trifluoromethyl)-hexafluorocyclobutanes
consisting essentially of 1,2- isomers.

3.2.1a   The infrared spectrum

The infra-red spectra of the isomers of di-(trifluoromethyl)-hexa-
fluorocyclobutane have previously been determined [4,122]. The infra-
red spectrum of the purified product indicated the presence of cis -
1,2-di(trifluoromethyl)-hexafluorocyclobutane by its characteristic
absorption at 1302 cm^{-1}, 1244 cm^{-1}, 1043 cm^{-1} and 724 cm^{-1}. The pre-
sence of the trans -1,2 isomer was established by the characteristic
absorption at 1324 cm^{-1}, 1065 cm^{-1} and in the region 743 cm^{-1} to
730 cm^{-1}. Small quantities of the 1,3 - isomers were indicated by the
absorption at 1125 cm^{-1}, 949 cm^{-1}, 844 cm^{-1} and 706 cm^{-1} which is not
observed for the other isomers. From the relative intensities at
1302 cm^{-1} and 1043^{-1}, those at 1324 cm^{-1} and 1065 cm^{-1}, and that at
1125 cm^{-1}, it was concluded that the composition of the mixture was
cis 48.1%, trans 50.6% and ~ 1.3% cis - trans -1,3 isomers.

3.2.1b The mass spectrum of di-(trifluoromethyl)-hexafluorocyclobutane.

The mass spectrum of di-(trifluoromethyl)-hexafluorocyclobutane
recorded as described in section 2.2.2b is given in Figure 3.6 The
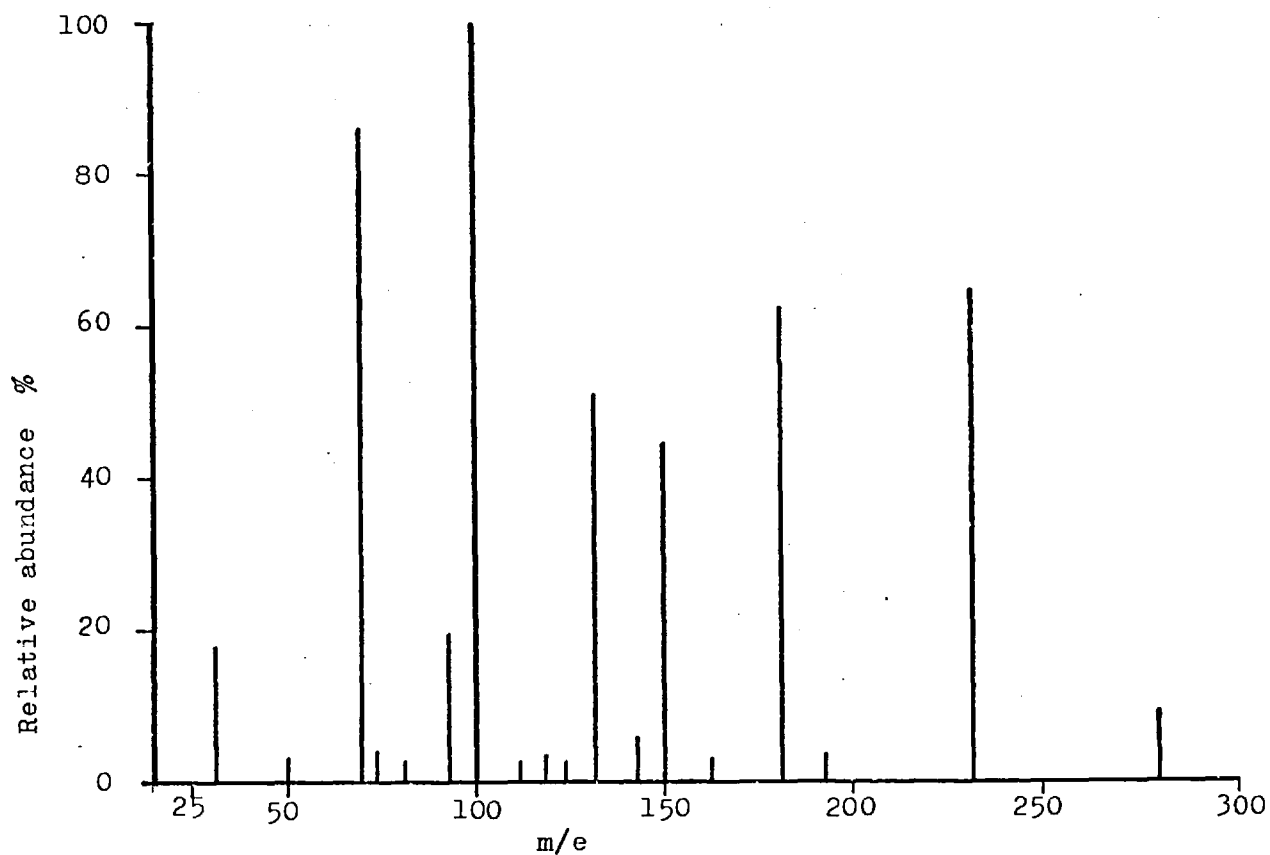
Ion	m/e	I% this work	I% (4) 1,2-trans	I% (4) 1,2cis	I%(4) 1,3
C_6F_{12}	300	0	0.1	0.15	0.11
C_6F_{11}	281	9	14	14	6
C_5F_9	231	64	84	85	5
C_5F_7	193	4	6	5	3
C_4F_7	181	62	83	75	14
C_3F_6	150	45	53	46	95
C_3F_5	131	50	49	46	100
C_2F_4	100	100	100	100	65
C_3F_3	93	19	21	20	13
CF_3	69	86	91	80	63
CF_2	50	3	10	10	-
CF	31	18	18	16	13

Figure **3.6** Mass spectrum of 1,2-ditrifluoromethylhexafluoro-
cyclobutane.

Ionization Potential was 80 eV. The tabular part of Figure 3.6 gives also the spectra of pure isomers as reported by Atkinson and Stockwell[4]. In the present spctrum the molecular ion peak (M^+) was not observed and some other minor differences are apparent. There is an increase of $CF_2 \overset{+}{\div} CF_2$ ions, possibly because of the higher Ionization Potential. However, the three metastable peaks corresponding to the non-integral masses of 189.9, 141,8 and 94.8 that can be represented by the equations

$$C_6F_{11}^+ = C_5F_9^+ + CF_2$$
$$C_5F_9^+ = C_4F_7^+ + CF_2$$
and $\quad C_4F_7^+ = C_3F_5^+ + CF_2 \quad\quad$ are still present.
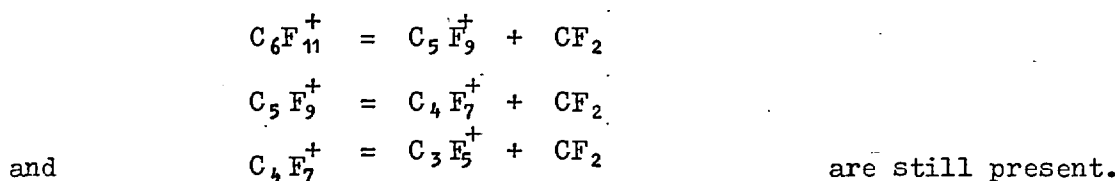
The symmetrical rupture, which dominates the mass spectrum of 1,2-dichlorohexafluorocyclobutane, is very much in evidence in this spectrum, too. The proposed mechanism for the breakdown of <u>cis-trans-</u>1,2-di(trifluoromethyl)-hexafluorocyclobutane (Fig. 3.7) also shows other similarities with the fragmentation pattern of the 1,2-dichlorohexafluorocyclobutane.

3.2.1c   The nuclear magnetic resonance spectrum

The ^{19}F NMR spectrum of the purified product of cyclodimerization of hexafluoropropene was reported by Stockwell. The eleven peaks observed were assigned to the isomers of di(trifluoromethyl)-hexafluorocyclobutane. Atkinson and Stockwell[4] reported the spectrum of each individual isomer. Solvent effects were avoided by using pure undiluted compound and employing trifluoroacetic acid (TFA) as an external standard. CCl_4 was used as solvent in some spectra of 1,3 isomers.
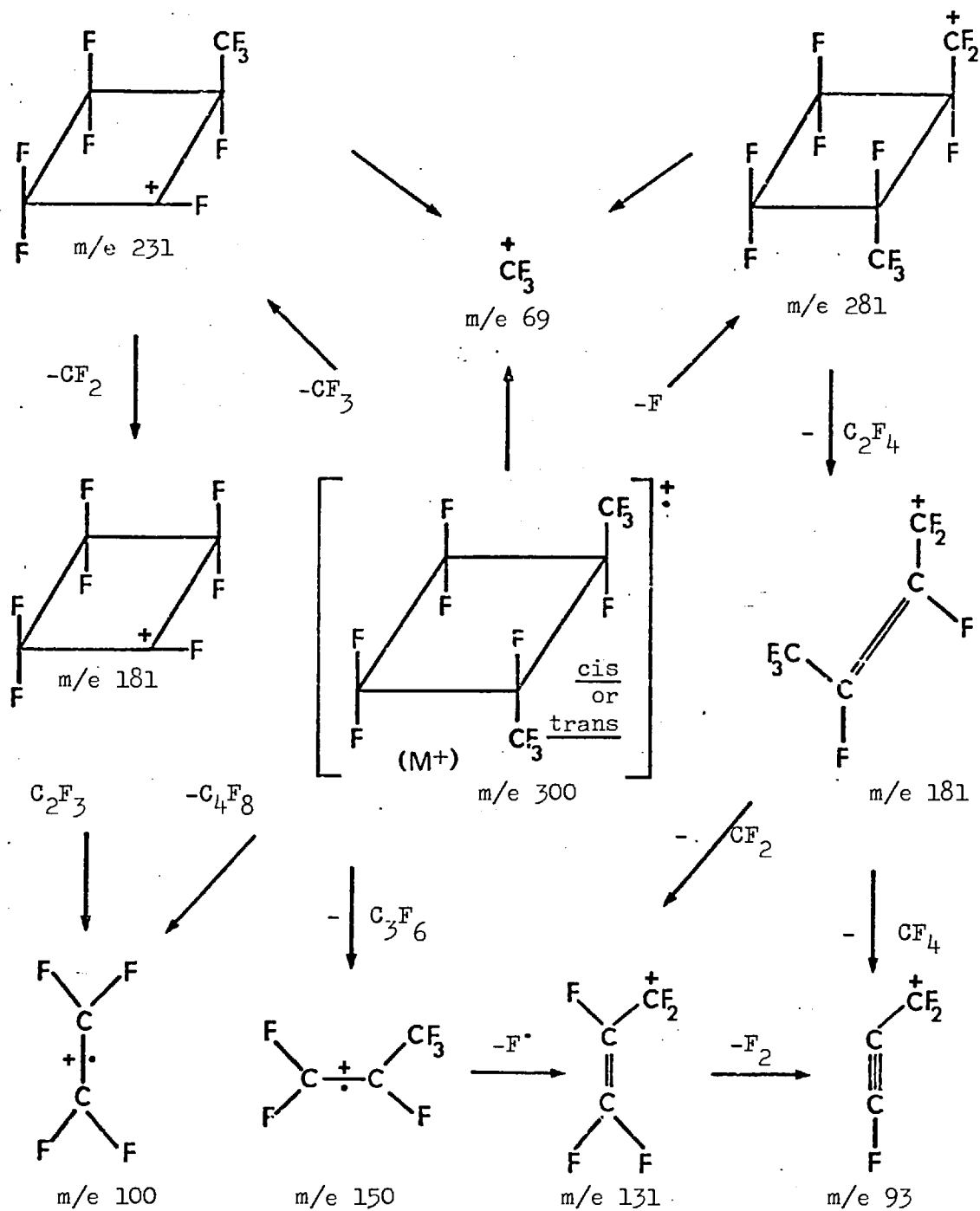
Figure 3.7   Proposed fragmentation mechanism for 1,2-di(trifluoro-

methyl)-hexafluorocyclobutane

The present ^{19}F NMR spectrum of di(trifluoromethyl)-hexafluorocyc-
lobutanes, recorded as described in 2.3.4, showed three groups of peaks,
as expected, at greatly differing fields. The most numerous group,
resonating at 3117 Hz - 3754 Hz downfield relative to hexafluoroben-
zene, is indicative of fluorine nuclei in the $-CF_2-$ groups. Some of
the eleven peaks of the entire spectrum were separated into two or more
overlapping peaks on higher resolution. The chemical shifts (C_6F_6 $\delta = 0$,
$CF_3 COOH$ $\delta = 86$) are almost identical with those reported by Atkinson
and Stockwell[4]. In the cis - 1,2 isomer, the coupling constant J of
the $-CF_2-$ AB pairs was 230 Hz .

GROUP	isomer	δ this work	δ (4)	isomer	δ this work	δ (4)
CF₃	cis-1,2	88.9	88.9	trans-1,2	88.9	88.9
	cis-1,3	89.8	91.0	trans-1,3	89.2	89.3
	cis-1,2	35.3	35.1	trans-1,2	34.5	34.3
	cis-1,2	33.5	33.5			
CF₂	cis-1,3	39.4	39.4	trans-1,3	37.0	36.5
	cis-1,3	39.8	39.7			
CF	cis-1,2	-30.6	-30.5	trans-1,2	-29.1	-29.0
	cis-1,3	-23.8	-23.7	trans-1,3	-26.6	-26.5
	cis-1,3	-25.4	-25.3	trans-1,3	-28.2	-28.0

The four isomers of di(trifluoromethyl) hexafluorocyclobutane
were also present in a sample separated from the products of co-di-
merization between hexafluoropropene and chlorotrifluoroethene. The
ratio of isomers cis-1,2 : trans-1,2 : cis-1,3 : trans-1.3, determined
from the $-CF_2-$ group peak areas, was 22 : 6 : 0.4 : 2.

The assignment of peaks to cis or trans -1,3 isomers is somewhat speculative based on the symmetry of the molecules and the effect of the -CF$_3$ group on adjacent -CF$_2$- groups.

3.2.2. The Preliminary experiments

A series of experiments was carried out in carefully controlled conditions. Pressure changes were monitored with the pressure transducer. The e.m.f. of the thermocouple was recorded continously. The reactor was well seasoned by a series of long qualitative pyrolyses of hexafluoropropene. Analysis of the reaction mixture by gas chromatography was carried out as described in the experimental section (2.1), although in the preliminary work conditions were not as rigorously controlled as in the later experiments. The total quantity of material extracted as samples during each experiment did not exceed 0.5% of the amount originally present. Analysis using the squalane column failed to give adequate separation of the starting material from the products.

In further experiments in which analyses were performed using a Poropak Q column, the peak area of the cyclic dimer of hexafluoropropene depended on the pre-history of the sampling valve. After much investigation including various blank analyses, it was found that the Viton O-rings were both absorbing and desorbing cyclic dimer and desorbing foreign material. These O-rings were replaced by Nitrile rings.

When after exhaustive tests, an entirely satisfactory performance of the gas sampling valve was obtained, a number of new experiments

were designed. Analysis of the reaction mixture was performed with strict adherence to the conditions specified in the experimental section.

In experiment B-16t at 689.7 K, purified hexafluoropropene was admitted to the reaction vessel. The initial pressure was 41.111 kPa after 2.5 minutes. The temperature was recorded continuously and no changes were observed. Samples were taken out of the reaction vessel after 2.10, 4.65 and 7.15 hours from the beginning of the reaction. The chromatographic peak areas were measured using a planimeter as in all subsequent experiments. Apart from the hexafluoropropene and the cyclodimer peaks, two minor peaks emerged, one attributed to tetrafluoroethene and the other to cyclobutane. Analysis of the reaction mixture at column temperature 358 K, ten degrees higher than usual, did not reveal any peaks beyond that of the cyclodimer. A 0.6 cm o.d, 150 cm long column packed with Poropak Q operating at 353 K achieved better resolution but did not indicate the presence of any more peaks.

In experiment B-17t at the same temperature (689.7 K) the initial pressure of hexafluoropropene in the reaction vessel was approximately the same i.e. 42.298 kPa but the reaction time at which the first sample was taken was 4.50 hours. Again, a slight increase in pressure was observed after 2.4 minutes.

Experiment B_16t

Pressure $(\frac{P_a}{Pa})$	Time $(\frac{t}{hours})$	$^{+}C_3F_6$xAtten.	$^{\ddagger}C_6F_{12}$xAtten.	Area ratio
41,131	0			
41,112	2.10	32.3 x 5	20.2 x 5	1.50 x 10^{-2}
40,578	4.65	37.4 x 5	23.6 x10	3.03 x 10^{-2}
40,082	7.15	41.7 x 5	37.0 x10	4.26 x 10^{-2}

Another experiment at lower pressure is detailed blow.

Experiment B_18t

26,262	0			
26,110	5.64	26.0 x 5	22.8 x 10	1.15×10^{-2}
25,830	8.20	25.2 x 5	31.0 x 10	1.48×10^{-2}

+ Area $= A_{r1} \times 10^{-8}$ A

‡ Area $= A_{r2} \times 2.4 \times 10^{-10}$

A typical chromatogram (Figure 3.8) of the analysis of one of these reaction mixtures clearly indicates that the only major product is the cyclic dimer. Calibration of the chromatographic analysis using mixtures of hexafluoropropene and its cyclic dimer, performed at this stage were used to calculate the figures given in Table III.2.1. This table also gives the results of several other experiments. It shows good reproducibility in measurements of rate divided by the square of pressure for experiments at the same temperature. Successive analyses within the one experiment B_16t indicated a decrease in rate possibly caused by back reaction.

The pressure of the reaction mixture P_t at any time is equal to the sum of the partial pressures of its constituents $P_t = \sum\limits_{i=1}^{s} P_i$. The sum of the concentration of the constituents, expressed as equivalent concentration of hexafluoropropene, should at any time be equal to the initial concentration of hexafluoropropene i.e.

$$C_o = \sum\limits_{i=1}^{s} v_i C_i \qquad \text{where } v_i \text{ is the}$$

number of moles of reactant equivalent to one mole of hexafluoropropene.

It had been found that the total pressure of a calibration mixture was indeed the sum of the partial pressures of the constit-
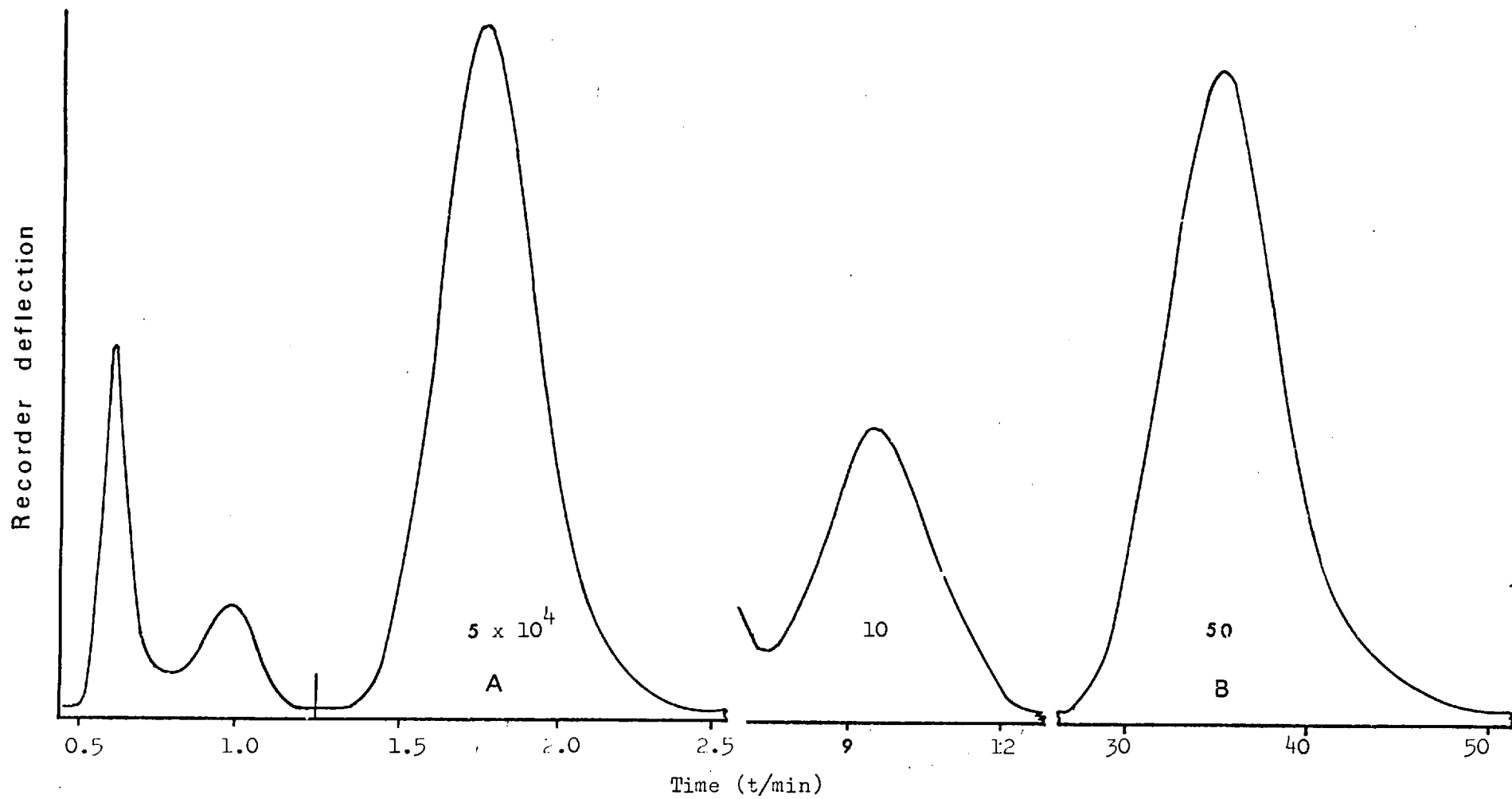
Figure **3.8** Chromatogram of hexafluoropropene Pyrolysis mixture

uents and that the results of the analysis were independent of the temperature (maximum 425 K) at which samples were taken.

It was expected that, within experimental error, the reaction mixture should satisfy these conditions. The results of the experiments as they appear in Table III.2.1. indicate that either the initial pressure was higher than that recorded, or, that there was a contribution of pressure increase from a side reaction. In support of a side reaction was the observed small initial pressure increase during the experiments B_16t to B_23t and the small amount of non-condensable gases present in the reaction mixture at the end of the experiment. The minor reaction products appearing in the chromatograms were not in sufficient amounts to account for the pressure increase.

In an attempt to learn more about the pattern of formation of minor reaction products, samples were taken shortly after the admission of hexafluoropropene into the reaction vessel. The formation of minor reaction products at detectable levels took place after two minutes (experiment B_20t). Tetrafluoroethene reached a maximum ($C_2F_4 < 4 \times 10^{-4} \, C_3F_6$) after 25-40 minutes (experiments, B_22t, B_23t T = 621.8 K) then its formation started to decline sharply.

Some loss of hexafluoropropene was thought to be due to the reaction

$$3SiO_2 + 2C_3F_6 = 3SiF_4 + 6CO$$ 3.2_2
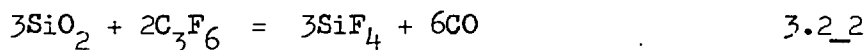
The pressure change will be expressed as

$$dP_r = dP_s + dP_a$$ 3.2_3

where P_s is the pressure of the products formed and P_a the pressure

of the reactant. For reaction 3.2_1 it follows that

$$dP_r = dP_s - \frac{2}{9} dP_s = -\frac{9}{2} dP_\alpha + dP_\alpha = -\frac{7}{2} dP_\alpha \qquad 3.2\_4$$

$$P_t = P_a + P_b + P_s \qquad 3.2\_5$$

where P_b is the pressure of dimer. The total amount of hexafluoro-

propene lost is

$$A = 2\Delta P - \frac{2}{9} \Delta P_s \qquad 3.2\_6$$

$$\therefore \qquad P_o = \sum_{i=1}^{s} \nu_i P_i = P_a + 2P_b + \frac{2}{9} P_s \qquad 3.2\_7$$

Form 3.2.4 and 3.2.6 it follows that

$$9P_o - 2P_t = P_a (7 + 16f) \qquad 3.2\_8$$

The quantities P_o and P_t were measured directly, where $f = \dfrac{Pd}{P_\alpha}$

f was determied by chromatographic analysis. Equation 3.2_7

was used to calculate P_a and for $P_s = 0$ it becomes

$$P_o - P_t = P_a \cdot f \quad \text{or} \quad P_o = P_a (1 + 2f) \qquad 3.2\_9$$

This correction (eq. 3.2_7) did not affect the results significantly

(Table III.2.1). Furthermore quantitative measurements by infra red

spectroscopy confirmed that the amount of the non condensable gases

was negligible. At the end of the experiment B_24t (75 hours,

$P_o = 23.774$ kPa) the bulk of the reaction mixture was condensed in

a trap cooled by melting toluene (178.1 K) until the pressure was reduced to 5.454 kPa (= 41 Torr). A sample of the vapour was taken. Its spectrum was compared with the spectrum of pure hexafluoropropene at the same pressure and no significant difference (d<2%) was observed.

In experiments B_16t to B_19t the amount of dimer formed is significant and the reverse reaction should be taken into account.

The specific reaction rate constants for the dissociation of the cis and trans 1,2-Di(trifluoromethyl)-hexafluorocyclobutane as given by Atkinson and Stockwell[4] are

$$k_{-2a} = 1.18 \times 10^{15} \exp \left(\frac{-268,620}{RT}\right) s^{-1}$$

and

$$k_{-2b} = 4.30 \times 10^{15} \exp \left(\frac{-268,620}{RT}\right) s^{-1} \text{ respectively,}$$

For the results of Table III.2.1. their average

$$\overline{k}_{-2b} = 2.74 \times 10^{15} \exp \left(\frac{-268,620}{RT}\right) s^{-1} \text{ was taken}$$

as the appropriate value. Later a more refined estimate was used (see Appendix II). The amount of the dimer dissociated $- \Delta B$ was calculated from the formula:

$$- \Delta B = B \exp \left(\overline{k}_{-2} \, t\right) - B \approx B \, \overline{k}_{-2} \, t$$

where t is the reaction time and B is the concentration of the cyclodimer as determined from the analysis. The last column of Table III.2.1. gives corrected values of the figures in column 9 calculated by adding ΔB to the experimental values for dimer yield.

The dependence of reaction rate on the pressure of reactants, all the other variables being kept constant, expressed as in

Table III.2.1.

Analyses and preliminary specific rate constants for the cyclodimerization of $CF_2 = CFCF_3$

Temp.	Exper.	Time t/min	Press. Pa/kPa	C_3F_6 +A_{ri}	c.$C_4F_6(CF_3)_2$ ‡A_{ri}	Area ratio	$P_r = \dfrac{c.C_4F_6(CF_3)_2}{C_3F_6}$	$\dfrac{P_r}{.t}\,(\dfrac{7}{2})$	$\dfrac{P_r}{P_a t}\,(\dfrac{6}{2x3})$	$\dfrac{k}{kPa^{-1}.min^{-1}}$
689.7 K	B_16t.1	126	41.11	32.3x5	20.2x5	150×10^{-4}	75.3×10^{-4}	5.97x*	14.5×10^{-7}	15.9×10^{-7}
	.2	279	40.80	37.4x5	23.6x10	303×10^{-4}	$152\ \times 10^{-4}$	5.45x*	13.4×10^{-7}	16.1×10^{-7}
	.3	429	39.97	41.7x5	37.0x10	426×10^{-4}	$214\ \times 10^{-5}$	4.98x	12.4×10^{-7}	16.3×10^{-7}
	B_17t.1	270	42.30	22.6x10	28.9x10	307×10^{-4}	$154\ \times 10^{-4}$	5.71x*	13.5×10^{-7}	16.2×10^{-7}
	.2	360	39.60	27.2x10	43.3x10	379×10^{-4}	$190\ \times 10^{-4}$	5.31x*	13.4×10^{-7}	17.0×10^{-7}
	B_18t.1	338	26.26	26.0x5	24.7x5	228×10^{-4}	$114\ \times 10^{-4}$	3.38x*	12.9×10^{-7}	16.1×10^{-7}
	.2	492	26.08	25.2x5	31.0x5	296×10^{-4}	$148\ \times 10^{-4}$	3.02x	11.6×10^{-7}	15.8×10^{-7}
	B_19t.1	378	15.66	34.3x2	22.2x2	155×10^{-4}	77.8×10^{-4}	2.06x*	13.2×10^{-7}	16.9×10^{-7}
	.2	532	15.61	32.6x2	26.0x2	192×10^{-4}	96.4×10^{-4}	1.81x	11.6×10^{-7}	16.2×10^{-7}
621.8	B_20t.1	250	24.89	16.0x5	3.2x1	9.6×10^{-4}	4.81×10^{-4}	1.92x**	7.73×10^{-8}	7.74×10^{-8}
	.2	372	24.79	16.8x5	4.4x1	14.7×10^{-4}	7.38×10^{-4}	1.98x	8.00×10^{-8}	8.02×10^{-8}
622.1	B_21t.1	1190	26.19	22.9x5	24.6x1	51.4×10^{-4}	25.7×10^{-4}	2.17x**	8.24×10^{-8}	8.28×10^{-8}
	.2	2760	25.78	25.2x5	31.5x5	$120\ \times 10^{-4}$	60.2×10^{-4}	2.18x**	8.46×10^{-8}	8.56×10^{-8}
	.3	3819	25.41	24.2x5	43.0x2	$160\ \times 10^{-4}$	80.4×10^{-4}	2.10x	8.29×10^{-8}	8.43×10^{-8}

A_{ri} = area x attenuation

+Area = A_{ri} x 10^{-8}A

‡Area = A_{r2} x 2.4 x 10^{-10}A

* = 10^{-5}

** = 10^{-6}

equation 3.1_2

reaction rate $\qquad r = \dfrac{dP_i}{dt} = k \prod_{i=1}^{s} P_i^{ni}$ $\qquad\qquad$ 3.1_2

indicated a second order reaction as can be seen from Table III.2.1. Column 9 gives k_2' for $n_i = 1$ and column 10 (11) give k_2' for a second order reaction. From the same table it can also be concluded that the reaction order is independent of temperature and pressure.

3.2.3 Treatment of experimental measurements

The chemical equation for the system is

$$2CF_2 = CFCF_3 \underset{k_{-2}}{\overset{k_2}{\rightleftharpoons}} \quad c - C_4F_6(CF_3)_2 \qquad\qquad 3.2\_1$$

or

$$2A \underset{k_{-2}}{\overset{k_2}{\rightleftharpoons}} \quad B \qquad\qquad 3.2\_11$$
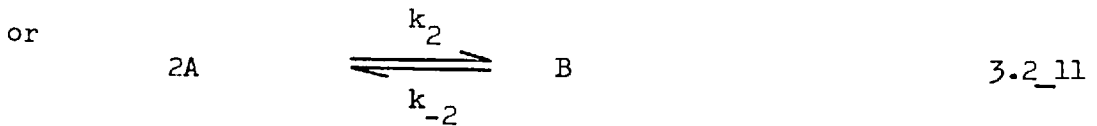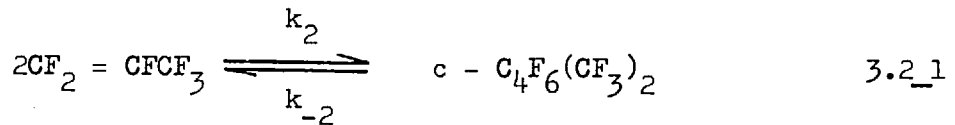
For the forward reaction k_2 is defined as

$$-\dfrac{dA}{2dt} = k_2 A^2 \qquad\qquad 3.2\_12$$

and it is expressed in $m^3\ mol^{-1}\ s^{-1}$. A is the concentration of monomer and B that of the cyclodimer.

The process is reversible. The direct second order reaction is opposed by one of the first order.

$$-\tfrac{1}{2}\dfrac{dA}{dt} = k_2 A^2 - k_{-2}B \qquad\qquad 3.2\_13$$

It can be easily seen that

$$-\tfrac{1}{2}\frac{dA}{dt} = \frac{dB}{dt} \qquad\qquad 3.2\_14$$

from equations 3.2_13 and 3.2_14 follows that

$$\frac{dB}{dt} = k_2 A^2 - k_{-2}B \qquad\qquad 3.2\_15$$

Since the change of A is very small the term $k_2 A^2$ may be regarded as constant

$$\frac{dB}{dt} = a - k_{-2}\,B \qquad\qquad 3.2\_16$$

Let $\qquad a - k_{-2}B = x$ $\qquad\qquad\qquad$ 3.2_17

$\therefore$ $\qquad\qquad\qquad -k_{-2}\,dB = dx$ $\qquad\qquad$ 3.2_18

and $\qquad\qquad\qquad \dfrac{dx}{x} = -k_{-2}dt$ $\qquad\qquad$ 3.2_19

Integration gives $\qquad\qquad x = C \exp(-k_2 t)$ $\qquad$ 3.2_20

at $\quad t = 0$ $\qquad\qquad C \equiv x_0 = a - k_{-2}B_0$ $\qquad$ 3.3_21

thus $\qquad a - k_{-2}B_0 = (a - k_2 B)\exp(k_{-2}t)$ $\qquad$ 3.2_22

therefore $\qquad a = k_{-2}\ \dfrac{B \exp(k_{-2}t) - B_0}{\exp(k_{-2}t) - 1}$ $\qquad$ 3.2_23

Since $\qquad \exp(k_{-2}t) = 1 + \dfrac{k_{-2}t}{1} + \dfrac{(k_2 t)^2}{2.} + \dfrac{(k_{-2}t)^n}{n.}$ $\quad$ 3.2_24

ignoring the higher terms one gets $\quad \exp(k_{-2}t) = 1 + k_{-2}t$ $\quad$ 3.2_25

$$\therefore \quad a = \frac{B (1 + k_{-2}t) - B_o}{t} \qquad 3.2\_26$$

Substitution gives $\quad k_2 = \frac{(B-B_o) + Bk_{-2}t}{tA^2} \qquad 3.2\_27$

where $A \equiv (A_o \cdot Af)^{\frac{1}{2}}$ is the geometric mean of the initial

and final concentration of the monomer and k_{-2} is the specific

rate constant for the dissociation of the cyclic dimer.

For $B_o = 0$ equation 3.2_23 becomes

$$k_2 = \frac{\exp (k_{-2}t)}{tA_o} \cdot f \qquad 3.2\_28$$

where $f = P_b : P_a$ is the dimer to monomer ratio as described by

chromatographic analysis.

Loss of material occuring as a result of taking samples was

taken into account in the calculation of the specific rate constant.

From equation 3.2_28 follows that

$$k_2 = \frac{B \exp (k_{-2}t)}{(t_1 + t_2)A_oA_f} = \frac{B' \exp (k_{-2}t)}{(t_1 + t_2)A_oA_f'} \qquad 3.2\_29$$

where $t_1 + t_2 = t$ and A_f' and B' are the concentrations of hexafluoro-

propene and its cyclodimer after taking the sample (ignoring the

small 'deadspace' effect). For multiple sampling, equation 3.2_29

may be written as

$$k_2 = \frac{B \exp (k_2 t_o)}{A_o \sum_{j=1} A_j t_j} \qquad 3.2\_30$$

where A_j is the concentration of hexafluoropropene at the end of the

period t_j ($=t_j - t_i$) and to the overall reaction time.

Alternatively each analysis may be treated as a separate

experiment by employing equation 3.2_27 in the form

$$k_2 = \frac{(B_j - B_i) + B_j k_{-2} t_j}{t_o A_i A_j} \qquad 3.2\_31$$

where B_i is the concentration of cyclodimer at the beginning of

period t_j and B_j the concentration at the end of this period before

sampling.

Equations 3.2_28, 3.2_30 and 3.2_31 were used to calculate

the specific rate constant.

3.2.4 Quantitative Measurement of the reaction rate in the region

570 K - 700 K

It was shown in sections 3.2.1 and 3.2.2. that the main reaction

of hexafluoropropene below 750 K is the formation of cis and trans

1,2-di(trifluoromethyl)-hexafluorocyclobutane and that the experi-

mental reaction order is two. It was also demonstrated that the

reaction can be followed to a reasonable degree of accuracy by gas

chromatography. It was by this means that the partial pressures

of the constituents were calculated and the specific reaction rates

were determined from equations. 3,2_23, 3.2_28 and 3.2_30 or 3.2_28.

Experiments were performed over the temperature range 570 K

to 700 K and the pressure range 7 kPa to 60 kPa. At each temperature

at least two experiments were performed. Some select replicate

experiments were performed in order to confirm the reproducibility
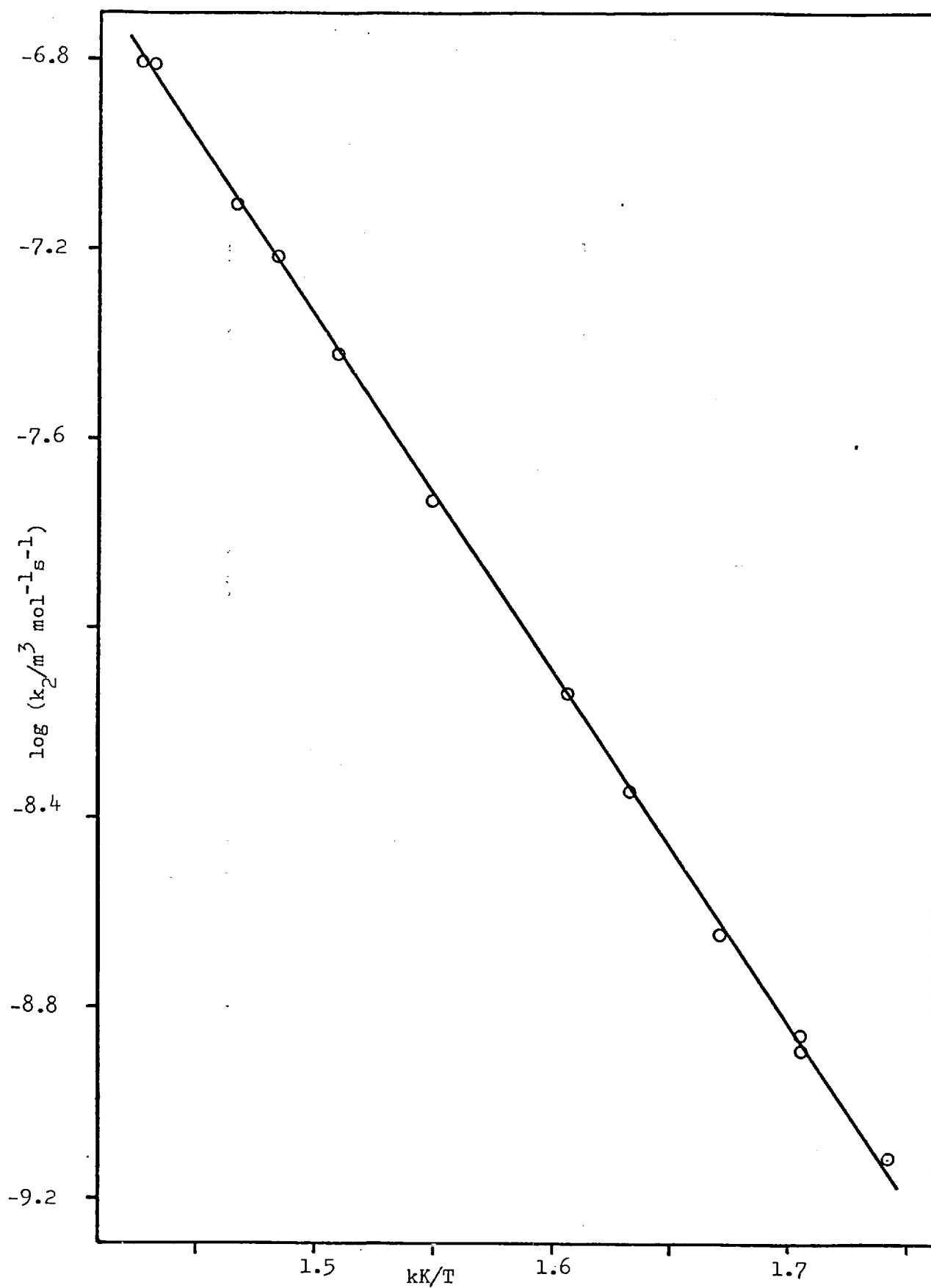
Figure **3.9** Graph of the logarithms of specific rate constants (k_2)

V. the reciprocal of temperature (K/T) for the cycloaddition of

hexafluoropropene

of the results. It was found that the specific rate constant was not affected by twofold variations of pressure or by the duration of the experiments. The concentration of cyclodimer produced was never more than 1.5 per cent of the hexafluoropropene concentration and usually only a few parts per thousand. Despite this restriction to low conversions the reaction times were rather long.

Comparison between specific rate constants derived from relatively high pressures and short reaction times and those resulting from relatively low pressures and long reaction times did not indicate any significant and meaningful differences.

Differences as high as 40% were observed in the value of the specific reaction constant if the reverse reaction was not taken into account. For experiments at which samples were taken at equal time intervals, lower values for the specific reaction constant were obtained as the reaction progressed. This was especially noticed in the upper end of the temperature range. For experiments performed at temperatures below 625 K such corrections for the back reaction did not normally exceed 0.3% which is well within the experimental error.

The results are given in Table III.2.2. and an Arrhenius graph of $\log k_2$ against $\frac{K}{T}$ is shown in Figure 3.9   A straight line for all the points was fitted by the method of least squares. The parameters of the straight line were then refined by excluding all the experiments in which the logarithm of the experimental value of k_2 differ by more than 0.03 from the calculated one using the parameters so obtained. The Arrhenius equation derived was

$$\log \left(\frac{k_2}{m^3 \, mol^{-1} s^{-1}} \right) = 3.91 \pm 0.02 - (7505 \pm 14) \frac{K}{T}$$

The errors shown are standard errors.

Table III 2.2.

Analyses and specific rate constants for the cyclodimerization of hexafluoropropene

Experiment	Temperature T/K	Pressure P_a/Pa	Time t/hours	$CF_2{:}CFCF_3$ [+]A_{r1}	$c\text{-}C_4F_6(CF_3)_2$ [‡]A_{r2}	$\dfrac{c\text{-}C_4F_6(CF_3)_2}{CF_2{:}CFCF_3} \times 10^4$	$\dfrac{k_2}{m^3\ mol^{-1}s^{-1}}$	$-\log k_2$	$\Delta\log k_2$
B31 - 1.1	574.2	40,078	14.08	27.4 <u>x 10</u>	7.3	3.2	7.05 $\left.\right]$ x 10^{-10}	9.152	0.006
.2		39,613	21.38	27.9	10.6	4.6	6.69	9.174	-0.016
B31 - 2.1	574.2	46,529	14.48	33.4	9.9	3.6	6.88 $\left.\right]$ x 10^{-10}	9.166	-0.008
.2		46,000	21.56	32.9	15.0	5.6	7.17	9.145	0.013
.3		45,479	37.60	32.7	25.9	9.5	7.30	9.137	0.021
.4		44,951	46.30	31.7	31.2	11.8	7.50	9.125	0.029
B31 - 3.1	574.4	52,815	14.30	37.7	13.0	4.2	7.14	9.147	0.007
.2		52.198	19.52	38.2	17.4	5.5	7.15	9.145	0.009
.3		51,629	24.95	37.3	21.7	7.0	7.20	9.143	0.011
B33 - 1.1	586.3	26,276	14.05	20.2	6.6	3.9	1.39 $\left.\right]$ x 10^{-9}	8.863	0.025
.2		25,962	20.15	20.3	9.4	5.6	1.37	8.864	0.024
.3		25,689	23.95	20.0	11.0	6.5	1.35	8.865	0.023
B33 - .1	586.3	45,943	13.63	35.0	18.7	6.4	1.29 $\left.\right]$ x 10^{-9}	8.889	-0.001
.2		45,380	20.58	32.5	25.1	9.3	1.28	8.892	-0.004
.3		44,864	24.08	32.3	28.5	10.7	1.27	8.896	-0.008

[+]A_{r1} = area in cm^2 $A \times 10^{-8}$ [‡]A_{r2} = area in cm^2 24×10^{-11} A

Table III 2.2. cont.

Experiment	Temperature T/K	Pressure P_a/Pa	Time t/hours	$CF_2\!:\!CFCF_3$ A_{r1}	$c\text{-}C_4F_6(CF_3)_2$ A_{r2}	$\dfrac{c\text{-}C_4F_6(CF_3)_2}{CF_2\!:\!CFCF_3} \times 10^4$	$\dfrac{k_2}{m^3\ mol^{-1}s^{-1}}$	$-\log k_2$	$\Delta\log k_2$
B30 - 1.1	598.6	46,680	15.00	32.5 ⎤ x 10	33.7	12.5	2.48 ⎤ x 10^{-9}	8.606	
.2		46,031	23.30	31.9 ⎥	25.3 x 2	19.1	2.35 ⎥	8.628	-0.003
.3		45,444	38.05	31.5 ⎥	40.2 x 2	30.6	2.35 ⎥	8.629	-0.004
.4		44,824	46.18	31.3 ⎦	18.5 x 5	35.6	2.40 ⎦	8.620	0.006
B30 - 2.1	598.6	36.478	14.25	25.3 ⎤ x 10	18.1	8.6	2.26 ⎤ x 10^{-9}	8.646	-0.021
.2		36.014	19.25	25.4 ⎥	25.5	12.1	2.25 ⎥	8.648	-0.023
.3		35,638	23.26	24.8 ⎦	30.1	14.6	2.28 ⎦	8.641	-0.016
B32 - 1.1	612.8	31.441	13.52	22.1 ⎤ x 10	25.3	13.8	4.54 ⎤ x 10^{-9}	8.342	-0.008
.2		30.985	18.52	21.6 ⎥	33.6	18.7	4.49 ⎥	8.347	-0.012
.3		30.605	22.53	21.8 ⎦	41.1	22.7	4.46 ⎦	8.351	-0.016
B32 - 2.1	612.8	21.790	14.37	31.3 ⎤ x 5	13.0	10.0	4.29 ⎤ x 10^{-9}	8.367	-0.032
.2		21.495	18.37	31.3 ⎥	16.1	12.4	4.30 ⎥	8.366	-0.031
.3		21,242	22.70	31.2 ⎦	19.5	15.1	4.16 ⎦	8.380	-0.039
B28 - 1.1	621.8	18.186	14.17	27.5 ⎤ x 5	14.8	13.0	7.14 ⎤ x 10^{-9}	8.146	0.017
.2		17.976	18.67	26.2 ⎥	18.6	16.9	6.93 ⎥	8.159	-0.001
.3		17.838	22.77	26.4 ⎦	23.5	21.5	7.10 ⎦	8.148	0.010

Table III 2.2. cont.

Experiment	Temperature T/K	Pressure p_a/Pa	Time t/hours	$CF_2{:}CFCF_3$ A_{r1}	$c{-}C_4F_6(CF_3)_2$ A_{r2}	$\dfrac{c{-}C_4F_6(CF_3)_2}{CF_2{:}CFCF_3} \times 10^4$	$\dfrac{k_2}{m^3\,mol^{-1}s^{-1}}$	$-\log k_2$	$\Delta\log k_2$
B28 - 2.1	622.4	47,628	14.77	37.4] x 10	18.9] x 5	34.7	7.13] x 10⁻⁹	8.147	-0.001
.2		46.725	19.02	31.9	23.7	45.5	7.57	8.124	0.022
.3		46,073	23.18	31.9]	29.3]	55.4	7.13]	8.147	-0.001
B28 - 3.1	622.4	20,289	13.08	30.1] x 5	18.3	14.7	7.22] x 10⁻⁹	8.142	0.004
.2		21.958	18.08	30.1	25.1	20.1	7.18	8.144	0.002
.3		21,647	22.08	30.6]	30.6	24.1	7.03]	8.153	-0.007
B28 - 4.1	622.4	25.834	12.37	35.4] x 5	22.7	15.4	7.18] x 10⁻⁹	8.144	0.002
.2		25,458	16.93	35.5	31.6	21.4	7.18	8.144	0.002
.3		25,122	21.32	36.0]	41.0	27.5	7.08]	8.150	-0.004
B29 - 1.1	645.2	25,562	14.55	35.2] x 5	33.2] x 2	45.4	1.84] x 10⁻⁸	7.735	-0.015
.2		25,027	18.80	35.3	42.8	58.4	1.86	7.729	-0.009
.3		24,655	22.85	34.3]	50.4]	70.6	1.88]	7.726	-0.006
B29 - 2.1	645.1	13.311	12.80	18.3] x 5	15.8	20.9	1.84] x 10⁻⁸	7.734	-0.012
.2		13.097	16.93	17.9	20.3	27.3	1.80	7.744	-0.022
.3		12,925	21.48	18.3]	25.3	25.3	1.78]	7.749	-0.027

Table III 2.2. cont.

Experiment	Temperature T/K	Pressure P_a/Pa	Time $t/hours$	$CF_2{:}CFCF_3$ A_{r1}	$c{-}C_4F_6(CF_3)_2$ A_{r2}	$\dfrac{c{-}C_4F_6(CF_3)_2}{CF_2{:}CFCF_3} \times 10^4$	$\dfrac{k_2}{m^3\,mol^{-1}s^{-1}}$	$-\log.k_2$	$\Delta\log k_2$
B29 – 3.1	645.2	49,838	4.03	36.3 x 10	15.0 x 5	24.7	1.85 x 10^{-8}	7.732	-0.012
.2		48,992	7.03	33.7	23.9	42.8	1.84	7.734	-0.014
.3		48,230	10.03	33.6	34.6	62.1	1.92	7.717	0.003
B26 – 1.1	662.7	25.764	4.00	36.5 x 5	38.4	25.4	3.86 x 10^{-8}	7.413	0.000
.2		25,410	7.00	36.2	33.3 x 2	44.4	3.88	7.411	0.002
.3		25,247	8.00	35.9	42.3 x 2	56.7	3.83	7.416	-0.003
B26 – 2.1	662.7	23,910	4.25	33.5 x 5	35.5	25.5	3.89 x 10^{-8}	7.410	0.003
.2		23,580	7.08	34.3	28.8 x 2	40.4	3.69	7.433	-0.020
.3		23,313	9.50	34.2	38.3 x 2	54.0	3.77	7.424	-0.011
B26 – 3.1	662.7	20,429	4.25	28.8 x 5	25.1	21.0	3.74 x 10^{-8}	7.427	-0.014
.2		20,168	7.55	30.3	45.9	36.5	3.70	7.432	-0.019
.3		19,950	10.50	30.0	30.9 x 2	49.6	3.70	7.432	-0.019
B24 – 1.1	673.7	24.087	14.20	22.9 x 5	22.3 x 5	117	5.86 x 10^{-8}	7.232	-0.004
.3		23.280	25.60	21.3	33.7	191	5.84	7.233	-0.005
B24 – 2.1	673.7	18.133	14.73	41.9 x 2	30.5 x 2	30.5	5.74 x 10^{-8}	7.241	-0.013
.2		17.678	19.23	40.9	38.7	114.1	6.00	7.222	0.006
.3		17.135	24.68	40.2	47.7	143	5.90	7.229	-0.001

Table III 2.2. cont.

Experiment	Temperature T/K	Pressure P_a/Pa	Time t/hours	CF_2CFCF_3 A_{r1}	$c\text{-}C_4F_6(CF_3)_2$ A_{r2}	$\dfrac{c\text{-}C_4F_6(CF_3)_2}{CF_2{:}CFCF_3} \times 10^4$	$\dfrac{k_2}{m^3\,mol^{-1}s^{-1}}$	$-\log k_2$	$\Delta\log k_2$
B27 – 1.1	681.4	16,288	4.10	23.9 ⎤ x 5	30.6	30.9	7.97 ⎤ x 10^{-8}	7.098	0.004
.2		16,036	7.00	23.9	25.5 x 2	51.4	7.82	7.107	−0.005
.3		15,829	9.85	23.7 ⎦	34.4 x 2	69.9	7.78 ⎦	7.109	−0.007
B27 – 2.1	681.4	15,491	4.05	22.7 ⎤ x 5	28.1	29.78	7.99 ⎤ x 10^{-8}	7.019	−0.004
.2		15,252	7.55	22.9	25.3 x 2	53.3	7.90	7.102	0.000
.3		15,043	10.50	21.9 ⎦	32.5 x 2	71.78	7.91 ⎦	7.102	0.000
B27 – 3.1	681.5	26,233	4.00	36.4 ⎤ x 5	37.7 x 2	49.9	8.19 ⎤ x 10^{-8}	7.087	0.013
.2		25,740	7.75	36.8	28.2 x 5	92.3	7.85	7.104	−0.004
.3		25,303	10.50	36.7 ⎦	37.5 x 5	123.2	8.35	7.078	0.022
B27 – 4.1	681.5	7,835	14.30	29.3 ⎤ x 2	23.1 × 5	47.4	7.96 ⎤ x 10^{-8}	7.099	0.001
.2		7,739	22.70	28.9 ⎦	23.1 × 5	43.0	8.12 ⎦	7.090	0.010
B27 – 5.1	681.5	61,165	2.05	21.2 ⎤ x 20	21.6 ⎤ x 10	61.38	7.92 ⎤ x 10^{-8}	7.101	−0.001
.2		59,859	4.00	21.0 ⎦	42.3 ⎦	121.3	8.37 ⎦	7.077	0.023
B27 – 6.1	681.3	45,149	2.00	32.6 ⎤ x 10	23.0 x 5	42.5	7.98 ⎤ x 10^{-8}	7.098	0.006
.2		44,416	4.00	32.1	23.0 x 10	86.4	8.03	7.095	0.009
.3		43,632	6.00	30.8 ⎦	32.8 x 10	128 . 3	8.33 ⎦	7.079	0.025

Table III 2.2. cont.

Experiment	Temperature T/K	Pressure P_a/Pa	Time t/hours	CF_2CFCF_3 A_{r1}	$c-C_4F_6(CF_3)_2$ A_{r2}	$\dfrac{c-C_4F_6(CF_3)_2}{CF_2:CFCF_3} \times 10^4$	$\dfrac{k_2}{m^3\,mol^{-1}s^{-1}}$	$-\log k_2$	$\Delta\log k_2$
B27 – 7.1	681.5	46.635	2.25	32.9⎤ x 10	26.3 x 5	48.2	7.60⎤ x 10^{-8}	7.119	0.019
.2		45,775	4.25	32.8	25.9 x 10	95.1	8.31	7.080	0.020
.3		44,928	6.30	31.6⎦	36.4 x 10	138.8	8.40⎦	7.076	0.024
B25 – 1.1	698.1	18.641	4.25	44.7⎤ x 2	20.7⎤ x 2	55.8	1.44⎤ x 10^{-7}	6.842	-0.004
.2		18,089	8.00	44.7⎦	34.2⎦	92.2	1.47⎦	6.833	0.006
B25 – 2.1	698.1	24,279	4.55	25,4⎤ x 5	16.1⎤ x 5	76.3	1.48⎤ x 10^{-7}	6.830	0.009
.2		23,384	8.55	24.8	27.3	132.4	1.46	6.836	0.003
.3		22,975	11.20	26.1⎦	36.0⎦	166	1.52⎦	6.818	0.021
B25 – 3.1	698.5	29,949	3.00	42.0⎤ x 5	24.6 x 5	70.6	1.47⎤ x 10^{-7}	6.833	-0.001
.2		28,924	5.00	41.9	19.9 x 10	114.6	1.57	6.804	0.028
.3		28.497	6.50	41.2⎦	23.9 x 10	140	1.49⎦	6.827	0.005
B25 – 4.1	700.4	51,493	3.10	32.4 x 10	35.7⎤ x 10	133	1.53⎤ x 10^{-7}	6.815	-0.012
.2		49,690	5.45	30.4 x 10	55.3⎦	216	1.60⎦	6.796	0.007

3.3   THE THERMAL CYCLOADDITION OF HEXAFLUOROPROPENE

        TO CHLOROTRIFLUOROETHENE

The reaction between chlorotrifluoroethene and hexafluoropropene

has not been reported previously. In trial experiments at 650 K,

chlorotrifluoroethene - hexafluoropropene mixtures containing 2%

of chlorotrifluoroethene were pyrolysed for a period of 2-5 hours

during which samples of the reaction mixture were taken for analysis.

In the chromatograms, apart from the usual peaks from pyrolysis of the

pure constituents of the mixture, a new peak emerged immediately after

the 1,2-di(trifluoromethyl)-hexafluorocyclobutane peak and preceeding

the 1,2-dichlorohexafluorocyclobutane peak (Figure 3.10)

The new compound was prepared and purified as described in 2.3.5.

3.3.1   Identification of 1-Chloro-2-trifluoromethyl-hexafluoro-

          cyclobutane

The infra red and mass spectra of material giving peak D

(Figure 3.10)was identified with those of 1,2-dichlorohexafluoro-

cyclobutane and the compound of peak B was identified spectroscopically

as 1,2-di(trifluoromethyl)-hexafluorocyclobutane. The material of

peak E was isolated and purified chromatographically by recycling it

four times and collecting only the central part of the peak (see also

section 2.3.5). The middle cut was used for spectroscopic measure-

ments. No traces of the starting material were observed but some

1,2-di(trifluoromethyl)-hexafluorocyclobutane (about 0.2%) was still

present.
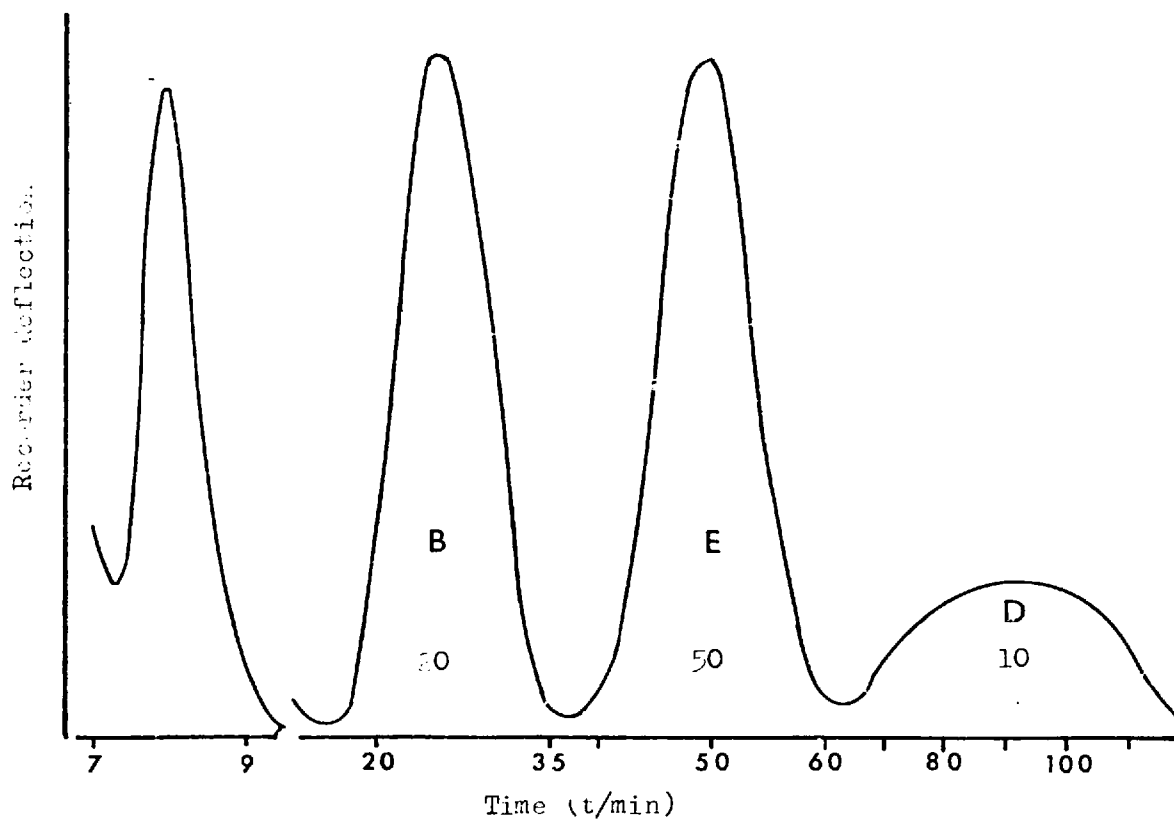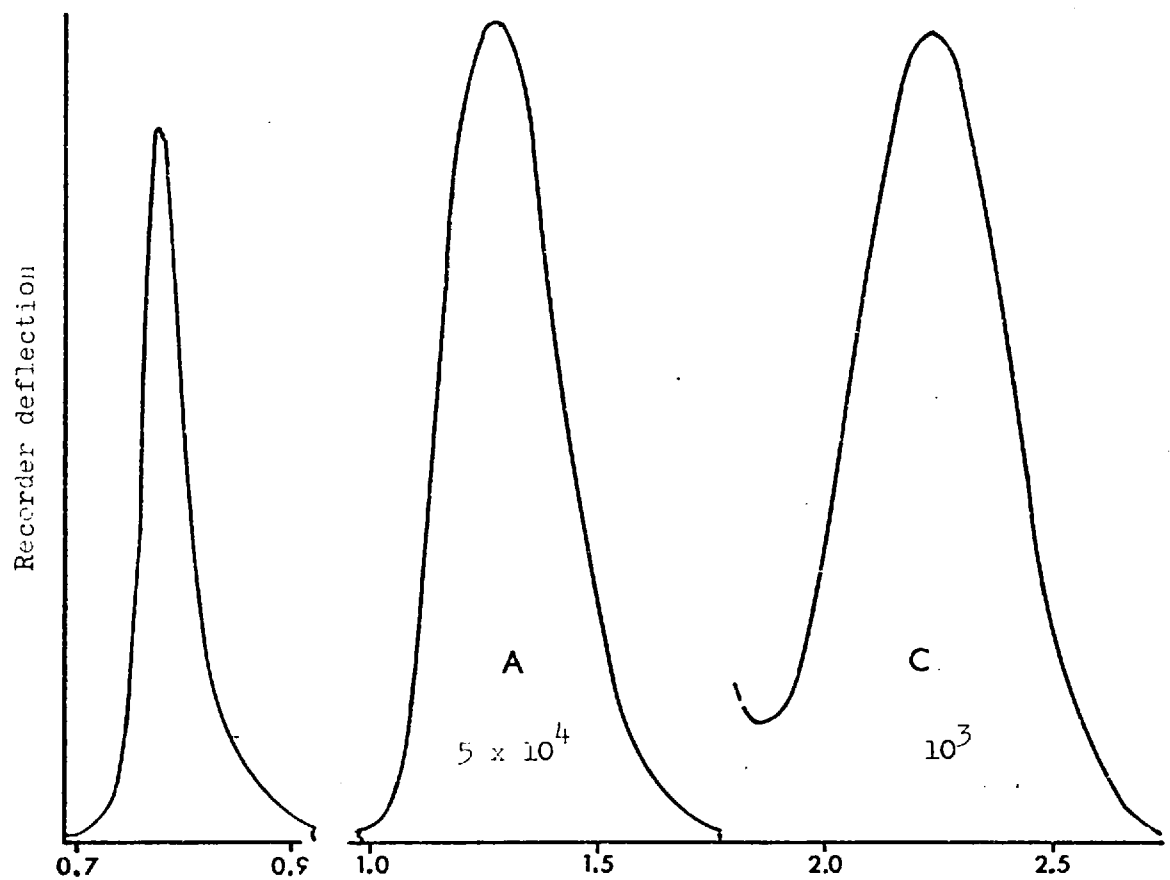
Figure **3.10** Chromatogram of hexafluoropropene-chlorotrifluoro-
ethene pyrolysis mixture

3.31a   Physical properties

The compound is a colourless liquid (room temperature) with an unpleasant smell.   Its physiological and toxicological properties are not known.

1.   Relative molecular mass

The relative molecular mass of the compound was estimated from vapour density measurements.   The vapours of the compound were admitted to one of the calibrated flasks (C in Figure 2.1.) and were allowed at 298 K to reach a pressure not exceeding 18 kPa.   The pressure was measured using the transducer adjacent to the calibrated flask.   Then the gas trapped into the flask was transferred by condensation at liquid nitrogen temperature to a pre-weighed bottle.   The weighing bottle was equipped with a 'rotaflo' greaseless valve to avoid gas absorption and desorption and errors arising from it.   The bottle was removed from the vacuum line and was allowed to reach room temperature before weighing.   In all the subsequent calculations it was assumed that the vapours obeyed the ideal gas laws.   The estimated molecular weight was found to be 266 ± 3.   The theoretical value is 266.5

2.   Vapour pressure

The vapour pressure of the isomeric mixture was measured over the temperature range 242 K to 313 K using an isoteniscope.   The results can be represented by the equation

$$\log P = (9.87 \pm 0.09) - \frac{1570 \pm 18}{T}$$

where P is the vapour pressure in Pascal.

The boiling point given from the previous equation is 322.8 K.

The value obtained by direct measurement was 323.5 K.

3.3.1b   Infrared spectrum
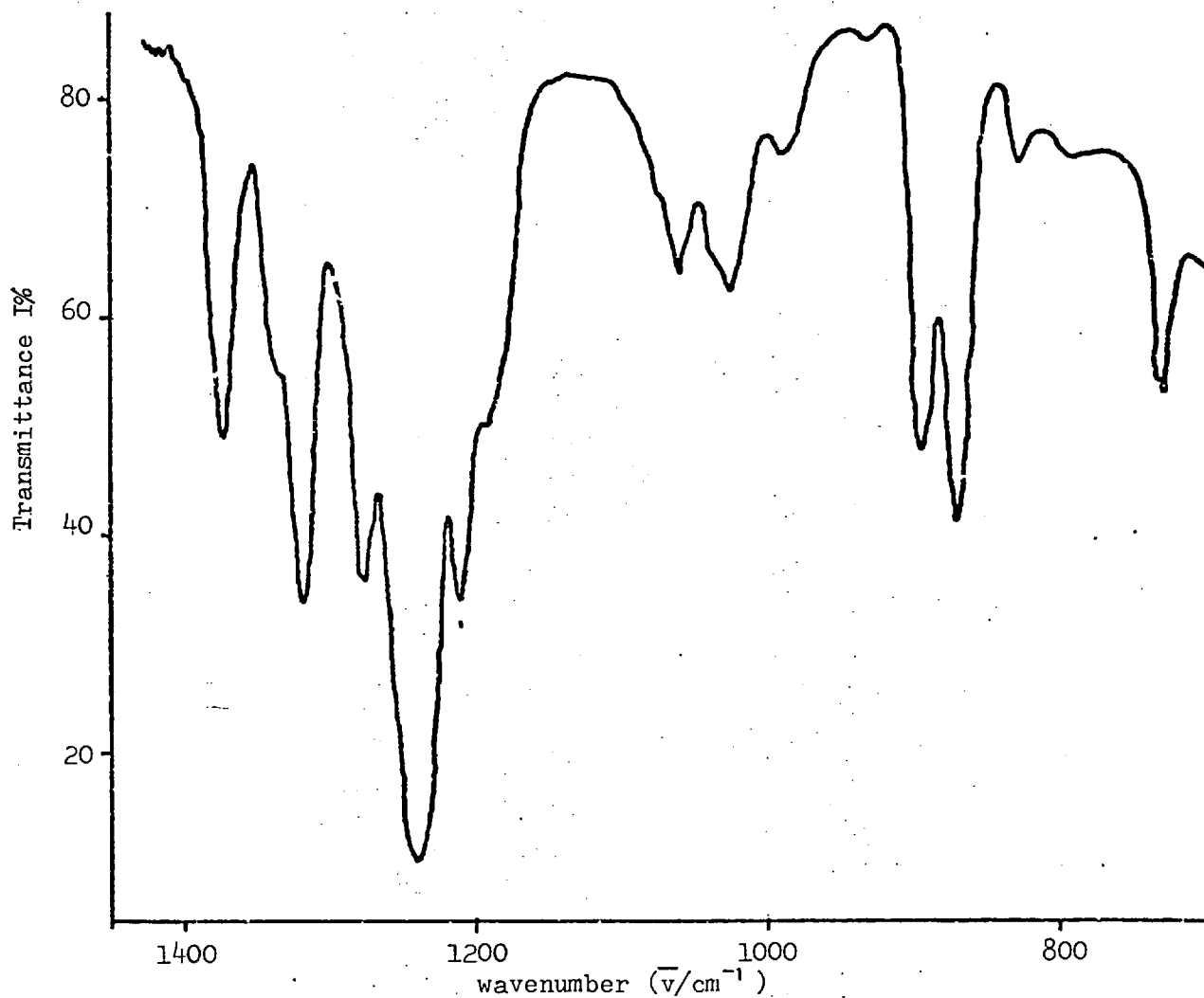
Figure 3.11   Infrared spectrum of 1-chloro-2-trifluoromethyl-hexa-

fluorocyclobutane

The infrared spectrum of 1-chloro-2-trifluoromethyl-hexafluoro-

cyclobutane from 4000 cm^{-1} to 650 cm^{-1} was recorded as described in

section 2.2.2a. Unfortunately it was necessary to use a cell with

rock salt windows which prevented the spectrum being observed in the

region below 650 cm^{-1}. However, since the complete analysis of the

infrared spectrum was beyond the objectives of the present work, this

omission was of little significance. Structural correlations in

fluorocarbons are restricted mainly in the region 1800 cm^{-1} -

800 cm^{-1}. The frequencies of the main absorptions of the isomeric

mixture are given in Table III.3.1. together with the relative

absorbancies.

The spectrum (Figure 3.11) is dominated by strong absorption in

the region of 1150 cm^{-1} - 1400 cm^{-1} probably associated with C-F

stretching vibrations.[125] Absorption in the range 1325 cm^{-1} -

1365 cm^{-1} as well as in the region 730 cm^{-1} to 745 cm^{-1} is associated

with the perfluoromethyl group in a $>CFCF_3$ group. The last region

falls within the domain of resonance (700 cm^{-1} - 750cm^{-1}) of stretching

vibrations of the C-Cl bond in monochlorocompounds. Absorption in the

region 750 cm^{-1} - 960 cm^{-1} is attributed [126] to ring deformation.

Ring stretching vibrations cover the range 1000 cm^{-1} to 1430 cm^{-1}.

The absence of resonance in the region 1650 cm^{-1} to 1800 cm^{-1},

indicated the absence of fluorolefinic double bond.

The relative absorbances of several bands varied, depending on the

conditions of sample formation. The bands 875 cm^{-1}, 997 cm^{-1} and

1285 cm^{-1} were more intense in samples prepared at high temperatures.

In the same spectra, a second group of bands 795 cm^{-1}, 900 cm^{-1},

1065 cm^{-1}, 1218 cm^{-1} and 1323 cm^{-1} appeared to diminish. Correlation

with the results of the analysis of the NMR spectrum suggests that

the first group of bands should be associated with the cis isomer.

Whether these bands are characteristic of each isomer or not, cannot be decided without complete separation of either of the two isomers.

Table III 3.1. Infrared spectrum of 1-chloro-2-trifluoromethyl-hexafluorocyclobutane

wavenumber $(\bar{\nu}/cm^{-1})$	Absorbance %	wavenumber $(\bar{\nu}/cm^{-1})$	Absorbance %
1382	45.3	1029	34.6
1345	38.4	997	13.2
1327	69.2	934	9.3
1323	70.4	900	48.3
1285	69.2	875	59.7
1247	100.0	833	20.6
1218	55.3	795	7.1
1190	39.0	737	30.2
1128	6.3	733	36.7
1083	15.7	729	27.2
1065	15.1		

3.3.1c   The mass spectrum

The mass spectrum of 1-chloro-2-trifluoromethyl-hexafluoro-cyclobutane at 70 eV Ionisation Potential (I.P.), recorded as

described in section 2.2.2b, is given in Figure 3.12 . The molecular

ion (M^+) peak is not observed, as expected, not even in the 16 eV I.P.

spectrum. The more intense peaks appearing at m/e 100 and 116 were

attributed to the ions $CF_2 \overset{+}{\underset{.}{-}} CF_2$ (base peak) and $CF_2 \overset{+}{\underset{.}{-}} CFCl$ respect-

ively. These ions may be produced directly from the molecular ion

peak by homolytic fission of the cyclobutane ring across two oppo-

site carbon-carbon bonds. Such a breakdown, a common feature between
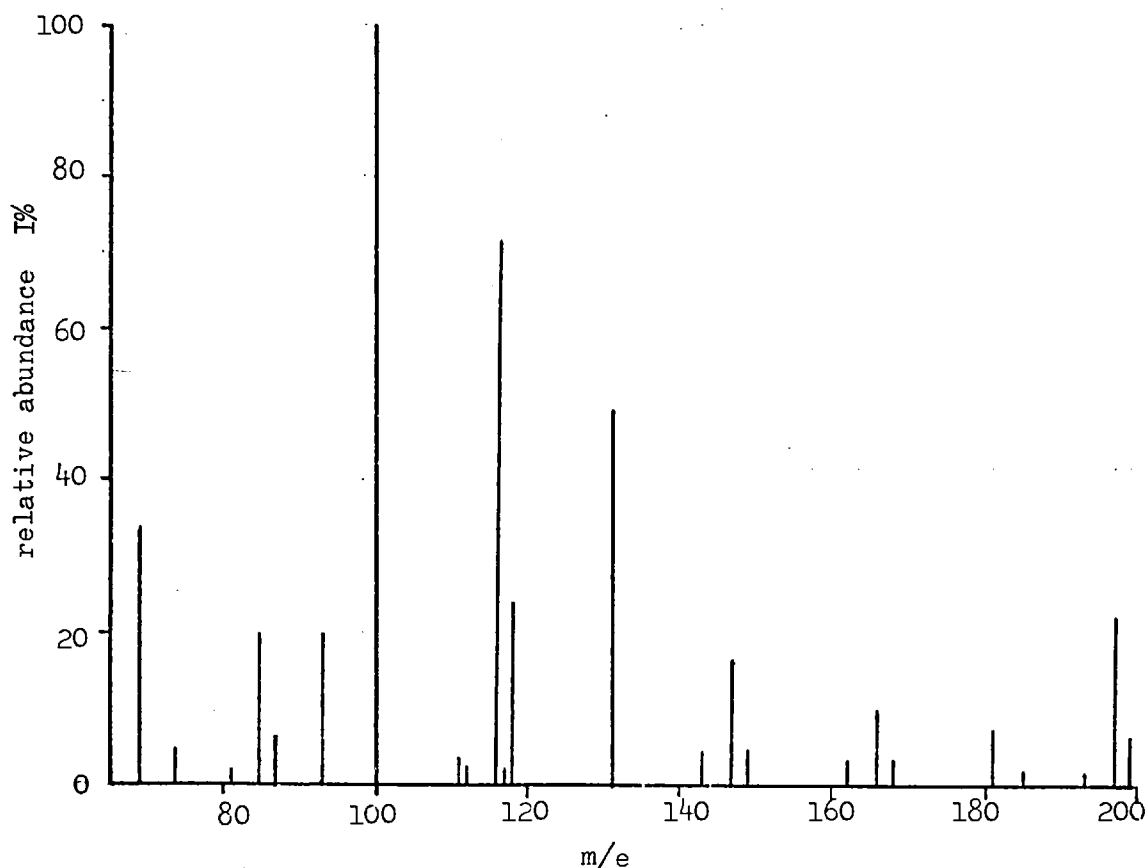
Figure 3.12. Mass apectrum of 1-chloro-2-trifluoromethyl-

hexafluorocyclobutane

Table III.3.2 Mass spectrum relative intensities of 1-chloro-2-

trifluoromethyl-hexafluorocyclobutane *

Ion formulae	m/e	relative intensity I%	Ion formulae	m/e	relative intensity I%
C_5F_9Cl	268	0.0	C_2F_3Cl	118	23.7
C_5F_9Cl	266	0.0	C_2F_3Cl	116	71.4
C_5F_8Cl	249	0.9	C_3F_4	112	2.5
C_5F_8Cl	247	2.9	C_3F_2Cl	111	3.3
C_5F_8	212	2.0	C_3F_2Cl	109	1.0
C_4F_6Cl	199	7.1	C_4F_4	105	1.0
C_4F_6Cl	197	21.7	C_2F_4	100	100.0
C_5F_7	193	1.5	C_2F_2Cl	97	0.9
C_3F_6Cl	187	0.6	C_3F_3	93	20.0
C_3F_6Cl	185	1.9	CF_2Cl	87	6.5
C_4F_7	181	7.6	CF_2Cl	85	19.8
C_4F_5Cl	178	0.7	C_2F_3	81	1.8
C_3F_5Cl	168	3.4	C_3F_2	74	4.3
C_3F_5Cl	166	10.1	CF_3	69	33.4
C_4F_6	162	2.6	$CFCl$	68	0.7
C_3F_6	150	1.2	$CFCl$	66	2.1
C_3F_4Cl	149	5.4	C_2F_2	62	1.2
C_3F_4Cl	147	16.5	C_3F	55	1.6
C_4F_5	143	5.0	CF_2	50	2.1
C_3F_5	131	49.0	CCl	49	0.6
C_4F_4	124	1.5	CCl	47	1.7
C_5F_3	117	1.8	C_2F	43	1.1

* Values below 0.5 and ions having m/e <45 are not included

$$CFCl = CF - \overset{+}{C}F_2$$
m/e 147

m/e 197

$\overset{+}{C}F_3$
m/e 69

$-CF_3$

C_2F_4

m/e 247

$-F$

$- \Big| C_2F_3Cl$

F CF$_2$ C C F F
m/e 131

$-C_4F_7$

$\overset{+}{C}F_2Cl$
m/e 69

cis or trans

m/e 266

$- \Big| F_2$

Cl F C + C F F
m/e 116

$-C_3F_6$

F F + C C F
m/e 93

$-C_2F_3Cl$

$-C_3F_5Cl$

$-C_2F_4$

F CF$_3$ C + C F F
m/e 150

F + F C C F F
m/e 100

Cl + CF$_3$ C C F F
m/e 166
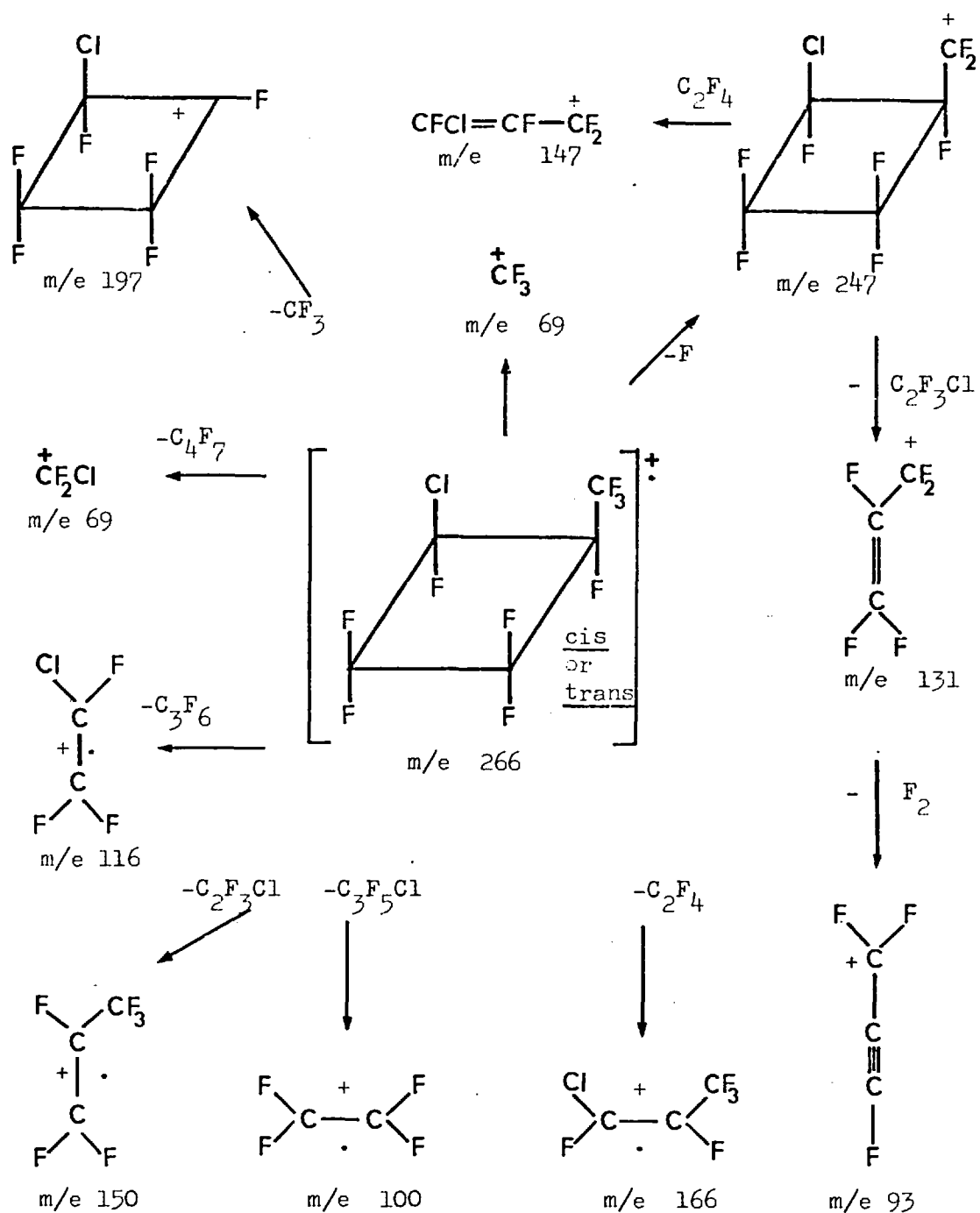
Figure **3.13** Proposed fragmentation mechanism for 1-chloro-2-trifluoromethyl-hexafluorocyclobutane

this compound and the spectra given in 3.1.1b and 3.2.1b, would also explain the intensity of the $C_3F_5Cl^+$ peak as well as that of $C_3F_5^+$. The CF_3 group, present in the mass spectra of substituted perfluorocyclobutanes, (see 3.1.1c) gives an intense peak in this spectrum too. The CF_3^+ can be formed by direct fragmentation or by re-arrangement.

Pairs of peaks were attributed to chlorine containing segments. The peak height ration of these pairs was always 3:1, characteristic of the presences of only one chlorine atom. Correlation of the evidence presented in 3.3.1a, 3.3.1b and the mass spectrum strongly supported the belief that a cyclic compound is produced.

3.3.1d   Nuclear magnetic resonance spectrum

Samples of 1-chloro-2-trifluoromethyl-hexafluorocyclobutane were prepared at 648 K and 678 K, and were purified as described in 2.3.5. The NMR spectrum of the samples was recorded as described in 2.2.2c. The spectrum of each sample comprised 20 well defined peaks. On higher resolution the peaks attributed to -CFCl- and -CFCF$_3$- groups separated each into two overlapping peaks.

The spectrum was interpreted by (non-perfect) first order analysis[127] in order to elucidate the structure of the compound. Doublets having spin-spin coupling constant $J \approx 220$ H$_z$ were assigned to fluorine of the -CF$_2$- groups. The peaks were allocated to two groups. The allocation was based on peak area measurement and on change in peak area ratios observed in recording the spectra of samples synthetized at various temperatures. The peak shapes were identical in

all spectra suggesting that only two isomers were mainly present in the sample and that the level of impurities, if any, was very low.

The effect of substitution by chlorine can be calculated[116]. The spectrum of chloroheptafluorocyclobutane reported by Stedman[112] indicates that substitution of fluorine by chlorine moves adjacent $-CF_2-$ groups by about 6.7 ppm and groups in β position to chlorine by about 3.7 ppm, both to low field (see section 3.1.1c).

Substitution by the $-CF_3$ group into the octafluorocyclobutane ring moves the adjacent $-CF_2-$ groups to low field but this effect has not been studied in detail and information[123] is not available to make full deduction. In the spectra of di(trifluoromethyl)-substituted polyfluorocyclobutanes reported by Atkinson and Stockwell the shift for 1,2 disubstitution is 7.0 ppm and, except for cis-1,2-, separation within the pair has $\delta=0.0$ (see also 3.2.1c).

The results of the analysis of the present spectrum indicate that its origin is cis and trans 1,2- isomers. In isomer A, the chemical shift between two fluorine nuclei in the group adjacent to chlorine is 9.34 ppm, whilst that for the $-CF_2-$ group in β position to the $-CFCl-$ group is only 2.49 ppm. In isomer B the chemical shift between the gem fluorines adjacent to chlorine is 8.05 ppm and for the β position only 4.05 ppm. These last figures are exactly what would be expected for a compound with fluorine replacing the $-CF_3$ group (see section 3.1.1c).

Analysis of figures for 1-chloro-2-trifluoromethyl-hexafluorocyclobutane indicate that the $-CF_3$ group has shifted the adjacent $-CF_2-$ group to low field by 4.69 ppm and the group in β position by 2.85 ppm. These figures are larger than would be predicted from the results for 1,2-di(trifluoromethyl)-hexafluorocyclobutane.

trans

A

cis

B
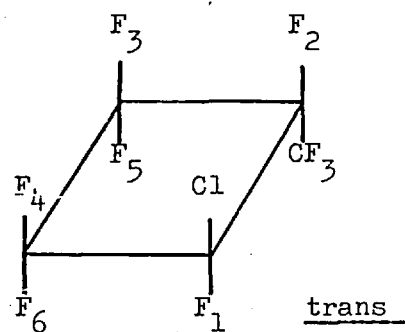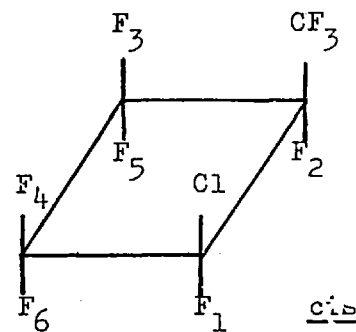
Peak	Frequency*	J	δ	Peak	Frequency*	J	δ
	2950				2999		
F_6	3165	215	32.64	F_6	3214	215	33.17
	3510		37.30		3500		37.19
	3856				3787		
F_4	4067	211	41.97	F_4	4002	215	41.22
	3117				3055		
F_5	3353	236	34.90	F_5	3289	234	34.06
	3401		36.14		3395		36.08
	3450				3502		
F_3	3684	234	37.39	F_3	3738	236	38.08
F_1	2279		24.22	F_1	2141		22.75
F_2	-1512		-16.07	F_2	-2337		-25.90
CF_3	8383		89.09	CF_3	8360		88.84

* Frequency is given as - $(H_i - H_r)$ expressed in Hz

Associated with isomer A is the peak at δ= -16.07 attributed to fluorine of the tertiary carbon atom. This is at much lower field than the corresponding peak of isomer B. The $\Rightarrow$CF fluorine in 1,2-di(trifluoromethyl)-hexafluorocyclobutane achieves resonance at still higher field (cis δ=-30.6, trans δ=-29.1). The presence of chlorine adjacent to the $\Rightarrow$C$_{ter}$—F group has shifted the resonance downfield. The fluorine of the tertiary carbon atom is nearer to chlorine and to the C-Cl bond in the trans isomer than it is in the cis. Thus, one might expect the C$_{ter}$—F fluorine nuclei in the trans isomer to be more influenced by the chlorine atoms, and to resonate at a lower field. On this basis isomer A is the trans isomer.

The chemical shift of the -CFCl- fluorine increases a little from cis to trans isomer. More substantial is the change (cis 3 ppm, trans 4.5 ppm) relative to chloroheptafluorocyclobutane (δ=19.7) indicating that the influence of the -CF$_3$ group is felt strongest in the trans isomer. Therefore, group B is from the cis isomer.

The evidence is sufficient to prove that the compound is the cis, trans -1-chloro-2-trifluoromethyl-hexafluorocyclobutane. The characterization of isomers, as cis or trans does not affect the kinetics of the system. The composition of the mixture ranged for 41% cis at 675 K to 47% cis at 648 K.

3.3.2   The Preliminary experiments

The preliminary experiments that were carried out were designed to provide information concerning factors affecting the formation of 1-chloro-2-trifluoromethyl-hexafluorocyclobutane (E) and to establish techniques for study of the reaction.

$$CF_2 = CFCl \quad \overset{k_3}{\underset{k_{-3}}{\rightleftharpoons}} \quad \begin{array}{c} F_2 \\ F_2 \end{array}\boxed{}\begin{array}{c} FCF_3 \\ FCl \end{array} \qquad 3.3.1$$

$$+$$

$$CF_2 = CFCF_3$$
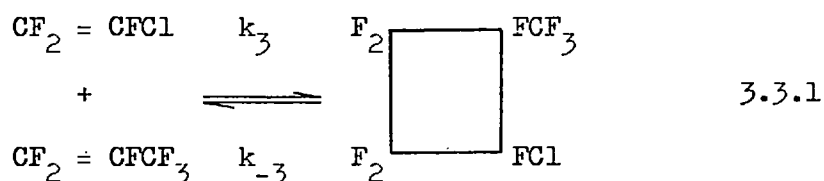
The formation of compound E proceeds concurrently with the cyclodimerization of the pure components. Observation of change in pressure would indicate the overall extent of the reactions taking place, without supplying any information on the extent of formation of compound E. Therefore, analysis provides the only satisfactory method for studying the reaction.

The rate of cyclodimerization of chlorotrifluoroethene is higher than that of hexafluoropropene (see 3.1 - 3.2). The cycloadditions are, in general, second order reactions and it was expected that the intermolecular reaction would also be of second order. It is possible that, by keeping the concentration of chlorotrifluoroethene relatively low, the formation of 1-chloro-2-trifluoromethyl-hexafluorocyclobutane might predominate over the cyclodimerization. It was thought appropriate to have the concentration of $CF_2=CFCl$ in the mixture in the region 2-6%. Under this condition the loss of chlorotrifluoroethene due to dimerization is roughly proportional to the loss of hexafluoropropene.

Two methods of introducing the mixture into the reaction vessel were tested. In the first method the two gases were admitted into the reactor separately. First a quantity of hexafluoropropene was introduced and then an amount of $CFCl=CF_2$, so that the mixture was formed inside the reactor. Its composition was calculated from pressure readings taken before and after each admission. The main disadvantages of this method were long time intervals (1-2 min.)between the first and

second gas admission and the size of error ($\pm$4-6%) in the compo-
sition of the mixture. In the second, more tedious method, the
pressure of the component contained in a certain volume was measured
accurately and then the components were brought together into one of the
calibrated flasks (C in Fig. 2.1) by condensation. The mixture
was brought to room temperature and homogeneity was ensured by mag-
netic stirring that continued until the sample was inserted into the
reactor. Analysis of samples from the storage flask taken before and
after the admission of the mixtures into the reaction vessel, as well
as those taken from the reactor did not differ by more than $\pm$3%.
With this method, strict adherence to the standard pyrolysis pro-
cedure (section 2.6) was observed.

In the first experiment C1-01T the ratio $CFCl=CF_2:CF_2=CFCF_3$ was
1.63:98.37 and the total pressure 49.730 kPa. The temperature of the
reactor was held at 647.6 K and it was checked periodically.
Pressure changes were recorded continuously and since there was no
significant pressure drop the reaction was left to proceed undisturbed
for a period of 250 minutes. At the end of that period a sample was
analyzed by gas chromatography using the Poropak Q column, section 2.2.1a
(column B,   page 79) operating at 348 K. The intercombination
product was observed but there was no peak for 1,2-dichloro-
hexafluorocyclobutane (compound D). A similar result was obtained
after 5.85 hours. The results of the analysis indicated that the
yield of the interdimer was high enough for accurate analysis.

Experiment Cl-01t

$*$Area ($\sigma/cm^2 \times 10^{-12}$ A)

Time ($\frac{t}{h}$)	Pressure $\frac{Pt}{Pa}$	C_3F_6	$CF_2=CFCl$	B	E
0	49,730				
4.15	49,431	30.4×10^4	29.2×10^2	$35.6 \times 2 \times 24$	$30.6 \times 2 \times 29$
10.00	48,831	30.2×10^4	$(24.8) \times 10^2$	$34.2 \times 5 \times 24$	$22.5 \times 5 \times 24$

$*$The second figure in the area value is the attenuation factor
and the third is chart speed correction factor.

In the second experiment Cl-02t the initial pressure
of the mixture was reduced to 35.647 kPa and a sample was taken
after 3 hours. Calculation for the rate of $CFCl=CF_2$ cyclo-
dimerization suggested that a detectable amount of compound D should
have been formed. Since the analysis did not produce the expected
peak but what appeared to be a shift in the base line, a second
sample was taken and analysis was performed with the column at 365 K.
A new peak, smaller in area, appeared, as expected, after the inter-
dimer peak.

At this stage trial analyses were performed to establish the best
column temperature for peak separation peak shape and analysis time.
It was decided to explore the range above 348 K but below 365 K at
which temperature the separation of $CFCl=CF_2$ from $CF_2:CFCF_3$ was
incomplete. For this purpose a mixture of the same composition
(98.37: 1.63) pyrolysed for two hours (experiment Cl-03t, initial
pressure 41.015 kPa) and samples were taken from it for analysis.
Best results were achieved with the column in the range 357-360 K.
The standard operating temperature chosen for this chromatographic

Table III 3.3

Experiment (647.6 K)	Time $\frac{t}{min}$	$C_3F_6\ \frac{P_a}{Pa}$	$C_2F_3Cl\ \frac{P_w}{Pa}$	$C_2F_3Cl\ \frac{P_c}{Pa}$	Interdimer $\frac{P_e}{Pa}$	$\frac{P_e}{P_a P_c t}$	$\frac{k^*}{Pa^{-1}min^{-1}}$
C1-01t	250	48,691	811	560	192	2.34×10^{-8}	2.34×10^{-8}
	600	48,299	810	390	351	2.16×10^{-8}	2.28×10^{-8}
C1-02t	180	35,070	572	393	67	2.17×10^{-8}	2.30×10^{-8}
C2-03t	120	34,468	2,215	1,801	187	2.26×10^{-8}	2.28×10^{-8}
	300	34,050	2,200	1,418	375	2.12×10^{-8}	2.25×10^{-8}

* Figures calculated by another approximate method

analysis was 358 K.

In the next experiment C2-03, all peaks were present. An approximate fourfold increase in the percentage of $CFCl=CF_2$ (6%) facilitated a high interdimer yield despite the lower initial pressure (36.811 kPa) and the relatively short reaction time.

Experiment C2-03

Time $(\frac{t}{h})$	Pressure $\frac{Pt}{Pa}$	Area $(\sigma/cm^2 . 10^{-12} A)$				
		C_3F_6	$CF_2=CFCl$	B	D	E
0.00	36,811					
2.00	36,478	20.4×10^4	$45.0 \times 2 \times 10^2$	$32.7::1 \times 12$	$38.5 \times 1 \times 24$	$61.6 \times 1 \times 24$
5.00	35,341	19.6×10^4	$34.9 \times 2 \times 10^2$	$37.9 \times 2 \times 12$	$65.8 \times 1 \times 24$	$24.3 \times 5 \times 24$

Having established the best column temperature, mixtures of hexafluoropropene and 1-chloro-2-trifluoromethyl-hexafluorocyclobutane, as well as hexafluoropropene-chlorotrifluoroethene were used for calibration (section 2). The peak areas were converted into partial pressures by using the calibration factors. Since all calculations are based on the partial pressure of hexafluoropropene, its value was estimated by subtracting the amount of hexafluoropropene consumed for cyclodimer formation and production of interdimer.

The partial pressures of the reaction mixture components, calculated as described previously, were used in the determination of the order of reaction and of the specific rate constant k_3. To calculate the quantities in column 7 in Table III 3.3 the pressure of chlorotrifluoroethene was taken as the geometric mean $\bar{P}_c = (p_{co} \, p_c)^{\frac{1}{2}}$, where p_{co} is the initial and p_c the final pressure.

The figures given in column 7 were obtained from equation 3.3_2

$$\frac{\Delta E}{\Delta t} = k'_3 \, \bar{P}_a \, \bar{P}_c \qquad\qquad 3.3\_2$$

The set of results in column 7 indicate that the order of reaction is initially two. For one experiment the value of k'_3 appears to depend on the progress of the reaction. However, application of equation 3.3_2 requires measurement of five components of the mixture thus increasing the probability of errors creeping up in the calculations. Furthermore, equation 3.3_2 becomes increasingly approximate as the reaction proceeds.

Having obtained good evidence that the reaction was second order more accurate equations for calculating the rate constant from the measurements were deduced. These are given in section 3.3.3. It will be seen later that the accurate calculations confirmed that the order of the reaction is two.

3.3.3   Treatment of experimental measurements

The chemical equation and specific rate constants for the system of reactions are

$$2\ CF_2=CFCl \quad \underset{k_{-1}}{\overset{k_1}{\rightleftharpoons}} \quad c-C_4F_6Cl_2 \qquad\qquad 3.1\_1$$

$$2\ CF_2=CFCF_3 \quad \underset{k_{-2}}{\overset{k_2}{\rightleftharpoons}} \quad c-C_4F_6(CF_3)_2 \qquad\qquad 3.2\_1$$

$$\begin{array}{c} CF_2=CFCl \\ + \\ CF_2=CFCF_3 \end{array} \underset{k_{-3}}{\overset{k_3}{\rightleftharpoons}} \quad c-C_4F_6 \!\!<\!\!\begin{array}{c} CF_3 \\ Cl \end{array} \qquad\qquad 3.3\_1$$
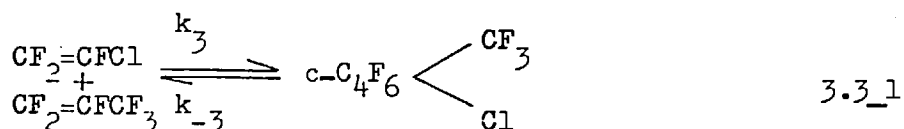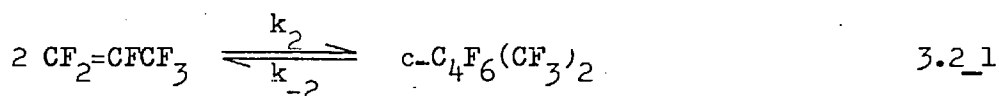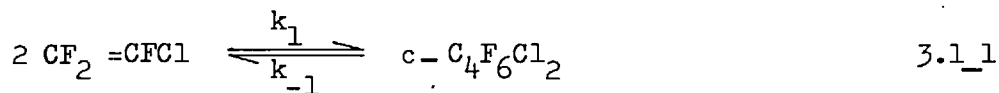
For the forward reaction k_3 is defined as

$$\frac{dE}{dt} = k_3 A C_m \qquad\qquad 3.3\_3$$

and it is expressed in $m^3 mol^{-1} s^{-1}$. A, B, C_m, D, E, are the concentrations of hexafluoropropene, 1,2-di(trifluoromethyl)-hexafluorocyclobutane, chlorotrifluoroethene, 1,2-dichloro-hexfluorocyclobutane and 1-chloro-2-trifluoromethyl-hexafluoro-cyclobutane respectively. The quantities k_1, k_2, k_{-1}, k_{-2} have been defined earlier (section 3.1 and 3.2).

The system is described by the following differential equations.

$$-\frac{dC_m}{dt} = 2k_1 C_m^2 k_3 A C_m - 2k_{-1} D - k_{-3} E \qquad\qquad 3.3\_4$$

$$-\frac{dA}{dt} = 2k_2 A^2 + k_3 A C_m - 2k_{-2} B - k_{-3} E \qquad\qquad 3.3\_5$$

$$-\frac{dE}{dt} = k_3 A C_m - k_{-3} E \qquad\qquad 3.3\_6$$

$$-\frac{dB}{dt} = k_{-2} B - k_2 A^2 \qquad\qquad 3.3\_7$$

$$-\frac{dD}{dt} = k_{-1} D - k_1 C_m^2 \qquad\qquad 3.3\_8$$

For low product yields, at temperatures below 670 K, the reverse reactions are negligible and can be ignored. Therefore

$$-\frac{dC_m}{dt} = 2k_1 C_m^2 + k_3 A C_m \qquad\qquad 3.3\_4a$$

$$-\frac{dA}{dt} = 2k_2 A^2 + k_3 A C_m \qquad\qquad 3.3\_5a$$

$$\frac{dE}{dt} = k_3 A C_m \qquad\qquad 3.3\_6a$$

It can, also, reasonably be assumed that the concentration of hexafluoropropene is invariant, since only a few parts per thousand of it are consumed. Then, equation 3.3_4a may be integrated without difficulty. Substituting the value of C_m obtained from 3.3_4a in equation 3.3_6a and integrating we obtain equation 3.3_9

$$\frac{E}{A} \cdot \frac{2k_1}{k_3} = \ln\left[\frac{C_{mo}}{A} \cdot \frac{2k_1}{k_3} + 1 - \frac{C_{mo}}{A} \cdot \frac{2k_1}{k_3} \exp(-k_2 At)\right] \quad 3.3\_9$$

The value of k_3 was determined by calculating

$$\ln\left[\frac{C_{mo}}{A} \cdot \frac{2k_1}{k_3} + 1 - \frac{C_{mo}}{A} \cdot \frac{2k_1}{k_3} \exp(-k_3 At)\right] = \Theta$$

and

$$\frac{E}{A} \frac{2k_1}{k_3} = \Gamma \qquad \text{for various values of } k_3 \text{ and plotting } \Gamma, \Theta \text{ against}$$

k_3 on the same graph. The point of intersection of the two lines gave the value of k_3. This method gave k_3 values differing by $\pm 5\%$ (see last column, Table III 3.3), but this is tedious and a minor fault is that it does not make full use of all the experimental measurements available.

A computer programme was written to determine k_3 by iteration, using equation 3.3_9. The first step was to calculate k_3 by equation 3.3_2 and the intitial value was then adjusted stepwise until equation 3.3_9 was obtained. The ratio E/A used was determined from the peak areas of the chromatograms determined as described in section 2.2. The final concentrations of hexafluoropropene A was

calculated by substracting from the initial concentration A_o the amount

consumed for interdimer formation and the production of cyclodimer

according to equation 3.2_2.

$$A = A_o - E - 2k_2 \, A_o \, A \Lambda t$$

As an improvement of the level of approximation it was assumed that the

loss of hexafluoropropene is proportional to the loss of chlorotri-

fluoroethene. This assumption is reasonable since the changes in

concentration are small, especially when the percentage of chlorotri-

fluoroethene is kept low.

Let $\quad A_o - A = g \, (C_{mo} - C_m)$
<div align="right">3.3_10</div>

then $\quad A = A_o - g \, (C_{mo} - C_m)$
<div align="right">3.3_11</div>

where g is the proportionality factor
<div align="right">3.3_16</div>

Equation 3.3_4a for the loss of chlorotrifluoroethene becomes

$$-\frac{dC_m}{dt} = 2k_1 C_m^2 + k_3 A_o C_m - k_3 C_m \, g \, (C_{mo} - C_m)$$
<div align="right">3.3_12</div>

$$= (2k_1 + gk_3) \, C_m^2 + (k_3 A_o - k_3 \, gC_{mo}) \, C_m$$
<div align="right">3.3_13</div>

put

$$C_m = y \quad (2k_1 + gk_3) = a \qquad (k_3 A_o - k_3 gC_{mo}) = b$$
<div align="right">3.3_14</div>

$$\therefore \quad -\frac{dy}{dt} = ay^2 + by$$
<div align="right">3.3_15</div>

Integration of 3.3_15 gives

$$y = \frac{b}{(\dfrac{ay_o - b}{y_o}) \exp (bt) - a}$$
<div align="right">3.3_16</div>

Introducing 3.3_16 in equation 3.3_6a

$$\frac{dE}{dt} = k_3 A C_m = k_3 C_{mo} - k_3 g\, C_{mo} C_m + k_3 g\, C_m^2 \qquad\qquad 3.3\_17$$

$$= by + k_3 gy^2 \qquad\qquad 3.3\_18$$

$$\therefore \quad \frac{dE}{dt} = \frac{b^2}{\dfrac{ay_o + b}{y_o}\, \exp(bt) - a} + \frac{k_3 gb^2}{\dfrac{ay_o + b}{y_o}\, \exp(bt) - a^2} \qquad 3.3\_19$$

substitute $\quad \dfrac{ay_o + b}{y_o} = m \qquad a = -n \qquad n + m\exp(bt) = x$

then $\quad dx = bm\,\exp(bt)dt = b(x-n)dt \qquad\qquad 3.3\_20$

Rearrangement of equation 3.3_19 gives

$$dE = \frac{bdx}{(x-n)x} \div \frac{k_3\, gb}{(x-n)x^2} \cdot dx \qquad\qquad 3.3\_21$$

Integration of 3.3_21 can be achieved by resolution into partial fractions.

$$\underline{A} \quad \int \frac{bdx}{x(x-n)} = b \int \frac{Ydx}{(x-n)} + \int \frac{Zdx}{x} \qquad\qquad 3.3\_22$$

$$Y = -Z = \frac{1}{n}$$

$$\therefore \quad \int \frac{bdx}{x(x-n)} = \frac{b}{n}\, \ln\left(\frac{x-n}{x}\right) + \text{Constant (1)} \qquad\qquad 3.3\_23$$

B

$$\frac{k_3 gb}{(x-n)x^2} \cdot dx = k_3 gb \left(\int \frac{U \, dx}{(x-n)} + \int \frac{V \, dx}{x} + \int \frac{W \, dx}{x^2} \right) \qquad 3.3\_24$$

$$= k_3 gb \ \frac{1}{n^2} \left[\ln \ \frac{x-n}{x} + \frac{1}{x} \right] + \text{Constant (2)} \qquad 3.3\_25$$

$$\therefore \quad dE = \frac{b}{n} \ \ln\left(\frac{x-n}{x}\right) + k_3 gb \left[\frac{1}{n^2} \ln \ \frac{x-n}{x} + \frac{1}{nx} \right] + \text{Constant} \qquad 3.3\_26$$

at $t = 0$, $E = 0$

$$- \text{Constant} = \frac{b}{n} \ln \frac{m}{m+n} + k_3 gb \left[\frac{1}{n^2} \ln \left(\frac{m}{m+n}\right) + \frac{1}{n(m+n)} \right] \qquad 3.3\_27$$

Introducing equation 3.3_27 into 3.3_26 we obtain

$$E = \frac{b}{n} \ln \left(\frac{x-n}{x} \ \frac{n+m}{m} \right) + k_3 gb \left[\frac{1}{n^2} \ln \left(\frac{x-n}{x} \cdot \frac{m+n}{m} \right) + \frac{1}{nx} - \frac{1}{n(n+m)} \right]$$

Substitution in

$$\ln \left(\frac{x-n}{x} \ \frac{n+m}{m} \right) \qquad 3.3\_29$$

gives

$$= - \ln \left[\frac{\dfrac{(ay_0+b) \exp (bt)}{y_0} - a}{\left(\dfrac{ay_0+b}{y_0}\right) \exp (bt)} \quad \frac{\dfrac{ay_0+b}{y_0}}{\dfrac{ay_0+b}{y_0} - a} \right] \qquad 3.3\_30$$

$$= \ln \big(\exp (bt) \big) + \ln \left[\frac{(ay_0+b)}{b} \ \exp (bt) - \frac{ay_0}{b} \right] \qquad 3.3\_31$$

$$= -\ln \left[\frac{ay_0}{b} + 1 - \frac{ay_0}{b} \ \exp (-bt) \right] \qquad 3.3\_32$$

Substitution in

$$\frac{1}{n^2} \ln \left(\frac{x-n}{x} \ \frac{m+n}{m} \right) + \frac{1}{nx} - \frac{1}{n(n+m)} \qquad 3.3\_33$$

gives

$$= \frac{1}{a^2} \ln\left(\frac{m \exp(bt)}{m \exp(bt)-a} \right) \frac{m-a}{m} - \frac{1}{a\left(m \exp(bt)-a\right)} +$$

$$+ \frac{1}{a(m-a)} \qquad 3.3\_34$$

$$= \frac{1}{a^2} \ln\left[\frac{b \exp(bt)}{\left(ay_o+b\right)\exp(bt)-ay_o} + \frac{y_o}{ab} - \frac{1}{a\left(\frac{ay_o+b}{y_o}\right)\exp(bt)-a^2} \right] \quad 3.3\_35$$

Therefore, introducing equations 3.3_32 and 3.3_35 in 3.3_28 we obtain equation 3.3_36

$$E = \frac{b}{a} \ln \frac{ay_o}{b} + 1 - \frac{ay_o}{b} \exp(-bt) - \frac{k_3 bg}{a^2} \ln\left(\frac{b \exp(bt)}{(ay_o+b)\exp(bt)-ay_o} \right)$$

$$+ k_3 \frac{y_o}{a} g - k_3 \frac{y_o}{a} g \left[\frac{1}{\frac{ay_o}{b}(\exp bt-1) + \exp(bt)} \right] \qquad 3.3\_36$$

Since $\dfrac{a}{b} = \dfrac{z}{Y_o} \equiv \dfrac{z}{C_{mo}}$ where $z = \dfrac{(2k_1+gk_3)\, C_{mo}}{k_3\,(A - gC_{mo})}$,

equation 3.3_36 may be written as

$$\frac{E}{C_{mo}} = \frac{1}{Z} \ln \left(Z + 1 - Z \exp(bt) \right)\left(1 - \frac{k_3}{a} g \right) +$$

$$+ \frac{k_3}{a} g \left(1 - \frac{\exp(-bt)}{1+z-z \exp(-bt)} \right) \qquad 3.3\_37$$

Equation 3.3_37 cannot be solved directly. It is possible, however, to find k_3 by iteration. The existing computer programme was extended and the value of k_3 obtained by equation 3.3_9 was used as the initial value.

Equation 3.3_37 requires the value of the proportionality factor g as defined in equation 3.3_10. For substitution in equation 3.3_10 the final value of chlorotrifluoroethene was calculated from equation 3.3_4a in its integrated form.

$$C_m = \frac{k_3\, A}{\left(2k_1 + \dfrac{k_3 A}{C_{m\,o}}\right) \exp\,(k_3 At) - 2k_1} \qquad\qquad 3.3\_4b$$

The values of A, C_m and g were recalculated in each iteration and a number of iterations could be carried out until two sets of values for g and the two sides of equation 3.3_37 did not differ by more than 1%.

In cases where the differences between the calculated and the experimentally determined concentration of each component exceeded the experimental error, it was possible to use the figures obtained from analysis.

The values of k_3 calculated by equation 3.3_37 were almost identical to three significant figures to those obtained from equation 3.3_9. Surprisingly, the values calculated using the much simpler equation 3.3_2 were also close to those obtained by equation 3.3_9 and 3.3_37, at least at the lower temperatures. However, as the temperature increased, the set of values of k_3 diverged and those obtained by 3.3_2 differ by a factor as high as two.

The consistency of the results for the entire range supported the indications for a second order reaction. Furthermore, pressures of the compounds of the mixtures calculated as described, were in concordance with those derived from chromatographic analysis (Table III.3.4).

The change in concentration occuring as a result of taking samples was also taken into account in interpreting the results. As initial pressure for the olefins was taken a weighed mean value

$$P_w = \frac{\sum_{i}^{n} (P_o - P_s)\, t}{\sum_{i}^{n} t_i}$$

where $\sum t_i$ is the overall reaction time $(t_j - t_o)$, P_o is the measured initial pressure of an olefin, P_s is pressure of gases, expressed as equivalent olefin, taken out of the reaction vessel prior to the period to which t_i refers, and t_i is the reaction time interval between two consecutive samples. To calculate $P_s = \sum_{i}^{n} v_i (1-\theta) P_i$ the pressure P_i of a component i, calculated described previously, was multiplied by $v(1-\theta)$, where $\theta = P'_{tj}/P_{tj}$, and is the number of molecules of product i. P_{tj} and P'_{tj} refer to the total pressure of the mixture before and after sampling.

In an alternative method, the pressure of the olefins at the end of a period t_i were taken as the starting pressures for the next period t_j. In this way each analysis could be treated as a separate experiment. The reaction time was taken as $t_j - t_i$ andthe product yield as $E_j - E_i$. Since the dependence of the reaction rate on concentration is more pronounced by this method, it attracted more attention in the early stages of the experimental work. Results

calculated in this way are marked with an asterisk. It is possible

that random errors in analysis will be amplified in the difference

$E_j - E_i$, especially in the upper end of the temperature range.

For this reason its application was restricted to cases where

$E_j \simeq 2E_i$. Values of k_3 calculated in this way were the same as those

obtained applying the first method.

3.3.4   Quantitative measurement of the reaction rate of hexafluoro-

propene to chlorotrifluoroethene cycloaddition in the region

570-700 K

The reaction of the system hexafluoropropene-chlorotrifluoroeth-

ene was studied over the temperature range 570 K to 700 K by

chromatographic analysis, and the results were treated as described

in the previous section.

At a given temperature, as a rule, two mixtures of different

composition were pyrolysed. Normally the percentage of chloro-

trifluoroethene in the second mixture was twice that of the first

mixture. Also, at least two samples of each mixture were pyrolysed

in order to observe and assess any pressure effects. The total pressure

of pyrolysed mixtures covered the range 8 kPa to 60 kPa. The compo-

sition of the mixtures varied widely, ranging from 1.6% to 15.5%

in chlorotrifluoroethene.

It was found that, within the chlorotrifluoroethene percentage

already mentioned, the composition of the mixture did not have any

effect on the specific rate constants. The value of k_3 was also

independent of the total pressure (Table III.3.4). Back reaction

was in evidence in prolonged experiments, especially in those per-

formed at the highest temperature of the range (698.3 K).

Table III.3.4.

Specific rate constants, calculated and experimental pressures for the cycloaddition of $CF_2=CFCF_3$ to $CClF=CF_2$

Exper.	In.Press. p_i^{**}	Temp T/K	Time t/min	$CF_2:CFCF_3$ P_a^{**}	Inter-dimer P_e^{**}	$CFCl=CF_2$ Exp.	$CFCl=CF_2$ Calc.	$1,2\text{-}cC_4F_5(CF_3)_2$ Exp.	$1,2\text{-}cC_4F_5(CF_3)_2$ Calc.	$1,2\text{-}cC_4F_6Cl_2$ Exp	$1,2\text{-}cC_4F_6Cl_2$ Calc.	$\dfrac{k_3}{m^3mol^{-1}s^{-1}}$
C11_28.1 * A =18165		698.3	120	17,940	105	435	432	55	59	31	32	
.2 C_m= 601			370	17,455	216		248		179		58	
.1.2			(250)	17,444	(113)		257		(117)		(29)	
C11_29.1 A =13900		698.3	167	13,713	89.1	327	320	46	48.3	25	25	
.2 C_m= 460			344	13,378	134	265	240	92	97	40	40	
.3			522	13,066	156	208	193	138	142	45	49	
C12_30.1 A =20064		698.3	135	19,635	265	780	756	75	81	121	138	10.5×10^{-6}
.2 C_m= 1296			324	19,066	433	451	429	177	199	163	212	10.5×10^{-6}
.3			506	18,677	499	355	303	264	290		237	
C12_31.1 A =15033		698.3	170	14,828	128	698	690	35	37	70	76	
.2 C_m= 971			351	14,486	229	480	461	89	96	130	136	
.3			545	14,154	282	385	333	142	156	150	170	
C12_32.1 A =11336		698.3	1	11,163	106	502	498	30	33	58	65	
.2 C_m= 732			353	10,784	163	398	363	59	64	92	97	
.3			523	10,553	179	312	301	84	89	108	115	
C9_22.1 A =23446		673.7	140	23,250	97.6	620	586	46	48	33	33	4.23×10^{-6}
.2 C_m= 749			341	22,828	199	422	427	106	116	56	59	4.18×10^{-6}
.3			521	22,499	261	337	333	162	174	70	72	4.10×10^{-6}

** Pressures P_a, P_b, P_c, P_d, P_e in Pascal

Table III.3.4. /Cont.

Exper.	In.Press. p_i^{**}	Temp. T/K	Time t/min	CF_2:$CFCF_3$ p_a^{**}	Inter-dimer p_e^{**}	$CFCl=CF_2$ Exp.	Calc.	$1,2$-$cC_4F_6(CF_3)_2$ Exp.	Calc.	$1,2$-$cC_4F_6Cl_2$ Exp.	Calc.	$\dfrac{k_3}{m^3 mol^{-1}s^{-1}}$
C9_23.1	A =17505	673.7	222	17,336	81.5	476	422	42	43	28	28	4.47×10^{-6}
* .2	C_m= 560		403	17,131	130	363	344	74	77	42	42	4.40×10^{-6}
.1 .1			(181)	17,120	50.1	363	342	(32)	32	(14)	14	4.37×10^{-6}
C9_24.1	A =13102	673.7	226	13,003	48.8	300	304		24	18	14	4.63×10^{-6}
.2	C_m= 308		423	12,851	79.3	250	252		45	23	22	4.38×10^{-6}
.3			1002	12,363	181	127	116	144	146	40	38	4.40×10^{-6}
C10_25.1	A =20203	673.5	150	19,983	140	808	819	38	38	70	72	4.59×10^{-6}
.2	C_m= 1104		330									
.3			532	19,310	335	458	457	129	130	146	148	4.24×10^{-6}
C10_26.1	A =15138	673.5	160	15,006	85.8	679	651	22	23	45	46	4.53×10^{-6}
.2	C_m= 827		345	14,776	155	526	511	48	49	70	78	4.38×10^{-6}
.3			536	14,579	197	406	419	72	74	95	100	4.00×10^{-6}
C10_27.1	A =11237	673.5	210	11,144	57.5	476	489	16	17	33	34	4.20×10^{-6}
* .2	C_m= 614		428	10,992	100	404	398	34	34	54	56	3.99×10^{-6}
.1 .2			(218)	10,956	(43)	403	396	(17)	(17)	(20)	(22)	3.84×10^{-6}

** Pressures P_a, P_b, P_c, P_d, P_e in Pascal

Table III.3.4 /Cont.

Exper.	In.Press. P_i^{**}	Temp. T/K	Time t/min	$CF_2:CFCF_3$ P_a^{**}	Inter-dimer P_e^{***}	$CFCl=CF_2$ Exp.	Calc.	$1,2-cC_4F_6$ $(CF_3)_2$ Exp.	Calc.	$1,2-cC_4F_6Cl_2$ Exp.	Calc	$\dfrac{k_3}{m^3 mol^{-1}s^{-1}}$
C2_3.1	A =34597	647.6	120	34,339	188	1801	1786	32	33	110	120	2.05×10^{-6}
* .2	C_m= 2215		300	33,673	379	1421	1367	18	81	125	132	1.96×10^{-6}
.1 .2			(180)	33,670	(190)	1418	1356	(48)	48	(106)	(109)	1.84×10^{-6}
C3_4.1	A =23925	647.6	226	23,725	138	1145	1042	29	30	76	80	1.96×10^{-6}
* .2	C_m= 1339		420	23,353	228	901	857	52	55	118	122	1.94×10^{-6}
.1 .2			(194)	23,301	(190)	901	852	(24)	(25)	(42)	(43)	1.94×10^{-6}
C3_5.1	A =17264 C_m= 967	647.6	300	17,118	103	755	753	22	21	53	55	2.10×10^{-6}
C4_6.1	A =29697	647.6	120	29,433	211	2371	2338	25	24	200	210	2.04×10^{-6}
.2	C_m= 2970		321	28,711	456	1697	1675	62	64	391	404	1.99×10^{-6}
C4_7.1	A =21206	647.6	180	21,018	147	1632	1654	19	19	135	159	1.89×10^{-6}
.2	C_m= 2120		393	20,701	279	1305	1287	39	40	246	271	1.87×10^{-6}
C4_8.1	A =15163 C_m= 1516	647.6	361	14,971	149	1100	1070	20	19	140	142	1.95×10^{-6}
C5_9.1	A =49581	647.6	120	48,989	448	2926	2755	67	68	318	323	2.10×10^{-6}
.2	C_m= 3851		314	47,938	920	(1802)	1786	187	174	549	562	2.08×10^{-6}

** Pressures P_a, P_b, P_c, P_d P_e in Pascal

Table III.3.4. /Cont.

Exper.	In.Press. P_i^{**}	Temp. T/K	Time t/min	$CF_2:CFCF_3$ P_a^{**}	Inter-dimer P_e^{**}	$CFCl=CF_2$ Exp.	Calc.	$1,2\text{-}cC_4F_6(CF_3)_2$ Exp.	Calc.	$1,2\text{-}cC_4F_6Cl_2$ Exp.	Calc.	$\dfrac{k_3}{m^3mol^{-1}s^{-1}}$
C5_10.1	A =35374 C_m= 2749	598.7	307	35,237	112	2,518	2,420		11	105	109	3.34×10^{-7}
C5_11.1	A =24787 C_m= 1927	598.7	330	24,716	57.6	1,832	1,751		6	55	59	3.2×10^{-7}
C5_12.1	A =17558 C_m= 1365	598.7	1080	17,453	87.3	1,151	1,104		9	85	87	3.14×10^{-7}
C6_13.1	A =21315 C_m= 2292	598.1	356	21,240	63.7	2,048	2,054		4	85	87	3.23×10^{-7}
C6_14.1	A =29357 C_m= 3157	598.1	780	29,086	230	2,415	2,327	(18)	18	270	300	3.11×10^{-7}
C6_15.1	A =21010 C_m= 2259	598.1	370	20,936	63.3	1,943	2,019		5	80	88	3.18×10^{-7}
C6_16.1 .2	A =14964 C_m= 1609	598.1	810 1280	14,882 14,756	69.8 100	1,295 1,241	1,355 1,238		5 8	90	92 133	3.26×10^{-7} 3.20×10^{-7}

** Pressures P_a, P_b, P_c, P_d, P_e in Pascal

Table III.3.4. /Cont.

Exper.	In.Press. P_i**	Temp. T/K	Time t/min	$CF_2{:}CFCF_3$ P_a**	Inter-dimer P_e**	$CFCl{=}CF_2$		$1,2{-}cC_4F_6$ $(CF_3)_2$		$1,2{-}cC_4F_6Cl_2$		$\dfrac{k_3}{m^3 mol^{-1} s^{-1}}$
						Exp.	Calc.	Exp.	Cal.	Exp.	Calc.	
C7_17.1	A =47403	573.7	392	47,194	192	6,180	6,184		7	386	379	1.25×10^{-7}
.2	C_m= 7135		1294	46,509	552	4,682	4,649	20	24	965	940	1.28×10^{-7}
C7_18.1	A =33842	573.7	421	33,725	105	4,513	4,560		4	193	214	1.22×10^{-7}
.2	C_m= 5094		1456	33,209	334	3,704	3,570	14	14	534	572	1.30×10^{-7}
*.1 .2			(1035)	33,195	(229)	3,703	3,560		(9)		(361)	1.33×10^{-7}
.3			1946	33,008	430	3,208	3,230	18	18	641	691	1.31×10^{-7}
*.2 .3			(490)	32,808	95.5	3,185	3,198		(4)		(118)	1.36×10^{-7}
C7_19.1	A =23162	573.4	525	23,093	62.8	3,170	3,172		2	118	126	1.24×10^{-7}
.2	C_m= 3486		1410	22,843	148	2,712	2,735		6	294	290	1.19×10^{-7}
.3			1845	22,746	323	2,513	2,453		8	330	323	1.22×10^{-7}
C8_20.1	A =45479	573.4	375	45,479	149	4,996	5,261		6	224	253	1.25×10^{-7}
.2	C_m= 5916		1420	44,640	483	3,884	3,951	20	24	664	719	1.26
.3			1830	44,330	559	3,631	3,534	28	31	769	809	1.23
C8_21.1	A =32305	573.4	435	32,207	86.9	3,886	3,799		4	153	151	1.24×10^{-7}
.2	C_m= 4187		1437	31,774	251	3,145	3,098		12	376	402	1.22
.3			1817	31,581	305	2,937	2,835		16	420	465	1.23

** Pressures P_a, P_b, P_c, P_d, P_e in Pascal

The value of k_3 appeared to diminish as the reaction progressed, suggesting that the reverse reaction cannot be regarded as negligible.

Taking into account the reverse reaction (see 3.3_4a) the exact value of k_3 was estimated from the equation.

$$k_{3a} = k_3 - bt \qquad\qquad 3.3\_32$$

The parameters k_3 and b were determined by solving the set of simultaneous equations corresponding to a given temperature. The quality b arises from the integrated form of equation 3.3_33

$$\frac{dE}{dt} = k_3 AC_m - k_{-3} (k_3 AC_m t) . \qquad\qquad 3.3\_33$$

$$\therefore \quad k_{3a} = k_3 - \tfrac{1}{2} k_{-3} k_3 t \equiv k_3 - bt \qquad\qquad 3.3\_34$$

The last equation may be used to estimate the value of k_{-3} from the relationship $k_{-3} = 2b/k_3$.

At 673.6 K the correction applied to the specific rate constant k_{3a}, determined from the analysis of the first sample, increased the value of k_3 by about 5%, depending on the duration of the first reaction period. Such a correction lies within the experimental error. However, for prolonged reaction periods, the correction becomes more significant (0.1 K_{3a}). At 698.3 K the correction applied to k_{3a} amounts up to 50% in cases of extended reaction periods. The corrected values of the specific rate constant appear in TableIII.3.4. Figure 3.14 is an Arrhenius graph of log k_3 against K/T. A straight line for all the points was fitted by the method of least squares. The Arrhenius equation for the points is:-
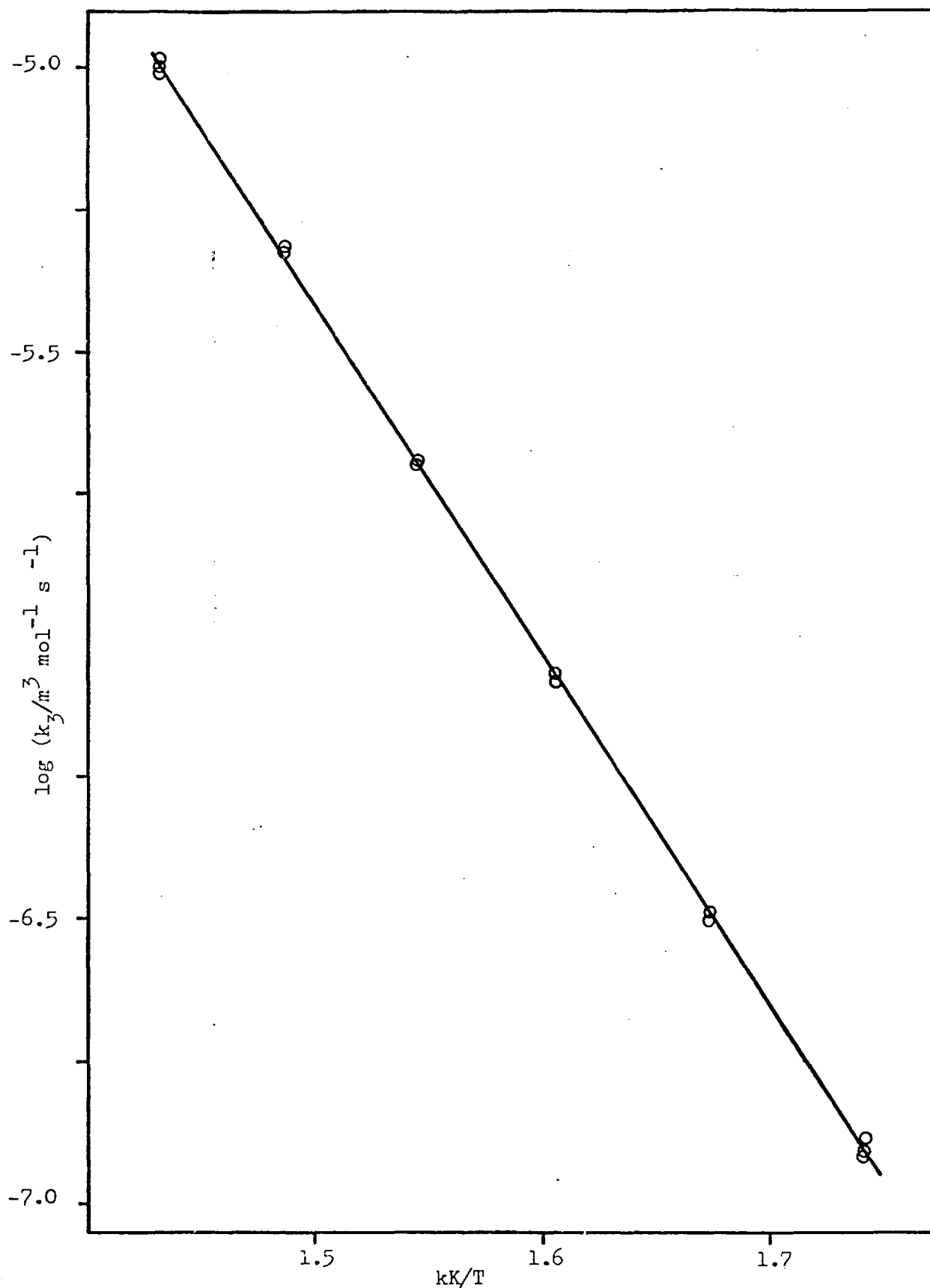
Figure **3.14** Graph of the logarithms of specific rate constants (k_3) $\underline{V.}$ the reciprocal of temperature (K/T) for the cycloaddition of hexafluoro-propene to chlorotrifluoroethene

$$\log \left(\frac{k_3}{m^3 mol^{-1} s^{-1}} \right) = (3.86^{\pm} 0.03) - (6182^{\pm} 15) \times \frac{K}{T}$$

These parameters were obtained by excluding all the points in which the value of $\log k_3$ differs by more than $\pm$ 0.033 from the one calculated by using the above parameters.

3.34a   The dissociation of 1-chloro-2-trifluoromethyl-hexafluoro-
cyclobutane

At 673.6 K the dissociation of 1-chloro-2-trifluoromethyl-hexa-fluorocyclobutane proceeds at a significant rate. The specific rate constant k_{-3}, estimated as outlined previously, had values $k_{-3} = 7.3 \times 10^{-6} s^{-1}$ at 673.6 K and $k_{-3} = 2.1 \times 10^{-5} s^{-1}$ at 698.3. Using these figures to calculate the pre-exponential factor A and the activation enery Ea, the values obtained A = 6.9×10^7, Ea = 167.3 kJ.mol^{-1}, are too low for ring opening reaction[128]. In an attempt to learn more about the kinetics of this dissociation reaction, experiments at 674.2 K, 697.5 and 725.6 K were carried out.

In the pyrolyses performed, the starting material was a mixture of roughly equal parts of cis and trans isomers containing about 3.8% di(trifluoromethyl)hexafluorocyclobutane. Despite attempts to reduce further the percentage of impurities, the similarity of the boiling points of the compounds and the proximity of the retention times in the Poropak column, made this exercise tedious and unprofitable. However, since recycling of the pyrolysed material was a better source for obtaining pure combination product than was the original pre-paration, the purity of samples used in the experiments at

697.5 K and 725.6 K was better than 98%

Pyrolyses were carried out at pressure ranging from 5.1 kPa to 18.3 kPa. The limiting factor preventing use of higher pressures was primarily the difficulty in preparing enough material for a series of experiments. Another limitation was non-ideal behaviour of the chlorotrifluoromethyl- hexafluorocyclobutane on the Poropak column. Some analyses were carried out, mainly to obtain information about the composition of the reaction mixture.

In the first set of experiments (D_101 to D_103) at 674.2 K, the change in pressure was significant so that reliable measurements could be made every two minutes. However, the value of k_{-3} obtained varied, diminishing with the progress of the reaction even when corrections were applied for 'dead space' and impurities. The value of k_{-3} obtained by a graphical method [119] ranged from $k_3 = 9.3 \times 10^{-6}$ s^{-1} at the early stages of the reaction, to $k_{-3} = 6 \times 10^{-6}$ s^{-1} after one hour or so. This trend was observed in the entire range of experiments.

Analyses carried out after suitable time intervals (15 minutes reaction time to three hours) revealed that hexafluoropropene and chlorotrifluoroethene were not the only reaction products. Three new peaks appeared between the peaks of chlorotrifluoroethene (R_t= 2.35 minutes) and di(trifluoromethyl)hexafluorocyclobutane, the most abundant compound appearing at R_t = 7.75 minutes. Attempts to isolate it using the preparative Poropak column were not entirely successful. The infrared spectrum of this compound with the cyclic products of co-dimerization showed absorption at 1780 and 1105 cm^{-1}. The mass spectrum of the unidentified compound appearing at R_t = 7.8 minutes,
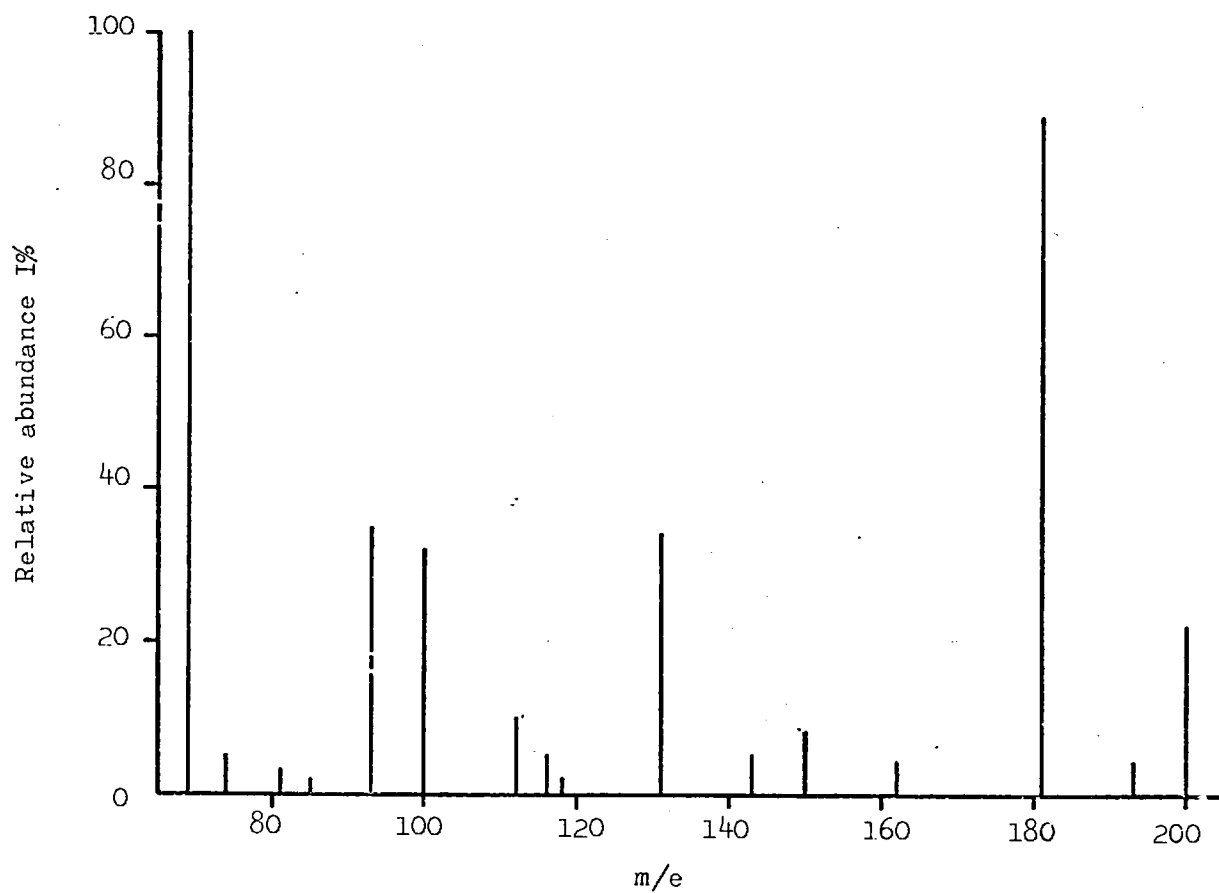
ion	m/e	I%	lm	m/e	I%
C_5F_9	231	2	C_3F_5	131	34
C_5F_8	212	2	C_2F_3Cl	116	5
C_4F_8	200	22	C_3F_4	112	10
C_5F_7	193	4	C_2F_4	100	32
C_4F_7	181	89	C_3F_3	93	35
C_3F_5Cl	166	2	CF_2Cl	85	2
C_4F_6	162	4	C_2F_3	81	3
C_3F_6	150	8	C_3F_2	74	5
C_3F_4Cl	147	2	CF_3	69	100
C_4F_5	143	5	CF_2	50	3

Figure 3.15   Mass spectrum of by-products of pyrolysis of

1-chloro-2-trifluoromethyl-hexafluorocyclobutane

somewhat contaminated by at least one other unidentified compound

(R_t = 5.7 min.) is given in Figure 3.15. The fragmentation

pattern is distinctly different from that characteristic of cyclo-

butanes. Fragments containing chlorine were observed as pairs, mainly

at n/e 85-87, 116-118, 147-149, 166-168. The highest m/e value in

the spectrum at 231 corresponds to fragment $C_5F_9^+$. It is thought

very difficult to determine the structure of a perfluoro-compound from

its mass spectrum [124]. Peak CF_3^+ is the base peak, common in per-

fluoroparaffins and perfluoroolefins alike [124]. The molecular

ion peak (M^+) is very small in the spectra of both classes but the

numerous exceptions, especially in the cis compounds, make it hazardous

to draw any conclusions. The presence of chlorine in the molecule,

the existence of a double bond, the appearance of the segment $C_4F_8^+$

which is absent in the mass spectra of perfluorocyclobutanes, and

the fragment $C_5F_9^+$ makes it plausible to assume that part of the

dissociation of 1-chloro-2-trifluoromethyl-hexafluorocyclobutane

may proceed by ring opening without the formation of hexafluoropropene

and chlorotrifluoroethene.

The pyrolysis carried out at 697.5 did not produce entirely

reliable results. Nevertheless, the mean value of k_{-3} at the early

stages of the reaction was $k_{-3} = 2.4 \times 10^{-5}$ s^{-1}, which is close to the

value estimated for the reverse reaction in the study of interdimeriz-

ation of hexafluoropropene to chlorotrifluoroethene. The results

obtained at 725.6 K were not so widely scattered, giving an average

value $k_{-3} = 9.6 \times 10^{-5}$ s^{-1}. Since at each temperature analysis indica-

ted a substantial formation (up to 35% relative to hexafluoropropene)

of products other than hexafluoropropene and chlorotrifluoroethene,

the value of k_{-3} is certainly not accurate. Also the ratio

$CF_2 = CFCF_3$: $CFCl = CF_2$ was greater than unity because of the partial dimerization of the chlorotrifluoroethene.

Although the activation energy Ea and the pre-exponential factor A for the reverse reaction cannot be calculated accurately because of the short temperature range and the large error involved in the value of the specific rate constants, the extent of opposing reactions in the formation of 1-chloro-2-trifluoromethyl-hexafluoro-cyclobutane was estimated correctly and the results for the forward reaction may be regarded as entirely reliable.

3.4   APPLICATION OF REACTION RATE THEORIES TO THE RESULTS

3.4.1   Arrhenius parameters

The specific rate constants of the cyclodimerizations described in sections 3.1 - 3.3 were given in equations of the general form.

$$\log k = A_c' + B\log T - \frac{C'}{T} \qquad 3.4\_1$$

In the cases of hexafluoropropene and the mixture hexafluoro-propene-chlorotrifluoroethene $B = 0$ and equation 3.4_1 was reduced to

$$\log k = A_c - \frac{C}{T} \qquad 3.4\_2$$

which is a logarithmic form of the integrated Arrhenius equation

$$\ln k = \ln A - \frac{E}{RT} \qquad 3.4\_2a$$

and the pre-exponential factors A and activation energies can be derived directly.

The results of cyclodimerization of chlorotrifluoroethene are given in the modified form of the Arrhenius equation

$$\ln k_i = \ln A_i + B\ln T - \frac{E_i'}{RT} \qquad 3.4\_1a$$

As a consequence of this modified Arrhenius equation

$$k_i = A_i' \, T^\beta \exp(-E_i/RT) \qquad 3.4\_1b$$

the pre-exponential factor and the activation energy are now both explicitly dependent on temperature. The relationship between

Table III.4.1

Pre-exponential factors, activation energies and specific reaction rates

reaction	A	k
$2C_m \longrightarrow D_{cis}$ or $2C_m \longrightarrow D_{trans}$	$5.86 \times 10^{-11} \times$ $(eT)^{4.321} m^{-3} mol^{-1} s^{-1}$	$k_1 \underline{cis}$ $k_1 \underline{trans}$ $= 5.86 \times 10^{-11} T^{4.321} \exp(-\frac{85.100}{RT}) m^3 mol^{-1} s^{-1}$
$D_{cis} \longrightarrow 2C_m$	$3.15 \times 10^{-5} s^{-1}$	$k_{-1}\underline{cis} = 3.15 \times 10^{15} \exp(-273,200/RT) s^{-1}$
$D_{trans} \longrightarrow 2C_m$	$1.19 \times 10^{15} s^{-1}$	$k_{-1}\underline{trans} = 1.19 \times 10^{15} \exp(-273,200/RT) s^{-1}$
$2A \longrightarrow B_{cis}$ or $2A \longrightarrow B_{trans}$	$4.1 \times 10^3 m^3 mol^{-1} s^{-1}$	$k_2 \underline{cis}$ $k_2 \underline{trans}$ $= 4.1 \times 10^3 \exp(-143,700/RT) m^3 mol^{-1} s^{-1}$
$B_{cis} \longrightarrow 2A$	$1.18 \times 10^{15} s^{-1}$	$k_{-2}\underline{cis} = 1.18 \times 10^{15} \exp(-268,600/RT) s^{-1}$
$B_{trans} \longrightarrow 2A$	$4.30 \times 10^{15} s^{-1}$	$k_{-2}\underline{trans} = 4.30 \times 10^{-5} \exp(-268,600/RT) s^{-1}$
$A+B \longrightarrow E_{cis}$ or $A+B \longrightarrow E_{trans}$	$3.6 \times 10^3 m^3 mol^{-1} s^{-1}$	$k_3 \underline{cis}$ $k_3 \underline{trans}$ $= 3.6 \times 10^3 \exp(-118200/RT) m^3 mol^{-1} s^{-1}$

A = hexafluoropropene

B = 1,2-Di(trifluoromethyl)-hexafluorocyclobutane

C_m = chlorotrifluoroethene

D = 1,2-Dichloro-hexafluorocyclobutane

E = 1,chloro-2-trifluoromethyl-hexafluorocyclobutane

the parameters of the equations 3.4_2a and 3.4_1b are

$$A = A' (eT)^\beta \qquad\qquad 3.4\_3$$

$$E = E' + \beta RT \qquad\qquad 3.4\_4$$

The pre-exponential factors, the activation energies and the specific rate constant equations for the cyclodimerization and the dissociation of the compounds studied are given in Table III.4.1. For the cyclodimerization reactions, analysis by spectroscopic methods provided some information about the relative rates of formation of the cis and trans isomers. At the early stages of the reaction approximately equal amounts of the isomers were produced. Therefore, it was assumed that the pre-exponential factor was the same for the cis and trans isomer, the transmission coefficient κ having a value of 0.5 for each isomer, and that the steric factor P was half the experimentally determined value.

3.4.2 - Steric factors for the cyclodimerization reactions

The collision theory of bimolecular reaction rates predicts a specific rate constant given by

$$k_{ij} = (8\pi k \frac{T}{\mu})^{\frac{1}{2}} d_{ij}^2 P \exp (- \frac{E_c}{RT}) \qquad\qquad 3.4\_5$$

where $d_{ij} = r_i + r_j$ is the molecular collision diameter, μ is the reduced mass, P is the steric factor and $E_c = E - \frac{RT}{2}$. Substitution in 3.4_5 gives

$$k_i = 2.753 \times 10^8 \ (\frac{T}{M_\mu})^{\frac{1}{2}} d_i^2 P \exp (- \frac{E_c}{RT}) \ m^3 mol^{-1} s^{-1} \qquad 3.4\_5a$$

$$= 2.753 \times 10^8 \; (\frac{T}{M_\mu})^{\frac{1}{2}} \; d_r^2 \quad \exp\;(-\frac{E_c}{RT} \quad m^3 \; mol^{-1}s^{-1} \qquad 3.4\_5b$$

where M_μ is expressed in relative atomic mass units. d_i is expressed in nm and d_r is the reactive collision diameter in nm. For a single gas (alike molecules) equation 3.4_5 becomes

$$k_i = 2 \; (\pi k \frac{T}{\mu})^{\frac{1}{2}} \quad d_i^2 \; P \; \exp\;(-\frac{E_c}{RT}) \qquad 3.4\_6$$

or $$k_i = 7.786 \times 10^8 \; (\frac{T}{M_\mu})^{\frac{1}{2}} \; r_i^2 \; P \; \exp\;(-\frac{E_c}{RT}) \; m^3 mol^{-1}s^{-1} \qquad 3.4\_6a$$

$$= 7.786 \times 10^8 \; (\frac{T}{M_\mu})^{\frac{1}{2}} \; r_r^2 \; \exp\;(-\frac{E_c}{RT}) \; m^3 mol^{-1}s^{-1} \qquad 3.4\_6b$$

Chlorotrifluoroethene was estimated to have d = 0.573 nm molecular diameter. At the upper end of the temperature range (823 K) E_c = 111216 J mol^{-1} while at the lower (426 K) E_c = 98610 J mol^{-1}. By substituting these figures into equations $3.4\_6a,b$, the values for the steric factor P and the reactive collision d_r obtained are listed together with those of hexafluoropropene and the mixture hexafluoropropene-chlorotrifluoroethene. For hexafluoropropene E_c = 141056 J mol^{-1} and it is assumed that d = 0.72 nm.

$CF_2 = CFCl$	823 K	P = 1.24×10^{-4}	$d_r = 6.39 \times 10^{-3}$
$CF_2 = CFCl$	426 K	P = 1.00×10^{-5}	$d_r = 1.81 \times 10^{-3}$
$CF_2 = CFCF_3$	636 K	P = 2.39×10^{-5}	$d_r = 3.52 \times 10^{-3}$
Mixture	636 K	P = 1.22×10^{-5}	$d_r = 2.26 \times 10^{-3}$

For the mixture, M_μ = 65.57, d_{ij} = 0.647 nm, and E_c = 115656 J mol^{-1}.

3.4.3 Application of the transition state theory

According to the transition state theory of reaction rates, the specific rate constant is given by the expression [129].

$$k_i = \kappa \left(\frac{k\ T}{h}\right) \exp\left(-\frac{\Delta H_i^{\ddagger}}{RT}\right) \exp\left(\frac{\Delta S_i^{\ddagger}}{R}\right) (RT)^{-\Delta n^{\ddagger}} \qquad 3.4.7$$

where κ is the transmission coefficient (usually κ=1) $\left(\frac{k}{h}\ T\right)$ is a universal frequency factor, and $\Delta n^{\ddagger}$ is the change in the number of moles accompanying the formation of an activated complex. k_i is expressed in concentration units (m^3 $mol^{-1} s^{-1}$).

For cycloaddition reactions studied $\Delta n^{\ddagger}$ = -1, and the transition state rate equation can be written as

$$\ln\left(\frac{k_i}{T^2}\right) = \ln\left(\kappa\ \frac{kR}{h}\right) + \frac{\Delta S_i^{\ddagger}}{R} - \frac{\Delta H_i^{\ddagger}}{RT} \qquad 3.4.8$$

where R = 8.205 x 10^{-5} atm m^3 K^{-1} mol^{-1}

Assuming that both the enthalpy and entropy of activation are independent of temperature over the range of rate measurements the results were expressed in the form

$$\ln\left(k_i/T^2\right) = A_i^{\ddagger} - B_i^{\ddagger}/T \qquad 3.4.9$$

by performing least squares calculations. Equating 3.4.8 and 3.4.9, one obtains

$$\ln\left(\kappa\ \frac{kR}{h}\right) + \frac{\Delta S_i^{\ddagger}}{R} = A_i^{\ddagger}$$

$$\frac{\Delta H_i^{\ddagger}}{R} = B_i^{\ddagger}$$

for hexafluoropropene ($\longrightarrow$ cis and trans, $k = \frac{1}{2}$)

$$\ln \left(\frac{k_2}{T^2} \right) = -5.899 - \frac{16014}{T}$$

and for the chlorotrifluoroethene - hexafluoropropene mixture

$$\ln \left(\frac{k_3}{T^2} \right) = -6.015 - \frac{12975}{T}$$

In the case of chlorotrifluoroethene there is ample evidence that the entropy and enthalpy of activation are temperature dependent. since

$$\Delta H_T^{\ominus} = \Delta H_0^{\ominus} + \int \Delta C_P^{\ominus} \, dT = \Delta H_0^{\ominus} + \Delta aT + \frac{\Delta bT^2}{2} \qquad 3.4\_10$$

$$\Delta S_T^{\ominus} = \Delta S_{T1}^{\ominus} + \int \Delta C_P^{\ominus} \frac{dT}{T} = \Delta S_{T1}^{\ominus} + \Delta a \ln (T/T_1) + \frac{\Delta b}{2} (T-T_1) \qquad 3.4\_11$$

$$\Delta G_T^{\ominus} = \Delta H_T^{\ominus} - T\Delta S_T^{\ominus} = -RT \ln K_P^{\ominus} \qquad 3.4\_12$$

and

$$\frac{d\ln K_p^{\ominus}}{d(1/T)} = -\frac{\Delta H_T^{\ominus}}{R} \qquad 3.4\_13$$

it follows that

$$\ln K_p^{\ominus} = \frac{\Delta S_{T1}^{\ominus} - \Delta a \ln T_1}{R} - \frac{\Delta H^{\ominus}}{RT} - \frac{\Delta a}{R} + \frac{\Delta a}{R} \ln T + \frac{3\Delta bT}{2R} - \frac{\Delta bT_1}{R}$$

$$3.4\_14$$

where T_1 is a reference temperature. The above equation can be recognized as the integrated van't Hoff isochore modified to take into account the variations of H and S with temperature. Introducing the relationship of equation 3.4_14 in 3.4_7 and omitting the terms containing b, for which there is not enough information to provide useful values, we obtain

$$\ln k_i = \frac{\Delta S^{\ddagger}_{T1} - \Delta a - \Delta a \ln T_1}{R} + \ln R + \ln \frac{k}{h} + \left(\frac{\Delta a}{R} + 2\right) \ln T - \frac{\Delta H^{\ddagger}_o}{RT} \qquad 3.4\_7a$$

Equating the parameters obtained for chlorotrifluoroethene with the terms of equation 3.4_7a and taking $T_1 = 300$ K as the reference temperature we have

$$H^{\ddagger}_o = 85.1 \text{ kJ mol}^{-1} \qquad a = 19.3 \text{ J K}^{-1}\text{mol}^{-1}$$

$$S^{\ddagger}_{300} = 179.9 \text{ J K}^{-1} \text{ mol}^{-1}$$

The entropies and enthalpies of activation for the reactions listed in section 3.4.1, calculated from equations 3.4_7 and 3.4_7a (mean temperature $T_m = 636$ K) are given in Table III.4.2.

3.4.4 Energetics of the reactions

For the cyclodimerization reaction $A + B \underset{k_{-i}}{\overset{k_i}{\rightleftharpoons}} D$
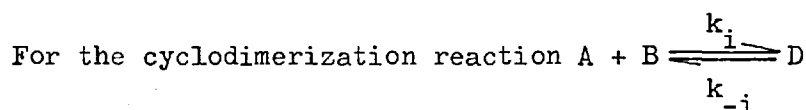
we have for the standard equilibrium constant K_i ($= K^{\ddagger}_P$, standard state: $P^{\ominus} = 101.325$ kPa)

Table III.4.2

Enthalpies and entropies of activation, entropies and enthalpies of reaction

reaction	$\Delta H_i^{\ddagger}$ kJ mol^{-1}	$\Delta S_i^{\ddagger}$ J K^{-1}mol^{-1}	$\Delta G_i^{\ddagger}$ kJ mol^{-1}	$\Delta H_i^{\ominus}$ kJ mol^{-1}	$\Delta S_i^{\ominus}$ J K^{-1}mol^{-1}	$\Delta G_i^{\ominus}$ kJ mol^{-1}
$2C_m \xrightarrow{k_1} D_{cis}$	97.4	-165.4	202.6			
$D_{cis} \xrightarrow{k_{-1}} 2C_m$	267.4	36.4	240.8	-169.2	-200.8	-32.0
$2C_m \xrightarrow{k_1'} D_{trans}$	97.4	-165.4	202.6			
$D \xrightarrow{k_{-1}'} 2C_m$	267.4	32.2	243.9	-169.2	-192.7	-37.6
$2A \xrightarrow{k_2} B_{cis}$	133.1	-168.4	240.9			
$B_{cis} \xrightarrow{k_{-2}} 2A$	262.3	27.9	241.9	-130.6	-198.0	4.5
$2A \xrightarrow{k_2'} B_{trans}$	133.1	-168.4	240.2			
$B_{trans} \xrightarrow{k_{-2}'} 2A$	262.3	38.7	234.0	-130.6	-208.7	11.8
$A+C_m \xrightarrow[k_3']{k_3} E$	107.9	-169.3	215.6			

$\Delta H_i^{\ddagger}$, $\Delta S_i^{\ddagger}$, $\Delta G_i^{\ddagger}$ refer to $T_m = 636K$ for cycloadditions $\Delta H_i^{\ddagger}$, $\Delta S_i^{\ddagger}$, $\Delta G_i^{\ddagger}$ refer to $T_m = 730$ K for dissociations

$\Delta H_i^{\ominus}$, $\Delta S_i^{\ominus}$, $\Delta G_i^{\ominus}$ refer to $T_m = 685K$

$$\ln K_i^{\ominus} = \ln K_{ic}^O + \Delta n \ln(\dot{RT}) = \frac{\Delta \bar{S}_i^{\ominus}}{R} - \frac{\Delta \bar{H}_i^{\ominus}}{RT} \qquad 3.4\_15$$

where K_{ic}^O is the standard concentration equilibrium constant

(standard state: $V_m = 1 \text{ m}^3 \text{ mol}^{-1}$) defined from

$$\ln k_i - \ln k_{-1} = \ln (A_i/A_{-i}) - \frac{(E_i - E_i)}{RT} = \ln K_{ic}^O \qquad 3.4\_16$$

and k_i is expressed in $\text{m}^3 \text{ mol}^{-1} \text{s}^{-1}$.

The principle of the microscopic reversibility demands that the dissociation proceeds along the same reaction path as the cyclodimerization. Combining equations 3.4_7, 3.4_15 and 3.4_16, it can be easily proved that

$$\Delta H_{iT} = \Delta H_i^{\ddagger} - \Delta H_{-i}^{\ddagger} = (E_i - E_{-i}) + \Delta n \, RT_m \qquad 3.4\_17$$

$$\Delta S_{ir} = \Delta S_i - \Delta S_{-i} = R \ln(A_i/A_{-i}) - R\Delta n - R\Delta n \ln(\dot{RT}_m) \qquad 3.4\_18$$

However, since the mean experimental temperature T_m for cyclodimerization differ from that for dissociation and since the variation of $H^{\ddagger}$ is not known, the formulae involving T_m were used. As average temperature for all the experiments was taken $T_m = 685$ K. The values of $\Delta H_{ir}^{\ominus}$ and $\Delta S_{ir}^{\ominus}$ derived using the above equations are given in Table III.4.2.

Chapter **4**

DISCUSSION

Introduction

Fluoroolefins have been used extensively in the study of $_{\pi}2 + _{\pi}2$ cycloaddition reactions and although a considerable body of semiquantitative kinetic measurements exists, the number of accurately determined equations for specific rate constans is still very small (section 1.4). Therefore this discussion concentrates more on results presented in this thesis than on results obtained from elsewhere.

4.1. Arrhenius parameters

The reactions reported in this thesis have pre-exponential factors that are fairly close to those for the few similar gas-phase cyclo-addition reactions that have been studied. For the cyclodimerization of tetrafluoroethene, Atkinson and Trenwith [63] obtained

$$- \frac{dC}{2A^2dt} = k = 5.15 \times 10^4 \exp (-106,270/RT) \quad m^3 mol^{-1}s^{-1}$$

while Lacker and others [111] found that

$$k = 8.25 \times 10^4 \exp (-110,040/RT) \quad m^3 mol^{-1}s^{-1}$$

The same investigators obtained for the intercombination of chloro-trifluoroethene to tetrafluoroethene [111]

$$k = 8.54 \times 10^4 \exp (-110,040/RT) \quad m^3 mol^{-1}s^{-1}$$

The differences between the pre-exponential factors of these cyclo-addition reactions (Table III.4.1.) are not always significant, as the A factors are derived quantities and small errors in the activation energy affect greatly the pre-exponential factor. The activation energies are also fairly similar (110-120 kJ) apart

from the notable exception of hexafluoropropene (144 kJ). The acti-
vation energy for this reaction is much greater than those for the

other reactions, the deviation being well above experimental errors.

The reactive collision diameters d_r given on page 200 range

from 2.2×10^{-3} nm to 6.4×10^{-3} nm. For the cyclodimerization of

tetrafluoroethene at 636 K, the value of $d_r = 8 \times 10^{-3}$ is close to

the value of $d_r = 7.4 \times 10^{-3}$, calculated from the results of Lacker

et al [111]. These values are higher by approximately a factor of

two but the deviation might be within experimental error. Since these

reactions produce basically the cyclobutane ring, the similarity of

the reactive collision diameters is not surprising. Bartlett and

Wheland [79] emphasized (page 45) the importance of the ease of

approach of reactants in formation of the initial new bond, in rea-

ctions proceeding via a diradical mechanism. The present results

indicate that the variation in hindrance of approach of olefins due to

different substituents is rather small. The similarity of the reactive

collision diameters and, therefore, the pre-exponential factors,

stresses the importance of the enthalpy of reaction. This work suggests

that the reactivity of a substituted fluoroolefin in a $_\pi 2 + _\pi 2$ cycloaddi-

tion is determined by the effect of the substituents on the stability

of the double bond to be broken, and on the stability of the formed

cyclobutane ring. Thus substitution of two gem fluorine atoms in the

weak C=C bond by $-CF_3$ groups would require a higher activation energy

for the reaction $CF_2 = C(CF_3)_2 \longrightarrow$ cyclic dimer to proceed. The pre-

sence of four $-CF_3$ groups would certainly increase the strain of the

cyclobutane ring so that dissociation would readily take place.

Indeed, the activation energies of 1,2-disubstituted fluorocyclo-

butanes decrease in the order $c\text{-}C_4F_8 > c\text{-}C_4F_4Cl_2 > c\text{-}C_4F_6(CF_3)_2$
[128]

Similar observations may be made in substituted cyclobutanes

with the notable exception of 1,1,3,3-tetramethylcyclobutane,

which shows high stability. However, systematic study of 1,3-

disubstituted cyclobutanes has yet to be undertaken.

Since there has been no direct measurement of the heat of

formation of the cyclic products, there is no way to check directly

the accuracy of the kinetically derived heats of reactions. It is,

however, generally accepted that kinetic measurement of the heat of

formation involves only a small error. Application of the group pro-

perties additivity scheme [30,31] to estimate thermodynamic quantities

of the compounds used in this work is hindered by the lack of appro-

priate data for groups participating in the structure of the com-

pounds studied. However, chemical statistics form a basis for

obtaining approximate values of thermodynamic quantities, especially

entropy for compounds of known structure and may provide information

about groups that are parts of the cyclic compounds.

4.2. Thermodynamic quantities from chemical statistics [*]

The partition function Q may be expressed as the product of the

translational, vibrational, rotational, electronic, nuclear spin

and free internal rotation contribution to the partition function

$$Q = Q_t \, Q_v \, Q_r \, Q_e \, Q_n \, Q_f \qquad\qquad 4.1\underline{\,1}$$

and computations are made easier by assuming a rigid rotor - harmonic

oscillator model for the molecule where

* the term chemical statistics is equivalent to statistical mechanics

$$Q_r = 8\pi^2 I_r^{\frac{1}{2}} (2\pi kT)^{3/2} h^{-3} \sigma^{-1} \qquad\qquad 4.1\_2$$

$$Q_f = (8\pi^3 I_f kTh^{-2}\eta^{-2})^{\frac{1}{2}} \qquad\qquad 4.1\_3$$

I_r is the product of the three principal moments of inertia, I_f is the 'reduced' moment of inertia and η the symmetry number of the internal rotation.

The involvement of the symmetry number σ in the rotational contribution to the partition function indicates that symmetry considerations should be taken into account in defining the standard state. The cis isomers of 1,2-dichloro, and 1,2-di(trifluoromethyl)-hexafluorocyclobutane belong to C_1 point group (or C_s if D_{4h} symmetry is assumed for the cyclobutane ring) and have a symmetry number of one. The trans isomers, however, belong to C_2 point group and have a symmetry number of two, but exist in two chiral (enantiomorphic) forms. The pure (+) or the pure (-) forms would contribute a factor of (-2) to Q_r or -Rln2 to rotational entropy S_r. If the standard state is taken as an inactive (+) - (-) mixture, and it is believed that this corresponds to the conditions of the present work, there will be an additional contribution of $-R\sum n_i \ln n_i$, $n_1, n_2 = \frac{1}{2}$ (i.e. Rln2) in the entropy, due to mixing. In the case of 1-chloro-2-trifluoromethyl-hexafluorocyclobutane, the cis and trans isomers belong to the C_1 point group and exist in enantiomorphic forms. Therefore, symmetry considerations make no net contribution to the differences in ΔS_i for the isomers of the molecules studied. Benson[30b] suggests that statistical calculations

should refer to the intrinsic partition function $Q(intrinsic)=Q.\sigma$

rather than to the state sum Q. The intrinsic entropy is, then,

$S^{\ominus}(intrinsic) = S^{\ominus} + Rln\frac{\sigma}{n}$ where n is the number of optical isomers

of the same energy.

4.2.1a Rotational partition function

Since the molecules produced have low molecular symmetry, neither

the positions of the three principal axes nor the centre of mass

are known. Therefore, the product of the three principal moments

of inertia I_r was calculated by means of the secular equation [135].

$$I_r = I_x I_y I_z = \begin{vmatrix} + I_{xx} & - I_{xy} & - I_{xz} \\ - I_{xy} & + I_{yy} & - I_{yz} \\ - I_{xz} & + I_{yz} & + I_{zz} \end{vmatrix} \qquad 4.1\_3$$

and since the coordinate frame of reference dia not coincide with

centre of mass, the moment of inertia coefficients I_{xx}, I_{yy}, I_{zz}

were calculated from

$$I_{xx} = \Sigma m_i (y_1^2 + z_i^2) - \frac{1}{M} (\Sigma m_i y_i)^2 - \frac{1}{M} (\Sigma m_i z_i)^2 \qquad 4.1.\_4$$

etc. and the (so-called) products of inertia from

$$I_{xy} = \Sigma m_i x_i y_i - \frac{1}{M} (\Sigma m_i x_i)(\Sigma m_i y_i) \quad etc. \qquad 4.1\_5$$

where m_i is mass of atom i with coordinates, x_i, y_i, z_i and

$M = \Sigma m_i$. As origin of the cartesian coordinates was taken the

centre of the cyclobutane ring (section 1.2) and the vectors

x_i, y_i, z_i were calculated by employing the MOLTER programme [45]

(section 1.3) which could be extended to perform these calculations. This particular frame of reference reduced the amount of calculation needed for different configurations and molecules. Thus, both the puckered and a planar ring were considered. For fluoroolefins, the vectors x_i, y_i, z_i were calculated using published bond distances and bond angles. The geometry of the ring in the cyclic compounds was assumed to be essentially that of octafluorocyclobutane (D_{2d}). The various permutational isomers, regardless of chirality, were constructed by replacing fluorine atoms with atoms or groups having appropriate bond distances [71] and angles. Equation 4.1_4 and 4.1_5 were, then, used to calculate the moments and products of inertia. For chlorotrifluoroethene, hexafluoropropene and 1a-chloro-2e-trifluoromethyl-hexafluorocyclobutane these are:

	I_{xx}^*	I_{yy}^*	I_{zz}^*	I_{xy}^*	I_{xz}^*	I_{yz}^*
$CF_2 = CFCl$	135	199	345	-45	0	0
$CF_2 = CFCF_3$	252	339	501	83	0	0
c_$C_4F_6ClCF_3$	836	803	997	-103	108	-30

Setting up the secular determinant (equation 4.1_3) the products of the principal moments of inertia are, respectively,

$Fx8.59x10^6$ Kg m^2, $Fx3.92x10^7$ Kg m^2, $Fx6.49x10^8$ Kg m^2 ($F=4.578x10^{-141}$)

The symmetry and the products of the principal moments of inertia I_{xyz} for 1,2-and 1,3- disubstituted perfluorocyclobutanes are given in Table IV.1. The values of I_{xyz} indicate that the rotational

* $I_{ij} = I_{ij}^* \times 1.6605 \times 10^{-47}$ Kg.m^2

Table IV.2.1.

Symmetry, product of principal moments of inertia and rotational

contribution to entropy of some 1,2 and 1,3 disubstituted perfluoro-

cyclobutanes
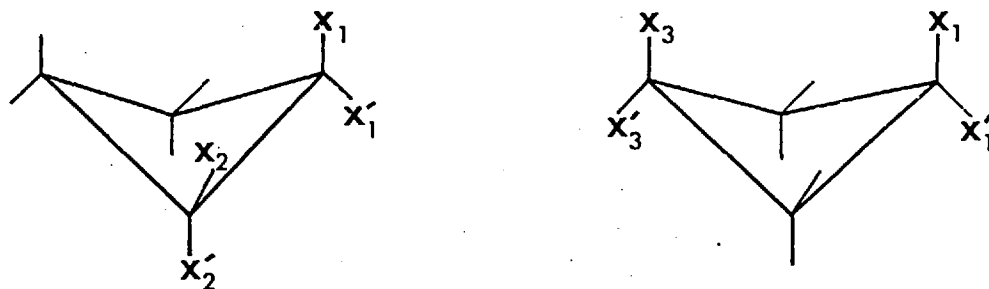
X		X		I^*_{xyz}	$^+S_{r \ 636}$	
		cis				
1	Cl	2	Cl	C_1	2.98	139.1	
1	CF_3	2	CF_3	C_1	11.18	144.6	
1	Cl	2	CF_3	C_1	6.49	142.3	
1	CF_3	2	Cl	C_1	5.85	141.9	
1	Cl	2	Cl	C_s	2.89	138.9	(a)
1	CF_3	2	CF_3	C_s	8.31	143.3	(a)
		trans				
1	Cl	2'	Cl	C_2	3.16	139.3	
1	CF_3	2'	CF_3	C_2	12.23	145.0	
1	Cl	2'	CF_3	C_1	6.29	142.2	
1	Cl	2'	Cl	C_2	3.00	139.1	(a)
1	CF_3	2'	CF_3	C_2	10.8	144.4	(a)

(a) planar model

Substituent					I^*_{xyz}	$^+S_{r_{636}}$
		cis				
1^1	Cl	2	Cl	C_1	3.07	139.2
1^1	CF_3	2	CF_3	C_1	13.81	145.5
1^1	Cl	2	CF_3	C_1	7.24	142.8
		cis				
1	Cl	3	Cl	C_{2v}	2.11	137.7
$1'$	Cl	$3'$	Cl	C_{2v}	3.08	139.2
$1'$	CF_3	$3'$	CF_3	C_{2v}	14.23	145.6
$1'$	CF_3	$3'$	Cl	C_s	6.94	142.6
		trans				
1	Cl	$3'$	Cl	C_s	3.1	139.2
1	CF_3	$3'$	CF_3	C_s	13.62	145.4
1	Cl	$3'$	CF_3	C_s	7.05	142.7
1	CF_3	$3'$	Cl	C_s	6.38	142.2
				C_s	0.008	124.3
				C_s	0.039	130.65
Compounds						
$CF_2 = CFCl$				C_s	0.008	124.3
$CF_2 = CFCF_3$				C_s	0.039	130.65

* $\times 10^8$, and $I = I^* \times (1.6605 \times 10^{-47})^3$ Kg m^2

+ calculated from Q.

contribution Q_r to the partition function for the 1,3-isomers would be roughly the same as that for the 1,2-isomers. The rotational entropy of a rigid rotor is calculated from

$$S_r = R\ln Q_r + RT d\ln Q_r/dT \qquad 4.1\_6$$

Expressing the products of inertia I_r^* in relative atomic mass units and m^{-20} (Angstrom $\overset{o2}{A}$) the rotational entropy is given by

$$S_r^O = R \left(\tfrac{1}{2}\ln I_r^* + \frac{3}{2} \ln T - \ln\sigma - 2.7106\right) \ J \ K^{-1}mol^{-1} \qquad 4.1\_7$$

Values obtained for the model molecules appear in Table IV.1.1.

4.2.1b   Vibrational partition function

The number of fundamental vibrational and internal rotational modes for the cyclic molecules is (3n-6) since the systems are non-linear oscillators. The vibrational partition function cannot be estimated without more spectroscopic evidence than is at present available. The case of 1-chloro-2-trifluoromethyl-hexafluorocyclobutane is worse than the rest, since the observed vibrational spectrum was not assigned for the two isomers. Were this accomplished, the frequencies of a number of fundamental vibrations occuring below 1.8×10^{-3} Hz (600 cm^{-1}) would, still remain unknown. Since the low frequency vibrations make the most important contributions to Q_v a fairly complete vibrational analysis for the cyclic molecules is evidently required. However a useful estimate can be made by using the available infrared and Roman data for these compounds (sections 3.1.1, 3.2.1, 3.3.1) together with the published [52,126]

wavenumbers for analogous molecules.

Six of the fundamental vibrations of the cyclic molecules result from the loss of three translational and three rotational degrees of freedom of the two molecules combined to produce it. Two of the six additional vibrations will be ring bending δ and another two ring stretching ones (ν). The remaining two additional vibrations involve CX_2 bending vibrations which we consider to be out-of-plane r_γ , one twisting and one wagging. This mode of motion would occur at wavenumbers above that of the ring puckering 95 cm^{-1} but below of the other ring deformation (283 cm^{-1}). Therefore, values of 160-19? cm^{-1} for twist and 250-275 cm^{-1} for wagging are reasonable [55].

Calculation of the vibrational contribution Q_v to the partition function Q requires the knowledge of all the fundamental frequencies. However, the vibrational contribution to differences of thermodynamic quantities i.e. $\Delta S^{\ominus}$, would come mainly from the six additional vibrations. A small contribution is expected from the small changes in frequency above 600 cm^{-1} occuring from the change in the molecular structure. The most significant of these changes are, perhaps, the C-C stretching at 1780 - 1800 cm^{-1} (two), replaced by the two ring deformations at 900 - 1000 cm^{-1}.

The rather arbitrary assignment of frequencies to the six additional vibrations may well introduce greater error than the error occuring from the omission of frequency differences. Nevertheless, such an assignment based on similar compounds is indicative of the size of expected differences in thermochemical quantities and has been proved successful in the treatment of 1,2-dichlorohexafluoro-cyclobutane by Stedman [112], and 1,2-di(trifluoromethyl)-hexafluoro-

cyclobutane by Stockwell [132]. Stedman's and Stockwell's assignments were based on inadequately interpreted published [55] assignments which, since then, have been revised.

| Type of motion | $1,2\text{-}c.C_4F_6Cl_2$ | | $1,2\text{-}c.C_4F_6(CF_3)_2$ | | $1,2\text{-}c.C_4F_6ClCF_3$ |
	Stedman*	This work	Stockwell*	This work*	This work*
ring fold	86	95	86	95	95
ring deformation	162	270	162	270	270
ring deformation		334		334	334
ring deformation	640	640	640	640	640
ring breathing		962		950	934
ring stretching	1047	1047	1047	1015	1029
CX_2 wagging	270	216	270	230	225
CX_2 twisting	334	162	334	162	162

* wavenumber $(\overline{v}/cm^{-1})$

However, apart from the different allocation of fundamentals the present treatment differs from those of Stedman and Stockwell only in the addition of two carbon-carbon double bonds stretchings at 1800 cm^{-1}.

Treating the additional vibrations as harmonic oscillators and using the frequency assignment given and the corresponding values of Einstein functions [133] at 685 K, the contribution for each fundamental mode is obtained by interpolation and summation.

Table IV.2.2

Vibrational contributions to the change of standard entropy and heat capacity

Type of motion	1,2-c.C_4F_6Cl			1,2-c.$C_4F_6(CF_3)_2$			1,2-c.$C_4F_6ClCF_3$		
	x	S_v	Cp_v	x	S_v	Cp_v	x	S_v	Cp_v
ring fold	0.1995	21.73	8.29	0.1995	21.73	8.29	0.1995	21.73	8.29
ring deformation	0.5671	13.14	8.09	0.5671	13.14	8.09	0.5671	13.14	8.09
ring deformation	0.7016	11.43	7.98	0.7016	11.43	7.98	0.7016	11.43	7.98
ring deformation	1.3443	6.45	7.17	1.3443	6.45	7.17	1.3443	6.45	7.17
ring breathing	2.0207	3.75	5.98	1.9955	3.83	6.03	1.9619	3.93	6.09
ring stretch	2.1992	3.26	5.64	2.1320	3.43	5.77	2.1614	3.36	5.71
CX_2 wagging	0.4537	14.96	8.17	0.4831	14.44	8.15	0.4726	14.65	8.16
CX_2 twisting	0.3403	17.32	8.23	0.3403	17.32	8.23	0.3403	17.32	8.23
C-C stretch*	3.7809	-0.93	-2.84	3.7809	-0.93	-2.84	3.7809	-0.93	-2.84
Sum		91.11	56.71		90.84	56.87		91.05	56.88

$x = (\bar{v}hc/kt) = 2.1005 \times 10^{-3} \bar{v}$ at 685 K. $\bar{v}$ is expressed in cm^{-1}

S_v is expressed in $J K^{-1} mol^{-1}$ Cp_v is expressed in $J K^{-1} mol^{-1}$

4.2.1c   Internal rotation

A contribution to the thermodynamic functions is expected from the $-CF_3$ group, participating in the structure of the molecules studied, due to internal rotation. The internal rotation is a hindered one and a substantial barrier[23, 81] is expected. The actual contribution of hindered internal rotation to entropy, S_h^o, is calculated from the relation

$$S_h^o = h \left(\tfrac{1}{2} + \ln Q_f\right) - \left(S_f^o - S_{hi}^o\right)$$

4.2.2.   Entropy and heat capacity

Calculations by chemical statistics of differences in thermodynamic functions between reactants and products for the models suggested earlier (pages 25, 213) can be made. Calculations of entropy and heat capacity changes for the reactions studied give:

a   chlorotrifluoroethene $\longrightarrow$ 1,2-dichlorohexafluorocyclobutane

S_t	=	-174.97	C_{p_t}	= 2.5 R
S_r	=	-109.40	C_{p_r}	$= -\dfrac{3}{2}$ R
S_v	=	91.11	C_{p_v}	= 56.71
$\Delta S_{636}^{\ominus}$	=	-193.26 J K^{-1}mol^{-1}	$\Delta C_p^{\ominus}$	= 23.45 J K^{-1}mol^{-1}

experimental $\Delta S_{cis}^{\ominus}$ = -200.8   J K^{-1}mol^{-1}

experimental $\Delta S_{trans}^{\ominus}$ = -192.7   J K^{-1}mol^{-1}

b   hexafluoropropene ⟶ 1,2-di(trifluoromethyl)-hexafluorocyclobutane

$$S_t = -178.36 \qquad\qquad C_{p_t} = -20.78$$

$$S_r = -116.50 \qquad\qquad C_{p_r} = -12.47$$

$$S_v = 90.84 \qquad\qquad C_{p_v} = 56.87$$

$$S_h = \underline{2.00} \qquad\qquad C_{p_h} = 18.58$$

$$\Delta S_{636}^{\ominus} = -202.02 \text{ J K}^{-1}\text{mol}^{-1} \qquad \Delta C_p^{\ominus} = 42.19 \quad \text{J K}^{-1}\text{mol}^{-1}$$

$$\text{experimental } \Delta S_{cis}^{o} = -198.0 \text{ J K}^{-1}\text{mol}^{-1}$$

$$\text{experimental } \Delta S_{trans}^{o} = -208.7 \text{ J K}^{-1}\text{mol}^{-1}$$

c   mixture $CF_2=CFCF_3 + CF_2 = CFCl$ ⟶ 1-chloro-2-trifluoromethyl-
-hexafluorocyclobutane

$$S_t = -176.68 \qquad\qquad C_{p_t} = -20.78$$

$$S_r = -112.80 \qquad\qquad C_{p_r} = -12.47$$

$$S_v = 91.05 \qquad\qquad C_{p_v} = 56.88$$

$$S_h = 1.00 \qquad\qquad C_{p_h} = 9.29$$

$$\Delta S_{636}^{\ominus} = -197.43 \text{ J K}^{-1}\text{mol}^{-1} \qquad \Delta C_p^{\ominus} = 32.92 \quad \text{J K}^{-1}\text{mol}^{-1}$$

The first two values of entropy change and are within experi-
mental error of the kinetically determined quantities. Complete vibra-
tional analysis of the reacting system would have improved the results.
The equilibrium of the system $CF_3CF=CF_2 + CF_2 = CFCl \rightleftharpoons$ 1-chloro-
2-trifluoromethyl-hexafluorocyclobutane has not been studied and the
experimental value of entropy change is not known. The present cal-
culations indicate, as suggested earlier (section 4.1), that it would
be $\Delta S_{r3}^{\ominus} = 200 \pm 8 \text{ J K}^{-1}\text{mol}^{-1}$.

Provided that the vibrational contribution to the partition function of the 1,3-isomers is the same as that for the 1,2-isomers, no significant difference in $\Delta S_r^{\ominus}$ for these two classes is expected.

4.3   Energetics from addition of group properties

The groups participating in the structure of the cyclic molecules are $\left[C - (C)_2 (F)_2 \right]$, $\left[C - (C)_2 (Cl) (F) \right]$, $\left[C - (C)_3 (F) \right]$ and $C - (C) (F)_3$ and of course (section 1.4), the ring.

<u>a</u> For 1,2-Dichlorohexafluorocyclobutane (D) one has

$$\Delta X^{\ominus} = 2 \times \left[C - (C)_2 (F)_2 \right] + 2 \times \left[C - (C)_2 (F) (Cl) \right] +$$

$$\text{ring correction}$$

$\therefore \Delta H_f^{\ominus} = 2 \times (-407.94) + 2 \times (-235.14)^* + 117 = -1169.16 \text{ kJ mol}^{-1}$

$\quad S^{\ominus} = 2 \times (74.48) + 2 \times (92.88)^* + 124.68 = 459.4 \text{ J K}^{-1}\text{mol}^{-1}$

$\quad \overline{C_p^{\ominus}} = 2 \times (54.70) + 2 \times (60.63) + 14.77 = 245.43 \text{ J K}^{-1}\text{mol}^{-1}$

$\therefore \Delta H_{650}^{\ominus} = H_f^{\ominus} + \Delta \overline{C_p^{\ominus}} (T_{650} - T_{300})$

$\quad S_{650}^{\ominus} = S^{\ominus} + \Delta \overline{C_p^{\ominus}} \ln (T_{650}/T_{300})$

$\therefore \Delta H_{f650}^{\ominus} = -1169.16 + 85.9 = -1083.26 \text{ kJ mol}^{-1}$

$\quad S_{650}^{\ominus} = 459.4 + 189.76 = 649.16 \text{ J K}^{-1} \text{mol}^{-1}$

<u>b</u> 1,2-Di(trifluoromethyl)-hexafluorocyclobutane (B)

$$\Delta X^{\ominus} = 2 \times \left[C - (C)_2 (F)_2 \right] + 2 \times \left[C - (C)_3 (F) \right] +$$

$$2 \times \left[C - (C) (F)_3 \right] + \text{ring correction}$$

$$\therefore \quad \Delta H_f^{\ominus} = 2 \times (-407.94) + 2 \times (-183.68) + 2 \times (-662.75) + 117$$

$$= -2391.74 \text{ kJ mol}^{-1}$$

$$\Delta S^{\ominus} = 2 \times (74.48) + 2 \times (-28.55)^* + 2 \times (177.82) + 124.68$$

$$= 573.18 \text{ JK}^{-1}\text{mol}^{-1}$$

$$\Delta \overline{C_P^{\ominus}}_{650-300} = 2 \times (54.7) + 2 \times (50.2)^* + 2 \times (64.43) + 14.77$$

$$= 353.45 \text{ J K}^{-1}\text{mol}^{-1}$$

and $\Delta H_{f_{650}}^{\ominus} = -2391.74 + 123.71 = -2268.03 \text{ kJ mol}^{-1}$

$$\Delta S^{\ominus}_{650} = 573.18 + 273.28 = 845.46 \text{ J K}^{-1}\text{mol}^{-1}$$

<u>c</u>   1-chloro-2-trifluoromethyl-hexafluorocyclobutane (E)

From groups in this compound it is obvious that

$$2 \text{ X}^{\ominus} \text{ (E)} = \text{X}^{\ominus} \text{ (B)} + \text{X}^{\ominus} \text{ (D)}$$

$$\therefore \quad \Delta H_f^{\ominus} = -1780.45 \text{ kJmol}^{-1}$$

$$\Delta S^{\ominus} = 654.34 \text{ J. K}^{-1}\text{mol}^{-1}$$

$$\Delta \overline{C}_{P_{650-300}} = 299.44 \text{ J K}^{-1}\text{mol}^{-1}$$

$$\Delta H_{f650}^{\ominus} + -1675.64 \text{ kJ mol}^{-1} \quad S_{650}^o = 747.31 \text{ J K}^{-1}\text{mol}^{-1}$$

<u>d</u>   Hexafluoropropene (A)

$$\text{X}^{\ominus} = \left[C_d - (F)_2 \right] + \left[C_d - (C) (F) \right] + \left[C - (C_d) (F)_3 \right]$$

* The asterisk indicates tentative values

$$\therefore \quad \Delta H_f^{\ominus} = (-329.25) + (-128.68)^* + (-662.75)^* = -1120.68 \text{ kJ mol}^{-1}$$

$$\Delta S^{\ominus} = (156.06 + (76.72)^* + (176.82)^* = 409.66 \text{ J K}^{-1}\text{mol}^{-1}$$

$$\overline{\Delta C_{p650-300}^{\ominus}} = (47.49) + (37.41)^* + (63.6)^* = 148.5 \text{ J K}^{-1}\text{mol}^{-\beta 1}$$

and $\Delta H_{f650}^{\ominus} = -10.68.7 \text{ kJ mol}^{-1}$ $\quad S_{650}^o = 459.52 \text{ J K mol}^{-1}$

e   Chlorotrifluoroethene (C_m) [134]

$$X^{\ominus} = \left[C_d - (F)_2 \right] + \left[C_d - (F) (Cl) \right]$$

$$\Delta H_f^{\ominus} = (-329.25) + (-165.25)^* = -494.5 (489.5 \pm 12)$$

$$\Delta S^{\ominus} = (156.06) + (186.1)^* = 342.16 \text{ J K}^{-1}\text{mol}^{-1}$$

$$\overline{\Delta C_p^{\ominus}} = (47.49) + (57.51)^* = 105 \text{ J K}^{-1}\text{mol}^{-1}$$

$$\Delta H_{f650}^{\ominus} = -494,500 + 105 \times (650-300) = -457.75 \text{ kJ mol}^{-1}$$

$$\Delta S_{650}^{\ominus} = 342.16 + 81.19 = 423.35 \text{ J K}^{-1}\text{mol}^{-1}$$

From the calculated quantities the entropies and enthalpies of the reactions investigated are estimated. Table IV.3.1 summarizes the results.

* The asterisk indicates tentative values

Table IV.3.1.

Experimental and theoretical thermodynamic quantities at 650 K

reaction	method	$\Delta H^{\ominus}_{ri}$	$\Delta S^{\ominus}_{ri}$	$\Delta C^{\ominus}_{p}$
$2CF_2 = CFCl$ $\rightarrow cC_4F_6 \begin{smallmatrix}Cl\\Cl\end{smallmatrix}$	Experimental (cis)	-169.2	-200.8	
	Experimental (trans)	-169.2	-192.7	
	Statistical Mechanics		-193.3	23.45
	Group properties	-167.8	-197.5	35.43
$2CF_2=CFCF_3$ $\rightarrow cC_4F_6 \begin{smallmatrix}CF_3\\CF_3\end{smallmatrix}$	Experimental (cis)	-130.6	-198.0	
	Experimental (trans)	-130.6	-208.7	
	Statistical Mechanics		-202.0	42.2
	Group properties	-130.6	-203.5	56.4
cis-1a,2e	MINDO calculations*	-124.3		
trans-1a,2a	(page 25)	-169.3		
trans-1e,2e		-205		
$CF_2=CFCl$ + $CF_3=CFCF_3$ $\rightarrow cC_4F_6ClCF_3$	Experimental			
	Statistical mechanics		197.4	32.92
	Group properties	-149.2	-200.5	45.94

The agreement between these methods on the value of the enthalpy of reaction is very good. The greater deviation of the values calculated by the MINDO method (page 24) are due to the sensitivity of the method to the interatomic distances used. MINDO calculations clearly favour the formation of the _trans_ isomers. However, the method is intended to estimate heats of formation rather than heats of reaction. In this sense the error involved ($<$ $\pm$ 3%) is quite small for such complicated systems.

The values of entropy change assigned to groups have given good agreement between the value of entropy estimated from statistical mechanics and that estimated from groups. Since the values assigned presently were based on information from groups not very similar to those participating in the molecules, the discrepancies are not surprising. Perhaps, a better approach would be the examination of the differences in groups arising from contributions due to changes in the rotational and vibrational entropy.

The value of entropy change for the reaction

$$CF_3CF = CF_2 + CF_2 = CFCl \rightleftharpoons c\_ C_4F_6ClCF_3$$
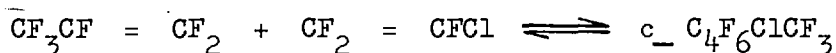
predicted from statistical mechanics and contribution from groups, is the one expected for such a system. The dissociation reactions for cyclobutane and polyfluorocyclobutane derivatives have pre-exponential factors [128] $A \approx$ 1-5 x 10^{15} s^{-1} and activation energies $E \approx$ 265-285 kJ.mol^{-1}. Assigning the value $A = 1.06 \times 10^{15} s^{-1}$ for the decomposition of the cis or trans isomer and assuming activation energy $E = 270.2$ kJ.mol^{-1} we obtain

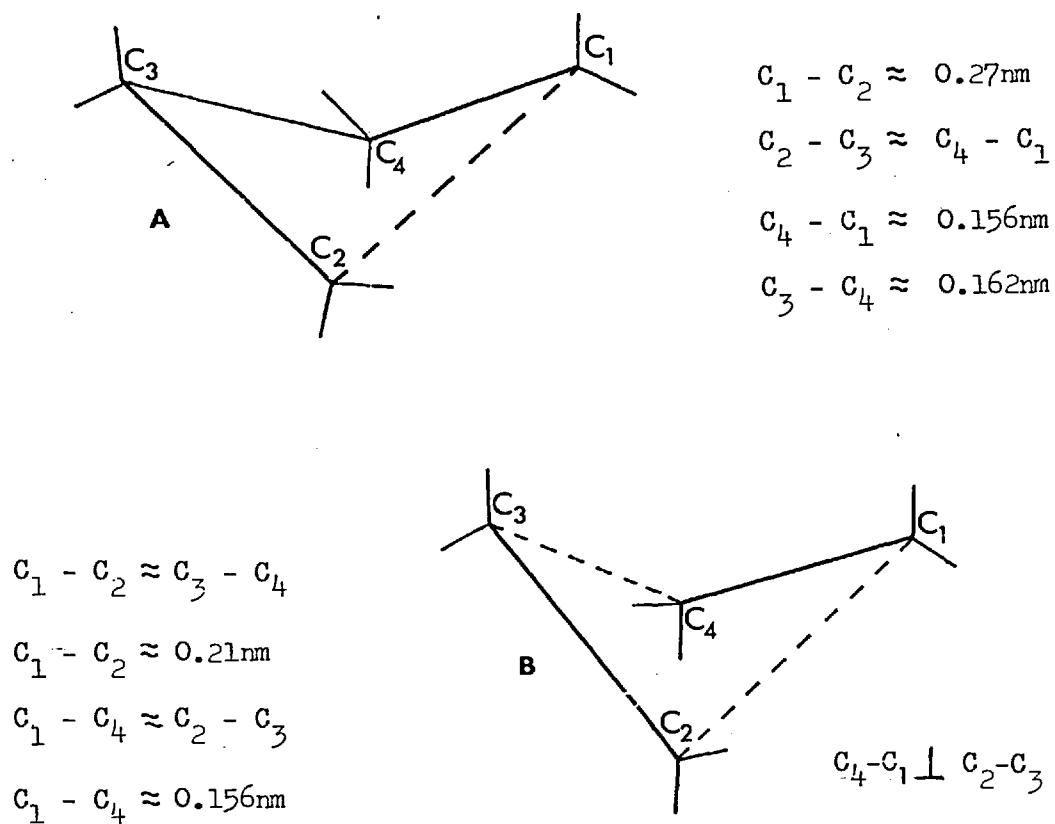$$S^{\ominus}_{r3} = -203.6 \text{ J } K^{-1}mol^{-1} \text{ and } H^{\ominus}_{r3} = -157.7 \text{ kJ.}mol^{-1}$$

4.4   Mechanism of the reaction

The entropy and enthalpy of activation provide information about the structure of the activated complex and are indicative of the factors affecting its formation as well as the probable course of the reaction. The entropy change in the transition state of similar $_\pi 2 + _\pi 2$ reactions has a value $-(160\text{-}170)$ J $K^{-1}mol^{-1}$ at 600 K - 700 K. The structure of the transition state is, therefore, characterized more by the loss of rotational and translational degrees of freedom of the reactants than by the widely varying sizes and masses of the substituents or their electronic properties.

The review of $_\pi 2 + _\pi 2$ cycloaddition reactions suggested that they may proceed by either a concerted or a stepwise mechanism (page 45). Epiotis [76], applying Perturbation MO, indicated that the smaller the size of substituents in a $_\pi 2_s + _\pi 2_a$ cycloaddition, the greater the rate of reaction   (page 44); the experimental results follow this trend. Furthermore, such a treatment predicts that these reactions would show regioselectivity favouring the formation of head-to-tail (HT) products (page 45). Formation of substantial quantities of 1,3 isomers simultaneously with the 1,2 isomers, would have indicated participation of a concerted process, since an HT addition (formation of 1,3 isomers) would not be favoured by a stepwise mechanism. However, Epiotis's approach is based on the relative size of the coefficient c_{ij} of the atomic orbitals (section 1.3, equations 1.3, 1.4) which depend on the type of approximations used. Although the, almost, exclusive formation of 1,2 isomers makes highly improbable participation of a concerted process, it does not rule out conclusively the involvement of such a reaction path and this mechanism should also be considered.

Figure 4.1.   Activated complex from a diradical intermediate

(A) and an allowed (s + a) concerted process (B)

$$C_1 - C_2 \approx 0.27\text{nm}$$

$$C_2 - C_3 \approx C_4 - C_1$$

$$C_4 - C_1 \approx 0.156\text{nm}$$

$$C_3 - C_4 \approx 0.162\text{nm}$$

A

$$C_1 - C_2 \approx C_3 - C_4$$

$$C_1 - C_2 \approx 0.21\text{nm}$$

$$C_1 - C_4 \approx C_2 - C_3$$

$$C_1 - C_4 \approx 0.156\text{nm}$$

B

$$C_4 - C_1 \perp C_2 - C_3$$

The stepwise process takes place _via_ a diradical intermediate which, according to Benson and others (page 47) should not be confused with the two transition states in the formation and the cyclisation of the radical. Ring closing involves a series of concerted events. In addition to the internal rotation which brings the radical ends C_1, C_4 into the proper _cis_ conformation, the bonding orbitals

must also be directed towards one another and the carbon bends must

bring the orbitals together. Therefore, the transition state for

cyclisation could be regarded as a diradical in the singlet state

in which the free electrons are paired. Furthermore, such an activated

complex implies a slightly elongated C_1 - C_4 bond and a rather 'loose'

C_1 - C_2 'bond'. The energetics of such a transition state may be cal-

culated from the groups participating in it if relevant information exists.

The method has been described in section 1.4. Entropy and heat

capacity may be calculated straightforwardly from statistical mechanisms

4.4.1 Calculation of thermodynamic properties of the transition states

and the diradical intermediate from group contribution

<u>A</u> Chlorotrifluoroethene ⟶ Cyclodimerization transition state

<u>1</u> Chlorotrifluoroethene (C_m)   see 4.3 <u>e</u>

<u>2</u> Diradical ($R'\colon$) = $\overset{\bullet}{C}FCl$ CF_2 CF_2 $\overset{\bullet}{C}FCl$

$HCFClCF_2CF_2CFClH$ $R'\colon$ + $2H^\bullet$

H_f^o (R^1H_2) = 2 x $\left[C\text{-}(F)\,(Cl)\,(H)\,(C)\right]$ +2 x$\left[C - (C)_2\,(F)_2\right]$

$\qquad\qquad$ = 2 x $(-279.5)^*$ + 2 x (-407.94) = -1374.9 $kJmol^{-1}$

S^o (R^1H_2) = 2 x $(175.2)^*$ + 2 x (74.5) = 501.3 J $K^{-1}mol^{-1}$

$\overline{C}^o_{p_{650\text{-}300}}$ (R^1H_2) = 2 x $(66.0)^*$ + 2 x (52.9) = 237.8

$\qquad\qquad\qquad\qquad\qquad\qquad\qquad$ J $K^{-1}mol^{-1}$

H_{f650}^o $(R^1\colon)$ = 2 $H_f^o(C\text{-}H)$ + H_f^o (R^1H_2) + 2 H_f^o $(H^\bullet)$

$\qquad\qquad$ + $\overline{C}^o_p$ $(T_2\text{-}T_1)$

$\qquad\quad$ = 866.1 - 1374.9 - 436 + 0.23 x 350 = -864.33

$$\Delta S^o_{650} \ (R^1:) \ = \ S^o \ (R^1 H_2) \ - \ 3 \ R\ln \ (\ \frac{R^1}{R^1 H_2} \ ) \ - \ 2 \ (C-H)_{3100} \ -$$

$$-2 \ (F{\overset{C}{\diagup}}{\diagdown}H)_{1450}, \ - \ 2 \ (Cl{\overset{C}{\diagup}}{\diagdown}H)_{700} \ -$$

$$-0.5 \ R\ln \frac{Ir \ (\ R \ :)}{Ir \ (R^1 H_2)} \ + \ R\ln g_i \ = \ 675.2 \ \ JK^{-1}mol^{-1}$$

$$\Delta \overline{C}^o_{P_{650-300}} \quad (R^1:) = 229.9 \ \ J \ K^{-1} \ mol^{-1}$$

<u>3</u>   Cyclic activated complex (C in Fig. 1.13)

$$\Delta H^*_{650} \ - \ H^o_f \ (R^1:) \ + \ H^o \ (CFCl \ CF_2 \overset{\bullet}{\longrightarrow} \infty)_{27}$$
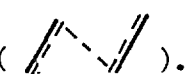
$$= \ -864.33 \ + \ 27 \ = \ -837.33 \ \ kJ \ mol^{-1}$$

$$\Delta S^* \ = \ S^o_{650} \ (R^1:) \ - \ (t\text{-}Bu \rightarrow \infty) \ + \ (C\text{-}C)_{900}$$

$$= \ 675.2 \ - \ 8.8 \ + \ 4.2 \qquad = \ 670.6 \ \ j \ K^{-1} \ mol^{-1}$$

The hindered rotation of a $-CFCl$ group is taken as the reaction co-ordinate. The weak link formed between the $C_1\text{-}C_2$ carbon atoms contributes one vibration at 800 cm^{-1}

<u>4</u>   'Open' activated complex (B on page 54)

The 'open' activated complex is depicted as ( ). Any significant structural differences between the model for cyclization (B) and that for geometrical (<u>cis-trans</u>) isomerization are expected to contribute to the entropy and enthalpy of activation. In the diradical mechanism, the central internal rotation of the 'open' activated complex becomes a free rotation. The carbon-carbon $(C_1\text{-}C_4)$ bond stretch is equated with the reaction co-ordinate. In addition, two skeletal bends involving the $C_3\text{-}C_4$ bond are loosened. Thus, for step $(d)_2$ (page 51) one has

$$X^o = X \ (R^1:) - X, \ 2 \ (t-Bu \rightarrow \infty) \quad - 2(C \overset{C}{\diagdown} C)_{420}$$

$$- (C-C)_{900} + (4e \ torsion)^*_{300} + (3e \ torsion)_{125}$$

$$+ \ (C \overset{C}{\diagdown} \cdot \ C)_{290}$$

$$S_{650} = 675.18 - 2 \times 8.8 - 2 \times 8.79 - 3.6 + 12.2 + 20.9 + 11.8 = 681.3 \ J \ K^{-1} \ mol^{-1}$$

$$H_{650} = -864.33 + 2 \times 23 \ (bond \ elongation) = -818.33 \ kJ \ mol^{-1}$$

In order to achieve concordance between experimental results and thermochemical quantities obtained from groups, it was necessary to adjust the value of energy required for hydrogen abstraction to 420 kJ H mol in the case of the diradical corresponding to the hexa-fluoropropene-chlorotrifluoroethene mixture, and to 412.5 kJ/H mol for that obtained from pure hexafluoropropene. The value quoted previously, 433 kJ/H mol, was derived from bond dissociation energy in fluorinated methanes and obviously is not applicable in the pre sent cases.

The thermochemical quantities for each reaction step, estimated from group contribution, are given in Table IV.4.1. These figures clearly indicate that the heat of reaction of the system

$$2CF_3CF = CF_2 \quad \longrightarrow \quad CF_3\overset{\bullet}{C}FCF_2CF_2\overset{\bullet}{C}FCF_3$$
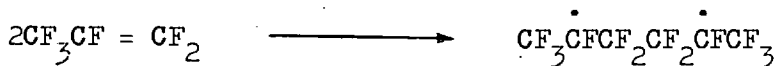
is about 99.7 kJ mol^{-1}, 48.5 kJ more than the heat of reaction

$$2 \ CF_2 = CFCl \quad \longrightarrow \quad ClCFCF_2\overset{\bullet}{C}F \ \overset{\bullet}{C}FCl$$
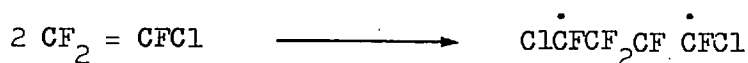
In calculating the entropy of activation the assignment of frequency values to three- and four-electron torsions is somewhat speculative, based on data from hydrocarbons[31, 135]. This approach

Table IV.4.1.

Changes in thermodynamic quantities for cyclization reactions <u>via</u> the diradical mechanism

Quantity	$2A \longrightarrow B^{\ddagger} \longrightarrow R: \longrightarrow C^{\ddagger} \longrightarrow D$				
	Change occuring at each step				
CF$_2$=CFCl					
$\Delta H^{\ominus}$	-915.5	97.2	-46.0	27.00	-245.96
$\Delta S^{\ominus}$	846.7	-165.4	- 6.1	-4.58	-21.44
$\Delta C_p^{\ominus}$	210.0	18.4	- 7.1	-4.47	20.0
CF$_2$=CFCF$_3$					
$\Delta H^{\ominus}$	-2137.40	133.3	-33.7	33.70	-263.93
$\Delta S^{\ominus}$	1048.96	-169.22	- 6.4	-6.10	- 21.78
$\Delta \overline{C}_p^{O}$	297.00	53.5	- 8.4	-5.17	16.52
Mixture					
$\Delta H^{\ominus}$	-1562.45	108.0	-38.2	30.10	-249.1
$\Delta S^{\ominus}$	947.83	-168.3	- 6.2	-5.34	- 20.68
$\Delta \overline{C}_p^{O}$	253.5	39.95	- 7.4	-4.8	18.26

$\Delta \overline{C}_p^{O} = \Delta \overline{C}_{p_{650-300}}^{O}$, $\Delta H^{\ominus}$, $\Delta S^{\ominus}$ refer to T = 650K

illuminates the pitfalls encountered in the application of the method to fluorocarbons and its shortcomings. More information about the thermochemical and spectroscopic properties of fluorocarbons and their diradicals will remove some of the present ambiguities. An alternative estimate of the entropy of the activation of the reactions studied may be obtained from statistical mechanics.

4.4.2   Entropy of activation from statistical mechanics

The relatively high entropy of activation $\Delta S_i^{\ddagger}$ for the compounds studied, indicates a 'loose' structure for the activated complexes. Cocks and Frey [130] suggested that the complex formed <u>via</u> a diradical intermediate is not planar but that it rather resembles a distorted cyclobutane, and that ring closing is more complicated than a simple shortening of the C_1-C_2 bond. The translational contribution to entropy for the activated complex is the same as that for cyclobutane and the rotational contribution does not differ by more than 1-2 J $K^{-1}mol^{-1}$ from the corresponding cyclic compound. Therefore, the difference in entropy change between activated complex and cyclic molecule, about 30-35 J K^{-1} mol^{-1}, is mainly due to different vibrational contribution. In the distorted structure of the activated complex, vibrations are shifted to or are replaced by torsions, at lower frequency (see 4.4.1.4). It is not possible to calculate accurately the increase in entropy but the value of 30-35 J $K^{-1}mol^{-1}$ does not seem excessive in view of the changes occuring. Assessing the changes, as before, we notice that while a C-C at 900 cm^{-1} does not contribute to entropy, the resulting three electron torsion at 125 cm^{-1} and four electron torsion at 300 cm^{-1} make a

net contribution of 29.5 J $K^{-1}mol^{-1}$ at 650 K. Similarly a number

of the CX_2 twisting, rocking and wagging vibtrations will occur at

considerably lower frequencies. It is possible that the dichloro-

and di(trifluoromethyl)- activated complexes attain such a con-

figuration (C_2, C_{2v}) so that the symmetry number is two, leading

to an entropy contribution of $-Rln2 \simeq -5.76$ J K^{-1} mol^{-1}. The value

of entropy change of 30-35 J $K^{-1}mol^{-1}$, adding all these contributions

together, does not seem unreasonable.

The model of the activated complex for an allowed concerted

process is not vastly different from the one previously discussed.

The elongated C_1-C_2 and C_3-C_4 bonds would not produce any signifi-

cant changes in the rotational contribution to entropy, neither

would the vibrational contributions have a dramatic effect. There-

fore, the change in entropy for such an activated complex is expected

to be roughly the same as that arising <u>via</u> a diradical. However,

an enthalpy estimate for the concerted process cannot be made.

Theoretical exploration of the potential energy surface along an

allowed (s + a) concerted path has not been undertaken yet and no

information is available.

The groups participating in 1,3-isomers are the same as those

in 1,2-isomers and it is expected that the heat of formation of these

compounds would not differ by more than 10 kJ mol^{-1}, unless the

effect of substituent interaction is greater than this value. There-

fore, the heat of reaction of these two classes will also be similar.

The MINDO calculations performed as part of the present work (page 45)

strongly suggest that this may be true. Such a difference in the

heat of formation does not explain the almost total absence of

1,3-isomers. Also, orbital symmetry restrictions apply equally

to the formation of 1,2-isomers as to 1,3-isomers. However, the heats of formation of diradicals leading to 1,3- disubstituted cyclo-buntanes may differ by more than 30 kJ mol^{-1} [7]. Such a difference would provide a plausible explanation as to why 1,3-isomers constitute only a few parts per thousand of the products. The comparatively high yield of 1,3-isomers in the cycloaddition of hexafluoropropene may be associated with the high enthalpy of activation of this reaction that enables formation of the diradical that produces the 1,3-cyclodimers.

The lack of stereoselectivity observed in these reactions is also associated with the enthalpy of activation. The results of Atkinson and his collaborators [,4] and the present work indicate that the highest barrier encountered in cycloaddition of fluoroolefins is the enthalpy of the 'open' activated complex. Therefore, it is expected that roughly equal amounts of isomers will be formed.

4.5   Conclusion and Suggestions for future work

The kinetic parameters and the thermodynamic quantities for the thermal cyclodimerization of pure chlorotrifluoroethene, hexafluoropropene and the intercombination cyclic product of the two compounds indicate that the reactivity of these compounds is determined from the stability of the olefinic double bond and the effect of the substituents on the stability of the cyclobutane ring. In this respect, the presence of the group $=CF_2$ enhances cyclo-addition by destabilizing the olefinic double bond and stabilizing the cyclobutane ring. The diradical mechanism explains the head-to-head cycloaddition, as well as, the formation of minute amounts of

1,3- isomers.

Previous kinetic studies in this laboratory [1,5] on the formation and dissociation of substituted polyfluoro- cyclobutanes and cyclopropanes have added considerably to the determination of thermodynamic quantities of fluorocarbons, as well as to the investigation of the mechanism of $_\pi 2$ + $_\pi 2$ cycloaddition. Further information about the energetics and the mechanism of cycloaddition may be obtained by extending the series of investigation to systems not possessing the group = CF_2, i.e. CFCl = CFCl, and to cyclic compounds not formed directly from cycloaddition such as 1,3- and 1,2,3- substituted cyclobutanes. The later case, the dissociation of 1,2,3-trisubstituted cyclobutanes will be most interesting and very profitable since it would provide information about the ease and position at which ring opening occurs. The added analytical complications may be largely overcome by using tubular columns for chromatographic analysis coupled with mass spectrometry. The reaction vessel (page 64) used in the present work would prove most helpful. Theoretical MO calculations about the potential energy surface along an allowed (s + a) reaction path would elucidate the present understanding of this process.

APPENDICES

&

REFERENCES

APPENDIX I

The MINDO/2 method

The MINDO method is a self-consistent-field MO theory, developed to fit experimental data (see page 49). Equation 1.1 (page 20) becomes

$$F\ C = S\ C\ E$$

where F is the Hatree-Fock Hamiltonian matrix, E is the orbital energy matrix, C is the matrix for linear expansion coefficients c_{ij} and S is the overlap matrix.

The Hatree-Fock Hamiltonian matrix elements have the general form

$$F_{ij} = H^c_{ij} + \sum_{k\ l} \left[P_{kl}\ (ij/kl) - P^a_{kl}\ (ij/kl) \right]$$

where the core Hamiltonian H^c_{ij} is given from

$$H^c_{ij} = \int \phi^*_i\ (1) \left[-\frac{1}{2} \nabla^2 + \sum_a^{atoms} \frac{Z_a}{r_{1a}} \right] \phi_j\ (1)\ dv$$

and

$$(ij/kl) = \iint \phi^*_i\ (1)\ \phi^*_k\ (2)\ (\frac{e^2}{r_{12}})\ \phi_j\ (1)\ \phi_1\ (2)\ dv_1 dv_2$$

The P_{kl} are elements of the total charge density-bond order matrix. The notation adopted here is similar to that used by Murrel and Harget [136].

According to the approximation suggested, the overlap integrals S_{ij} are neglected unless i = j. The two-, three- and four-centre integrals of the type (ij/kl) are set equal to zero unless i = j and k = 1. The remaining integrals are futher simplified by the approximation:-

$$(ii/jj) = \gamma_{ab} \quad (i \text{ on } A, \; j \text{ on } B)$$

where the two centre repulsion integral γ_{ab} between AOs of a given pair of atoms, A and B, is approximated as the Coulomb integral $(S_a S_a / S_b S_b)$ involving valence shell s-type orbitals of the atoms A and B with which i and j are respectively associated. Some other penetration integrals are neglected, too; thus, the attraction $< i/ V_b / i>$ between an electron in an AO $_i$ of atom A and the core of atom B, is assumed to be

$$<i / V_b / i> = -Z_b \gamma_{ab}$$

where $Z_b e$ is the core charge of atom B, i.e. the atomic number less the number of inner shell electrons.

With these approximations the elements of the core matrix H^C and the Hartree-Fock matrix F for a closed shell of electrons are:

(A,A) $\quad H^C_{ii} = U_{ii} - \sum_{b \neq a} Z_b \gamma_{ab} \qquad (i \text{ on } A)$

(A,A) $\quad H^C_{ij} = 0$

(A,B) $\quad H^C_{ij} = \beta^c_{ij}$

$$F^c_{ii} = U_{ii} + \frac{1}{2} \; q_i \; (ii/ii) +$$

$$\sum_{j \neq i}^{a} q_i \left[(ii/jj) - \frac{1}{2} (ij/ij) + \sum_{b \neq a} (Q_b - Z_b) \gamma_{ab} \right]$$

$$F^{aa}_{ij} = P_{ij} \left[\frac{3}{2} (ij/ij) - \frac{1}{2} (ii/jj) \right] = P_{ij} (\frac{3}{2} h_{ij} - \frac{1}{2} g_{ij})$$

$$F^{ab}_{ij} = \beta^c_{ij} - \frac{1}{2} P_{ij} \gamma_{ab}$$

where β^{c}_{ij} is one-electron resonance integral determined from empirical parameters, U_{ii} are the one-centre core-electron attraction integrals, and

$$g_{ss} \quad g_{sp} \quad g_{pp} \quad g_{pp'} \quad h_{sp} \quad h_{pp'}$$

are the one-centre electron repulsion integrals.

The atomic parameters for hydrogen, carbon and fluorine, given by Dewar and Lo [43], are

	U_{ss}	U_{pp}	g_{ss}	g_{pp}	g_{sp}	$g_{pp'}$	h_{sp}	$h_{pp'}$
H	-13.595		12.848					
C	-52.89	-40.28	12.23	11.08	11.47	9.84	2.43	0.62
F	-130.96	-105.03	16.92	16.71	17.25	14.91	4.83	0.90

APPENDIX II

Average specific rate constant k_{-2}

Atkinson and Stockwell [4] found that the decomposition of <u>trans</u> 1,2-di(trifluoromethyl)-hexafluorocyclobutane into two molecules of hexafluoropropene proceeeds faster than that of the <u>cis</u> isomer. They also found that isomerization occurred at rates very close to that of decomposition. The system of reactions may be represented as
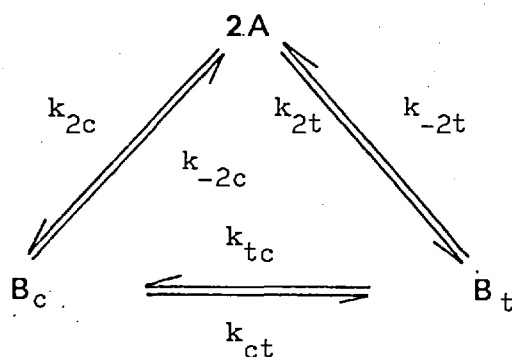
where A refers to hexafluoropropene, B_c and B_t to <u>cis</u> and <u>trans</u> 1,2-di(trifluoromethyl)-hexafluoropropene respectively.

At equilibrium

$$k_{ct}B_c = k_{tc}B_t \qquad 2I\_1$$

$$k_{2c}A^2 = k_{-2c}B_c \qquad 2I\_2$$

$$k_{2t}A^2 = k_{-2t}Bt \qquad 2I\_3$$

$$\therefore \quad \frac{k_{tc}}{k_{2t}} = \frac{k_{tc}}{k_{ct}} \cdot \frac{k_{-2c}}{k_{-2t}} = \frac{B_c}{B_t} = 0.6937 \qquad 2I\_4$$

$$\text{and} \quad \frac{B_c}{B_t + B_c} = 0.41 \qquad \frac{B_t}{B_t + B_c} = 0.59 \qquad 2I\_5$$

The equilibrium position of the isomers B_c and B_t is

$$\frac{B_c}{B_t} = \frac{5.84}{2.31} \text{, and } \frac{B_c}{B_t+B_c} = 0.717, \quad \frac{B_t}{B_t+B_c} = 0.283 \qquad 2I\_6$$

From equation $2I\_5$

$$k_{-2} = 0.41 \ k_{-2c} + 0.59 \ k_{-2t} \qquad 2I\_7$$

and from equation $2I\_6$

$$k_{-2} = 0.717 \ k_{-2c} + 0.283 \ k_{-2t}$$

taking the average and introducing the values of k_{-2c} and k_{-2t},

then $k_{-2} = 2.54 \times 10^{15} \exp (64,200/RT) \ s^{-1}$

APPENDIX III

"Dead" Space correction

A very small volume of the reaction vessel is at a temperature different to the one at which the reaction takes place and therefore a correction should be applied. [137]

The distribution of moles in the reactor is given by the equation

$$_o n_h \, R \, \frac{T_h}{V_h} \; = \; _o n_c \, R \, \frac{T_c}{V_c} \qquad\qquad 3 \; I\_1$$

where the subscripts refer to the hot ($_h$) and cold ($_c$) parts of the system, and n, T and V are respectively, number of moles, thermo-dynamic temperature and volume.

Let dn_n moles react. The decrease in the number of moles is $(1-q) \, dn_h$, where

$$q = \frac{dn_d}{dn_h} = \frac{\mu}{\nu} \qquad (\; \nu C \longrightarrow \mu E \qquad \nu > \mu)$$

is the ratio of the number of moles produced by the reaction to the number of moles consumed. This creates a pressure difference between the hot and the cold parts of the system. As a result, a number of moles enter the hot section to equalise the pressure: it is assumed that no diffusion takes place between the two sections.

Material balance requires

$$n_c + h_h + q^{-1} \, n_d \; = \; _o n \; = \; _o n_c + _o n_h \qquad\qquad 3 \; I\_2$$

$$dn_c + dn_h + q^{-1} dn_d = 0 \qquad\qquad 3\ I\_3$$

Since the pressure is at equilibrium

$$P_t = n_c R \frac{T_c}{V_c} = (n_h + n_d)\ R\ \frac{T_h}{V_h} \qquad\qquad 3\ I\_4$$

and $\quad n_c b = n_h + n_d \qquad\qquad 3\ I\_5$

where $\qquad b \equiv \dfrac{T_c\ V_h}{T_h\ V_c} \qquad\qquad 3\ I\_6$

Introducing equation 3 I_5 into equations 3 I_2 and 3 I_1 one
obtains

$$\frac{n_h}{b} + \frac{n_d}{b} + h_n + q^{-1}nd = \frac{-n_h}{b} + {}_o n_h \qquad\qquad 3\ I\_7$$

$$n_d \left(\frac{1 + b/q}{b} \right) = {}_o n_h \left(\frac{1 + b}{b} \right) - n_h \left(\frac{1 + b}{b} \right) \quad 3\ I\_8$$

$$n_d = {}_o n_h \frac{(1+b)}{(1+b/q)} - n_h \frac{(1 + b)}{(1 + b/q)} \qquad\qquad 3\ I\_9$$

For a reaction $\nu C \rightarrow \mu E$ of order a, the specific rate constant
is defined by

$$- \frac{1}{\nu} \frac{dC_h}{dt} = k\ C_h^a \qquad\qquad 3\ I\_10$$

or $\qquad \dfrac{\xi}{V_h} \quad \dfrac{1}{\mu V_h} \cdot \dfrac{dn_d}{dt} = k\left(\dfrac{n_h}{V_h}\right)^a$ $\qquad$ 3 I_10a

$\therefore \qquad \dfrac{dn_d}{dt} = \mu\, k\, n_h^a\, V_h^{1-a}$ $\qquad$ 3 I_11

Substitution of 3 I_11 in 3 I_3 and 3 I_5 gives

$$\dfrac{dn_h}{b} + \dfrac{dn_d}{b} + dn_h + \mu q^{-1} k\, n_h^a\, V_h^{1-a}\ dt = 0 \qquad \text{3 I\_12}$$

$$\dfrac{dn_h}{n_h^a}\left(\dfrac{1+b}{b}\right) = -\mu k\ V_h^{1-a}\ \dfrac{(1+b/q)}{b}\ dt \qquad \text{3 I\_13}$$

Integrating

$$n_h^{1-a} - n_h^{1-a} = \left(\dfrac{b/q+1}{b+1}\right)\ \mu k\ \dfrac{t}{V^{a-1}} \qquad \text{3 I\_15a}$$

or $\qquad C_h^{1-a} - {}_oC_h^{1-a} = \dfrac{(b/q+1)}{(b+1)}\ \mu\, k\, t$ $\qquad$ 3 I_15b

or $\qquad P_h^{1-a} - {}_oP_h^{1-a} = \dfrac{(b/q+1)}{(b+1)}\ \mu\, k_p\, t$ $\qquad$ 3 I_15c

where C_h and P_h are, respectively, the concentration and pressure of reactant in the hot section of the reactor.

Substituting equation 3 I_9 into 3 I_4 one obtains

$$P_t = \left[n_h + \frac{(1 + b)}{(1 + b/q)} ({}_o n_h - n_h) \right] \frac{RT_h}{V_h} \qquad 3\ I\_17$$

$$= \left[n_h \frac{b}{q} (\frac{1 - q}{1 + b/q}) + (\frac{1 + b}{1 + b/q})\ {}_o n_h \right] \frac{RT_h}{V_h} \qquad 3\ I\_18$$

$$(1 + b/q)\ P_t = n_h \frac{b}{q} (1 - q) \frac{RT_h}{V_h} + (1 + b)\ P_o \qquad 3\ I\_19$$

$$\frac{1}{n_h} = \frac{b}{q} (1 - q) \frac{RT_h}{V_h} \cdot \frac{1}{(1 + b/q)\ P_t - (1 + b)P_o} \qquad 3\ I\_20$$

Substitution of equation 3 I_20 in the general solution

(eq 3 I_15) facilitates the determination of k in terms of experi-

mental quantities P_t and P_o order reaction (a 2) of the type

$$2A = B \qquad (q = \tfrac{1}{2},\ \mu = 1)$$

equation 3 I_15a becomes $\quad n_h^{-1} - {}_o n_h^{-1} = \frac{1 + 2b}{1 + b} k \frac{t}{V_h} \qquad 3\ I\_21$

and $\quad n_n^{-1} = b \frac{RT_h}{V_h} \cdot \frac{1}{(1 + 2b)P_t - (1 + b)P_o} \qquad 3\ I\_22$

$$\therefore \quad k = \frac{1 + b}{1 + 2b} \frac{RT_h}{t} \left[\frac{b}{P_t(1 + 2b) - P_o(1 + b)} - \frac{1}{P_o} \right] 3\ I\_23$$

REFERENCES

1. A.B. Trenwith, Ph. D. Thesis, London University, 1952

2. B. Atkinson and V.A. Atkinson, J. Chem. Soc., 1957, 2086

3. B. Atkinson and M, Stedman, J. Chem. Soc., 1962, 512

4. B. Atkinson and P.B. Stockwell, J. Chem. Soc. (B), 1966, 740, 984.

5. D.J. McKeagan, Ph. D. Thesis, London University, 1967

6. J.D. Roberts and C.M. Sharts, Org. Reactions, 1962, 12, 1

7. P.D. Bartlett, Science, 1968, 159, 833

8. P.D. Bartlett, Quar. Reviews, 1970, 24, 473

9. L. Pauling 'The Nature of the Chemical Bond' 3rd. Ed., Cornell Univ. Press, New York, 1960

10. M.J.S. Dewar 'The Molecular Orbital Theory of Organic Chemistry' McGraw-Hill, 1969

11a R.S. Berry, Chem. Rev., 1969, 69, 533

  b R. Milstein and R.S. Stephen, J. Chem. Phys., 1971, 55, 4146.

12. C.R. Patrick 'Advances in Fluorine Chemistry', 1961 Vol.2, 1

13. C.R. Patrick, Chem. in Britain, 1971, 7, 154

14. T.M. Reed 'Fluorine Chemistry' (ed. J.H. Simons) Vol.5, 133 Academic Press, 1964

15. J.S. Rowlinson 'Liquids and Liquid Mixtures' 2nd. ed., 283, Butterworths, 1969

16. C.H. Chang, A.L. Andreassen and S.H. Bauer, J. Org. Chem., 1971, 36, 920.

17. E.J.M. van Schaick, H.J. Geise, F.C. Mijloff and G. Renes, J. Mol. Struct., 1973, 16, 23

18. N.C. Craig, L.G. Piper and V.L. Wheeler, J. Phys. Chem., 1971, 75, 1453

19. G.A. Crowder and P. Pruettiagkura, J. Mol. Struct., 1973, 18, 177

20. H. Hilderbrandt, A.L. Andreassen and S.H. Bauer, J. Phys. Chem.,
    1970, 74, 1586

21. E.J.M. van Schaick, F.C. Mijlhoff, G. Renes and H. Geise,
    J. Mol. Struct., 1974, 21, 17

22. W.A. Bernett, J. Org. Chem., 1969, 34, 1772

23. R.J. Abraham and K. Parry, J. Chem. Soc. B, 1970, 539

24. R. Stephens and J.C. Tatlow, Quar. Reviews, 1962, 16, 44

25a A. Streitwieser and D. Holtz, J. Am. Chem. Soc., 1967, 89, 692

  b A. Streitwieser, A.P. Marchand and A.H. Pudjaatmaka, ibid.,693

26. K.J. Klabunde and D.J. Burton, J. Am. Chem. Soc., 1972, 94,5985

27. J. Hine, N.W. Flachskam, J. Am. Chem. Soc., 1973, 95, 1179

28. J. Hine and F.E. Rogers, J. Am. Chem. Soc., 1968, 90, 6701

29. W.A. Sheppard and C.M. Sharts, 'Organic Fluorine Chemistry',
    W.A. Benjamin, 1969

30a S.W. Benson and J.H. Buss, J. Phys. Chem., 1958, 29, 46

  b S.W. Benson 'Thermochemical kinetics', J. Wiley and Sons, 1968

  c S.W. Benson, F.R. Cruickshank, D.M. Golden, G.R. Haugen,
    H.E. O'Neal, A.S. Rodgers, R. Shaw and R. Walsh,
    Chem. Rev., 1969, 69, 279

31. H.E. O'Neal and S.W. Benson, J. Phys. Chem., 1968, 72, 1866

32. JANAF Thermochemical tables, 2nd. Ed., NSRDS-NBS, 37, 1971

33. R.D. Chambers, 'Fluorine in Organic Chemistry', p.6,
    J. Wiley and Sons, 1972

34 A.D. Walsh, Trans. Faraday Soc., 1947, 43, 60

35. H.A. Bent, J. Chem. Phys., 1960, 33, 1258

36. J.A. Pople and M. Gordon, J. Am. Chem. Soc., 1967, 89, 4253

37. W.H. Herhe and J.A. Pople, J. Am. Chem. Soc., 1970, 92, 2191

38. L. Radom, W.H. Herhe and J.A. Pople, J. Am. Chem. Soc., 1971,
    93, 289

39. J.A. Pople, D.L. Beveridge and P.A. Dobosh, J. Chem. Phys.,
    1967, 47, 2026

40. J.A. Pople and D.L. Beveridge 'Approximate Molecular Orbital
    Theory', Chap. 3 and 4, McGraw-Hill, 1970

41. N.C. Baird and M.J.S. Dewar, _J. Chem. Phys._, 1969, 50, 1262

42. M.J.S. Dewar and L. Haselbach, _J. Am. Chem. Soc._, 1970, 92, 590

43. M.J.S. Dewar and D.H. Lo, _J. Am. Chem. Soc._, 1972, 94, 5296

44. M.J.S. Dewar, Private Communication

45. B. Atkinson, Private Communication

46. N.D. Epiotis, _J. Am. Chem. Soc._, 1973, 95, 3087

47. A. Liberles, A. Greenberg and J.E. Eilers, _J. Chem. Ed._, 1973, 50, 676

48. R.B. Davidson and L.C. Allen, _J. Chem. Phys._, 1971, 54, 2828

49. S.W. Benson and H.E. O'Neal, 'Kinetic data on gas phase unimolecular reactions' NSRDS-NBS 21, 1970

50. E.M. Engler, J.D. Andose and P. von R. Schleyer, _J. Am. Chem. Soc._, 1973, 95, 8005

51. R.G. Rathjens, Jr., N.K. Freeman, W.D. Gwinn and K.S. Pitzer, _J. Am. Chem. Soc._, 1953, 75, 5634

52. J.M.R. Stone and I.M. Mills, _Mol. Phys._, 1970, 18, 631

53. F.A. Miller and R.J. Capwell, _Spec. Acta_, 1971, 27A, 947

54. S. Meiboom and L.C. Snyder, _J. Chem. Phys._, 1970, 52, 3857

55. R.P. Bauman and B.J. Bulkin, _J. Chem Phys._, 1966, 45, 596

56. C.H. Chang, R.F. Porter and S.H. Bauer, _J. Mol. Struct._, 1971, 7, 89

57a J.S. Wright and L. Salem, _J. Am. Chem. Soc._, 1969, 91, 5947

  b J.S. Wright and L. Salem, _ibid._ 1972, 94, 322

58. J.L. Nelson and A. Frost, _J. Am. Chem. Soc._, 1972, 94, 3727

59. R. Pasternak and A.Y. Meyer, _J. Mol. Struct._, 1974, 20, 351

60. F.A. Miller and R.J. Capwell, _Spect. Acta_, 1971, 27A, 1113

61. W.C. Harris and D.B. Young, _J. Mol. Struct._, 1973, 18, 257

62. Ref. 54 in (R.M. Moriarty 'Cyclobutane and heterocyclic analogs') 'Topics in Stereochemistry' Vol. 8, p.304, J. Wiley and Sons, 1974

63. B. Atkinson and A.B. Trenwith, _J. Chem. Soc._, 1953, 2082

64. R. Huisgen, R. Grashey and J. Sauer in 'The Chemistry of Alkene' S. Patai, Ed. (Interscience, New York 1964) Chap. 11

65. R.B. Woodward and R. Hoffmann, 'The Concervation of Orbital Symmetry' Academic Press, 1970

66. H.C. Longuet-Higgins and E.W. Abrahamson, J. Am. Chem. Soc., 1965, 87, 2045.

67. E.B. Wilson, Jr., J.C. Decius and P.C. Cross, 'Molecular Vibrations', App. X, McGraw-Hill, 1955

68. J.S. Wright and L. Salem, J. Am. Chem. Soc., 1972, 94, 322

69. M.J.S. Dewar, Angew. Chem. Int. Ed., 1971, 10, 761

70. H.E. Zimmerman, Acc. Chem. Res., 1971, 4, 272

71. T.N. Margulis, Acta Crystal. 1965, 19, 857

72. H. Fujimoto, S. Yamabe and K. Fukui, Bull. Chem. Soc. Jap. 1972, 45, 2424

73. K. Fukui, Acc. Chem. Res., 1971, 4, 57

74. W.C. Herndon, Chem. Rev., 1972, 72, 157

75. R.F. Hudson, Angew. Chem. Int. Ed., 1973, 12, 36

76. N.D. Epiotis, J. Am. Chem. Soc., 1972, 94, 1924, 1935

77. R.F. Lake and H. Thomson, Proc. Roy. Soc., 1970, 315, 323

78. N.D. Epiotis, J. Am. Chem. Soc., 1973, 95, 5624

79. P.D. Bartlett and R.C. Wheland, J. Am. Chem. Soc., 1972, 94, 2145

80. H.E. O'Neal and S.W. Benson, J. Chem. Eng. Data, 1970, 15, 266.

81. H.E. O'Neal and S.W. Benson, Int. J. Chem. Kin., 1969, 1, 221

82. L. Salem and C. Rowland, Angew. Chem. Int. Ed., 1972, 11, 92

83. L.M. Stephenson and T.A. Gibson, J. Am. Chem. Soc., 1971, 94, 4599

84. R. Hoffmann, S. Swaminathan, B.G. Odell and R. Gleiter, J. Am. Chem. Soc., 1970, 92, 7091

85. P.J. Hay, W.J. Hunt and W.A. Goddard, III, J. Am. Chem. Soc., 1972, 94, 638

86. J.A. Pople, Int. J. Quantum Chem., Symp. 1971, 5, 175

87. L.M. Stephenson, T.A. Gibson and J.I. Brauman, J.Am. Chem. Soc., 1973, 95, 2849

88. W. von E. Doering and K. Sachdev, J. Am. Chem. Soc., 1974, 96, 1168

89. J.D. Cox and G. Pilcher, 'Thermochemistry of Organic and Organometallic Compounds', 143, Academic Press, 1970

90. P.C. Beadle, D.M. Golden, K.D. King and S.W. Benson, J. Am. Chem. Soc., 1972, 94, 2943

91. B. Atkinson and D. McKeagan, Chem. Comm., 1966, 189

92. Standards for Petroleum and its products, Part I, 732, Institute of Petroleum, London, 1967

93a National Physical Laboratory, Notes of App. Acience No. 9, London, H.M.S.O., 1962

93b B.S. 2520: 1967 British Standards Institution, London, 1967

94. T. Boddington, P. Gray and B.J. Tyler, 2nd Int. Symp. on Gas Kinetics, Swansea, 1971

95a NBS Monograph 125, National Bureau of Standards (US), Washington, D.C., 1974

95b 'Handbook of Chemistry and Physics', 52nd Ed., E94, The Chemical Rubber Co., Cleveland, 1971

96. D.H. Fine, P. Gray and R. McKinven, 72nd Symp. on Combustion, The Combustion Institute, 1969, 545

97. C.A. Clemons and A.P. Altschuller, Anal. Chem., 1966, 38, 133

98. C.A. Coulson and D.R. Humphries, Gas Chromatography, 1970, 344

99. R.N. Bright and R.A. Matula, J. Chromatog., 1986, 35, 217

100. A. Foris and J.G. Lechman, Sep. Science, 1969, 4, 225

101. R.P.W. Scott, 'Advances in Chromatography' Vol. 9, 193 M. Dekker Inc., New York, 1970

102. A.F. Williams and W.J. Murray, Talanta, 1963, 10, 937

103a E.G. Young and W.S. Murray J. Am. Chem. Soc., 1948, 70, 2814

103b W.F. Edgell, ibid., 1948, 70, 2816

103c F.A.M. Buck and R.L. Livingston, ibid., 1948, 70, 2817

104a J.R. Nielson, H.H. Claassen and D.C. Smith, J. Chem. Phys., 1952, 20, 1916

104b A.B. Harvey and L.Y. Nelson, ibid., 1971, 55, 4145

105a J. Harmon, U.S. Patent 2,404,374 (1946)

105b J. Harmon, U.S. Patent 2,436,148 (1948)

106. A.L. Henne and R.P. Ruh, J. Am. Chem. Soc., 1947, 69, 279

107. M.W. Buxton, D.W. Ingram, F. Smith, M. Stacey and J.C. Tatlow, J. Chem. Soc., 1952, 3830

108. W.T. Miller, in 'The Preparation, Properties and Technology of Fluorine and Organic Fluorine Compounds', 567, National Nuclear Energy Series, Div. VII, 1, McGraw-Hill, 1951

109. J.D. Park, H.V. Holler and J.R. Lacher, J. Org. Chem., 1960, 25, 990

110. W.C. Solomon and L.A. Dee, J. Org. Chem., 1964, 29, 2790

111. J.R. Lacher, G.W. Tompkin and J.D. Park, J. Am. Chem. Soc., 1952, 74, 1693

112. M. Stedman, Ph.D. Thesis, London University, 1960

113. J.R. Lacher, A. Buckler and J.D. Park, J. Chem. Phys., 1952, 20, 1014

114. W.F. Edgell and F.E. Kite, J. Chem. Phys., 1947, 15, 882

115. J.H. Beynon, R.A. Saunders and A.E. Williams, 'The mass spectra of organic molecules', Ch.7, 376, Elsevier, 1968

116. J. Feeney, L.H. Sutcliffe and S.M. Walker, Mol. Physics, 1966, 11, 117

117. W.D. Phillips, J. Chem. Phys., 1956, 25, 949

118. D. Margerison in 'Comprehensive Chemical Kinetics', Vol.1, Ch.5, Elsevier Publishing Co., 1965

119. P.D. Lark, B.R. Craven and R.C.L. Basworth, 'The handling of chemical data' Ch.5., Pergamon Press, 1968.

120. R.A. Matula, J. Phys. Chem., 1968, 72, 3054

121. H.C. Brown, J. Org. Chem., 1957, 22, 1256

122. M. Hauptschein, A.H. Fainberg and M. Braid, J. Am. Chem. Soc., 1958, 80, 842.

123. J.W. Emsley and L. Phillips in 'Progress in NMR Spectroscopy', Vol.7. Pergamon Press, 1971.

124. J.R. Majer, 'Advances in Fluorine Chemistry', Vol.2, 1961

125. L.J. Bellamy, 'The infra-red spectra of complex molecules',
     p. 329, Methuen, London, 1958

126. J.R. Durig and J.N. Willis, Jr., J. Chem. Phys., 1971, 54, 1547

127. R.A. Hofmann, B. Forsén and B. Gestblam, in 'NMR Basic principles
     and progress' Vol.5, Springer-Verlag, Berlin, 1971.

128. H.M. Frey and R. Walsh, Chem. Rev., 1969, 69, 103

129. S. Glasstone, K.J. Laidler and H. Eyring, 'The theory of rate
     processes', McGraw-Hill, New York, 1941

130. A.T. Cocks and H.M. Frey, J. Chem. Soc. (A), 1969, 1671

131. G.J. Janz, 'Estimation of thermodynamic properties of organic
     compounds', Academic Press, New York, 1958

132. P.B. Stockwell, Ph.D. Thesis, London University, 1965

133. J Sherman and R.B. Ewell, J. Phys. Chem., 1942, 46, 641

134. J.R. Lacher and H.A. Skinner, J. Chem. Soc. (A), 1968, 1034

135. M.I. Page, Chem. Soc. Rev., 1973, 2, 295

136. J.N. Murrell and A.J. Harget, 'Semi-empirical self-consistent-
     field molecular orbital theory of molecules' Wiley-
     Interscience, 1972

137. P.J. Robinson, Trans. Faraday Soc., 1965, 61, 1655.